University of Zurich[UZH]

Impacts of current and future deglaciation on water and sediment availability in the Lötschental, Valais.

GEO 511 Master's Thesis

Author
Matthias Nyfeler
12-925-707

Supervised by
Dr. Holger Frey
Prof. Dr. Christian Huggel

Faculty representative
Prof. Dr. Andreas Vieli

30.04.2019
Department of Geography, University of Zurich

MASTER'S THESIS

Impacts of current and future deglaciation on water and sediment availability in the Lötschental, Valais

Author:	Matthias Nyfeler	matthias.nyfeler@uzh.ch 12-925-707
Supervised by:	Dr. Holger Frey Prof. Dr. Christian Huggel	holger.frey@geo.uzh.ch christian.huggel@geo.uzh.ch
Faculty representative:	Prof. Dr. Andreas Vieli	andreas.vieli@geo.uzh.ch

University of Zurich[UZH]

Department of Geography

Handed in on the 30th of April 2019 / GEO 511 / University of Zurich / Department of Geography

«Ja, das ischt äs Zeychnd, das friäjer oich uisgaabräd ischt. Hiä die Schpäält! Wa ich in 70är Jaarn da bin gsi, ischt das nid äso gsi. Duä sind d Schpäält zuä gsi, vill me Schnee hets ghabäd. Guät, dizz Bild muäs schpaat im Herpscht sii, wil dr Bärg uif oich uisgaabräd ischt, schtaarch uisgaabräd. Und äbn d aabru Schtella uf im Gletschär firha chemmd.»

Pius Henzen, Bergführer

«Yes, that's a sign that [it] also became free of snow. Here those crevasses! When I was there during the seventies, it didn't look like that. There the crevasses were closed, a lot more of snow was around. Well, this picture has to be late in fall because the mountain is free of snow and ice too, in a severe manner. And therefore the snow free places on the glacier appear.»

Pius Henzen, mountain guide

Cover: Galcier tongue area of Nästbach, captured during the photogrammetric survey on the 21st of September 2018. (Source: Elias Kaiser)

Postcard / Quote: Already in the early 20th century the glaciers became snow-free in high altitudes during fall. (Source: Werner Bellwald)

PREFACE

«Natur, Ruhe, Mythen - Erlebe das magische Tal.»
«Nature, Silence, Myths - Experience the magic Valley.» (LÖTSCHENTAL MARKETING AG, 2019)

With this slogan Lötschental tourism advertises and attracts tourists into the beautiful and isolated valley. My great grandparents already visited the remote place on mules over one hundred years ago and began the family tradition as regular visitors. It lived onward until today and I was lucky to spend a lot of my youth in the valley, helping out the local people with hay-making, experiencing hot and dry summers or bridging the time during valley closings due to avalanche danger in 1999 during several days. Even if I grew up in the agglomeration of Basel, I learned about the alpine environment and was impressed by the close interaction of the beauty and roughness of nature (FIG. 01). Maybe these experiences led to my interest about climate, glaciers and natural hazards.
During the first 28 years of my life, the glacier tongue of the Langgletscher lost about 400 m of its length and every year the path to the glacier tongue needs to be extended many meters. It is unmistakable that such processes have a big impact on the environment and act as mouthpiece for other geomorphological processes in the valley.

FIG. 01: View from «Galn», inside the Birchbach catchment, towards the Lötschenlücke at around 2'700 m a.s.l. on the 15th of September 2018. (Source: own photography)

The inhabitants of the Lötschental have to face upcoming challenges while increasing temperatures and changing precipitation patterns influence the alpine living more and more. The Lötschental itself resembles a holy goblet, sourrounded by smooth landscapes in the north-west and the rough and peaky nunatak Bietschhorn (3'934 m a.s.l) on the south-east, sitting enthroned on top of the valley and representing the highest vanguard of the near four-thousanders. A goblet where the effects of global change and glacier retreat can be exemplarily studied regarding to the local population. With this thesis, I want to give the valley a perspective to help to understand the processes which are already happening and regarding the upcoming future,.
The obvious glacier retreat represents the initial position from where the problems of water and sedi-

ment availability are discussed. While the vanishing glacier melt leads to a decrease in fluvial runoff, the mobilised sediments are affecting the local population. Both processes have to be assessed regarding their triggering, their effects and their risks which is the aim of the present study.
This thesis was conducted at the University of Zurich in Glaciology and Geomorphodynamics under the supervision of Dr. Holger Frey and Prof. Dr. Christian Huggel, whom I thank in particular for their support, flexibility and confidence in my work. I thank my mother Edith Nyfeler for her detailed correction of my work and of course I thank my partner in crime, Kathrin Kuhn, for her endless support and appreciation regarding the sometimes challenging task. My personal thanks go out to the following people who supported me:

- Bruno Bellwald, President of Kraftwerke Fafleralp AG
- Christoph Graf, Mountainflyers 80 Ltd.
- Daniel Siegen, former Technical Manager of Wiler
- David Liechti, Institute for Snow and Avalanche Research SLF
- Edith Oosenburg & Marco Hostettler, Federal Office for Environment BAFU, Department Hydrology
- Elias Kaiser, Photographer
- Elmar Ebener, President Foundation Blatten
- Hans-Jakob Rieder, Mayor Wiler
- Horst Machguth, World Glacier Monitoring Service WGMS
- Jean-Christoph Lehner, Mayor Blatten
- Jules Seiler, Geoplan AG
- Jürg Wegmüller, Mountainflyers 80 Ltd.
- Leonard Murisier, SRP Ingenieur AG Brig
- Lucas Kalbermatten, President of the Valley Council Lötschental
- Martin Ebener, Community Recorder Ferden
- Michel Bovey, Institute for Snow and Avalanche Research SLF
- Michel Salzgeber, EnAlpin AG
- Mirjam Baumann, Federal Office for Meteorology and Climatology EDI, MeteoSwiss
- Nadja Jeitziner, Mayor Ferden
- Nico Mölg, PhD University of Zurich
- Nina Brunner, Support for hydrological modellings
- Pascal Tourneur, IT-Support
- Patrick Manz, Berner Kraftwerke BKW
- Randy Muñoz, PhD University of Zurich
- Reinhard Tannast, Mayor Kippel
- Richard Bellwald, Ranger Lötschental
- Ruben Rieder, Municipal Council Wiler
- Siegmund Jungkunz, Community Recorder Kippel
- Simon Oberli, Gletschervergleiche.ch
- Susan Ivy-Ochs (PD Dr.), Quaternary Geologist
- Stefan Ebener, Werkhof Blatten
- Urban Paris, SRP Ingenieur AG Brig
- Urs Marti (Dr.), Swisstopo
- Werner Bellwald (Dr.), Cultural Historian

... and finally everybody who gave me a hint without even knowing it.

CONTENT

REGISTER

PHOTOS / GRAPHS / ILLUSTRATIONS

TABLES

ZUSAMMEN-FASSUNG

Der Klimawandel trifft die Welt in vielfältiger Art und Weise. Aufgrund der Empfindlichkeit der Alpen werden diese durch die zukünftigen Veränderungen stark betroffen sein. Während die Temperaturen steigen und sich das Niederschlagsbild verändert, beeinflussen die abschmelzenden Gletscher die Wasserversorgung der alpinen Regionen und lassen grosse Sedimentansammlungen zurück. Beide Prozesse bedrohen die lokale Bevölkerung durch Murgänge und Wasserknappheit. Die vorliegende Arbeit untersucht die Wasser- und Sedimentverfügbarkeit im Lötschental von heute und bis zum Ende des angebrochenen Jahrhunderts.

Basierend auf zwei Einzugsgebiete des Hauptflusses Lonza, wird die Wasserverfügbarkeit in monatlicher Auflösung modelliert und durch die Parameter Regen, Schneeschmelze, Gletscherschmelze und Evapotranspiration definiert. Mögliches Grundwasser wird vernachlässigt. Das Modell basiert auf der vorhandenen Gletscherfläche und auf stündlichen Messwerten von Temperatur und Niederschlag. Die Zukunftsprognosen werden anhand der «Representative Concentration Pathways» (RCP) Szenarien 2.6, 4.5 und 8.5 berechnet, welche auch auf die Nebenflüsse übertragen werden. Es wird angenommen, dass die Nebenflüsse das Abflussverhalten der benutzen Wasserquellen widerspiegeln. Aufgrund des Vergleiches zwischen dem lokalen Wasserverbrauch und der Wasserverfügbarkeit, kann eine Aussage über eine mögliche Wasserverknappung gemacht werden. Die Resultate zeigen eine starke Abhängigkeit von den existierenden Eismassen. Sie sind für 46 % des gesamten Abflusses des Lötschentals verantwortlich. Die zukünftigen Szenarien geben zudem einen Abflusseinbruch von etwa -45 % für das pessimistische RCP8.5 Szenario an. Dieses Resultat wird gestützt durch die Ergebnisse der Nebenflüsse, welche modellierte Abflussrückgänge von bis zu -75 % verzeichnen. Eine zukünftige Wasserknappheit konnte nicht erkannt werden, trotzdem muss berücksichtigt werden, dass das Modell auf monatlichen Mittelwerten beruht und deshalb keine kurzzeitige Veränderungen abbilden kann.

Die Sedimentverfügbarkeit wird anhand der Differenz zwischen zwei Höhenmodellen von 2011 und 2018 quantifiziert, wobei letzteres als Teil dieser Arbeit mittels Photogrammetrie erzeugt wurde. Die Materialverfügbarkeit, wie auch die vorausgesetzten Prozesse, um einen Murgang auszulösen, werden durch Vergleiche zwischen erkannten Oberflächenverschiebungen und vorhandenen Berichten über Murgänge bestimmt. Die Sedimentreservoirs konnten in die Gruppen der «Massive», der «Überdeckung» und der «Streuung» eingeteilt werden, wobei die «Überdeckung» die grösste Wahrscheinlichkeit beinhaltet, als Murgang ausgelöst zu werden. Die Sedimentverfügbarkeit konnte der Platzierung schuttbedeckter Eismassen, der Topographie und dem Untergrund zugeordnet werden. Es kann angenommen werden, dass die Murgangaktivitäten zurückgehen, die Intensität der einzelnen Murgänge aber zunehmen wird.

Aufgrund der Resultate kann ausgesagt werden, dass das Lötschental in naher Zukunft starke Veränderungen in der Wasser- und Sedimentverfügbarkeit erfahren wird. Die einsetzenden Prozesse hängen von der Gletscherrückzugsrate ab und werden das zukünftige Lebensumfeld der lokalen Bevölkerung bestimmen.

ABSTRACT

Climate change is affecting the world in manifold ways. Based on its fragility, the Alps are impacted by the upcoming transformations in a distinctive way. While temperatures will increase and precipitation patterns will change, the glacier retreat influences the water supply of alpine regions and provides large sedimentary accumulations on former glaciated areas. Both processes can endanger the local population through debris flow events or water scarcity. This study analyses the water and sediment availability in the Lötschental for today and until the end of the century.

The water availability is modelled for two catchments of the main river Lonza and is defined by the parameters of rain, snow melt, glacier melt and evapotranspiration. Any groundwater existence is neglected. The model is based on the glacier coverage and on measured hourly temperature and precipitation values which are averaged to monthly results. To get future projections, the representative concentration pathways RCP scenarios 2.6, 4.5 and 8.5 are applied, also onto the tributary torrents. They assumably reflect the runoff behaviour of the used springs in the valley. Statements about possible water scarcity are made based on the correlation between the local water consumption and the water availability. The results reveal a strong dependency on the present ice masses today. They deliver 46 % of the total runoff of the whole valley. The projected scenarios reveal a runoff decrease for the Lötschental of around -45 % for the pessimistic RCP8.5 scenario which is supported by the results of the tributary torrents. The smaller sized the catchments reveal less possibility of runoff compensation and therefore a future runoff decrease of up to -75 % is calculated. A possible upcoming water scarcity was not detectable, even though it has to be considered that the model is based on averaged monthly values which are not able to picture short-time phenomenons.

The sediment availability is derived from the difference between two elevation models originating from 2011 and 2018, while the latest elevation model was photogrammetically generated as part of this study. The material availability and the required processes to trigger a debris flow are retrieved out of the correlation between recognised surface differences and existing reports of debris flow events. The sediment reservoirs could be classified into the three main groups of «Massifs», «Coverage» and «Scatter», while the «Coverage» reveals the highest probability of being triggered as debris flows. The sediment availability could be allocated to the location of debris covered ice masses in consideration of the topography and the existing underground. It is assumed that the debris flow activity will decrease while the intensity of single events will increase.

Based on the results, it can be concluded that the Lötschental will experience severe changes in water and sediment availability in the near future. The instating processes are depending on the rate of the glacier retreat and will determine the future living environment of the local inhabitants.

1 INTRO-DUCTION

1.1 Initial situation and background

2018 was a year of records. METEOSWISS (2019a) writes that the Swiss nationwide mean annual temperature of 6.9 °C is the highest measured value since the beginning of records in 1864 and it was more than a degree warmer than the preceding reference period from 1988-2017 (5.7 °C). 2018 represents one of the fourth warmest years since 2011 and includes nine months which were warmer than the average, thereof six in an extreme way.

While the winter temperatures were in average representative for the period of 1981-2010 (with distinct differences between the months), the snow height revealed up to 200 % of the averaged value which was also reflected by various road closings of avalanche endangered valleys like the Mattertal and the Lötschental (ibid.). In high altitudes, locally 2.5-6 m of snow height were measured until the end of January 2018 which covered the glaciers with 70 % more snow than in average (SCNAT, 2018). Winter ended with cold temperatures and a warm spring set in. In April the nationwide mean annual temperature was 3.9 °C higher than the reference period (1981-2010), followed by an extreme warm summer which was 2 °C above the long-term temperature. Beside the hot temperatures, the overall dry conditions with only 20-40 % of the average precipitation in June led to a century water shortcoming in parts of Switzerland . Fall represented a small relief, but the temperatures were still 1.8 °C above the average including ongoing dry conditions on the northern face of the alpine ridge (METEOSWISS, 2019a).

The Federal Office for Environment (BAFU) reported in August 2018, that the runoff of rivers and lakes is heavily below-average with the exclusion of water systems with glaciated catchments (BAFU, 2018).

The hot temperatures led to a veritable decomposition of smaller glaciers. It is assumed that swiss glaciers lost about 1.5-2 m ice thickness (SCNAT, 2018) which led to an above than average runoff and which in turn compensated the missing precipitation (FIG. 02).

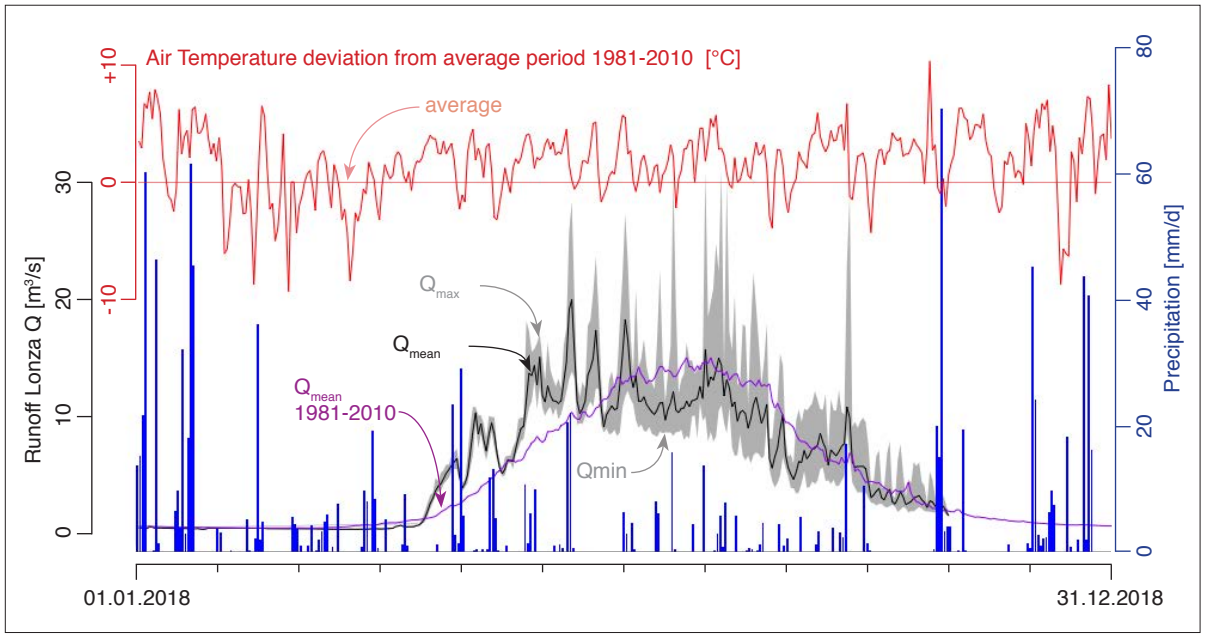

FIG. 02: Overview about the relation between the runoff of Lonza, precipitation and air temperature in Blatten (2018) compared to the averaged period (1981-2010). During summer less precipitation was measured and not every runoff peak is correlated to a precipitation input. (Source: BAFU, 2019b & METEOSWISS, 2019b)

The summer drought affected the Valais and also the Lötschental in a severe way and was the worst since more than 100 years. Different municipalities had to restrict their water consumption (VS, 2018). Based on the clustered heat waves in the past 20 years, the canton Valais published in 2013 an heat-wave-plan to handle the risks and effects of the high temperatures which was used in 2018 (KANTON WALLIS, 2018).

Beside 2018, the years 2015, 2014 and 2011 were the fourth warmest since the beginning of records with a yearly averaged temperature above 6.5 °C. As FIG. 02 shows, in Blatten a mean annual temperature of 1.57 °C above the average value (1981-2010) was measured in 2018 (METEOSWISS, 2019a). With an increasing temperature, glaciers will melt and the precipitation patterns will change (CH2018, 2018) and will inevitably affect Switzerland as «Water Castle», especially alpine regions which are directly depending on local water supply. Because the ice is melting, the glacial runoff will increase in the first phase and decrease afterwards (HUSS & HOCK, 2018). It is assumed, that the «peak water» is reached within 20 to 60 years - depending on the size of the glacier (CHY, 2009). But the main problem is the relation between water input and usage. If the consumption is bigger than the supply, a water shortage (so called «water scarcity») develops (UN WATER, 2019). To avoid such critical situations, it has to be known from which sources and in which relation the used water is composed. Already 1999, SECKLER et al. (1999) wrote a paper about future water scarcity problems in 2025, they argued mainly with a lowering of the groundwater table based on the population growth and increased water consumption and neglected the first signs of climate change. HAEBERLI & HOHMANN (2008) made local researches and state on page 5: *«Despite the large water resources in the Alpine region, water stress could become a problem in some parts of Switzerland during the hot/dry season (...).*

Conflicts about water use are likely to grow and options for adaptation - for instance, redefinition of the use of reservoirs at high-altitude (irrigation and summer power production rather than winter power production) - should be investigated as early as possible.» In the scope of changing alpine catchments, different researches have been conducted: BELLWALD (2009) analysed the glacier change in the Lötschental until 2005 and WELPMANN (2003) measured and modelled the surface temperatures in the valley. In the near surrounding several analysis were conducted on the retreat of Aletschgletscher where possible overdeepenings were modelled, including the area of Langgletscher (LINSBAUER et al., 2012; HAERBERLI et al., 2016). Beside the glacier correlated water availability, the climate change also influences the sedimentary availability which is affected by retreating glaciers too (DELANEY et al., 2018).

The first year with an annual mean temperature above 6.5 °C was 2011 (regarding 1864). It was a year of destiny for the Lötschental. It was above-average warm and dry, but in fall the weather changed and on the 10th of October heavy floods set in. Different rivers drained huge amounts of water. Milibach, a small mountain torrent on the Petersgrat side was estimated to have discharged up to 32m^3/s in maximum (RÖSSLER et al., 2013) which corresponds to the EHQ scenario (GEOPLAN AG, 2007) and describes around the half of the maximal runoff of the main river Lonza in Blatten. EnAlpin AG, the operator of the hydroelectricity powerplant in Ferden at the valley entrance, assumed a sedimentary input into the basin of around 200‘000 m^3 which is more than 10 % of the maximum catchment volume (GEOPLAN AG, 2012). In total the damage in the Lötschental was estimated to 20 million Swiss franks (DER BUND, 2011). RÖSSLER et al. (2013) analysed that the event was based on a fast change between a snow intensive cold front which was abruptly followed by a warm front with strong but local rainfall. The overlap of those two water sources (snow and rain) led to the former unknown runoff volume and the massive sedimentary flux. Based on the 2011 event BÖCKLI & RICKENMANN (2015) modelled the sedimentary flux of each contributory torrent and reconstructed the process. Beside the huge event in 2011, regular debris flows are reported on the north faced Bietschhorn ridge (GEOPLAN AG, all reports). The trigger events are based on moderate to heavy rain events or on melting dead ice (GEOPLAN AG, all reports), while the preconditions always differ. GEOPLAN AG (2013) writes that a clustering of debris flow events has to be expected with an ongoing climate change. Especially in cases of mountain torrents, where the catchments are characterized by both permafrost and glaciers. Sedimentary processes in the valley are already analysed by WELPMANN (2003) and STOFFEL et al. (2006), while OTTO et al. (2009) analysed the sediment storage of the Turtmanntal, directly south of the Rhonetal with a similar height as the Lötschental. SCHADEGG (2019) wrote his master thesis about a landslide above Ferden. Beside the local researches, the University of Bozen has an ongoing multiannual project called «GLORI - Glaciers to rivers sediment transfer in alpine basins» which analyses the processes of the sedimentary transfer on two basins in the southern Tirol (GLORI, 2018).

The year 2018 showed that the so called «Water Castle» Switzerland can be affected by longtime dry conditions. Even though the country is privileged by the topography and geology, the missing of glacier masses and the missing refilling of groundwater resources can impact the population in a severe way. Beside some exclusive hot years in the recent past, the all in all continuous increase of the global temperature changes the alpine environment significantly.

The processes of water and sediment availability in correlation to the glacier melt are multilayered and affect the local population in different ways. Cascading events can result in hazardous results. HUGGEL et al. (2005) developed an approach *«(...) to assess the maximum event magnitude and the influence of occurrence of glacial hazards* [ice avalanches, glacial lake outburst floods and debris

flows].» (ibid.:1068) in an alpine environment. The understanding about the occurrence and the size of processes is crucial for a changing landscape. The UN writes on their homepage: *«Water scarcity can mean scarcity in availability due to physical shortage, or scarcity in access due to the failure of institutions to ensure a regular supply or due to a lack of adequate infrastructure.»* (UN WATER, 2018). To be able to implement possible measures against a developing water scarcity, the susceptibility of the system and the system itself have to be understood. In regard of an assumed increase in sedimentary flux, the management of the water household is critical. As HAEBERLI et al. (2017) already discussed in their paper *«Increasing risks related to landslides from degrading permafrost into new lakes in deglaciated mountain ranges»*, future lakes, artificial or not, can be easily affected by various processes. B. Bellwald, head of the Fafleralp power plant corporation (KW Fafleralp AG) and partner of the power plant association in Blatten (Genossenschaft Elektrizitätswerk Blatten), told that the northern slope of the Bietschhorn ridge is more or less constant regarding debris flow activity, but the Petersgrat side reveals an increasing rate of debris flows which represents a rising problem for the power plants and the water reservoirs. Questions about hydroelectricity and water storage are directly influenced by sedimentary and glacial fluxes and have to be assessed in relation to each other.

1.2 Aim of the thesis

This thesis wants to investigate the impacts of glacier retreat onto sediment and water availability in the Lötschental in a widespread manner and wants to give an overview about the ongoing processes with a glimpse into the future.
We want to investigate the following research questions, split into two main sections:

- Water availability
  - What are the different contributors to the runoff of the Lonza river and how can they be quantified? How do glaciers influence the runoff?
  - How does the runoff change in future?
  - Is there a possibility of a developing water scarcity in the valley?

  The questions will be assessed with a developed model, based on the present measured runoff behavior of the main river Lonza (Chapter 3).
- Sediment availability
  - Where are the main sedimentary reservoirs? And how did they form?
  - How could they be triggered as mass flows and why?
  - Is an effect of decreasing permafrost visible or assumable?

  The sedimentary analysis are conducted on the south-eastern valley side (shadow side) and the required topographical informations are retrieved with photogrammetry (Chapter 4).

2 THE VALLEY

2.1 General situation

The Lötschental is the most eminent side and high valley north of the Rhonetal in the Canton Valais (WELPMANN, 2003: 16 & references therein). The north western ridge of the main valley is dominated by the glaciated Petersgrat, the border to the canton of Berne, while the south eastern ridge includes the nearly 3‘934 m high Bietschhorn. In total, the valley which covers around 145 km^2, also represents the catchment of the main river Lonza and is surrounded by nine peaks higher than 3‘500 m a.s.l. BÖRST (2006) separated the valley into three parts: a first narrow and short part in right angle to the Rhonetal (Lonza gorge), then a second south west to north east oriented 7 km wide main valley (residential zone), concluded in the third part by the merging of the northern and southern ridge in the north east at the Lötschenlücke (unoccupied zone), which represents a pass to the Aletsch region.

- Lonza gorge

  In Ferden the valley abruptly changes direction and turns southward which includes a change from the U-shaped valley into a steep and narrow Lonza gorge between Niwen (W) and Hogleifa (E). In this gorge, Lonza reveals an average slope of 10 % and the gorge opens just before Gampel at the bottom of the Rhonetal. At 1‘216 m a.s.l. Goppenstein is located in the middle of the gorge. It represents the infrastructural gate to the Lötschental, where the train station for personal transport and car shuttles ensures the connection to the Mittelland and to the Rhone valley, and where the only road enters the Lötschental. Goppenstein builds the Achilles‘ heel regarding natural hazards, and was already affected several times. It caused emergency supplies and evacuations by helicopter due to avalanches or debris flows.

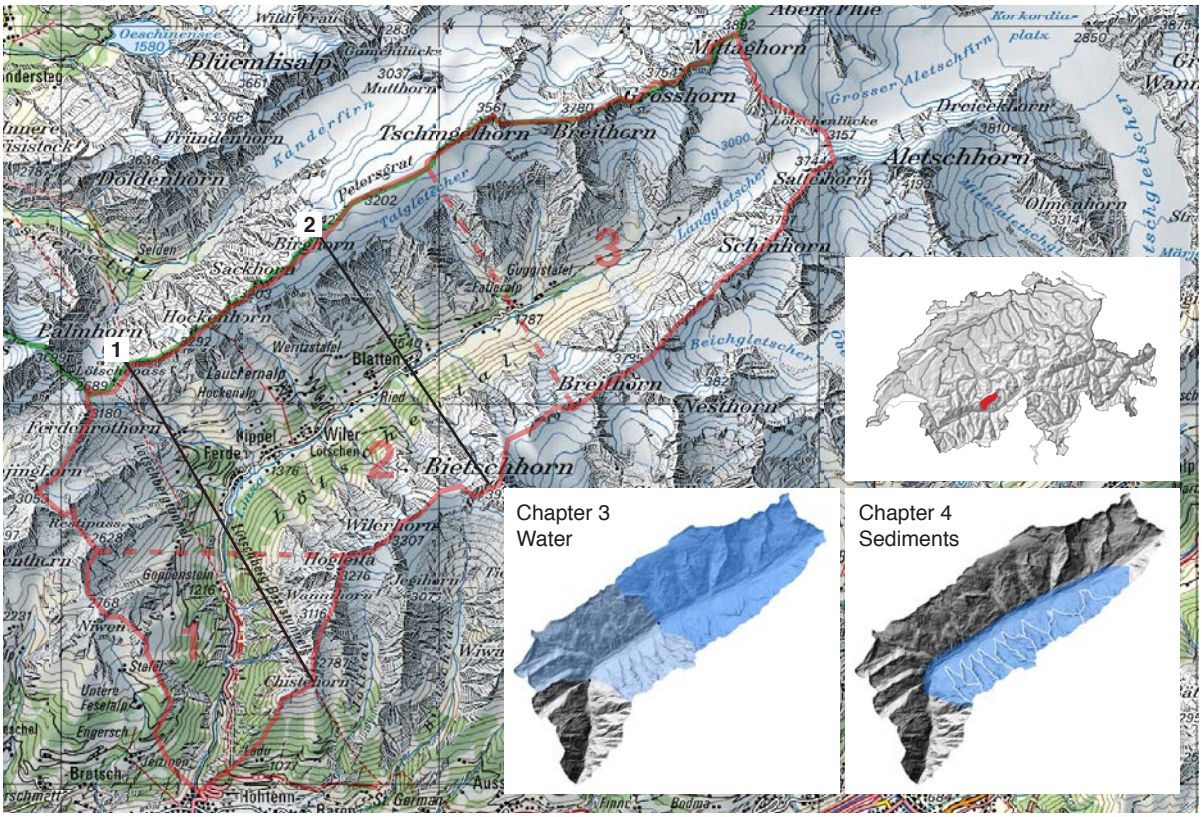

FIG. 03: Overview about the Lötschental (red outlined). The different sections of the research areas are shown. The colour grade for chapter 3 is based on two different catchments. The black lines illustrate the location of the cross sections of FIG. 07. (Source: SWISSTOPO, 2018a)

- Residential zone

  Between the two parallel mountain ridges in section two, the residential zone (WELPMANN, 2003: 16 & BÖRST, 2006: 40) reveals the permanent settlement of Blatten, followed by Wiler, Kippel and Ferden whereas every village also represents its own municipality. Additionally the hamlets of Ried, Weissenried and Eisten are also perennially occupied. The Lötschental hosts around 1‘500 residents, distributed on the different villages and hamlets.

- Unoccupied zone

  The upper third section (FIG. 03) between Lötschenlücke and the hamlet Fafleralp is sparsely vegetated and is dominated by periglacial processes. The Langgletscher which is flowing down from Lötschenlücke and which is laterally supported by Anengletscher characterizes the landscape. Lonza meanders from the preglacial zone at 2‘000 m a.s.l. through a gorge north of Grundsee to the Fafleralp. BÖRST (2006: 41) describes the area as *«(...) weitgehend anthropogen unbeeinflusste Wildnis.»*

The valley is meteorologically impacted by two different sections of Switzerland: by the southernly Valais with the Rhonetal and through the northerly input from western central Switzerland (HÄFELIN, 1955). Therefore the actual weather is based on both systems which congregate over the valley. In summer and fall convective low pressure and anticyclonic north wind conditions are present, while in winter and spring cyclonic west wind conditions dominate the weather. During summer convective weather systems predominate the valley (by 65.3 %) while during the rest of the year, convective and advective conditions are nearly balanced (BÖRST, 2006). Based on the orientation and the height of

the surrounding mountains, the valley is influenced by Lee effects originating from northwesterly and southeasterly wind systems. The effect is measured in lower rates of precipitation than it is measured in the surrounding (BÖRST, 2006 and references therein; RÖSSLER et al., 2013; SPREAFICO & WEINGARTNER, 2005).

The meteo station in Blatten, from which data of this thesis are taken for many aspects and is operated by MeteoSwiss, measured between 2002 and 2018 an average yearly temperature of +4.11 °C, with fluctuations from +2.8 °C (2005) up to +5.1 °C (2015) (METEOSWISS, 2019b). The three warmest years with averaged temperatures above 5 °C appeared within the last five years. The mean sunshine endurance between 2013 and 2018 is 126.4 hrs per year, with a peak of 218.36 hrs in August (maximum measured: 265.4 hrs in August 2015). The yearly mean precipitation sum between 2002 and 2018 is 1038.3 mm, whereas the year of 2018 (1205.6 mm) was the wettest since 2007 (1352.8 mm) (ibid.). In the valley the dominant advection condition in summer builds thunderstorms which lead to a short but heavy precipitation input, while during April and September a depression of rainfall is noted (BÖRST, 2006).

As FIG. 04 shows, no trend is visible regarding changes in precipitation or temperature patterns. Even if the variance is high (especially for the precipitation), the mean values seem to be stable.

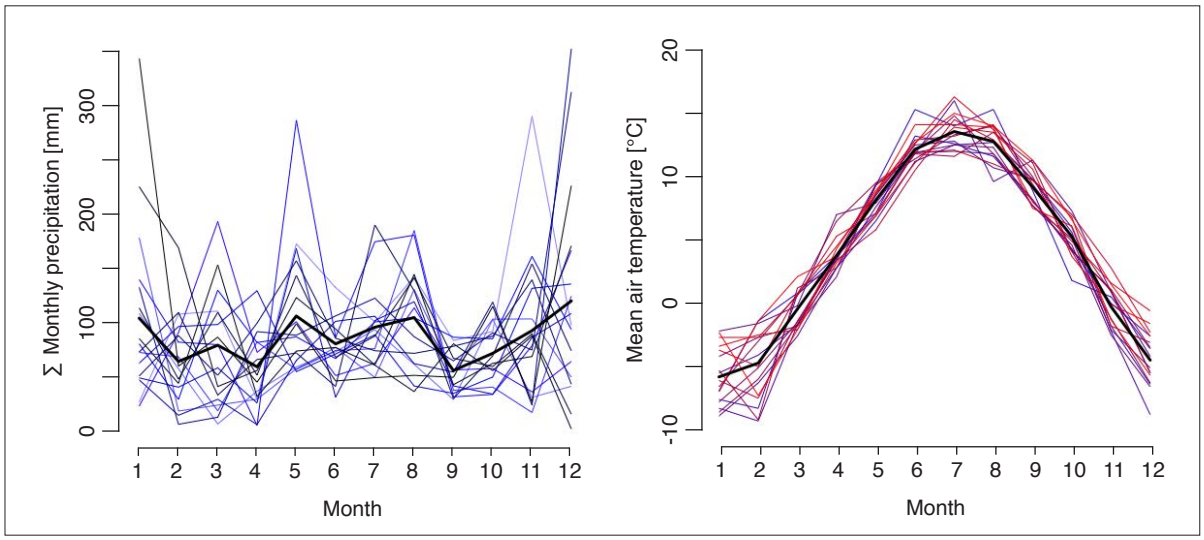

FIG. 04: Trend illustration from monthly mean data measured by BAFU and MeteoSwiss in Blatten (2002-2018). Left: Precipitation from dark (2018) to bright (2002), due to readability not illustated as barplots. Right: temperature from blue (2002) to red (2018). The thick black line represents the mean between 2002 and 2018. The colour change is not visible, because no trend is visible. The curves superimpose each other.
(Source: BAFU, 2019b & METEOSWISS, 2019b)

The southern Bietschhorn ridge shadows the valley widely, especially during the winter months with low solar radiation and a low solar path. This reveals huge local temperature differences and has an impact on the local wind systems. In summer, when the sun hits the measurement station in Blatten, the wind turns from north-east to south-west and represents a classical valley-wind system (FIG. 05). But it is also observed that the shaded side reveals more downwind while the warm side is heated and experiences thermal conditions. This effect presumably leads to a horizontal wind system spin, rolling inside the valley.

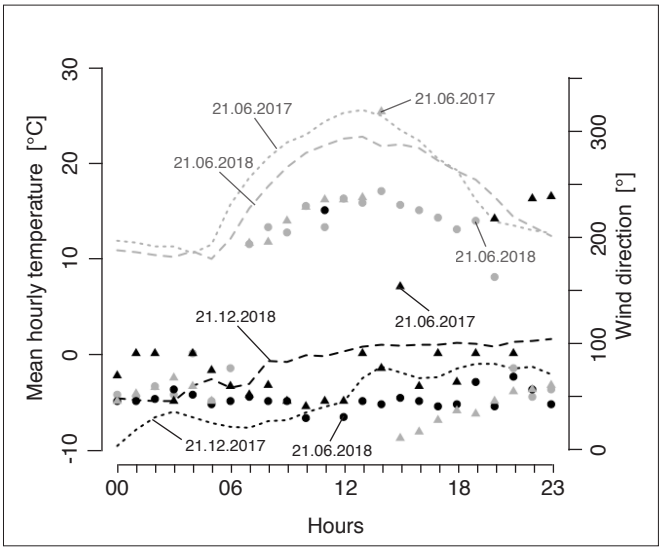

FIG. 05:
Illustrated are the wind (points) and the temperature (lines) pathways in Blatten in 2017 and 2018. Represented are the measurements of the summer solstice (21.06., grey) and the winter solstice (21.12., black). During the winter solstice, the station is shadowed and indicates mainly northeasterly winds. During the summer solstice the station experiences a transition from shadowed (by the Bietschhorn ridge) to sun exposed conditions at around 05:00 AM, including a change in wind direction.
(Source: METEOSWISS, 2019b)

2.2 Geology

Geologically the valley lies in the central Aaregranite and represents the weakness between the subunits of Gasterngranite in the north and the Bietschhorngranite (Central-Aaregranite) in the south. Enclosed are carbonic and mesozoic sediments (HÜGI et al., 1988) which are overprinted by metamorphosis and constitute the availability of small ore occurrences around Ferden and Goppenstein. The originally covering mesozoic sediments (Helvetic nappes) on top of the stratigraphy were shifted northwards and the sole remnants can be found as dark formations on the Hockenhorn, Elwerdätsch and the Rothörner (BÖRST, 2006). On the opposite southern ridge the highest summits (Bietschhorn, Breitlauihorn, Breithorn and Lonzahörner) are built out of the bright and massive Bietschhorngranite and reveal the sharp transition into the darker granitic gneisses on their steep north faces (FIG. 06). The dark rock with pleices of diverse biotite gneisses, amphibolites, pegmatite- and aplitlenses (sometimes also wired by aplitic-pegmatitic veins) is streaked by several bands of amphibolites which includes feldspar and mica (HÜGI et al., 1988; STECK, 1983).

FIG. 06: Photographs of geological phenomena. Left: A massive boulder found during the fieldwork (27.07.2018) in the Nästbach-catchment. It represents the granitic gneisses including plaices of biotite gneiss, amphibolites and small aplite lenses. Right: The transition between Bietschhorngranite and the darker granitic gneiss zone is visible on the north face of the whole Bietschhorn ridge (21.09.2018). (Source: own photographies)

Going from the southern ridge towards Petersgrat (FIG. 07), the amount of chlorite and sericite increases while the granitic proportion decreases until mainly biotite sericite gneisses and schists (including chlorite) are present. Those relatively soft gneisses and schists in the centre of the valley revealed nearly no erosional resistance and rivers as well as the glaciers deepened between the stable granitic shoulders into the surface. The slight asymmetry between the south faced Petersgrat slope (around 35°) and the north faced Bietschhorn slope (around 40°) can be explained with the steep inclination of the old crystalline units (BÖRST, 2006).

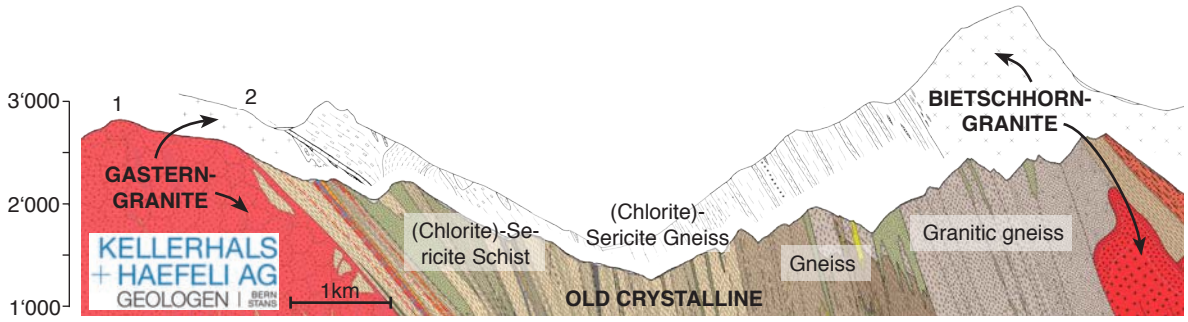

FIG. 07: Geological cross sections (location shown in FIG. 03) across the Lötschental. The lower coloured one is from the Lötschberg-Basistunnel and was provided by the geology company Kellerhals+Häfeli, while the upper illustration is from the geological atlas, written by HÜGI et al. (1988). The elevation is represented in m a.s.l.

2.3 Glacial history

Based on the main topic of this thesis, the glacial history of the Lötschental should be outlined on the existing researches. It is not the aim to draw a detailed picture even though the valley offers a huge amount of moraines and therefore potential dating options.

The glacial history is traceable from the late Pleniglacial. Around the last glacial maximum (LGM) at 24 ka BP (CLARK et al., 2009; IVY-OCHS 2015) the Lötschental was covered under a layer of up to one kilometre of ice (BINI et al., 2009) and the ancient Lötschental glacier flowed into the ice masses of the Rhone glacier (FIG. 08), which itself reached the Mittelland around Solothurn (JOUVET et al., 2017). At this time the Lötschental was shaped significantly by ice flow velocities of around 100 to 1'000 m per year and by a basal shear stress of approximately 1.0-1.5 bar to the ground (HAEBERLI & PENZ, 1985). The extension of the LGM is visible today at the «Trogschultern» on the shadow side at around 2'000 m a.s.l. (FIG. 09).

After the maximal extent of the Rhone glacier at approximately 21.1 ka BP (IVY-OCHS et al., 2004), the glacier retreated until 17 to 16 ka BP followed by the buildup of the Gschnitz moraines (IVY-OCHS, 2015; IVY-OCHS et al., 2006). In the Lötschental no frontal Gschnitz moraines are existing because the glacier tongue of the Langgletscher still reached the base of the Rhonetal (FIG. 09), but lost a lot of volume compared to the LGM (AUBERT, 1980). Based on the illustrations of AUBERT (1980) and visual interpretations of the valley, the glacial surface of Gschnitz was approximately at the altitude which is represented by todays treeline. The different hamlets of Faldum-, Lauchern- and Weritzalp (place name: Netzbord) are built on the assumed lateral moraines of the stadial (FIG. 09).

The remains of the following Daun stadial are elusive in the scope of this thesis, therefore no assumptions are made. But REITNER et al. (2016) describe, that the formerly known Daun stadial can be correlated with the currently used definition of the Egesen stadial. Therefore no Daun moraines could

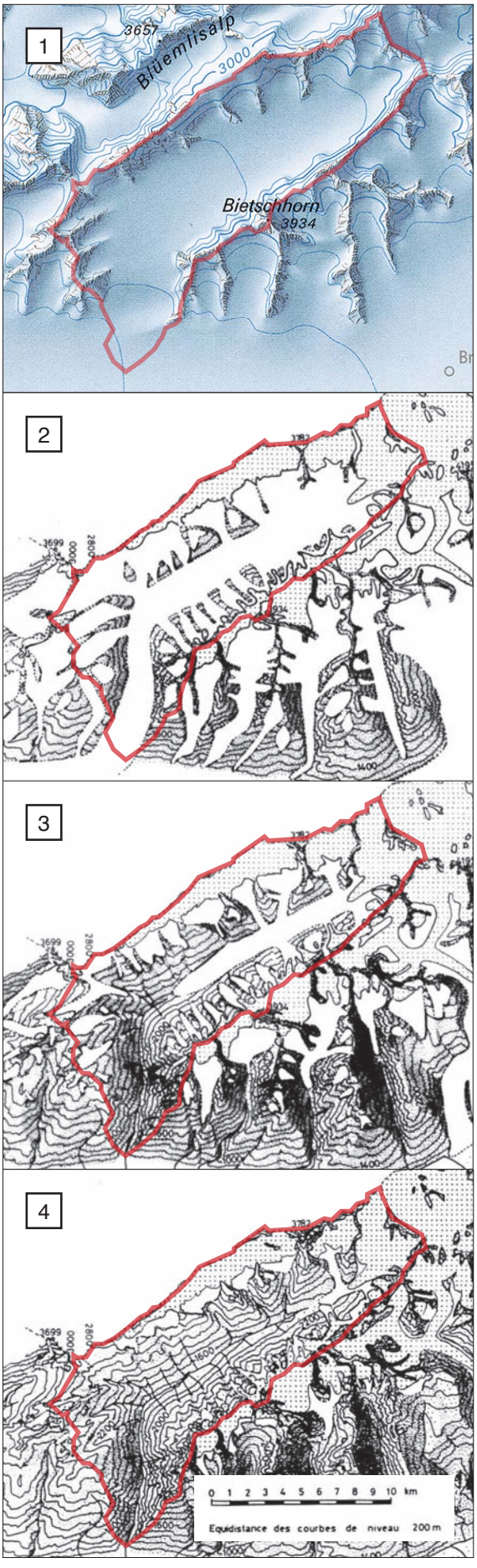

FIG. 08:
Sequence of glacier retreats and possible extensions in the Lötschental for four time steps:

1. LGM situation. Valley filled with ice. (BINI et al., 2009)
2. «Moraines basses»: Gschnitz stadial around Oldest Dryas with a frontal moraine around 600 m a.s.l. after AUBERT (1980: 55+61)
3. «Moraines intermédiaires»: assumed Daun (today: Egesen) stadial around Younger Dryas with a frontal moraine around 1350 m a.s.l. in the area of Kippel and Wiler. AUBERT (1980: 55+61)
4. «Moraines élevées»: glacial stage around 1850, post-glacial, with a frontal morain at 1800 m a.s.l. AUBERT (1980: 55+61)

The actual extension (dotted areas) refer to the extension around 1980. The red outline was inserted to visualize the extension of the valley.

be accessed. With the beginning of the Greenland Interstadial 1 (GI-1) around 14.6 ka BP, the Bølling-Allerød oscillations changed the climatic conditions until 12.9 ka BP dramatically (SEIERSTAD et al., 2005; RASMUSSEN et al., 2014). Within a short timespan, the temperatures climbed several degrees celsius and the glaciers retreated significantly with the result, *«that not only the main valleys* [of the alps] *but also the tributary valleys were ice-free at the beginning of the Bølling or just before.»* (IVY-OCHS, 2015: 305). Therefore the Lötschental was presumably ice free and the temperature dependency of the treeline (ELLENBERG & LEUSCHNER, 2010) changed the vegetation and appearance of the valley. BURGA (1988) reveals an interpretation of the development of the Central Alpine forest belt of Switzerland since the Late-Würmian, which is based on an already overwrought timescale. It is assumed, that the peak at 11‘000 ka BP (Figure 13 in BURGA, 1988) refers to the Bølling-Allerød period and therefore the treeline can be reconstructed to approximately 1‘600 m a.s.l. Even though the temperatures were in average higher than during the Oldest Dryas, the phase included two cold phases (Older Dryas and Intra Allerød Cold Phase IACP) each approximately 200 years in duration and with around 2 °C lower temperatures in comparison with the preceding setting (see APP-A1, page 109; RASMUSSEN et al., 2014). How those cold phases influenced the valley is out of the scope of this thesis. After the Allerød period, at 12.9 ka

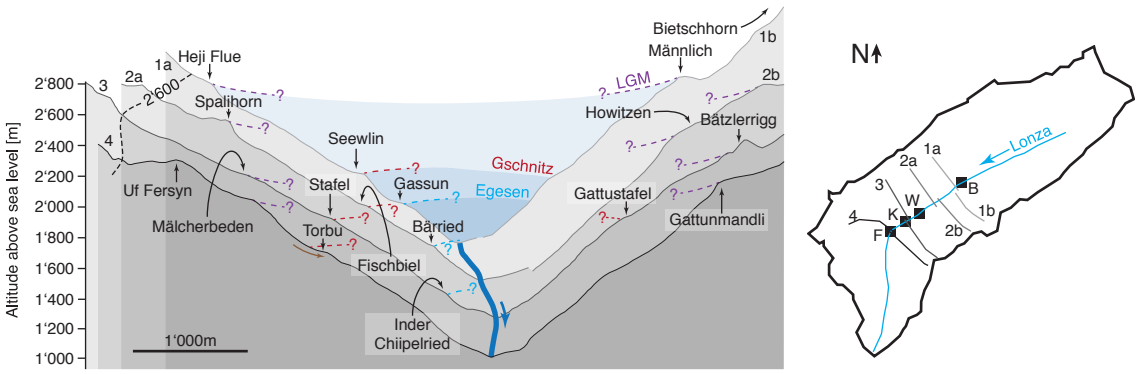

FIG. 09: Cross sections of the Lötschental, indicated are the assumed moraines of LGM, Gschnitz and Egesen. On cross section no. 4, no Egesen moraine is identifiable. The 2'600 m a.s.l. altitude acts as reference due to the scaling and shift of the different crosssections (indicated on top left). Due to the glacier advances, Egesen and Gschnitz are convex, while LGM is illustrated concave after BINI et al. (2009). (Source: own illustration based on SWISSTOPO, 2018a)

BP the Younger Dryas (YD) set in (ibid.: 17). The period, congruent with the Greenland Stadial 1 (GS-1), was shaped by lower temperatures similar to the average during the Oldest Dryas (APP-A1; HEIRI et al., 2014). It can be said, that *«(...) the interval was characterised by drier, more continental conditions (around 70% of modern precipitation), with a lowering of the mean annual temperature of 2.5-4 °C, the higher value affecting the drier central parts of the Alps.»* (VAN HUSEN, 1996: 117). The unstable climatic situation resulted in a series of glacier retreats and advances which built a sequence of moraines, defined as the Egesen stadial (KERSCHNER, 2009; MAISCH, 1987). The newly formed Langgletscher tongue reached the region of today's villages Kippel and Wiler (AUBERT, 1980) (FIG. 09). IVY-OCHS et al. (2008) write on page 567: *«(...) Egesen is defined as a series of morphologically fresh, steep-walled and often well-preserved moraines downvalley form the LIA moraines. The maximum Egesen advance is characterised by a clear morphological boundary (...). Two and sometimes three distinct groups of moraines can be distinguished.»* Even if for this thesis no specific geological research was undertaken, the remains of the frontal Egesen moraines are assumed to be found at around 1'600 m a.s.l. east of Wiler on the north (Rufiwald) and south (east of the apex of Wilerbach) flanks. On the north flank the lateral moraines can be followed until Faflerstaffel. They presumably build the terraces of the hamlets Bärried (1'635 m a.s.l) and Weissenried (1'705 m a.s.l.), followed by the terrace of Schwarzsee (1'860 m a.s.l.) between Blatten and Fafleralp and a nameless terrace below the Chrindellicke (north of Fafleralp at 1'995 m a.s.l) (FIG. 09).

With the beginning of the Holocene at 11.7 ka BP (RASMUSSEN et al., 2014: 17) a warmer and drier climate set in. The so-called Holocene Climate Optimum was based on a higher northern summer insolation which led to higher summer temperatures and therefore shorter glaciers (NUSSBAUMER et al., 2011). IVY-OCHS (2009) writes on page 2141: *«Glaciers were smaller than today for most of the time and forest growth was possible in areas that are presently ice covered. Glaciers advanced during a few short phases, the magnitude of the advance depending on the size of the glacier.»* The glaciers in the Lötschental were smaller than today and the response time was shortened down to years and decades (JOHANNESSON et al., 1989). The short-time climatic fluctuations based on other mechanisms could have led to severe glacier fluctuations in the valley (NUSSBAUMER et al., 2011). JOERIN et al (2006 & 2008) recognized at least 12 recession phases during the Holocene in the Swiss Alps with a duration of around 5'100 years in total. The glacier advances maximally reached the extension of the Little Ice Age

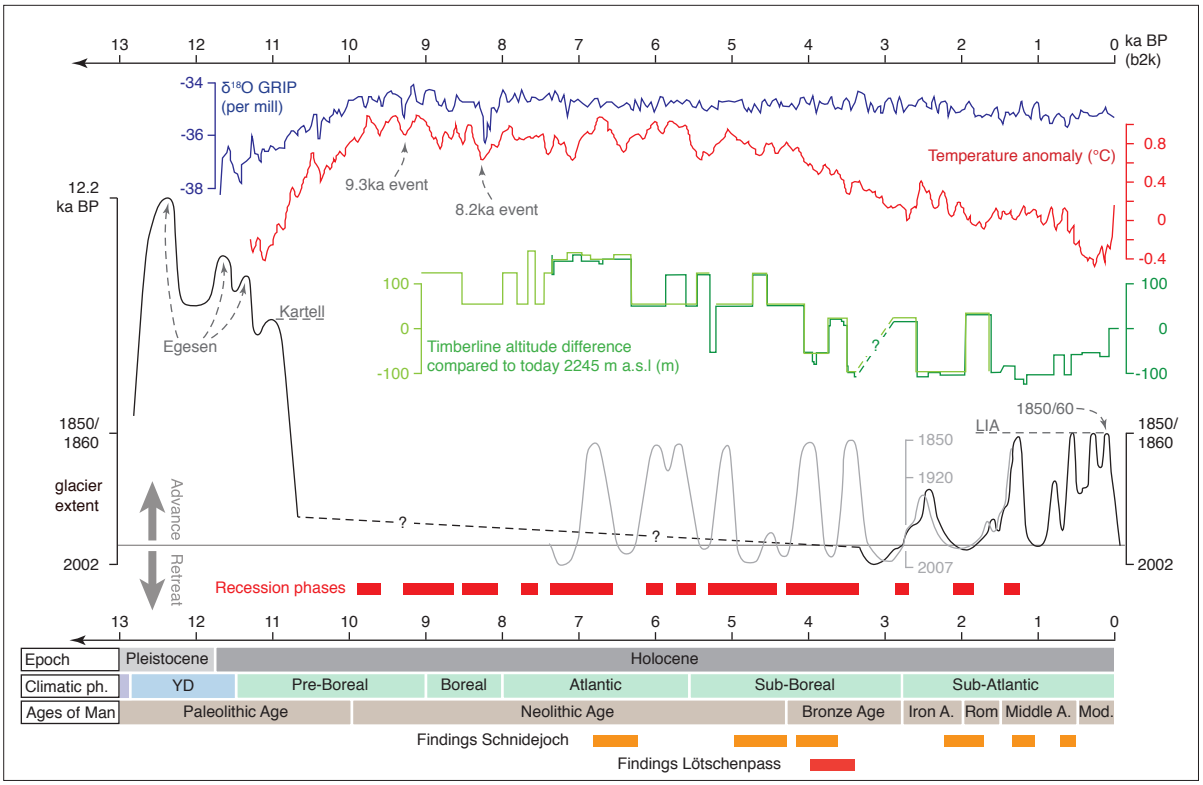

FIG. 10: Modified overview about the Holocene based on different sources. Shown is a correlation of the GRIP measurement (blue: UCPH, 2018), temperature (red: MARCOTT et al., 2013), timberline altitude (light green: NUSSBAUMER et al., 2011, dark green: NICOLUSSI et al., 2005), glacial extension (grey: NUSSBAUMER et al., 2011, black: IVY-OCHS, 2009), glacial recession phases (red: JOERIN et al., 2006) and the timeline (GEORGOPOULOU et al., 2015) regarding findings at different places (red: HAEBERLI et al., 1999, orange: GROSJEAN et al., 2007). Ph.: Phase, YD: Younger Dryas, A: Age.

(LIA) (IVY-OCHS, 2009). TINNER & THEURILLAT (2003) studied the uppermost timberline altitude between 9-3 ka BP at Lengi Egga (13 km distance to Blatten Lötschen, north of Belalp) and defined it to be 120-180 m higher than today at around 2‘500 m a.s.l., reaching up to the rocky terrain of todays valley. The Holocene is the period, wherein leftovers of human appearances were dated and which reveal a close relation of the alpine population to the glacial coverage.

Archaeological findings on the westerly lying Schnidejoch (33 km west of Blatten) and on the Lötschenpass during the summers of 2003 and 2017 (GROSJEAN et al., 2007; HAFNER, 2015) emphasizes the fluctuations of glacier extents «*which suggest that at the archaeological site this glacier* [Schnidejoch] *was smaller in 2003 than at any time during the past 5000 years.*» (GROSJEAN et al., 2007: 1) The latest findings at the Lötschenpass are not dated yet, but are assumed to originate from 3‘000 to 4‘000 BP latest (according to Werner Bellwald, 23.10.18).

After 3.3 ka BP *«(...) prolonged glacier advances became more frequent and periods of recession were shorter, leading finally to the LIA advances from the 14th century AD until 1850/60.»* (IVY-OCHS, 2009: 2144) The glaciers of the Lötschental and especially Langgletscher presumably advanced and culminated around 2.6 ka BP, 500-600 AD, 800-900 AD and 1‘100-1‘200 AD similar to Aletschgletscher (ibid.) (FIG. 10).

During the Roman climate optimum at 1‘500 BP humans settled in the valley and left back the oldest indications for constant occupation in the Lötschental (BELLWALD, W., 2009).

The LIA extent of the Langgletscher was presumably reached again in the 14th, 17th and 19th centuries (IVY-OCHS, 2009 & references therein). In 1850/60 the glaciers finally reached their last maximal ice

extent and began to retreat afterwards.

ZEMP (2006: 35 & references therein) described the recent glacier fluctuations between 1850 and 2003 as following: Since 1850 the general glacier retreat can be correlated to the warming trend during this period. He assumes *«(...) a negative winter precipitation anomaly (...) during the second half of the 19th century (...)»* as cause for the beginning retreat which was interrupted by *«(...) glacier advances in the 1890s, 1920s and 1970-1980s (...) and can be explained by earlier wetter and cooler periods with reduced sunshine duration and increased winter precipitation.»* Langgletscher followed the general trend and lost between 1888 and 2017 818 m length, 50 % of it since 1990 (GLAMOS, 2018) (FIG. 11/12).

FIG. 11: The tongue of Langgletscher with ten years difference. Captured and provided by Simon Oberli. (Source: GLETSCHERVERGLEICHE, 2019)

BELLWALD W. (2009) analysed the glaciers of the valley and showed, that between 1927 and 2005 the glaciated area shrunk about 28.8 % and lost around 0.44 km^3 ice volume between 1927 and 2003. He stated that the area loss is bigger for the small glaciers on the Bietschhorn ridge (-38 %) than for the big ice masses of the Petersgrat ridge (-30.24 %) and the Langgletscher (-23.21 %). The new Swiss Glacier Inventory SGI (FISCHER et al., 2014) mapped the glaciated areas of the alps for the year 2010 and revealed a glacier coverage of 20.25 km^2 for the Lötschental, which represents a coverage loss of 22.4 % during 5 years (BELLWALD, 2009: 26.09 km^2). The ongoing ice melt is also visible in other research topics: in 2012 and 2013, RUTISHAUSER et al. (2016) conducted helicopter-borne ground-penetrating radar investigations on Petersgrat, Anen- and Langgletscher. The data, which was provided by Dr. Andreas Bauder (Laboratory of Hydraulics, Hydrology and Glaciology VAW of ETH), reveal an ice thickness of around 100 m or less for Langgletscher and Petersgrat.

Today the main ice masses are located between 2‘800 and 3‘300m a.s.l and are dominated by Petersgrat and Anengletscher. The ongoing monitoring of the Langgletscher by GLAMOS (2018) shows the discussed glacier retreat, speeding up since the millennium (FIG. 12).

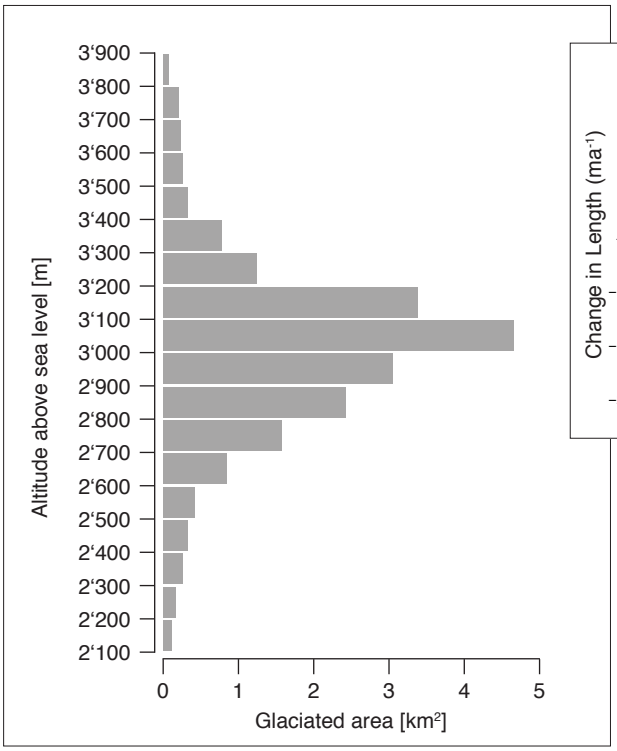

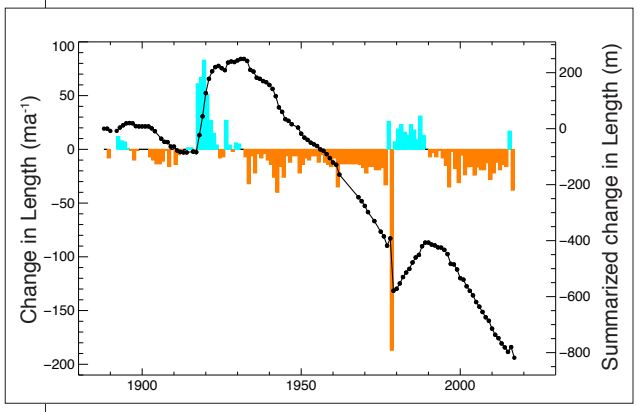

FIG. 12:

Left: Hypsography for the Lötschental, based on SGI 2010 (FISCHER et al., 2014). The main ice is located between 3‘000 and 3‘100 m a.s.l.
Up: Change in length of Langgletscher in the Lötschental. (modified after GLAMOS, 2018)

2.4 Geomorphology

The valley is strongly characterized by the past glaciations and is already described by several authors (e.g. HÜGI et al., 1988). Due to the sedimentary focus of this thesis, this chapter discusses the geomorphological processes on the valley floor.

The summits above 2‘500 m a.s.l., especially the Bietschhorn, were nunataks during the LGM and are therefore sharp-edged while lower areas are more smoothened by glacial erosion. The Lötschental itself acts as trough valley for the Rhonetal, but several fluvial overprinted smaller trough valleys can be found on the north and the south side of Lonza at altitudes of around 2‘200 m a.s.l. (BÖRST, 2006) wherein forms like the «Bätzlerfridhof» or «Blauseeli» reveal glacial cirques. The trough valleys on the south side drain through steep rocky gorges into Lonza, while the northern torrents reveal wider riverbeds, presumably due to the softer and more erodible underground (schists and quaternary sediments). The main valley floor (Ferden - Blatten) is relatively flat and reveals a general slope of 1.5° (direction south west) which is regurlarly interrupted by alluvial fans originating mostly from the southern through valleys. The fans reveal coalesced aggredation surfaces and the sizes differ between Kippel (Bätzlabach 0.1 km²) and Fafleralp (Loibinbach 0.8 km²). Between Ferden and Kippel, the Gitzibach reveals practically no fan but is surrounded by two plateaus («Chastel» opposite of Ferden and «Biel» opposite of Kippel). Additional plateaus can be assumed on the north side of the valley, represented by the village of Kippel (1‘369 m a.s.l). Without further geological research it is assumed that those terraces are remnants of a former higher fluvial plane (lake or river bed). Because the incision of Lonza into the terraces begins around the fan of Tännerbach and the highest terraces are around the same altitude, it can be assumed that the blockage led to a former sediment catch basin in the

Lötschental, which extended up to Tännera, sedimenting relatively flat areas. The smaller terraces represent several repetitions of such occlusions, preventing Lonza of eroding into the underlying ground (sediment or bedrock). During the Bølling-Allerød oscillations, the glacier retreated significantly (see chapter 2.3) and gave way to erosive processes in the whole valley (SCAPOZZA, 2016). It is possible that during this period a valley damming around Goppenstein could have taken place (FIG. 13). As AUBERT (1980) wrote and as it is assumed based on field observations, the former Langgletscher advanced and reached again the area of Wiler and Kippel during the following Egesen stadial, removing all sedimentary deposits of the valley higher up. Because the fans of «Bätzlabach», «Wilerbach» and «Tännerbach» have flat areas around themselves («Elsigen», «Nidru Mattä» and «Obru Mattä»), they had to be coexistent or need to be younger regarding the valley blockage. As the Egesen extent is lower in altitude than the the former upper sediment plane indications at Tännerbach, the lake and the debris fans need to be younger than the lowest Egesen stadial (discrepancy marked as black circle in FIG. 13), dating back to 12-11 ka BP.

To locate the occlusion which assumably dammed Lonza, the terraces can be followed to the most southern point at «Fischertellä», south of today's Ferden dam. This actually proves the possibility of occlusion events in the steep Lonza gorge, probably originating from areas like the «Egguwald» and «Wandschluichen» south of Ferden. It is not in the scope of this work to give a detailed analysis about the development of the alluvial fans and the given assumptions are based on interpretations and field observations. It would need further geological investigations to reveal more concrete results.

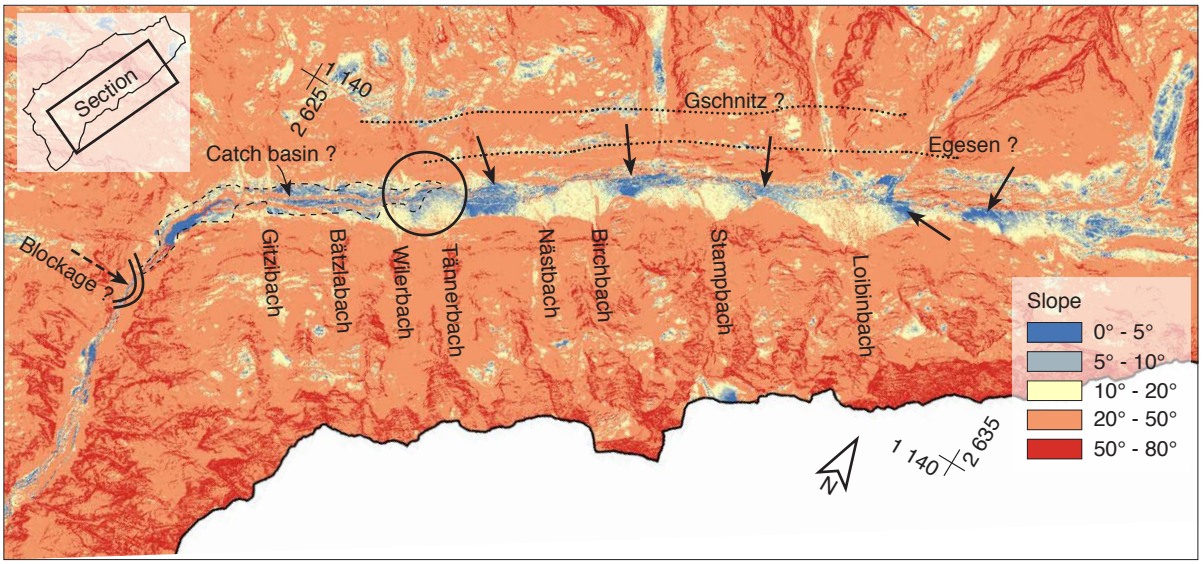

FIG. 13: Slope map of the south-western part of the Lötschental. The arrows indicate planes behind debris cones. (Source: SWISSTOPO, 2018a)

Apart from the fan ages, nearly every alluvial fan is in contact with a plane on the hydrological upper direction (marked with arrows in FIG. 13). It is assumed that every plateau represents a former small lake or aggradation plane, filled with fluvial sediments transported by the main river Lonza. A debris flow event on the 9th of August 2009 has shown, that even a relatively huge mass input can not stop the main river Lonza adequately to cause a long time blockage (FIG. 14). Within 45 minutes the river managed to cut through the sediment (GEOPLAN AG, 2010). Damming situations leading to the now existing planes, had to be more massive. It is not clear if the planes were built based on a single blockage event or step by step through different smaller occlusion. Even if there were several small events, the sedi-

FIG. 14: Occlusion of the main river Lonza by a debris flow of Birchbach on the 9th of August 2009. (Source: Lukas Kalbermatten)

mentary input needed to be very high during a short time to be able to dam the river. DEBRET et al. (2010: 2192) analysed Lake Le Bourget (French Alps) and they could reveal a higher sedimentation rate of 5.5 mm/a during the late Pleistocene and early Holocene until 10 ka, going back to 1mm/a until ca 4 ka (FIG. 15). Afterwards the rates increased to nearly 3 mm/a before falling again to 1 mm/a in the modern ages. GIGUET-COVEX et al. (2011) made a similar research on Lake Anterne (north-east of Lake Le Bourget and 25 km south-west of Martigny) and concluded a similar picture with a stronger increase in the past 5 ka. Interesting are the correlations between higher sedimentation rates and retreated glacier tongue at 5.3, 3 and 2 ka BP (shaded in FIG. 15). Assumed that the sedimentation pattern in the central alps was throughout the same, the researches by DEBRET et al. (2010) and CIGUET-COVEX et al. (2011) lead to the question which of those events could have triggered the occlusions in the Lötschental. Based on the preceding argumentation it has to be assumed that the fans and the correlated fluvial planes in the Lötschental originate from the deglaciation phase directly after the Egesen stadial. As SCAPOZZA (2016) based on JORDA & ROSIQUE (1994) writes the phase *«probably corresponds to the Grande phase d'éboulisation postglaciaire (litt. «Big phase of postglacial erosion») (...)* [which] *is characterising the long period of enhanced sediment transfer following the deglaciation. During this*

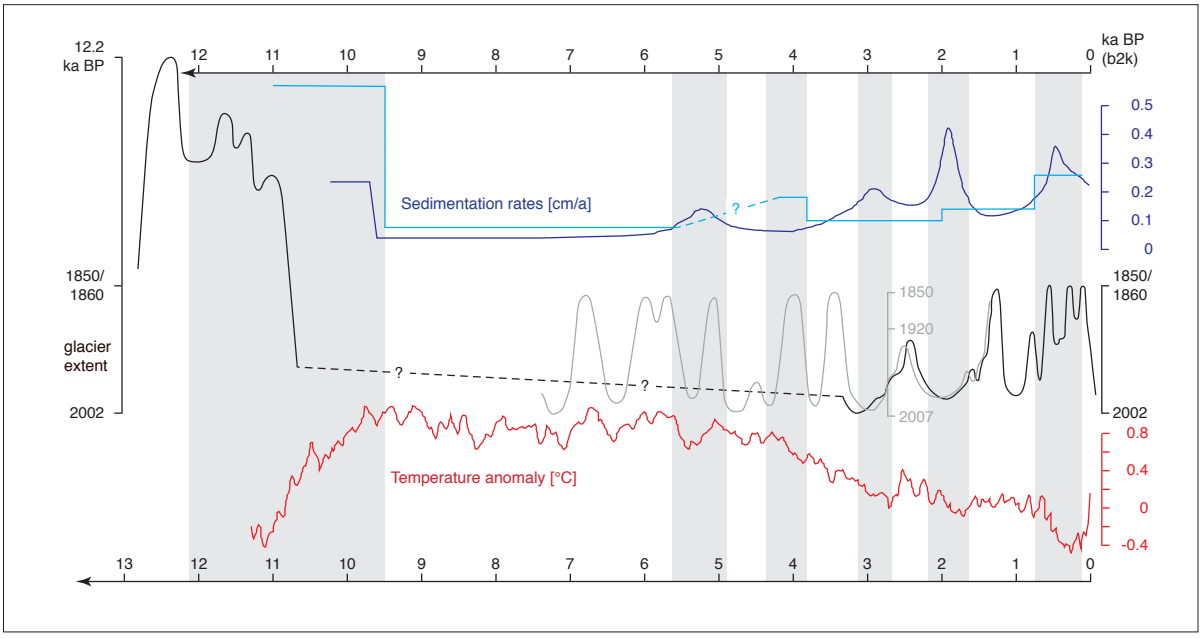

FIG. 15: Modified overview based on FIG. 11 including data of sedimentation rates (cm/a) by DEBRET et al., 2010 (light blue) and CIGUET-COVEX et al., 2011 (dark blue). The shadowed areas highlight periods with increased sedimentation rates. They can be correlated vaguely with retreating glaciers and temperature changes.

second phase (...) erosion (...) formed the main part of periglacial talus slopes and (...) released deposits that will constitute intact rock glaciers in the followings millennia.» Because of the glacial periods and the reciprocating glacier movement during the Egesen stadial, a lot of sediment was available and was transported fast. During the Mid-Holocene climate optimum 9.5-6.3 ka BP (BURGA et al., 2001) the activity of the fans presumably decreased and reactivated around 6 ka with a lower intensity.
HÜGI et al. (1988: 44) writes in the geological description of the valley, that Lonza transports a sedimentary fraction of 0.03 mm/a today, which is low compared to the overall picture of DIXON et al. (2016) with a calculated erosion rate of 0.17-0.24 mm/a for the central alps. WITTMANN et al. (2007: 6) however measured cosmogenic nuclide-derived denudation rates and retrieved an actual value of 1.28±0.32 mm/a for the Lötschental.
During the implementation of a geothermal heating, a hole was drilled into the alluvial fan of Birchbach at 2‘629‘113.0 / 1‘140‘851.9 which reached massive bedrock in 78 m depth (according to Elmar Ebener, 03.07.2018 / FIG. 16). Because of the proximity to the northern bedrock formations on the surface (in 90 m distance), it is assumed that the depth reveals approximately the deepest point of the cross section. Based on a simplified volume calculation of the Birchbach fan (35 Mio. m^3) with an applied time span of 10 ka (see FIG. 15), a sedimentation rate of 0.14 cm/a was calculated which supports the assumption, that the fan is estimated to be as old as the Egesen stadium.

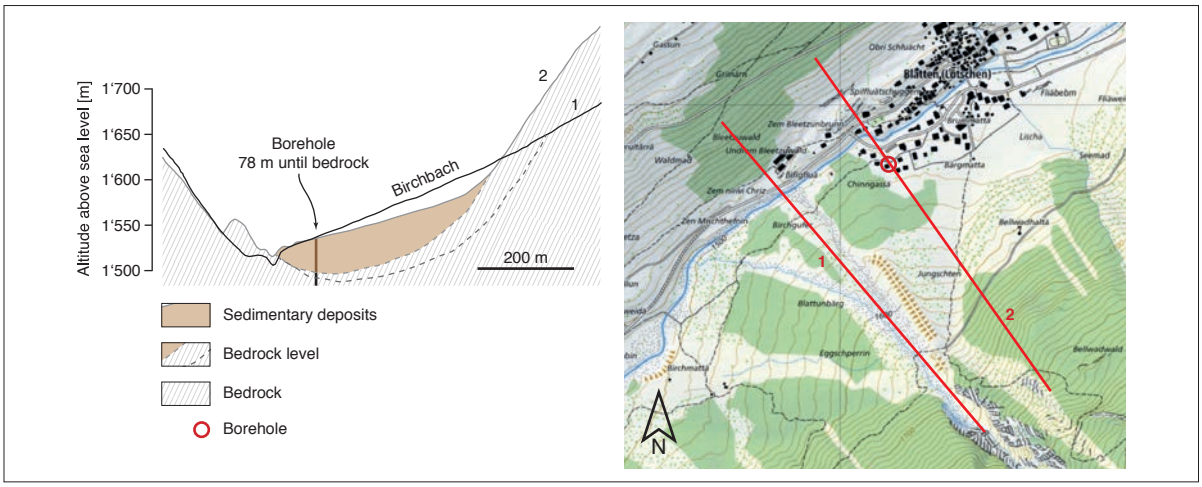

FIG. 16: Assumed situation on the Birchbach fan, based on two cross sections including one borehole. (Source: own illustration)

But the alluvial fans and erosional processes are not only built on debris flows, also avalanches transport high percentages of sedimentary fractions. STOFFEL et al. (2006) dendrochronologically analysed the Birchbach debris fan and retrieved patches from different ages on the fan. The north-eastern forest, between Blatten and the Birchbach channel, began to grow around 1870, while the south-western forest grew from 1920 on. The areas were mainly influenced by avalanche activity and not by debris flows, but every catchment reveals its own specific and mixed processes. In the early spring of 2018 the avalanches of Birchbach and Tännerbach transported huge amounts of snow. Even though the catchments are directly beneath each other, the Tännerbach avalanche included more debris (and boulders with a volume up to 30 m^3) than the Birchbach avalanche (FIG. 17). Therefore the processes are manifold and superimpose each other.
The processes endanger the local inhabitants and infrastructure. Different measures are already implemented to dam, hinder or deflect possible debris flows and avalanches. Therefore channels, basins

and dams guide the mass flows in specific directions. Despite the already applied measures, the existing artificial structures like roads are endangered by a remaining risk. If a mass flow is leaving the guidance, it could result in large deposits what is normally followed by high costs for reconstruction.

FIG. 17: Comparison of debris content of the Tännerbach avalanche (left) and the Birchbach avalanche (right) on the 13th of May 2018. View downwards. (Source: own photographies)

2.5 Hydrology

The Lötschental also represents the catchment of Lonza which is supported by over 27 lateral torrents flowing down in regular intervals. Based on the given geology with little sedimentary backfilling in the valley floor, nearly all the water is directly drained and a groundwater body is nearly not existent (HADES, 2018).

The glaciers of the valley roughly separate the catchment in an upper glaciated and a lower non-glaciated area. Those sections are measured by the stations of BAFU in Blatten (catchment BLA) and by EnAlpin which operates the hydroelectric power plant in Ferden (catchment FER) (FIG. 18). While in the upper section an «a- to b-glaciaire» regime is measured, the lower part is described as «a- to b-glacio-nival» (PFAUNDLER & ZAPPA, 2002; SCHÜRCH et al., 2010). WEHREN et al. (2010) writes on page 36, that the regimes *«(...) differ primarily in terms of the flow characteristics during the months of May to September, i.e. the period during which ice and snow are melting (...). Discharges in May and June are largely dictated by snowmelt, while those in the July to September period are influenced by glacier melt.»* The difference in the regime is also visible in the mean annual runoff which reveals over 1‘600 mm above Blatten and 1‘100-1‘200 mm below Blatten (SCHÄDLER & WEINGARTNER, 2002).

Based on the monthly mean values between 2013 and 2018, FER reaches its maximum in June with a peak at 17.6 m^3/s, while BLA peaks in July with 12.4 m^3/s (FIG. 18). As WEHREN et al. (2010) writes, the differences are caused by dissimilar percentages of glaciated and snow covered areas. The catchment of BLA is covered by 18.9 km^2 ice, whereas FER has only 1.34 km^2 more glaciated area - however FER is nearly twice as big as BLA.

The quantity of rivers and runoff volumes is predestined for the construction of small hydroelectric power plants and therefore, several systems have been built in the last years. Due to the steep slopes

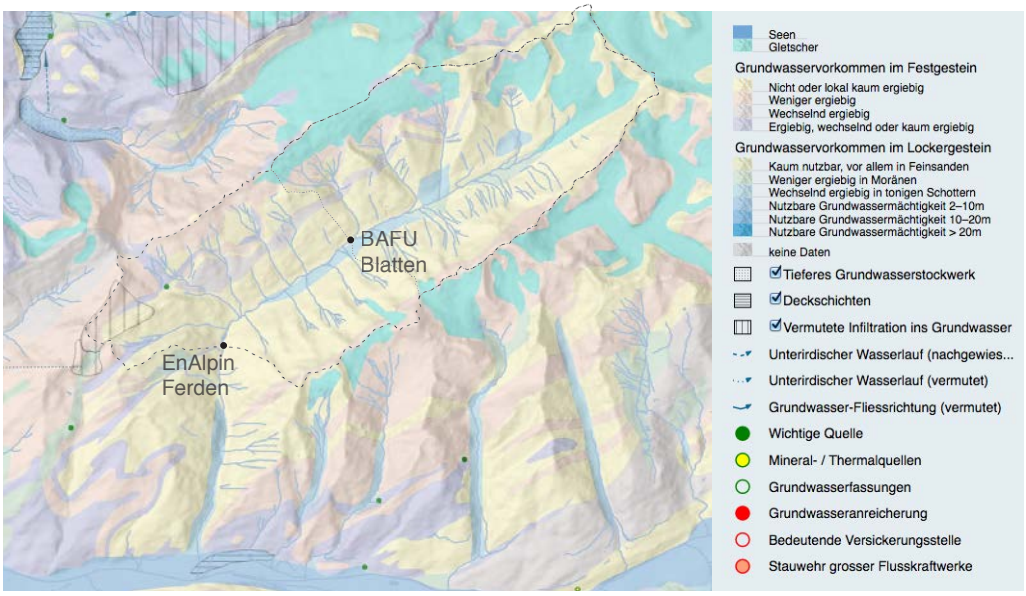

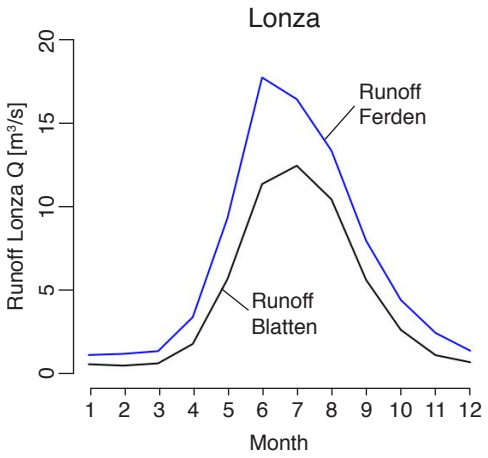

Regime	a-glaciaire	b-glaciaire	a-glacio-nival	b-glacio-nival
	Jan Jun Dec	Jan Jun Dec	Jan Jun Dec	Jan Jun Dec
Rank	1. July 2. August 3. June 4. September	1. July 2. August 3. June 4. September	1. July 2. June 3. August 4. May	1. June 2. July 3. August 4. May
Cv (Jun)	21	21	16	17
Cv (Jul)	11	13	14	21
Basin characteristics	mA >2400 Gla ≥36	mA >2100 Gla 22–35.9	mA >2400 Gla 12–21.9	mA 1900–2300 Gla 6–11.9

Rank: Based on mean monthly flow [m^3/s] mA: Mean altitude [m asl]
Cv: Coefficient of variation % Gla: Glaciation ratio %

FIG. 18: On top: the Lötschental as epresented on the HADES platform, possible groundwater is neglectable (modified after HADES, 2018). On the bottom: the mean monthly runoff of Lonza is pictured. It is measured in Blatten and Ferden between 2013 and 2018 and compared to the given fluvial regimes. (Source: BAFU, 2019b; EnAlpin AG, 2018; WEHREN et al., 2010)

of the south side in correlation with avalanches and debris flows, all power plants are located along the Lonza or on the northern tributary torrents. For consumption purposes the water of springs is also collected on the southern slope of Petersgrat. It is distributed via the water network (FIG. 19) to the different consumers for domestic purposes, agriculture and in winter for snow production.

In the last years the valley implemented an automatic surveillance water system which collects all data about inflow, outflow and usage of the springs and reservoirs. While the system of Kippel and Wiler is already running since two years, Ferden (June) and Blatten (November) are connected since 2018 (FIG. 20). Therefore the database for detailed analysis is incomplete. Old data about the reservoirs and springs are not available.

Based on the given data, today the consumption is multiple times covered by the reservoir inflow (FIG. 20). But the usage varies significantly between the municipalities (TAB. 01) and is with a mean of 948 litre well above the Swiss average of 162 litre per day and person (WWF, 2012: 7). The water consumption increases during summer and reaches the maximum around July. It is assumed that tourism

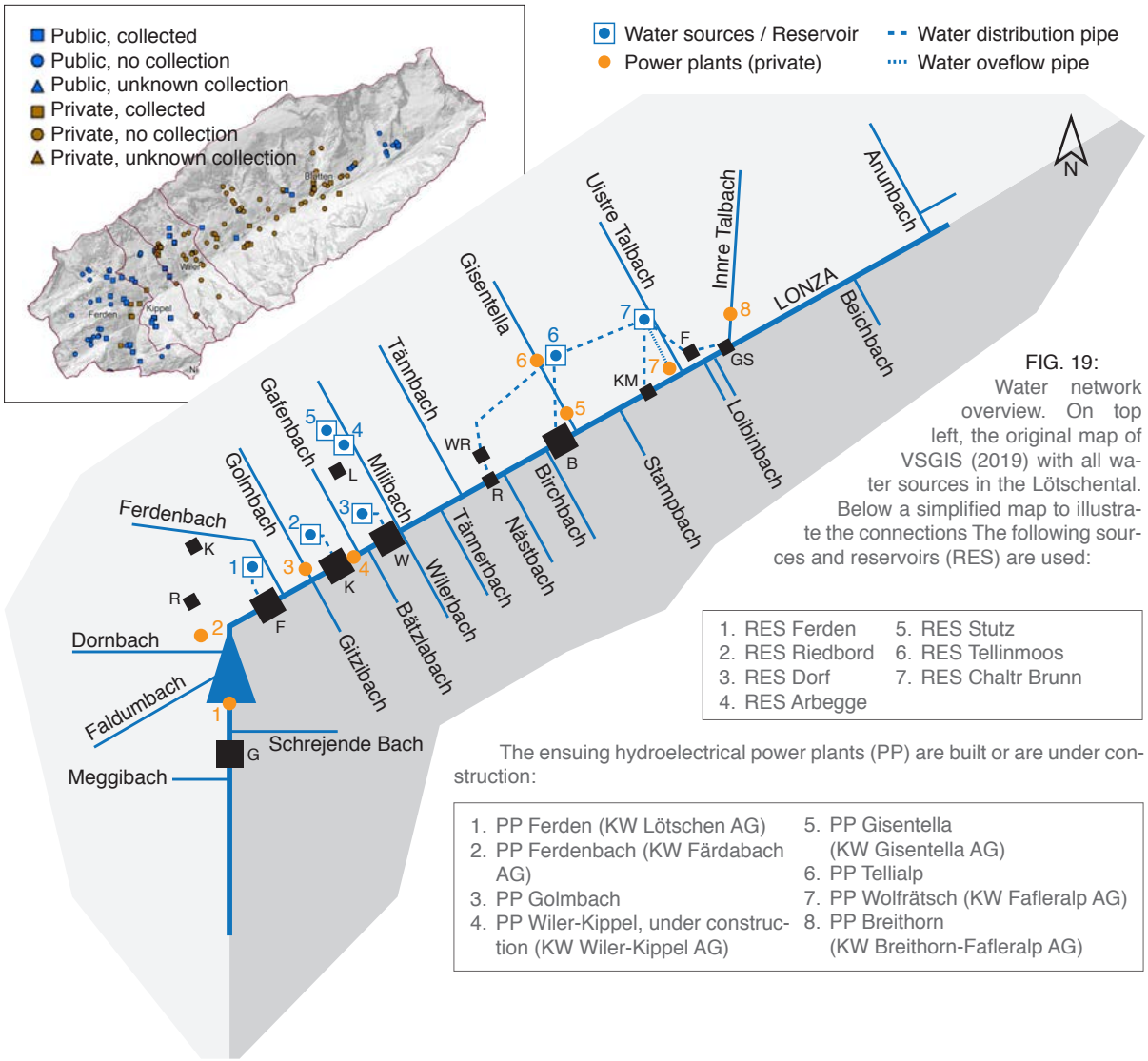

FIG. 19: Water network overview. On top left, the original map of VSGIS (2019) with all water sources in the Lötschental. Below a simplified map to illustrate the connections The following sources and reservoirs (RES) are used:

1. RES Ferden
2. RES Riedbord
3. RES Dorf
4. RES Arbegge
5. RES Stutz
6. RES Tellinmoos
7. RES Chaltr Brunn

The ensuing hydroelectrical power plants (PP) are built or are under construction:

1. PP Ferden (KW Lötschen AG)
2. PP Ferdenbach (KW Färdabach AG)
3. PP Golmbach
4. PP Wiler-Kippel, under construction (KW Wiler-Kippel AG)
5. PP Gisentella (KW Gisentella AG)
6. PP Tellialp
7. PP Wolfrätsch (KW Fafleralp AG)
8. PP Breithorn (KW Breithorn-Fafleralp AG)

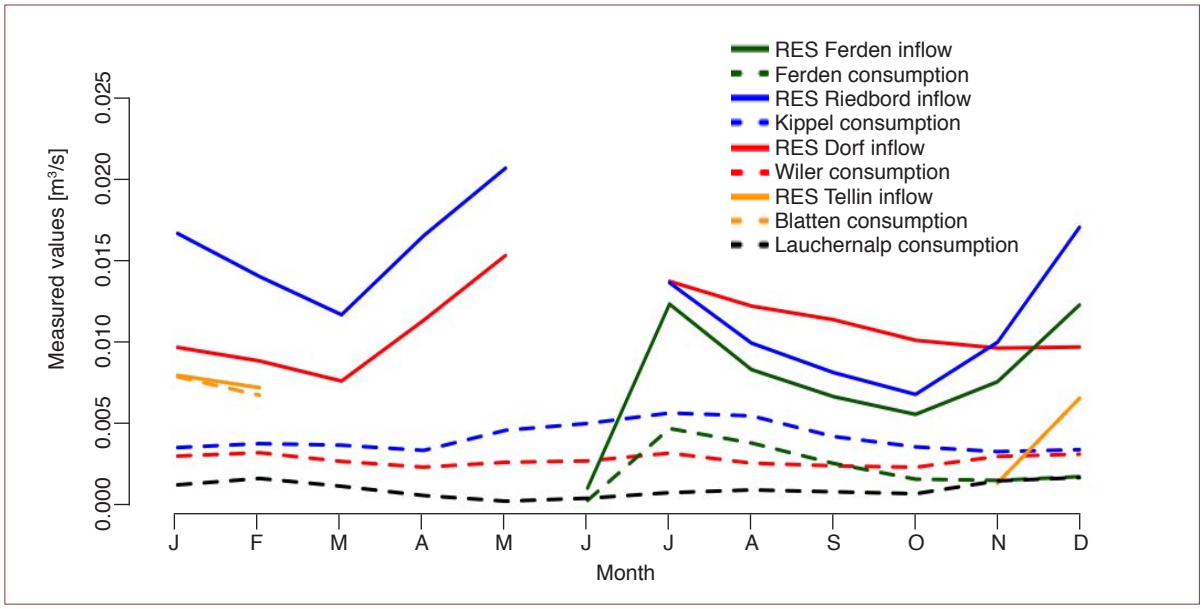

FIG. 20: Measured values of reservoir inflows and the consumption of the municipalities. For this study the ski resort Lauchernalp is only of interest regarding the water consumption, therefore no respective reservoir is illustrated. In June no inflow data of Kippel and Wiler was measured. Ferden got onto the system in June, Blatten in November 2018. January and February measurements of Blatten are already from 2019. (Source: municipalities)

TAB. 01: Overview about the water consumption of the municipalities. (Source: municipalities)

Municipality	Inhabitants (2008)	∑ yearly water consumption [m³]	Consumption per inhabitant & day [l]
Ferden	277	41‘811 (Jul-Dec)	820
Kippel	374	129‘232	946
Wiler	550	86‘160	429
Blatten	317	55‘995 (Dec-Feb)	1‘962

and water use for agriculture lead to the higher values. For the winter ski resort Lauchernalp, the consumption reaches its maximum in February and decreases until May, based on the seasonality of the inhabitation. The overall high water consumption of the valley can be explained with an old leaking water distribution system (according to Daniel Siegen, 05.10.2018) and several wells per village which are running nearly throughout the whole year. Additionally, it is common in wooden houses to let the water running through the winter months to prevent freezing conduits (according to Werner Bellwald, 07.06.2018). The tourism with 194‘000 overnight stays in 2014 (KANTON WALLIS, 2016) also increases the consumption, especially in winter and in summer.

How the springs are fed and how the parameters (precipitation, snow melt, glacier melt and evapotranspiration) are composed for each catchment is not specifically known. Based on the measured data of the surveillance system, the graphs show a peak around Mai or June with a decrease until winter (October-March) and with an increase afterwards (FIG. 20). The relatively flat characteristic and the peak in early summer of the reservoir inputs of Ferden, Kippel and Wiler is interpreted as nival runoff regime which is dominated by snowmelt. For the reservoir of Blatten not enough data is available to make an assumption.

Because the water collections are near mountain torrents, the torrents are assumed to reflect the water input relatively into the reservoir. This assumption is supported by the comparison between the torrents and the respective reservoir inputs (FIG. 20/21). The respective runoffs (modelled by the companies and measured) show big differences in behaviour (FIG. 21). While the runoff of all investigated rivers begins to increase slowly in March, Faldum-, Ferden- and Dornbach reveal a runoff with flatter curve

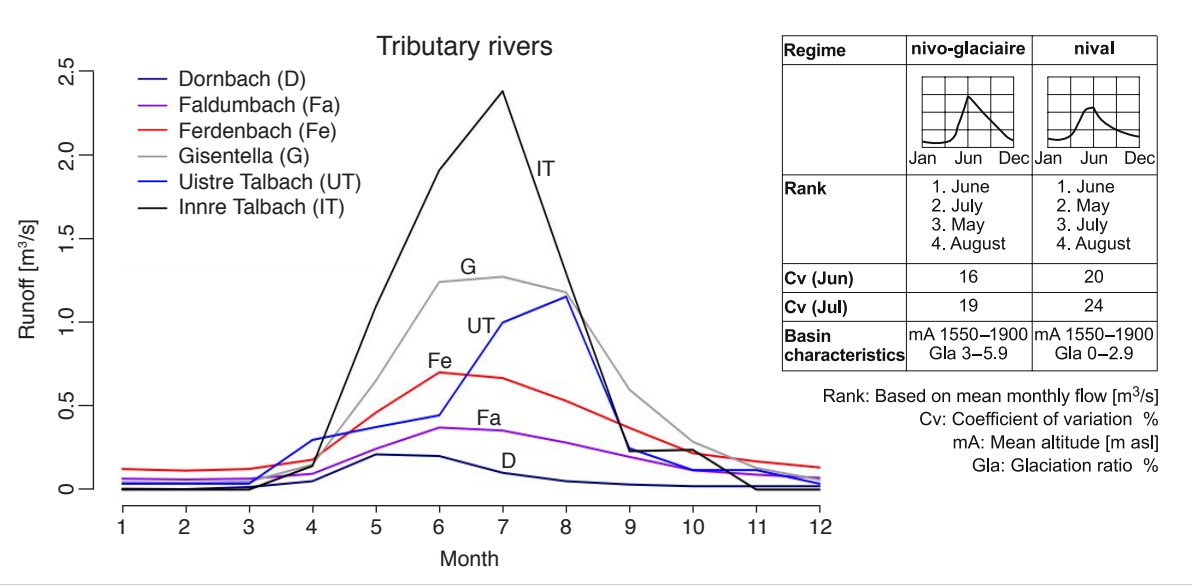

FIG. 21: Mean monthly runoff of different tributay torrents of the northern side. (Source: SRP AG, 2008; EnAlpin AG 2018; WEHREN et al., 2010)

than Uistre und Innre Talbach. While the Innre Talbach increases relatively stable from nearly no runoff up to 2.38 m^3/s in July, the Uistre Talbach shows a stepped curve with an intermediate hold from April to June at around 0.37 m^3/s, followed by a jump up to 1.15 m^3/s in August and a stepped decrease until November. The stepped runoff curve (SRP AG, 2008: 6) implies an external influence which was not rectifiable. Based on the overall similarity of the catchments, it is assumed that Uistre and Innre Talbach reveal a more or less similar runoff pattern. Hence, the runoff during the summer months is cut off by the increased water consumption of Blatten.

Dornbach reveals an increase until May (0.21 m^3/s) and a decrease afterwards until October. Faldum- and Ferdenbach show a similar curve with differences in the runoff volume. Both torrents increase in runoff volume until June (Faldumbach: 0.37 m^3/s, Ferdenbach: 0.70 m^3/s), followed by a long a constant decrease until December. Gisentella increase in runoff until June and stays relatively stable until August at 1.2 m^3/s, followed by a slow decrease until December.

Based on the runoff-patterns, Faldum-, Ferden- and Dornbach reveal a nival runoff-regime, while Uistre (and the Innre) Talbach is nivo-glacial (ibid.) and Gisentella glacio-nival dominated.

3 WATER

3.1 Study area

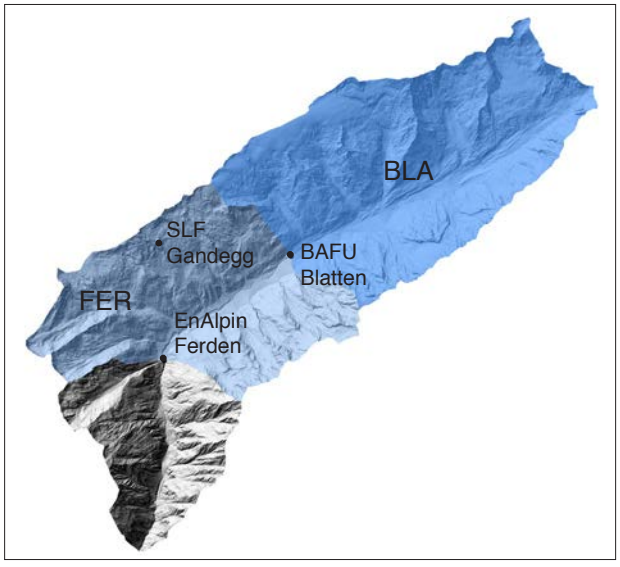

FIG. 22: Overview about the analysed catchments in the Lötschental. (Source: SWISSTOPO, 2018a)

The research area is based on the two catchments of FER and BLA (FIG. 22).

«BLA» describes the catchment of the measurement station of the Federal Office of Environment (BAFU) of the main river Lonza at Blatten (77.38 km^2, 48 % of the valley area). «FER» covers the valley until the Ferden dam, including the catchment BLA and 82 % of the total valley surface (131.78 km^2). The Ferden dam is operated by EnAlpin AG and reveals a barrier for the main river Lonza. Due to the delimitation of the catchments, BLA and FER reveal suitable areas for hydrological modellings.

The meteorological station of the Institute for Snow and Avalanche Research SLF is located at Gandegg (2'710 m a.s.l.) and will be used as reference for temperature and snow calculations.

3.2 Data and methods

3.2.1 The model system

To calculate the water availability in the Lötschental a simplified model (modified after WULF et al., 2016: 153) with a monthly resolution is applied:

$$Q_{Out} = M + P_{Rain} - ETc \quad (1)$$

$$M = Sm + Gm \quad (2)$$

The output of the system (Q_{Out}) is based on the different input parameters snow melt (Sm), glacier melt (Gm) and rain (P_{Rain}) while evapotranspiration (ETc) describes the only system loss. Based on HADES (2018) the valley reveals only a small quantity of possible groundwater existence (FIG. 18). It is assumed that the groundwater quantity is negligible small or inexistent. Even if some amounts of water will infiltrate the upper layer of the soil, the flowing water is considered to behave as direct surface runoff. The proportions into the values of Gm, Sm and P_{Rain} are unknown and therefore the model (FIG. 23) reflects a process where the input values have to be calculated out of the given data. Hence, the model is separated into the four different main parameters «Snow», «Evapotranspiration»,«Rain» and «Glacier» which are explained in the following chapters. «Snow» and «Rain» are summarized as «Precipitation».

Due to the fast changing behaviour of precipitation in an alpine environment, including variously changing runoff characteristics, calculations based on given monthly average temperature and precipitation would not have been detailed enough. The snowfall altitude can change within hours and could lead to very different runoff patterns (RÖSSLER et al. 2013). To manage this issue, the model is based on a high temporal and spatial resolution for the input values of «Precipitation» and «Glacier».

- Temporal: the model is based on an hourly resolution, based on the data availability of MeteoSwiss and BAFU (see TAB. 02), which reproduces a detailed picture of the runoff behaviour of Lonza and the precipitation input at Blatten itself.
- Spatial: the valley is sectioned into 27 bands of 100m altitude (elevation band = EB), going from 1‘200 to 3‘800 m a.s.l. Each represents an assumably homogenous area with steady conditions.

Based on this high resolution the monthly, catchment specific pattern was calculated and integrated into the final model.
Because the measurements of MeteoSwiss in Blatten are available between 2013 until 2018 (METEOSWISS, 2019b), this period acts as reference and forms the fundament on which the model is built.

3.2.2 Main Parameters

Precipitation - Sm & P_{Rain}

P_{Rain} is hourly measured at Blatten, but MeteoSwiss includes rain and snow into the definition of precipitation (METEOSWISS, 2016). This leads to:

$$P_{tot} = P_{Rain} + P_{Snow} \quad (3)$$

If snow is falling, it is melted first and measured in fluvial condition afterwards. This inconspicuous fact could create a huge error in calculations because the physical property of a snow flake is highly dif-

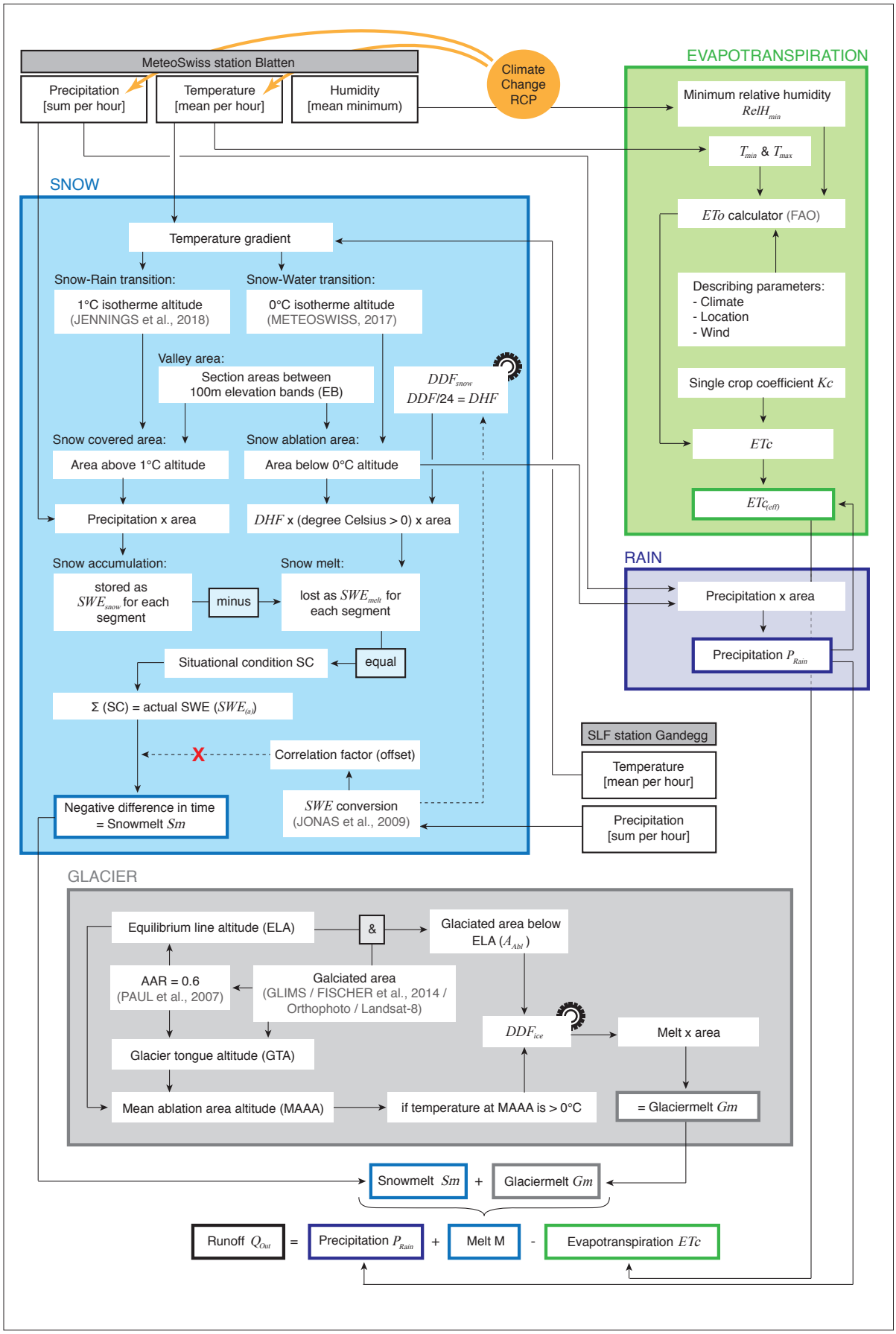

FIG. 23: System overview about the applied hydrological model. For further information, all factors can be found in the text. Every parameter with a cogwheel acted as tuning factor. The climatic changes (RCP factors) are only applied onto the measured precipitation and temperature values. (Source: own illustration)

TAB. 02: Overview of the used parameters for the hydrological model with the source (Src), the description and used values. «Cal» describes parameter which are used to calibrate the modell.

Src	Parameter	Value / Description	Sm	P_{Rain}	ETc	Cal
Blatten BAFU	Precipitation (P_{tot})	Measured and supplied by MeteoSwiss in Blatten [mm/hr]. Timespan used: between 31.05.2013 and 05.11.2018.				
	Temperature (T)	Measured and supplied by MeteoSwiss in Blatten [$°C_{mean}$/hr]. Timespan used: between 31.05.2013 and 05.11.2018.				
		Measured and supplied by MeteoSwiss in Blatten [$°C_{min}$/month], [$°C_{mean}$/month], [$°C_{max}$/month] Timespan used: between 03.2001 and 10.2018 T_{min}= -25.5°C, T_{max}= 30.5°C				
	Runoff (Q_{Out})	Measured and supplied by BAFU in Blatten [m^3_{mean}/hr]. Acts as reference to the modelled discharge of BLA. Timespan used: between 01.01.1974 and 01.08.2018.				
	Minimum Relative Humidity ($RelH_{min}$)	Measured and supplied by MeteoSwiss in Blatten [%]. Timespan used: between 03.2001 and 10. 2018. Total average value for the dataset: $RelH_{min}$= 27.8%.				
Gandegg SLF	Precipitation (P_{tot})	Measured and supplied by SLF at Gandegg [mm/hr]. Used for *Sm* calibrations. Timespan used: between 20.11.1996 and 07.11.2018.				
	Temperature (T)	Measured and supplied by SLF at Gandegg [$°C_{mean}$/hr]. Used for *T*-gradient calculations in relation to Blatten. Timespan used: 01.01.2018 - 05.11.2018.				
Ferden EnAlpin	Runoff (Q_{Out})	Measured and supplied by EnAlpin in Ferden [Σ m^3/month]. Acts as reference to the modelled discharge of FER. Timespan used: between 08.2001 and 09.2018.				
FAO	Single Crop Coefficient (*Kc*)	Based on the tabulated coefficients of the «Food and Agriculture Organization of the United Nations» (FAO). Monthly values [without dimension].				
	Reference evapotranspiration (*ETo*)	The *ETo* [mm/d] was calculated with the «*ETo* Calculator», developed and freely provided by the FAO.				

Parameter	Value
Station Coordinates Blatten BAFU	46°25‘N 7°49‘E / 1535 m a.s.l
Climate	arid to semi-arid (Valais)
Location	interior location (valley)
Wind	light to moderate winds in the area (isolated system)

ferent from a rain drop. The main issues are wind field deformations around the measurement gauge (wind-induced error) or *«splashing of rain drops or blowing of snow flakes out or into the gauge»* (JOSS et al., 1997: 97). In order to separate snow and rain, the following conditions and settings are defined:

- From January to November 2018, 84 % of the time both stations at Gandegg and Blatten measu-

red falling precipitation, while Gandegg measured in average +0.54 mm more precipitation. During 7 % of the time only Gandegg measured precipitation, while Blatten measured dry conditions. Based on these results, no vertical or horizontal gradient was applied.

- There is no barrier effect by mountains. No shadowing or lee effects are assumed.
- Temperature is controlling the physical state of the water droplet (frozen or fluvial). P_{tot} is only equal to P_{Rain}, if the temperature is higher than 0 °C. Below 0 °C the accumulation of snow is presumed.
- The calculated runoff is measured at Blatten without any delay.

Based on those definitions the fraction of Sm in P_{tot} has to be retrieved first. The problem of snowmelt is based in the delay between input (snowfall) and output (melt) due to temperature correlated processes. A correlation between runoff and precipitation can only be achieved, if all calculations are based on the snow water equivalent (SWE). SEIBERT et al. (2014: 101) writes: *«The S_{WE} is defined as the amount of liquid water that would be obtained upon complete melting of the snowpack per unit ground surface area. S_{WE} (mm), snow depth (d(m)), snow density (ρs (kg m^{-3})), and water density (ρw = ~ 1,000 kg m^{-3}) are directly related.»* But because precipitation is always measured in fluvial condition, the gauge already measures the SWE even if snow is falling.

To retrieve the snow melt out of the measured precipitation input, the following steps are applied:

1. While the MeteoSwiss station at Blatten acts as reference, a vertical temperature gradient is applied and for every EB (elevation band) the temperature is calculated. The EBs below the 0 °C altitude register falling rain and the water drains as direct runoff (P_{Rain}). The corresponding areas are multiplied with the measured precipitation at Blatten. The sum of all EBs during one hour of one catchment represent the total runoff. Based on the hourly resolution, an average monthly valley runoff is calculated for each month between 2013 and 2018. In a second step, the average of all equal months is retrieved out of the given five years.

2. Falling snow transforms into rain at a temperature of approximately 1 °C (JENNINGS et al., 2018). The measured precipitation at Blatten is multiplied with the corresponding EB areas above the 1 °C altitude, describing the accumulation of falling snow as P_{Snow} in SWE_{snow}.

3. Based on physical effects and in contrast to the falling snow, the snow cover begins to melt if the temperature is above 0 °C. Snow melts with a Degree Day Factor (DDF), which describes how much snow (SWE) is melted per day and per degree Celsius above 0 °C [mm/d/°C], is defined e.g. by HOCK (2003) to a value of 5.3 mm/d/°C (DDF_{snow}) or 0.22 mm/h/°C as Degree Hour Factor (DHF_{snow}). For each EB the hourly melt is calculated as multiplication of the DHF with the corresponding EB areas above 0 °C (= SWE_{melt}).

4. For each EB and hour, P_{Snow} - SWE_{melt} describes the situational condition (SC).

5. To model the actual $SWE_{(a)}$ of the snowpack, each hourly SC is compared to the preceding hour and describes the snow development for each EB. Values smaller than 0 are zeroed due to a not existing negative snow height.

6. If the SC at a specific time is smaller than one hour before, the difference is released as runoff (Sm). If the SC is higher than one hour before, no melt happened and the value is set to zero. The sum of Sm on every EB describes the total runoff due to snowmelt of the whole catchment during one hour. An average monthly catchment runoff is calculated for each month and year between 2013 and 2018. In a second step the average of all equal months is retrieved out of the given five years.

The applied temperature gradient is calculated out of the local difference between the measurement stations of Gandegg and Blatten from the year 2018. Results showed that the standardized 0.65 °C/100m (BARRY & CHORLEY, 1987) were not accurate enough. A mean temperature gradient of 0.46 °C/100m could be retrieved. It is not the focus of this thesis to analyse in detail why the gradient is smaller than standard 0.65 °C/100m. But different solar input, the position of the two stations (Gandegg is on the sunny side of the valley and Blatten in the valley floor) and other factors, could interfere with the gradient and thus lowering the value.

Evapotranspiration - ETc

The crop evapotranspiration coefficient ETc [mm/d] is the result of the multiplication of the Kc and ETo [mm/d] coefficients and describes the amount of water which is evapotranspirated by crops into the atmosphere during one day under standard conditions, while standard conditions are defined by the Food and Agriculture Organization of the United Nations FAO as: *«No limitations are placed on crop growth or evapotranspiration from soil water and salinity stress, crop density, pests and diseases, weed infestation or low fertility»* (FAO, 2018b)

- The Kc coefficient [dimensionless] is tabulated by the FAO and it *«incorporates crop characteristics and averaged effects of evaporation from the soil. For normal irrigation planning and management purposes, for the development of basic irrigation schedules, and for most hydrologic water balance studies, average crop coefficients are relevant and more convenient than the Kc computed on a daily time step using separate crop and soil coefficient (...)»*. (ibid.) For the simplified hydrological model, the vegetated area of the Lötschental is considered to be equally covered by larches and grasslands. Other vegetation is neglected. Therefore a FAO average mid-term Kc value of 0.6 was retrieved for BLA (1/3 larches, 2/3 grassland) and 0.7 for FER (1/2 larches, 1/2 grassland) with larches Kc = 1 and grasslands Kc = 0.4. Kc was assumed to stay constant during the seasons.
- The ETo calculator, developed by the FAO (FAO, 2018a), calculates the reference evapotranspiration ETo out of the data given by TAB. 03. It describes the evaporation by an homogenous grassy area and is therefore idealized.

TAB. 03: Retrieved ETo results based on the «ETo-Calculater» by the FAO. (Source: FAO, 2018b)

ETo	Jan	Feb	Mar	Apr	Mar	Jun	Jul	Aug	Sep	Oct	Nov	Dec
[mm/d]	1.2	1.7	2.6	3.8	5.2	6.3	6.2	5.4	4.0	2.8	1.8	1.1

Out of the given data ETc was calculated. Because the evapotranspiration is based and limited on precipitation, $ETc_{(eff)}$ is retrieved out of the conclusion, that if the calculated ETc is smaller than the precipitation input, the value of ETc is applied. If the retrieved ETc is higher than the available P_{Rain}, the ETc is multiplied with a factor of 0.1 due to limited biologic activity.
It has to be notified, that the result reflects a coefficient for a non stressed and well-managed crop in subhumid climates which is an assumption for the Lötschental. Climatic anomalies are not taken into account.

Glacier - Gm

Based on the retrieved values for Sm, P_{Rain} and ETc and due to the fact, that Q_{Out} is measured at Blatten and Ferden, Gm could be calculated out of the formulas *(1)* and *(2)*. But the model should depend on future glacier extensions and therefore Gm has to be calculated independently.

A glacier is not affected by melt homogeneously and reveals accumulation and melting processes. The theoretical existing equilibrium line describes the position, where the ablation equals the accumulation and the mass balance is zero (ELA: equilibrium line altitude). The ELA various during one year but can be located as snow line altitude (SLA) in the transition between summer and fall, when high temperatures melt the maximum of snow coverage (YUWEI et al., 2014). The relation between the ablation and accumulation area (AAR), which is dependent on the ELA, determines the state of the glacier. PAUL et al. (2007) calculated an AAR for a steady state glacier of 0.6, describing that 60 % of the glacier has to be accumulation area. If the value is lower than 0.6 then the glacier begins to retreat, if it is higher the glacier advances. All processes occur with delay due to the response time between the environmental changes and the adaptation of the glacier. Therefore small glaciers react faster than large ones. These relations revealed the following definitions for the model calculations regarding Gm:

- The glaciers are assumed to be in steady state.
- Only the area between ELA and the lowest point of the glacier (GTA: glacier tongue altitude) is affected by melting processes.
- The located ELA and the GTA are constant for the chosen time series.
- The melting process acts homogeneously and is defined by the Degree Day Factor of ice (DDF_{ice}) by HOCK (2003) to 11.7 mm/d/°C.

The glaciated area is retrieved out of the dataset of the Swiss Glacier Inventory SGI (FISCHER et al., 2014) and the Glacier Monitoring Switzerland GLAMOS (GLAMOS, 2018). The areas of the last extension recording from 2010 are used and the following steps are required to calculate Gm:

1. Based on the data, the GTA (lowest point) and the ELA (AAR = 0.6) are calculated.
2. Because the temperature decreases with height and therefore not every EB of the glacier reveals the same air temperature (which influences the melt), the mean ablation area altitude (MAAA) between GTA and ELA acts as reference. Is the MAAA > 0 °C, it is assumed that the whole ablation area experiences uniform ice melt based on the applied DDF_{ice}. If the MAAA is below 0 °C, no melt occurs.

To get a first indication of a possible ELA, the Glaciological Report No. 135/136 «The Swiss Glaciers 2013/14 & 2014/15» (EKK, 2017) was consulted wherein the glaciers of Rhone (ELA 2‘915 m a.s.l) and Tsanfleuron (ELA 2‘835 m a.s.l) are listed. The Lötschental is located approximately in the middle of both and the median of 2‘875 m a.s.l was used as representative total ELA for the valley.
First calculations with the model showed, that the ELA is probably too low, which was supported by impressions during fieldwork and helicopter flights in the summer and fall of 2018 - even if the summer of 2018 was very warm and maybe not representative for years, pictures of 2015 revealed a similar situation. Following personal photographs and Landsat-8 satellite images, the ELA was located at 3‘100 m a.s.l for the year of 2018 (FIG. 24). To verify the assumption, an AAR of 0.6 was applied to the glaciated area of the valley. For FER the ELA was calculated to 2‘966.5 m a.s.l. and for BLA to 2‘970.6 m a.s.l. This small difference between the steady state AAR of 0.6 and the current state of transformation of the ELA is evident, due to the fact that the glaciers in the valley are not in a steady state and are retreating significantly. Based on those calculations and the fact that the model is built on datasets until 2010, the ELA was calibrated to 3‘000 m a.s.l.
The GTA is difficult to define for the whole valley. Like for the ELA the glacier tongue is influenced by different parameters and varies from glacier to glacier. Out of randomly chosen 30 glacier tongues in the

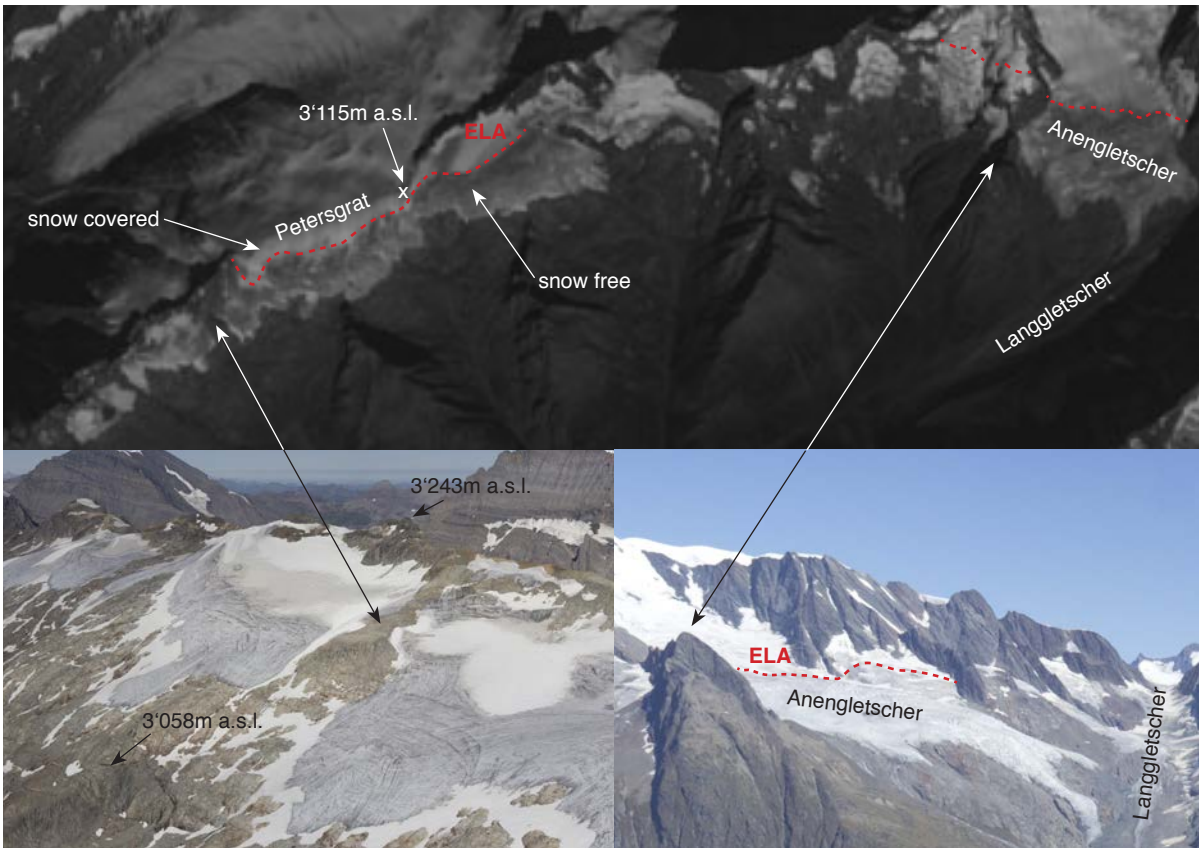

FIG. 24: Interpreted ELA based on the extract of the red band Landsat-8 image with view onto the Petersgrat, captured on the 9th of October 2018 [top], a picture of the remnants of the Tellingletscher (Petersgrat) on the 31st of July 2015 with indications of a high ELA [bottom left] and an image from the Birchbach catchment (from 2‘800 m a.s.l) in direction to Anengletscher on the15th of September 2018 [bottom right]. Marked is the ELA (red) at an altitude of approximately 3‘100 m a.s.l. (Sources: REMOTEPIXEL (2018) [top] & own photographies [bottom]).

valley the lowest glacier tongue (Langgletscher at 2‘095 m a.s.l) was nearly 1 km lower than the highest one (ice field north of Schwarzhorn at 2‘968 m a.s.l) while a mean of 2‘716 m a.s.l. was calculated. The retreat of the tongue occurs with delay in time due to the inertia of the system and therefore the GTA is almost never in a state of balance and would be higher if the actual environmental conditions would stay until the glacier has reached its equilibrium state. Based on the assumption of steady-state conditions, the GTA is reflected by the lowest point of all glaciers and therefore represented by the tongue of Langgletscher.

3.2.3 Tributary torrents

The tributary torrents are flowing directly aside of the used water sources and are therefore assumed to behave like the springs in the valley. Hence, the analysis concentrates on the rivers Faldumbach, Ferdenbach, Dornbach, Gisentella and Uistre and Innre Talbach which are covered with a complete monthly data series and are in vicinity of a tapped spring (TAB. 04). The modelling is based on the calculations and the composition of the runoff of Lonza. Every torrent is compared to the modelled output of Lonza (in respect to the main catchments FER and BLA) and is adapted based on the respective fluvial regime (see chapter 2.5). Therefore, the nival rivers Faldum-, Ferden- and Dornbach are modelled without glacial input. Because a separate modelling for every river would be too time consuming, the correlation is roughly processed with the following method:

TAB. 04: Used datasets for the tributary torrent analysis

Torrent	Source
Faldumbach	EnAlpin AG (no year) [l/s_{mean} per month]
Ferdenbach	EnAlpin AG (no year) [l/s_{mean} per month]
Dornbach	Salzman Ingenieure AG (no year) [l/s_{mean} per month]
Gisentella	SRP AG (2014) [m^3/s_{mean} per month]
Uistre Talbach	SRP AG (2008) + Werkhof Blatten [l/s_{mean} per month]
Innre Talbach	SRP AG (2011) [l/s_{mean} per month]

- Neglecting non-existent parameters (e.g. glaciation)
- Applying gradients to increase or decrease the impact of parameters
- Shifting the curve based on calculated differences in volume (reference: January and month of peak) and time (reference: month of peak). This basal offset acts as summarized gradient for unknown system specifications.

3.2.4 Calibration and validation

To adjust the model to the existing measurements, the factors of DDF_{snow} and DDF_{ice} act as tuning factor while the Nash-Sutcliffe coefficient represents the model efficiency. The Nash-Sutcliffe model efficiency coefficient NSE *«proposed by Nash and Sutcliffe (1970) is defined as one minus the sum of the absolute squared differences between the predicted and observed values normalized by the variance of the observed values during the period under investigation.»* (KRAUSE et al., 2005: 90) and is described mathematically as following (NASH & SUTCLIFFE, 1970):

$$NSE = 1 - \frac{\Sigma_{t=1}^{T} (Q_m^t - Q_o^t)^2}{\Sigma_{t=1}^{T} (Q_o^t - \overline{Q_o})^2} \quad (4)$$

with: Q_m^t *modeled discharge at time t*; Q_o^t *observed discharge at time t*; $\overline{Q_o}$ *mean of observed discharges*

The NSE ranges from 1 (perfect fit) to -∞, while values <0 represent a not valuable result. The NSE value should be located within 0.75 and 1.00 to represent a «very good» result (MORIASI et al., 2006).

3.2.5 Future

This thesis wants to give a perspective into the future. To model possible scenarios, the following pre-settings are used:

System definitions

Because a dynamic model would go beyond the scope of this thesis, the model describes temperature related states of equilibrium, meaning the ELA is in steady state and the glacier is in balance. Such behaviour includes the following assumptions:

- The glaciers are represented as homogenous areas without any vertical extent or geometry. Calculations are surface and not volume related.
- The model does not take any flow behaviour or surface changes of the ice into account.
- The melt is produced by applying the defined melting factors onto the respective area.
- The developed hydrological model presumes all future processes to act linear.

Temperature and precipitation

To model the upcoming climate change related scenarios, the CH2018 report was taken as reference. It focuses on four main changes (CH2018, 2018: 180):

1. *«**Dry summers**: decrease in summer precipitation and increase in summer temperature and in the maximum number of consecutive dry days (CDD)»*
2. *«**More hot days**: increase in the temperature of the hottest day of the year (...) and in the number of very hot days (...)»*
3. *«**Heavy precipitation**: increase in frequency and intensity of rare (...) to extreme (...) precipitation events»*
4. *«**Snow-scarce winters**: reduction in snow cover and frequency of snowfall and rise of zero-degree line due to rising winter temperature»*

The report is based on three different Representative Concentration Pathways (RCPs) (FIG. 25). RCPs were defined for the Fifth Assessment Report of IPCC from 2013 and *«they are identified by their approximate total radiative forcing in year 2100 relative to 1750: 2.6 Wm^{-2} for RCP2.6, 4.5 Wm^{-2} for RCP4.5 (...) and 8.5 Wm^{-2} for RCP8.5. (...) For (...) RCP8.5, radiative forcing does not peak by year 2100; for RCP2.6 it peaks and declines; and for RCP4.5 it stabilizes by 2100.»* (IPCC, 2013: 45). The RCPs are dependent on CO_2 concentrations (RCP2.6: 421 ppm, RCP4.5: 538 ppm, RCP8.5: 946 ppm) and for CO_2-equivalent CH_4 and N_2O concentrations by the year 2100 (ibid.).

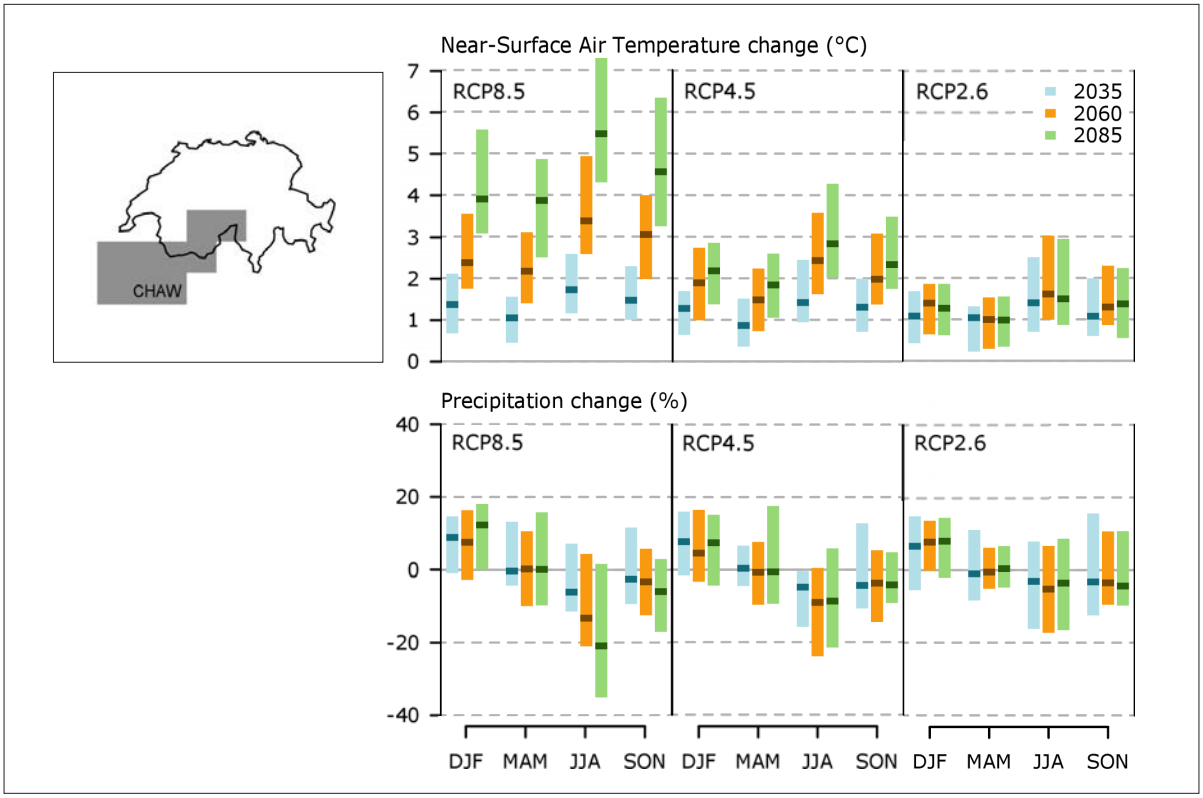

FIG. 25: *«Projected future change in median temperature (°C) [and precipitation (%)] for winter (DJF: December-February), spring (MAM: March-May), summer (JJA: June-August) and autumn (SON: September-November) in (...) [the] western Alps (CHAW). Projections are for 30-year averages centred at 2035 (blue), 2060 (orange), and 2085 (green) with respect to the reference period 1981-2010. Three emission scenarios are considered: RCP8.5 (...), RCP4.5 (...), and RCP2.6 (...). The lower and upper bounds of the colored bars represent the empirical quantile range, spanning the lower (5 %) and upper (95 %) bounds of the ranked data points (i.e., 90 % of the model ensembles fall within this range). The middle line is the median estimate of the ensemble.»* (CH2018, 2018: 58). (Source: modified after CH2018, 2018)

TAB. 05: Applied climatic changes for south western Switzerland, referencing to pre-industrial conditions. (Source: CH2018, 2018)

Climatic parameter change for 2085 (50% value)	RCP	DJF	MAM	JJA	SON
Temperature increase [°C]	8.5	3.9	3.87	5.47	4.56
	4.5	2.18	1.84	2.83	2.33
	2.6	1.27	0.98	1.49	1.37
Precipitation change [%]	8.5	12.3	0.1	-20.9	-6
	4.5	7.4	-0.6	-8.7	-4.2
	2.6	8	0.4	-3.6	-4.4

The CH2018 (2018) report calculated the corresponding temperature and precipitation changes during the four main seasons and for three different years (2035, 2060 and 2085). But for the applied model, the three time periods are too specific due to the fact, that it does only represent equilibrium state conditions. Therefore only the median (50 %) values of 2085 are applied, representing conditions around the end of the 21st century (TAB. 05). Due to the fact, that the RCP scenarios refer to pre-industrial conditions (CH2018, 2018), the mean temperature increase of 1.0 °C until 2018 (ALLEN et al., 2018) is subtracted from the provided RCP projections to model future temperature increases. The temperature and precipitation changes are applied onto the existing measurements of the period between 2013 and 2018. Three scenarios (RCP2.6, RCP4.5 and RCP8.5) are calculated for BLA and FER with the respective temperature and precipitation factors of 2085 (TAB. 05).

Glacier

While in the accumulation area no melt and no change in glacier extent is assumed, the ablation area is calculated relatively to the position of the ELA. RABATEL et al. (2013: 9) describes a mean ELA change of 100 m during the period of 1984 to 2010 in the western alps. During nearly the same period of 1979 to 2010, FOSTER & RAHMSTORF (2011: 6) analysed a global temperature increase of +0.5 °C and the CH2018 (2018: 52) report an increase of +0.6 °C from 1981 to 2010. Those two variables correlated represent an ELA change of 200 m in altitude per 1 °C change.

Comparing to the results of 150 m/°C (KUHN, 1980) and 140 m/°C (PAUL et al., 2007) the value is relatively high. It is assumed, that possible inertia could lead to an offset of the measured ELA change. Taking all points into consideration, an overall gradient of 170 m/°C is used (describing the mean). Based on the RCP scenario and the respective temperature increase, the ELA is calculated for future projections. As the model does not include any delay and therefore the RCP values for the year 2085 (CH2018, 2018) are used and modelled, assuming a steady state condition around the end of the 21st century. It is supposed, that the glacier extent above the ELA stays constant and no lateral melt occurs. After applying the ELA to the respective RCP scenario for the year 2085, the accumulation area is known based on the data of the SGI (FISCHER et al., 2014). Further on, the AAR of 0.6 defines the ablation area based on the accumulation area. The sum of the given ablation and accumulation area represents the total modelled glaciated area in relation to the temperature for the RCP projection.

To retrieve the GTA the total modelled ablation area is relatively distributed over the glaciated area. For today, the glaciated area per EB is set in relation to the total ablation area (percentage) which acts as factor. This ice distribution is applied onto the projected ablation area, representing an area correlated glacier extent in the future (illustrated in FIG. 26). The procedure leads to an offset in melt if big ice masses are concentrated in specific elevation bands (for example «Petersgrat»). Out of the relatively distributed glaciated areas, the lowest glaciated point is retrieved (accuracy: 100 m) which describes the GTA.

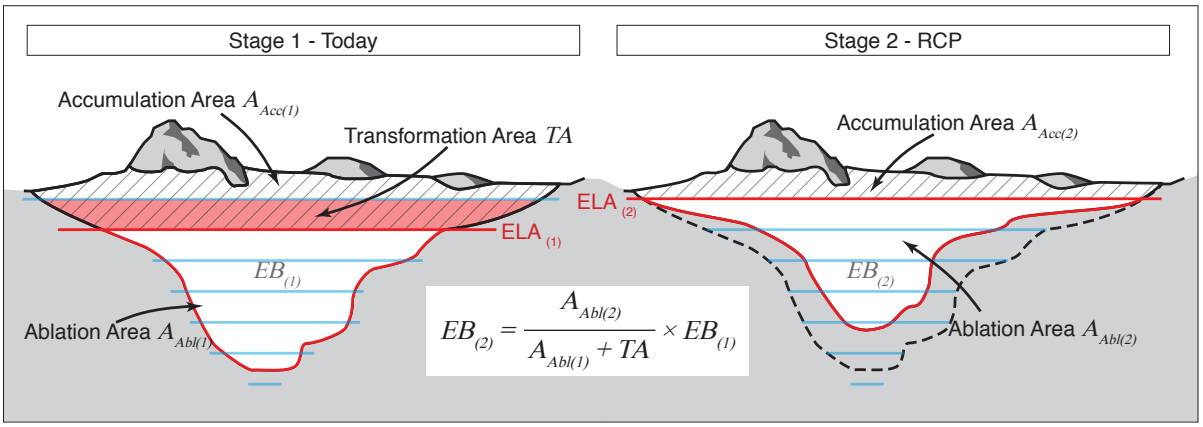

FIG. 26: Illustration about the glacier area projections for future RCP scenarios. The sources for ELA, accumulation and ablation areas are given in FIG. 24. The red outlined area illustrates the ablation area, while the blue lines indicate EBs. The transformation area (TA) is crucial for the calculation of the future glacier extent. (Source: own illustration)

3.2.6 Water supply of the Lötschental

Because the torrents of the water sources are not specifically modelled, the modelling of future scenarios has to be made on gradients which are applied to the situation of today. The used gradients are retrieved from the CH2018 (2018) report (P_{Rain}) and in relative values from the Lonza model itself (Sm, Gm and ETc) in respect of the main catchments FER or BLA.

3.3 Model results for present conditions

3.3.1 Result Lonza

Based on the model inputs, the $DDF_{snow\ \&\ ice}$ were adjusted within the listed limits by SCHAEFLI et al., (2005). The given values in TAB. 06 («Before calibration») acted as first reference, whereas the second column indicates the values used after the calibration.

TAB. 06: Used calibration factors before and after calibration.

Index	Before calibration	After calibration
DDF_{snow}	5.3 mm/d/°C (HOCK, 2003)	4 mm/d/°C
DDF_{ice}	11.7 mm/d/°C (HOCK, 2003)	9 mm/d/°C

With this factors applied, the following results were achieved (FIG. 27):

January: BLA reveals nearly no runoff. Little snow melt and missing rain input lead to a total runoff of 0.21 m³/s, while FER is modelled with a total runoff of 0.64 m³/s due to higher P_{Rain}.

February: It is the month where both catchments reveal the minimum Q_{Out} (FER: 0.39 m³/s, BLA: 0.14 m³/s) based on a minimal input of rain and snow melt.

March: In March Sm begins to increase (FER: 1.2 m³/s, BLA: 0.6 m³/s) while for both catchments P_{Rain} is three times as high as in February. The loss of water is still minimal and for FER & BLA smaller than 0.05 m³/s.

April: With a monthly averaged temperature above 0 °C in Blatten, Sm triples and acts as main water input into the valley runoff in April (FER: 3.4 m³/s, BLA: 1.8m³/s). FER reveals nearly double as much runoff as modelled for BLA.

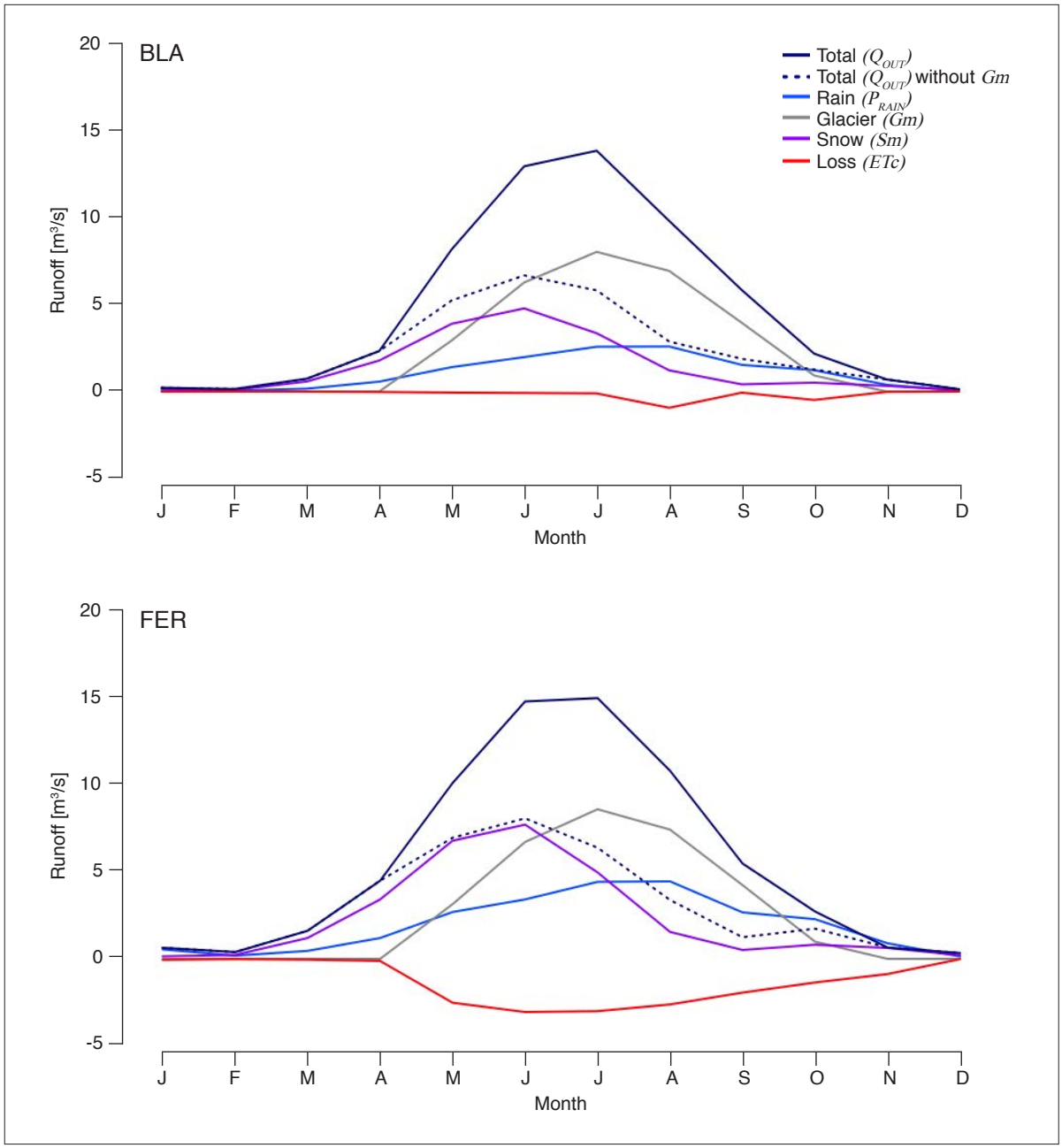

FIG. 27: Shown are the modelled runoff compositions (mean values) of Lonza in Blatten and in Ferden for the applied period between 2013 and 2018. The dashed line shows the total runoff of today without the inclusion of ice melt. (Source: own graph)

May: In May the temperature increase (8.2 °C) reaches the glaciated areas and Gm rises significantly. The contribution of ice melt is 2.9 m³/s for BLA, respectively 3.2 m³/s for FER, whereas the evapotranspiration increases mainly in FER (FER: -2.5 m³/s, BLA: -0.06 m³/s). Differences exist also in the relative proportioning: while in FER Sm (6.8 m³/s) is bigger than the sum of P_{Rain} and Gm, in BLA the glacier melt (2.9 m³/s) is nearly as big as the snow melt (3.9 m³/s).

June: In June Sm peaks (FER: 7.7 m³/s, BLA: 4.8 m³/s) and decreases afterwards. The month reveals the second highest runoff volumes with values up to 14.8 m³/s (FER) and 12.9 m³/s (BLA). For FER the amount of water loss increases up to the annual

maximum of -3.06 m³/s.

July: Only in the catchment of BLA, Gm was already higher than Sm in June. In July both catchments reveal the highest amount of glacial melt (FER: 8.6 m³/s, BLA: 8.05 m³/s) while Sm decreases significantly to a value between the months of April and May. It is also the month with the maximum Q_{Out} with peaks of 15.0 m³/s for FER and 13.9 m³/s for BLA. During July and August, P_{Rain} reaches also the annual maximum in both catchments.

August: August is the first month with a decreasing total runoff (around 30 %). While the precipitation input is on a similar level like in July, Gm and Sm decreases. In FER the runoff loss also decreases (0.4 m³/s), but in BLA ETc reaches the maximum value of -0.9 m³/s.

September: In September the catchment of BLA (5.8 m³/s) measures a bigger Q_{Out} than FER (5.5 m³/s) because the glaciers reveal the highest runoff volumes in BLA (77 % of Q_{Out}). This is based on the nearly not existing ETc in BLA, while FER is modelled with a loss of -1.9 m³/s gets nearly 50 % of Q_{Out} as P_{Rain}.

October: It is the last month with glacial runoff (FER: 0.9 m³/s, BLA: 0.9 m³/s) which is smaller than the modelled P_{Rain}. BLA reveals a last vegetational increase of ETc (-0.5 m³/s) while FER since June steadily decreases (-1.4 m³/s).

November: During November, in FER the loss (-0.9 m³/s) is bigger than the total runoff (0.6 m³/s) which is nearly equal to Sm (0.6 m³/s). BLA reveals 0.1 m³/s more in Q_{Out} than FER and is mainly based on P_{Rain}.

December: The total runoffs go back to the annual minimum (FER: 0.3m³/s, BLA: 0.1m³/s).

Comparing the two catchments, BLA is responsible for 71 % of the calculated runoff of FER, while BLA reveals 51 % ice melt input and FER 46 %.

The calculations with the composition of today, but without the existing glaciers, show that the main peak of total runoff would be reached in June and that the mean annual runoff would be around 50 % lower than today (FIG. 27, dotted line).

3.3.2 Discussion Lonza

The retrieved runoff patterns reveal comprehensible results and are comparable with other researches (COSTA et al., 2018; FARINOTTI et al., 2011; SEIBERT et al., 2014) while the calculated NSE of 0.943 (BLA) and 0.923 (FER) represents a «very good» result (MORIASI et al., 2007) and is therefore representative. The values are very high, compared to the offsets, illustrated in FIG. 28. It is assumed that the small number of only 12 values is not representative enough to reveal a sufficient data base. The over- and underestimations between the modelled results and the observed data are equalling each other (the table with all data listed is under APP-C2/3). Nevertheless the following aspects have to be considered:

Offset

The good coverage which is pictured by the NSE values is based on the runoff volume and is during summer higher than during winter. In winter small modelling differences between the model and the measurements reveal huge relative offsets due to the small existing runoff. Therefore the offset has to be carefully taken into account. Based on the relative offset, the model can be separated into five different phases (see FIG. 28):

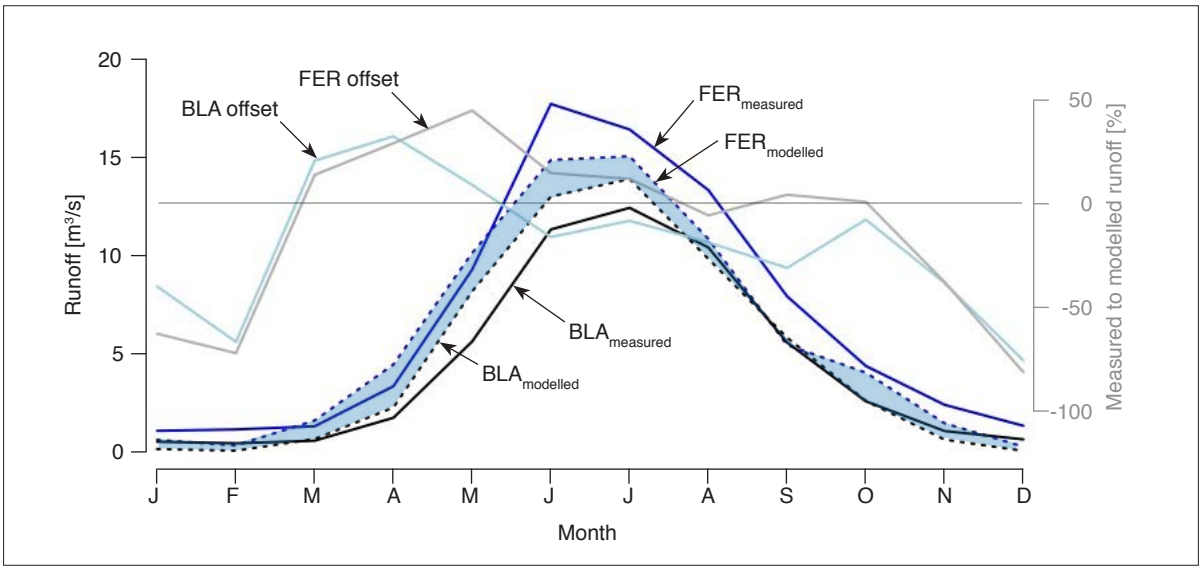

FIG. 28: Comparison between the measured and the modelled averaged values between 2013 and 2018, including the relative offset between the two curves (background). The main differences appear during the winter season due to small runoff volumes which implies huge variabilities. Blue shaded is the difference between the models. (Source: own graph)

- Jan-Feb: BLA and FER reveal an underestimation of around -70 % while the error is little higher for BLA.
- Mar-May: Both catchments illustrate an overestimation. While FER reveals its maximum in April (32.3 %) and is in May congruent with the measured values, BLA reaches its maximum in May (+44.7 %) which decreases until August.
- Jun-Aug: BLA reveals an overestimation and FER an underestimation. In August both catchments are modelled with an underestimation, where FER has a bigger offset than BLA.
- Sep-Oct: BLA is relatively stable and congruent with the measured values, while FER reveals in September an underestimation of around -30.9 %. In October both catchments are nearly congruent with the measurements.
- Nov-Dec: After October both catchments begin to underestimate the runoff until around December an offset of -80 % is reached.

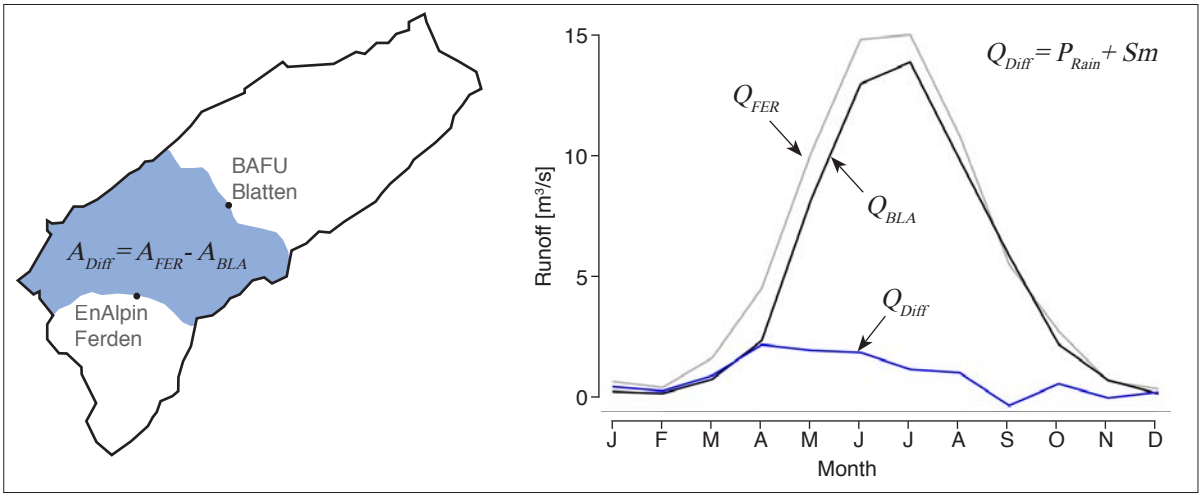

FIG. 29: Difference between FER and BLA. The main runoff measured in Ferden originates from BLA. (Source: own illustration)

The curves look similar, with a small difference in June, which reveals a problem of the model. The only variability between the two catchments is the area difference between FER and BLA (FIG. 29). The difference begins to develop from February until April and stays constant until June. In July the difference decreases and nearly disappears in September, increases again in October and decreases until December. The model is based on the different input parameters snow melt (Sm), glacier melt (Gm) and rain (P_{Rain}) while evapotranspiration (ETc) describes the only system loss. The glacier area varies minimal (BLA: 18.9 km², FER: 20.2 km²) and therefore has nearly no impact on any possible model differences, but precipitation (rain and snow) is assumed to be homogeneously distributed - which is reproduced as runoff difference Q_{Diff} between BLA and FER (FIG. 29).

Snow and Sm

A further issue is based in the snow modelling. To evaluate if a calculated SWE_{xnow} offset between Blatten and the measurements at Gandegg (2‘717 m a.s.l) exists, the logged data of Gandegg was compared to the modelled results of the corresponding EB (2‘700- 2‘800 m a.s.l). The measured snow height of Gandegg was converted into the specific SWE, based on the formula by JONAS et al. (2009) with the given and tabulated parameters for a, b (≥ 2‘000m a.s.l.) and the offset (region 4, Valais):

$$SWE_{(mod)} = HS_{obs} \cdot (a \cdot HS_{obs} + b + offset) \quad (6)$$

The SWE conversion was extrapolated to the whole EB to get comparable results to the model output. The correlation showed an underestimation by a factor of 0.313 of the modelled values. Later trials with application of this factor led to a big overestimation of the total runoff based on snowmelt. The station is assumed to show higher values compared to the surrounding stations (according to D. Liechti, project-leader of the measurement-stations of SLF, 08.11.2018). Based on those two indications of a possible overestimation, the factor was not applied.

It is presumed that the position of the measurement station could be influenced by aeolian snow accumulation due to its lee-sided position, regarding the mainly blowing westerly winds. Further on, the northern ridge of the Lötschental is influenced by Bernese and Valais weather phenomena, resulting in snow inputs from two different regions. Beside the not correlatable SWE data of the SLF station, the Gandegg pattern of snow accumulation and ablation was used to verify the model in time (FIG. 30).

Because the model refers to simplified assumptions (e.g. specific and unchanging temperature gradients, homogenous snow coverage without the influence of wind or avalanches), the measurements at Gandegg reveal sharp changes in the SWE. The model output shows a smoothed curve, only influenced by the change of the 0 °C altitude. While the point of the beginning snow accumulation and the rates of accumulation and ablation are relatively comparable, the point of total snow cover disappearance (TSCD) reveals an offset of around 15 to 30 days (FIG. 30). While the accumulation is regulated by the 0 °C altitude, the melt is controlled by the DDF_{snow}. As described in 3.3.1 the DDF_{snow} is set to 4 mm/d/°C. To model an earlier time of snow cover loss in spring, the DDF_{snow} needs to be higher. But the steeper rate of ablation leads to an overestimation in the total runoff compared to the measured values. The meltwater is drained too early. Therefore the DDF_{snow} of 4 mm/d/°C was not changed. The comparison to other researches which applied a DDF_{snow} within the valley or in the near surrounding of the Lötschental showed, that

TAB. 07: Overview of DDF_{snow} values applied in the extended research area.

Index	DDF_{snow} [mm/d/°C]
Applied in the modell	4
COSTA et al. (2018)	3.6
RÖSSLER et al. (2012)	2
SCHÄFLI et al. (2005)	6.1
HOCK (2003)	5.3

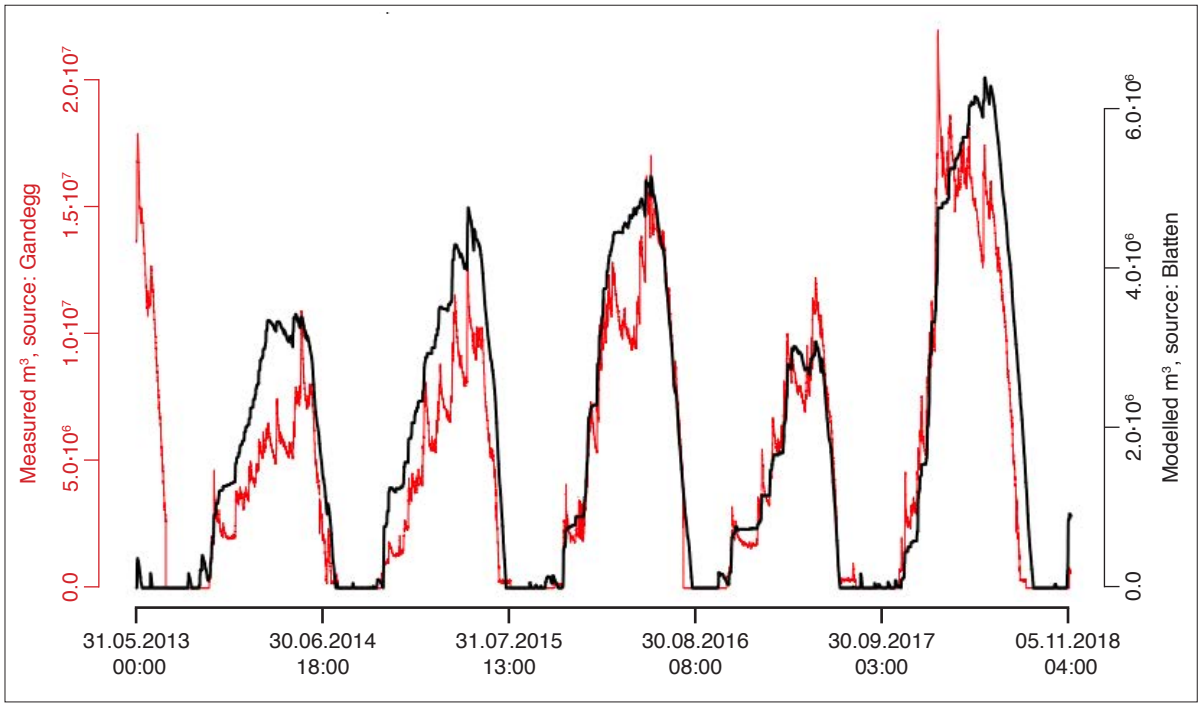

FIG. 30: Comparison between the measured m³ SWE at Gandegg and the modelled and the extrapolated values based on Blatten for the EB 2'700-2'800 m a.s.l. The accumulation point reveals a good correlation while the point of total melt out is modelled too early. The different scales are applied due to a better readability of the time related snow accumulation and ablation processes. The volume differences are discussed in the text. (Source: own illustration based on data of METEOSWISS, 2019b)

the inserted DDF_{snow} is within the range of the median (TAB. 07) and therefore can be assumed to be representative.

The delay of TSCD is estimated to be influenced by different rates of solar radiation (see chapter 2.1). Gandegg is positioned on the northern ridge of the valley at high altitudes, and Blatten acting as root for the model is located on the valley floor. While the solar input on Gandegg is high, the melting process starts earlier than in the model, which includes not only the sunny and warm north side, but also the cold and shady north face of the southern ridge. The mean of solar radiation of the whole valley is assumably lower than the mean of solar radiation at Gandegg. In conclusion: the amount of snow is higher compared to the model of Blatten, but the loss of the snow cover is earlier due to assumably different rates of solar radiation and ablation.

While BLA is overestimated, FER is underestimated. In reality the difference between $FER_{measured}$ and $BLA_{measured}$ is bigger than in the model (A_{Diff}) which peaks in June. It is not clear, how representative the used data of 2018 are. While the temperature gradient can be assumed to be more or less stable (only the 0°C altitude is shifting), the precipitation pattern reveals more anomalies. Beside the snow accumulation rates, which were measured higher at Gandegg than in Blatten, also the scenario of the floods in 2011 showed a very concentrated rain pattern (RÖSSLER et al., 2013). It has to be assumed, that the north western ridge in the Lötschental, especially between Petersgrat and Lötschenpass, gets more precipitation than other parts of the valley. The higher amount of precipitation is represented in the measured data und underestimated in the modelled runoff (for FER). Therefore the peak in June has to be based on the maximum of Sm (FIG. 28).

METEOSWISS (2017) referred to the complex behaviour of the snowline altitude and revealed the rule of thumb, that the snowline altitude is around 200 m to 400 m lower than the 0 °C line altitude. This

rule is not applied directly, but with the assumption of a snow fall altitude at the 1 °C elevation with an applied vertical gradient of 0.46 °C/100 m, the SLA would lay 200 m below the 0 °C elevation. If in the model the SLA would be set lower, the model would be affected with higher amounts of snow and less direct runoff. Based on the simplicity of the developed model and the fact, that the retrieved total output fits very good to the measured data, the lowered snowline altitude was not taken into account. Nevertheless the temperature gradient has a huge impact on the model and should be treated carefully. SEIBERT et al. (2014) listed further influencing factors based on DEWALLE & RANGO (2008), which influence the melt and would lead to a more detailed model if implemented:

- *Seasonal influence*
  Change in albedo, short-wave radiation and snow density
- *Open area versus forest*
  Shading effects and lowering of wind speeds leading to less melt
- *Snow-cover area*
  Spatial variability of the snow cover distribution
- *Snowpack pollution*
  Lower albedo due to dust and pollution deposited on the surface
- *Precipitation*
  Rainfall supplies sensible heat (Seeder-Feeder-Effect; RÖSSLER et al., 2013), and shading of clouds
- *Snow versus ice*
  Snow reveals a higher albedo than ice and therefore different melt rates
- *Meteorological conditions for certain air temperatures*
  Change of the melt factor for a specific temperature based on differences in wind speeds, radiation and moisture

Glacier and *Gm*

Beside the acknowledge of scientific researches, the ELA is defined by visual interpretations and the correlation of the late summer SLA as ELA. YUWEI et al. (2014) could show that the ELA can vary several 100 m in elevation from the SLA. Hence the SLA is not always representative. If the used ELA reflects the given conditions can not be said but the retrieved ELA represents the best fit to the measurements. Additionally it can be discussed, if a *Gm* based on the MAAA is representative. The problem of the mean altitude is based on the fact, that the whole ablation area drops into melting processes even if not the whole ablation area is below the 0 °C altitude. Based on the orientation of the Lötschental the glaciers are affected by a strong solar radiation gradient across the valley. The southern glaciers reveal much less solar input than the northerly and easterly lying glaciers. This fact was neglected, but it could be an explanation why BLA reveals an overestimation between March and July. The model calculates the melting processes (*Sm* and *Gm*) on given and extrapolated temperatures, which are (in contrary to the reality) assumed to be homogeneously distributed over the valley. Therefore other more sophisticated runoff models calculate the melt based on solar radiation, which includes possible effects of shading or exposure

TAB. 08: Overview of DDF_{ice} values applied in the extended research area.

Index	DDF_{ice} [mm/d/°C]
Applied in the modell	9
COSTA et al. (2018)	6.1
RÖSSLER et al. (2012)	3.9
SCHÄFLI et al. (2005)	7.1
HOCK (2003)	11.3

(FARINOTTI et al., 2011; HOCK, 1999/2003; SEIBERT et al., 2014).
The applied DDF_{ice} of 9 mm/d/°C reveals the best fit between the model and the measurements. Even the value seems to be high, other researches in the area estimated similar gradients (TAB. 08). Like for DDF_{snow}, the different values can be attributed to differences in temporal resolution, dataset length, thresholds for P_{Rain} and melt and other climatic variabilities. The table with the modelled glacier areas in correlation to the increasing temperatures is given in APP-C1.

Loss - Soil and ETc

The sole system loss is represented by evapotranspiration. Because the value is based on the vegetated area, FER and BLA reveal different patterns. It is difficult to assess the correctness of the result. COSTA et al. (2018: 520) states, that: *«(...) evaporation indeed plays a secondary role in the long-term water balance in Alpine environments, compared to precipitation and snowmelt (...), especially at high elevations such as in the case of the Massa and Lonza sub-catchments.»* while HERRNEGGER et al. (2012) analysed the upper Enns basin in the north-central Austrian Alps which is in elevation and surface coverage comparable to the Lonza catchment. They concluded that evapotranspiration calculations only based on temperatures are not sufficient, especially in high alpine regions where temperatures are relatively low and an underestimation results. Further on, the developed model does not differentiate in elevation coverages. A patch of larches on the valley floor is assumed to transpire the same amount of water like it would be located on 2'000 m a.s.l. Therefore the results of the ETc calculations seem to be realistic, but have to be handled carefully. For example, losses by sublimation are neglected which could have a huge impact, especially in wind exposed areas (STRASSER et al., 2008). Unfortunately, no useful comparison to other scientific researches could be found and no quantitative assessment about the credibility can be made.
It can be stated that the retrieved values of ETc are realistic, but the uncertainties are high, hence further researches would be needed to investigate the detailed processes in the valley.

Inertia and groundwater

In reality the runoff reveals also a certain delay based on system inertia. Because nearly no groundwater is involved in the Lötschental, the existing process is strongly simplified and no internal procrastination is present. Nevertheless the model assumes a «direct» runoff, meaning the input happens at the same time as it is measured at the corresponding data logger. This assumption is helpful but is in contrary to the existing processes. The monthly averaged runoff of fluvial inputs is not influenced by hourly or even daily delays. The main factor which is sensitive to a possible delay in the treated system is Sm, but with a temperature correlated DDF this problem could be solved. Therefore the system delay error is minimised and not critical for the model.

3.3.3 Results tributary torrents

To achieve the best correlation between the given datasets and the model, the adaptions of TAB. 09 were used. The retrieved NSE is within the defined limits (Faldumbach: 0.95, Dornbach: 0.90, Ferdenbach: 0.96, Gisentella: 0.98, Uistre Talbach: -1.05, Innre Talbach: 0.89) with the exception of Uistre Talbach. The model assumes a steady and a non-clipped runoff, therefore the NSE reveals a misleading result for this river.

The runoff pattern of the different torrents (shown in FIG. 31) shows the following results:
Faldumbach is mainly influenced by snow melt and rain water supply. Because no glacier coverage is present, Gm is missing. This missing input is compensated by the late beginning of Sm increase. Simi-

TAB. 09: Applied values for the torrent correlation.

Torrent	Time offset	Basal offset	*Sm* factor	*Gm* factor	Reference
Faldumbach	Runoff was one month too early	+0.04 m^3/s	not applied	no ice	FER
Dornbach	not applied	-0.02 m^3/s	0.8	no ice	FER
Ferdenbach	Runoff was one month too early	+0.07 m^3/s	not applied	no ice	FER
Gisentella	not applied	+0.02 m^3/s	0.7	1.0	BLA
Uistre Talbach	not applied	+0.02 m^3/s	0.8	1.5	BLA
Innre Talbach	not applied	-0.03 m^3/s	0.8	1.5	BLA

lar to Faldumbach, also Dornbach receives no input of ice melt. Because the model overestimated the runoff, a negative basal offset was applied. In comparison to Faldumbach, the *Sm* is modelled to peak already in June (Faldumbach: July). Ferdenbach reveals a similar runoff pattern as Faldumbach with a higher amount of water (nearly double). The small existing glaciers in the catchment of Ferdenbach are neglected and therefore not calculated.

Gisentella can be located not only geographically but also based on the runoff pattern between

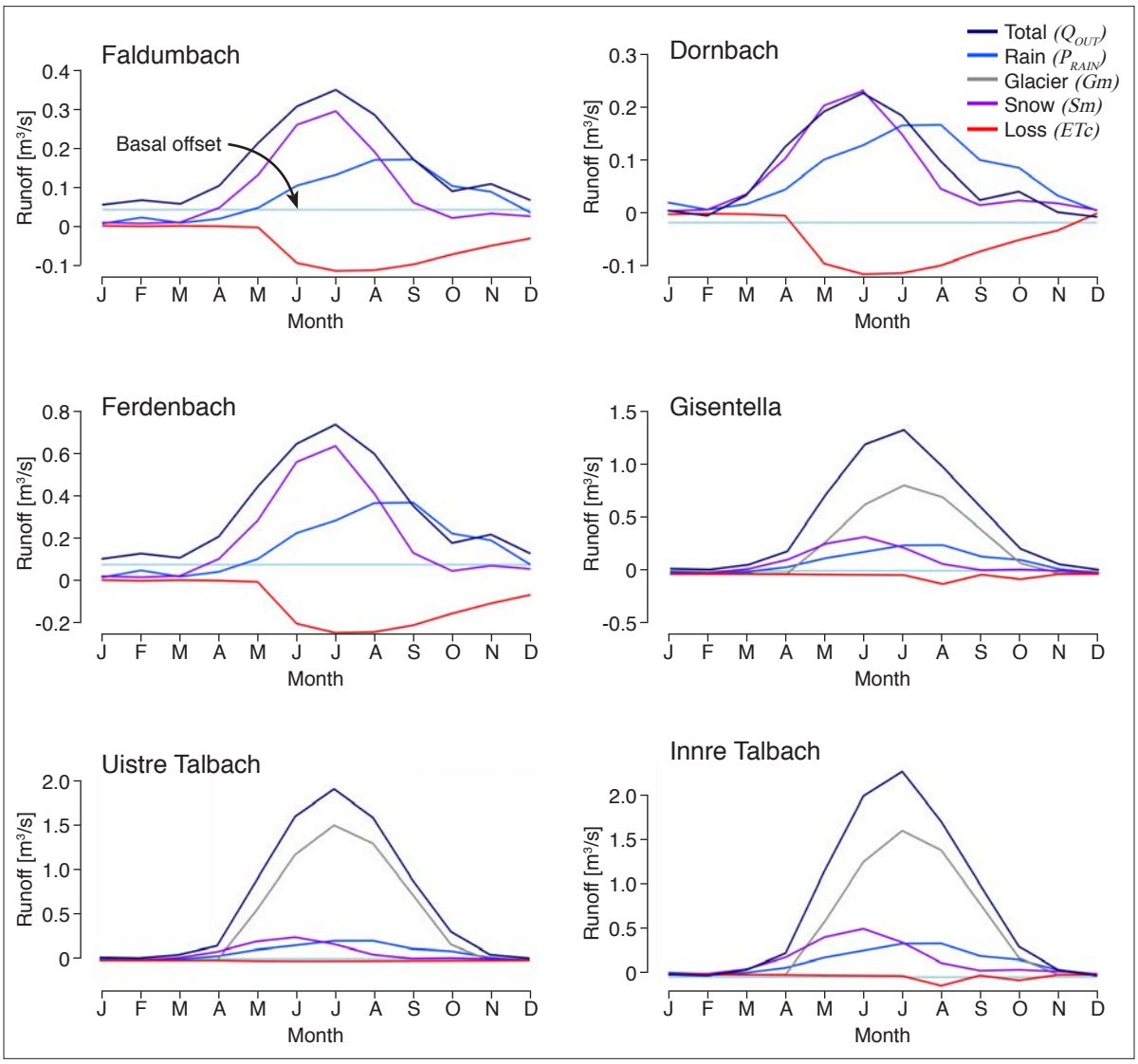

FIG. 31: Overview about the modelled runoff patterns of the tributary torrents on the north side of the Lötschental today. The lightblue line indicates the applied basal offset. (Source: own graphs)

Ferdenbach and Uistre and Innre Talbach. The runoff of Gisentella is relatively similar to the runoff model of BLA. Uistre and Innre Talbach are influenced by huge amounts of Gm. Therefore both reveal a strong increase during May with a peak in July. Innre Talbach has more Sm input, but loses more through ETc compared to Uistre Talbach.

3.3.4 Discussion tributary torrents

Because the torrent models are derived from the Lonza model, the pattern is comparable and reveals only the differences which were applied to correlate the given data with the models. Based on the discussion in chapter 3.2.2, the retrieved results are comprehensible and in correlation to the already named scientific researches (COSTA et al., 2018; FARINOTTI et al., 2011; SEIBERT et al., 2014). Nevertheless some calculations show differences in the monthly values of up to 400 % (see FIG. 32; Dornbach, Uistre and Innre Talbach) which have to be discussed.

Time offset

The main criteria which led to a shift of the whole modelled time series, especially for lower catchments, is based on Sm. It is questionable how useful it is, to shift a time series of runoff patterns to

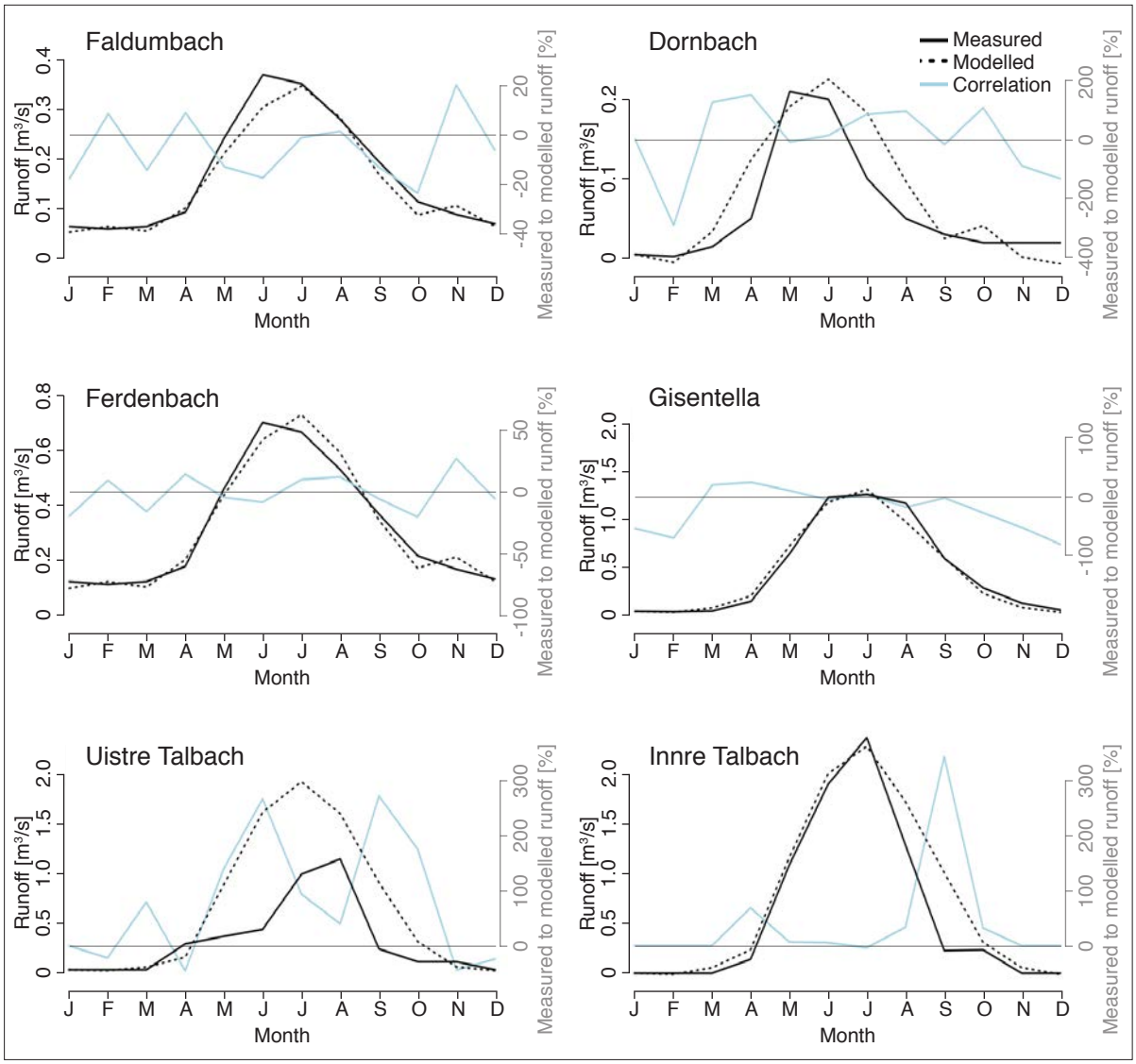

FIG. 32: Comparison between the measured and the modelled values of the tributary torrents, Included is the relative offset between the two curves (shaded). (Source: own graphs)

adapt themself. Based on solar radiation and other environmental conditions, it is assumed that Sm is able to set in at different times within a single catchment in dependency of the catchment size. The Lötschental with its powerful gradients and shading effects in northwest-southeast direction is predestined for delayed runoff scenarios. But the catchments of Faldum- and Ferdenbach are not comparable to the main valley. They have a terrain opening in direction east-northeast and do not reveal any steep flanks which would delay Sm in such a severe manner. The in between lying Dornbach was calculated without a time shift and shows a high grade of correlation. Therefore the fact that the snow melt begins with one month delay compared to the other torrents, does not make sense, but fullfils the aim to fit with the given data. Faldum- and Ferdenbach are modelled with the lowest offset in correlation to the measurements.

Basal offset

The basal offset is applied to minimise a systematic error. The particular offsets reflect 24 % (Faldumbach), 33 % (Dornbach), 22 % (Ferdenbach), 31 % (Gisentella), 6% (Uistre Talbach) and 5 % (Innre Talbach) of the measured mean runoff. The percentages correspond to the different system parameters. Uistre and Innre Talbach are mainly dominated by a glacial runoff, while lower catchments reveal different traits and therefore uncertainties in the attribution to the parameters.

Factors - Sm and Gm

The factors influence the domination of a certain parameter. The domination of a process is based on different environmental conditions: while the catchment of Lonza covers a large area and differences can be equalized, smaller catchments are more affected by small changes.
In respect to the assumed precipitation patterns in the Lötschental (western part is more humid than the eastern part), the runoff of the catchments has to be affected by those processes in the same way. A Gm factor was applied for the three glaciated catchments. Uistre and Innre Talbach reveal a huge offset (around 300 %) in September, which is assumably based on the influence of P_{Rain}; the used factor for snow melt led to a good correlation for the Innre Talbach.

Relative offset

The comparison between the measured and the modelled values are mainly based on differences for low runoff volumes which give back a big error for small varieties.

3.4 Model results for future conditions

3.4.1 Results Lonza

The parameter setting of chapter 3.3 was used and no changes were applied. A summary for every modelled catchment is given in FIG. 33. The description of the parameter projections of Lonza for the end of the 21st century is based on FIG. 34.

Rain and P_{Rain}

Up to temperatures of RCP4.5, the fluvial precipitation does not change a lot. The summer runoff decreases in small amounts while the winter runoff increases. The big jump appears between RCP4.5 and 8.5 with relatively stable values during July and September. For FER the mean P_{Rain} runoff increases from 1.06 m^3/s (today) up to 2.52 m^3/s (RCP8.5) and in BLA from 1.06 m^3/s (today) up to 1.37 m^3/s (RCP8.5), describing a total increase of nearly 30 %.

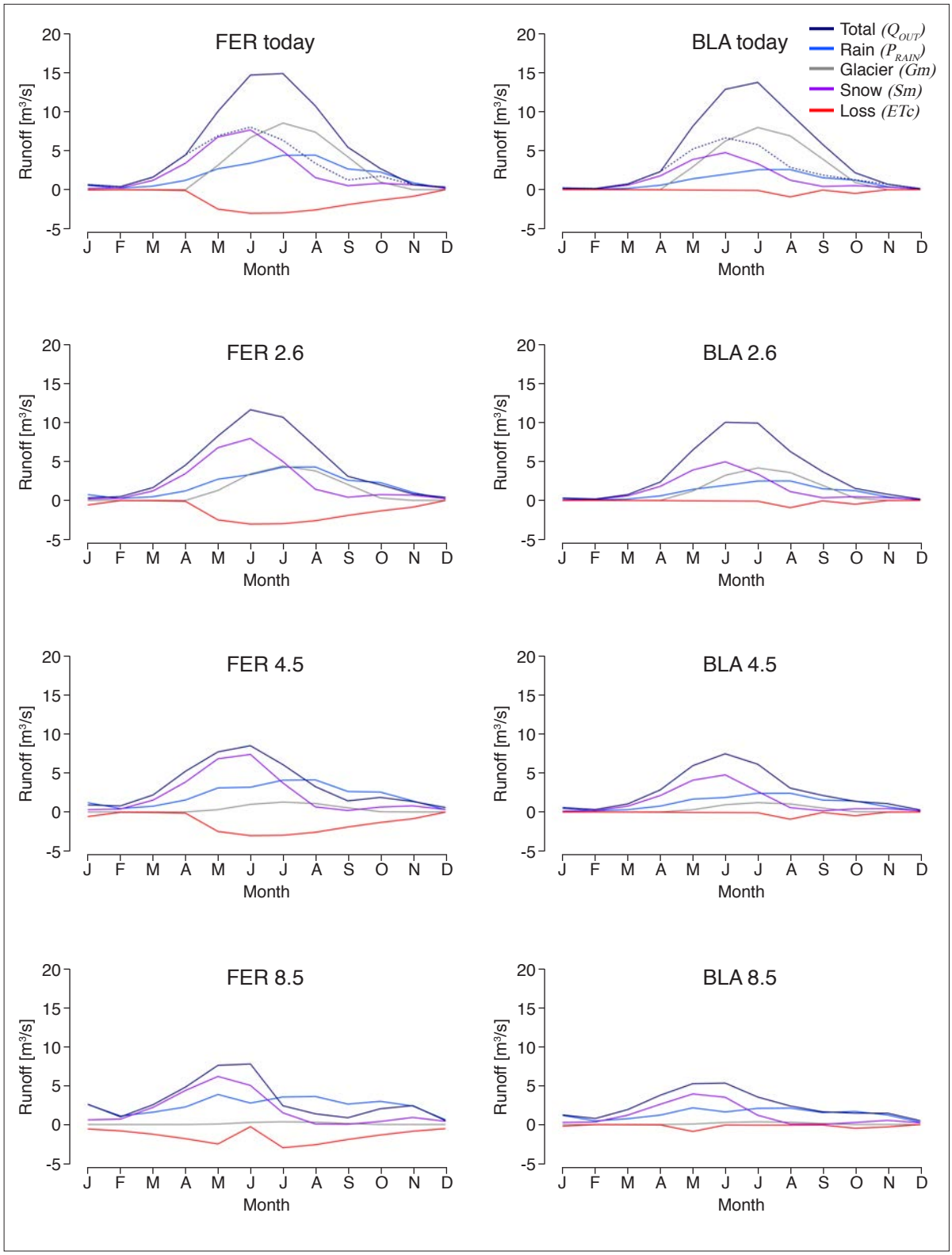

FIG. 33: Overview about the future runoff projections based on the RCP scenarios 2.6, 4.5 and 8.5 (2085). (Source: own graphs)

Snow and *Sm*

The runoff based on snow melt reveals in June a small increase of 1 % for the RCP2.6 scenario, while the other months seem to be stable. RCP4.5 is modelled with a higher runoff from January to May, in June the curve is on the same level as today (BLA) or already below it (FER), followed by less runoff

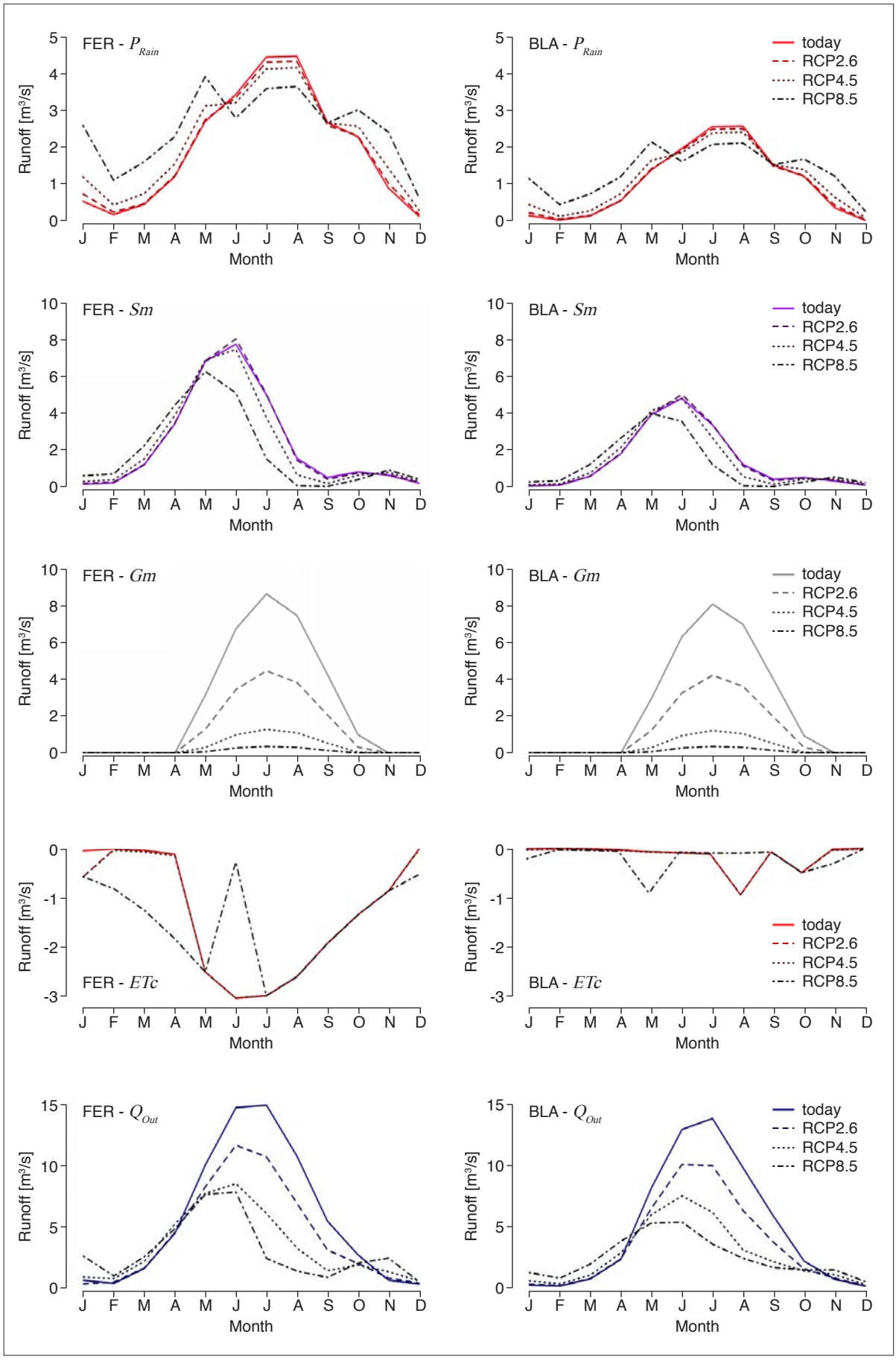

FIG. 34: Modelled parameter projections of Lonza for the end of the 21st century. (Source: own graphs)

during the summer months until October, where the curves begin to exceed the curve of today again. The shift to an earlier and smaller peak is emerged by RCP8.5. FER and BLA reveal the maximum runoff a month earlier in May, with a decrease of 1.47 m^3/s (FER) and 0.82 m^3/s (BLA) accompanied by an increase in January of 0.45 m^3/s (FER) and 0.22 m^3/s (BLA).

Glacier and Gm

The glacier retreat is significant and reveals a fast melt of the ice. With the assumption, that the steady state is reached, the increase of +1.5 °C leads to a coverage loss of around 46 % for both catchments, followed by similar losses if higher RCPs are applied. The altitude related glacier coverage (FIG. 37) shows that the huge ice masses around 3'000 m a.s.l. lead to a delay in the melt signal. While between BLA and FER a difference in the glaciated area of 1.34 km^2 exists today, the difference continuously disappears and is neglectable after a warming of +3 °C from 2018 on.

Loss - Soil and ETc

The ETc projections can be mainly separated into two situations: today and RCP8.5. BLA reveals a shift in maximum ETc from August (today) to May (RCP8.5) including the conservation and small extension from October until February. FER is impacted differently and increases the ETc period from April to December today to a perennial loss in the RCP8.5 scenario, with a strong decrease in July. In BLA, the RCP scenarios 2.6 and 4.5 follow the curve of today, in FER they show differences in January where the ETc increases.

Total runoff - Q_{Out}

The runoff curves show a negative trend for both catchments. Between today and the RCP8.5, BLA loses in average 2.30 m^3/s (today: 4.77 m^3/s, RCP8.5: 2.47 m^3/s) and FER 2.56 m^3/s (today: 5.60 m^3/s, RCP8.5: 3.03 m^3/s). The sum of the runoff reveals the same trend: BLA experiences between today and RCP8.5 a runoff volume loss of -38.4 % and FER of -46.0 %, accompanied by a shift of the maximum runoff from June/ July to May/ June. While the summer months get drier (runoff volume July: -74.26 % BLA / -83.74 % FER) the winter months increase in Q_{Out} (in January minimal a quadruplication). April and October reveal nearly stable conditions between today and RCP8.5.
In BLA the runoff decrease develops constantly from the values of today until the RCP8.5 scenario, FER however decreases until RCP4.5 and while Q_{Out} max in June is nearly constant, the months July to September collapse.

3.4.2 Discussion Lonza

Temperature

Because the temperature values are given data, the results are not discussed widely. The model is based on a homogeneously distributed temperature increase, published by CH2018 (2018). The temperature rise for the western alpine part of Switzerland (CHAW) is estimated to be higher than for other parts of the country (CH: +4.3 °C, CHAW: +4.5 °C for RCP8.5/ 2085). For all scenarios the heating will be stronger during the summer months (June-August) than during winter (December-February) which is represented in FIG. 35 for RCP8.5 (2085).
Beside the mean temperatures, the extreme values also increase significantly. The hottest day of the year is modelled up to +8.7 °C from today's temperatures (CH2018, 2018: 210).

Rain and P_{Rain}

Like for the temperatures, the rates for P_{Rain} changes are given by CH2018 (2018) and are therefore

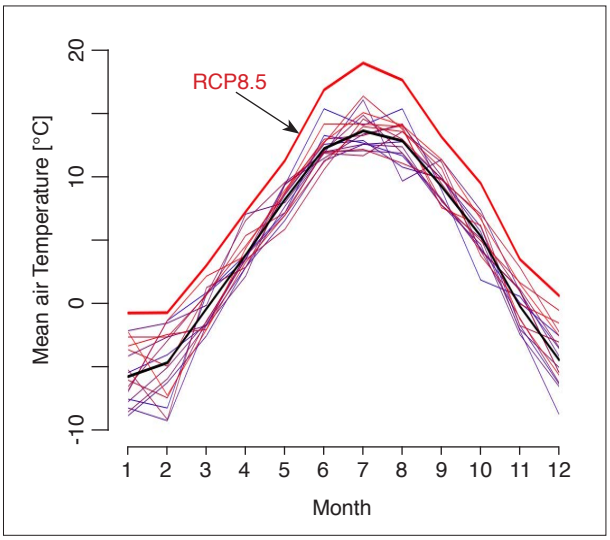

FIG. 35: Modified graph of Blatten after FIG. 04. Shown is the temperature increase following the RCP8.5 (2085) scenario red). (Source: CH2018, 2018 & METEOSWISS, 2019b)

not widely discussed. All in all the result shows a flattening of the curve. Summer months get drier and winter months wetter, while the mean between today an RCP8.5 increases around 30 % (BLA today: 1.06 m^3/s, RCP8.5: 1.37 m^3/s). The fact of increased runoff is well known, variously discussed on scientific platforms (MEEHL et al., 2005 & references therein) and already observed (STOFFEL & CORONA, 2018). But the precipitation events will change in intensity. The global temperature rising is accompanied by an increasing amount of water vapour in the atmosphere (6-7 % per °C) which is expected to be in correlation with future heavy precipitation events (CH2018, 2018). In contrary a trend towards longer periods without rain is expected for future summer. Effects which can not be replicated by the model.

Snow and *Sm*

The shift of *Sm* with a peak a month earlier than today (RCP8.5) is in correlation with the CH2018 (2018: 63): *«The widespread decrease in winter snowfall sums (...) means reduced snow accumulation at the surface; as such, this decrease will influence surface snow cover (...). Furthermore, rising temperatures can be expected to accelerate the melt process and thus the ablation of the surface snowpack.»* But like for the other parameters, the variabilities can not be reproduced with a monthly scaled model. The model itself shows a peak decrease of 0.8 m^3/s (BLA) and 1.5 m^3/s (FER).

The snow melt is mainly depending on the 0 °C altitude which is modelled by CH2018 (2018: 92) around 500 m higher by the end of the century compared to today. While the model is based on a temperature gradient of 0.46 °C/100 m, the CH2018 (2018) report applied a lapse rate of 0.5-0.67 °C/100 m which results in different outputs. Here the steady state assumption of the model limits the output. The projection by CH2018 (2018) reveals significant changes below 2'000 m a.s.l. (up to -80 % of snow fall) which can not be described by the model.

Glacier and *Gm*

Like *Sm* the glacier melt is based on the temperature and on the corresponding ELA. The model is based on a relative glaciated area distribution below the ELA to describe a possible delay in ice melt. This fact reveals assumably wrong results due to the fact, that all other parameters are calculated with a steady state scenario. If applied the glaciers would be totally disappeared. The model for example calculates small remnants of Petersgrat at 3'000 m a.s.l. if the ELA already climbed to 3'300 m a.s.l. (FIG. 36). Going stringent with the steady state presetting, the glacier should not be included. Because this scenario is highly unrealistic, *Gm* was assigned to bridge the differences between the model environment and the real occuring processes in a timid way. The model is seriously affected by the fact, that the melt is based on a DDF_{ice} which is homogeneously applied on a glacier surface without a three dimensional extension, but limited by the ELA. Due to the complexity of the model, and the aim

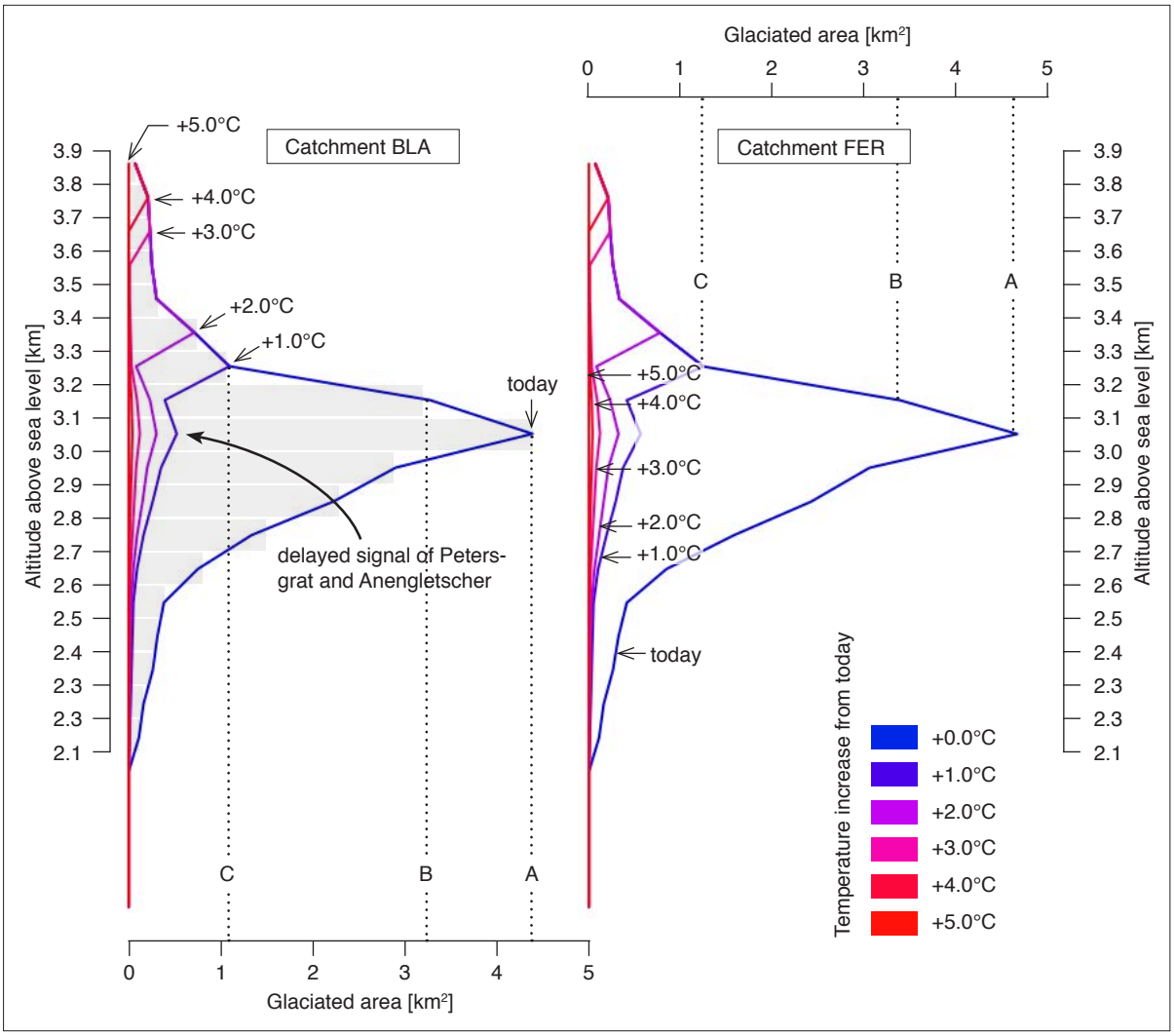

FIG. 36: Glacier hypsography in correlation to the RCP scenarios. The modelled glacier retreat shows a delayed melt around 3'000 m a.s.l. based on the concentrated ice masses at this altitude (see chapter 2.3). One of the main contributors is the Petersgrat. A rapid ice loss in the early stages is recognisable which leads to a foregoing increased fluvial runoff in the rivers in the Lötschental. The marked points (A to C) act as reference. Because a graph only based on bar plots would not be readable, they are replaced by mean altitude points which are connected (illustrated by the shaded bars). (Source: own graph)

of giving a future perspective and not a real prediction of a time related situational description, this approach reveals a sufficient grade of detail. The final result, that the glacial coverage will be disappeared until the end of the century (RCP8.5) due to an ELA above the maximum topographic altitude, corresponds to the calculations by FARINOTTI et al. (2011). It is speculated that the DDF_{ice} also reveals an increase due to higher solar radiation, higher temperatures and less snow coverage.

Including the discussed uncertainties, the results are comparable to other scientific researches (FARINOTTI et al., 2011; HUSS et al., 2010; LINSBAUER et al., 2013).

Loss - Soil and *ETc*

The model does not include any groundwater existence (see chapter 2.5) but based on the geology it can be assumed, that during heavy rainfall events a delayed signal is created through the subsurface flow in the sediments. The revealed 78 m depth in Blatten (see chapter 2.4) could include a periodically ground water storage. Some of the discussed flat areas behind the debris cones (chapter 2.4) show indications of mire and therefore the possibility of (sequentially) ground water existence

(JUTEBRING et al., 2018). The evapotranspiration however reveals an interesting result. This pattern is based on the calculation method with different inputs for Kc values which seems to be erroneous, even though it describes the vegetated areas in a comprehensible manner. Here the detailed analysis would go beyond the scope of this thesis. But the increased temperature has a significant impact onto the vegetation which was modelled by RÖSSLER et al. (2012) for the Lötschental. They could show that especially below 1'800 m a.s.l. the vegetation will be exposed to increasing droughts. Here the model is not useful and assumably affects the accuracy of the result in a negative way. For future projections the Kc value should be changed due to changes in the surface vegetation (higher tree line) which was not applied in the present study and therefore influenced the model output.

Total runoff - Q_{Out}

The total runoff shows the assumed results and BLA reflects a more glaciated area than FER. For the RCP8.5 scenario of BLA, the peak in July decreases more than 50 % to June and FER reveals around -50 %, describes a peak in May which is similar to the RCP4.5 scenario. The retrieved runoff pattern is comparable to FARINOTTI et al. (2011) who analysed the catchment of Aletschgletscher and the result correlates with the depicted future scenarios of CH2018 (2018). For BLA also a flattening of the runoff peak can be seen which illustrates the loss of glacier ice in the catchment. The catchment differences between RCP4.5 and 8.5 during spring can be explained with the increasing input of P_{Rain} and the decreasing Sm runoff. BLA is higher and receives more Sm than FER, therefore FER is more influenced by rain, why BLA still shows a snow influenced catchment.
Due to the steady state assumption, the short-time increased runoff based on higher melt rates called «peak water» (HUSS & HOCK, 2018) is not reproduced.

3.4.3 Results tributary torrents

To model future projections of the tributary torrents, the results of chapter 3.3.3 were multiplied with the respective RCP factors (APP-C4). The results (FIG. 37) can be separated into two groups: one group is modelled without (Faldum-, Ferden-, Dornbach) and one group with glaciers (Gisentella, Uistre & Innre Talbach).
The first group is exemplarily described by the Faldumbach: Between today and RCP2.6, the river receives only minor changes (maximal -8 % in December) which begins to differ for RCP4.5 where the months July to September are up to -44 % below today (August). In this scenario May reveals a similar value like today and the winter and early spring months (November - April) show a positive trend of around +5 %. December is the only month with a severe negative result of -36 %. The maximum peak jumps from 0.35 m^3/s (today) to 0.28 m^3/s. For RCP8.5 the peak in June reveals the same runoff as for RCP4.5. August decreases for additional -30 % and reveals only 0.07 m^3/s, compared to 0.28 m^3/s today. It is the driest month of the summer which is followed by a relatively stable fall and a runoff of around 0.1 m^3/s. In November Faldum- and Ferdenbach reveal a significant negative Q_{out}, while Dornbach indicates a small negative balance.
The second group shows a steady decrease in runoff and is discussed on Innre Talbach: compared to Faldumbach, Innre Talbach reveals already a reduced runoff for RCP2.6 (-30 % in June) while the months November-April are congruent. For the RCP4.5 the peak shifts from July to June and decreases from 2.29 m^3/s (today) to 0.91 m^3/s (RCP4.5) while August loses -74 % of the runoff. In spring the runoff increases in small amounts (March: +33 %). Compared to RCP4.5, RCP8.5 reveals less decrase, nevertheless, the comparison with today shows significant runoff changes. While today

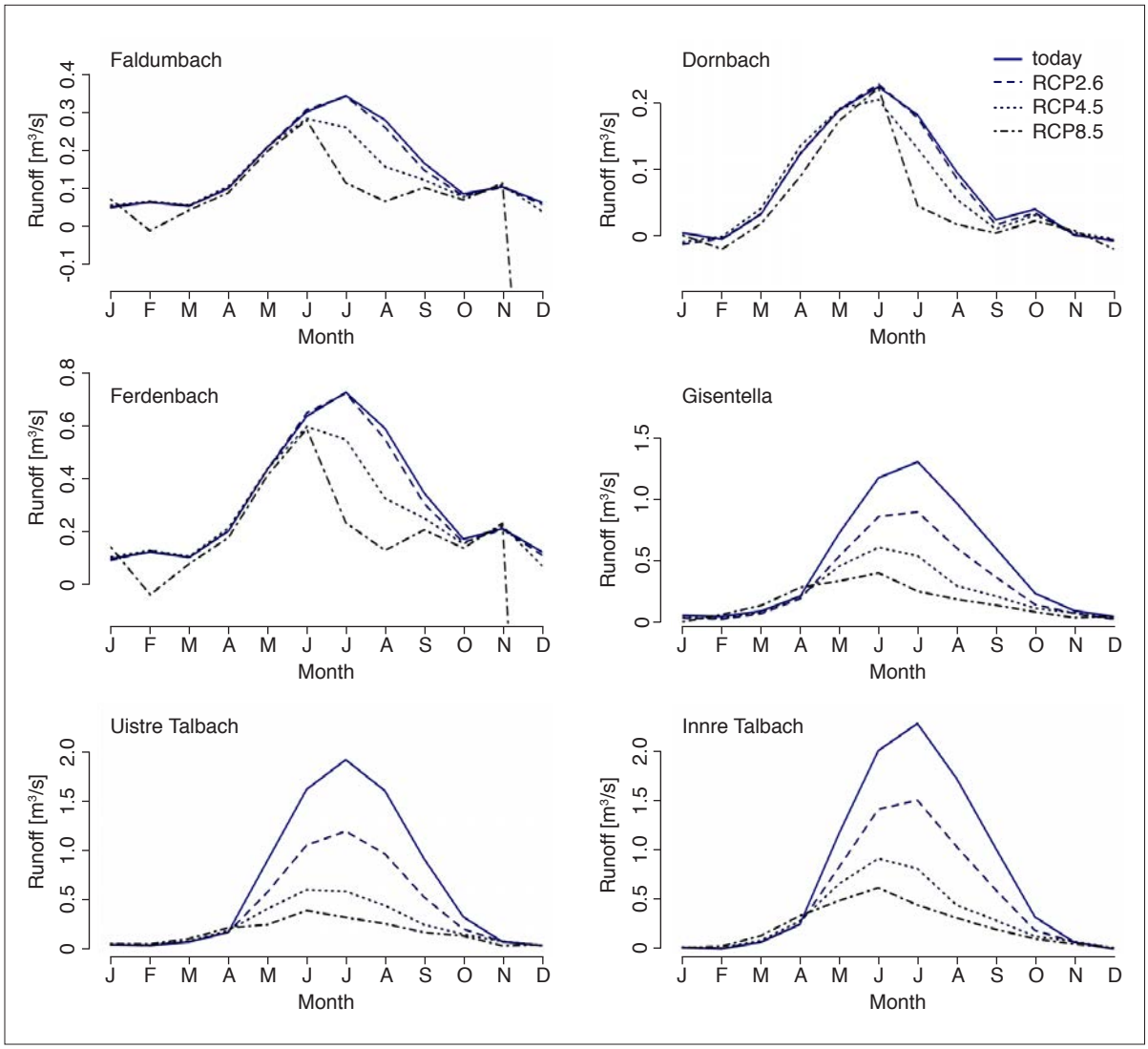

FIG. 37: Modelled Q_{Out} projections of the tributary torrents. (Source: own graphs)

in March 0.06 m³/s are measured, the RCP8.5 scenario calculates an increase of 119 % to 0.12 m³/s. On the other side, the summer months lose up to 82 % (August today: 1.72 m³/s, RCP8.5: 0.3 m³/s).

3.4.4 Discussion tributary torrents

The results illustrate the applied catchment specification (FER / BLA) and are therefore similar to the result of Lonza. Nearly every catchment reveals a shift for the maximal runoff from July to June with the exclusion of Dornbach, where no time offset was applied. Based on the calculated data, the model retrieved no ETc for June and therefore the missing loss resulted in an overestimation of the total runoff. It can be assumed, that with the application of the missing ETc the runoff of Dornbach would resemble the one of Faldum- and Ferdenbach. Because the applied factors are based on the main catchments FER and BLA, altitude depending factors like Sm are crucial. Because the mean altitude of Faldum-, Dorn- and Ferdenbach are lower (maximum 2‘244 m a.s.l.) than the one of FER (2‘507 m a.s.l.), the Sm runoff is overestimated for future projections. For November and December the model reveals also wrong results due to the fact that ETc increases in an unrealistic way and the total runoff becomes negative. The same issue can be seen in February. Why in February the ETc projection is erroneous can

not be specified but it is assumed, that the applied factors are misleading. Nevertheless, the reduced runoff of 0.1-0.2 m^3/s illustrates the snow and rain depending catchment and is in correlation to BAVAY et al. (2013) and FARINOTTI et al. (2011).

Based on the glacier retreat, the glaciated catchments react stronger to the RCP scenarios. The results are comparable to the runoff calculations at Rhonegletscher by HUSS et al. (2010) who retrieved a peak shift from from July to end of May and a decreased runoff volume of around -94 % (Innre Talbach: -82 %) between today and their most severe scenario (similar to RCP8.5). Due to the applied factor to project future developments, the torrents still reveal some Gm runoff (Innre Talbach: 20 % of total runoff) which is, compared to the result of Lonza with a zeroed Gm, an overestimation. The increased runoff in spring is in correlation to other researches (FARINOTTI et al., 2011; BAVAY et al., 2013).

3.5 Today versus future

The water availability will change significantly in the future. While the glaciated catchments (Gisentella, Uistre & Innre Talbach) lose around -70 % of the mean runoff, the snow and rain dominated areas (Faldumbach, Dornbach, Ferdenbach) reveal -40 % less runoff during the year (FIG. 37). Regarding the seasons, the changes affect mostly spring, summer and fall. Winter is constant with small differences and a small increase in total runoff.

Regarding water supply the increase in winter is positive for the winter tourism in the valley. The additional amounts of water are needed to compensate the missing natural snow. But the rising temperatures can also reduce the capability of snow production during warm winter days. The higher amounts of fluvial precipitation can lead to a fast runoff if snow packs are missing. Therefore water collection basins are presumably needed in the near future.

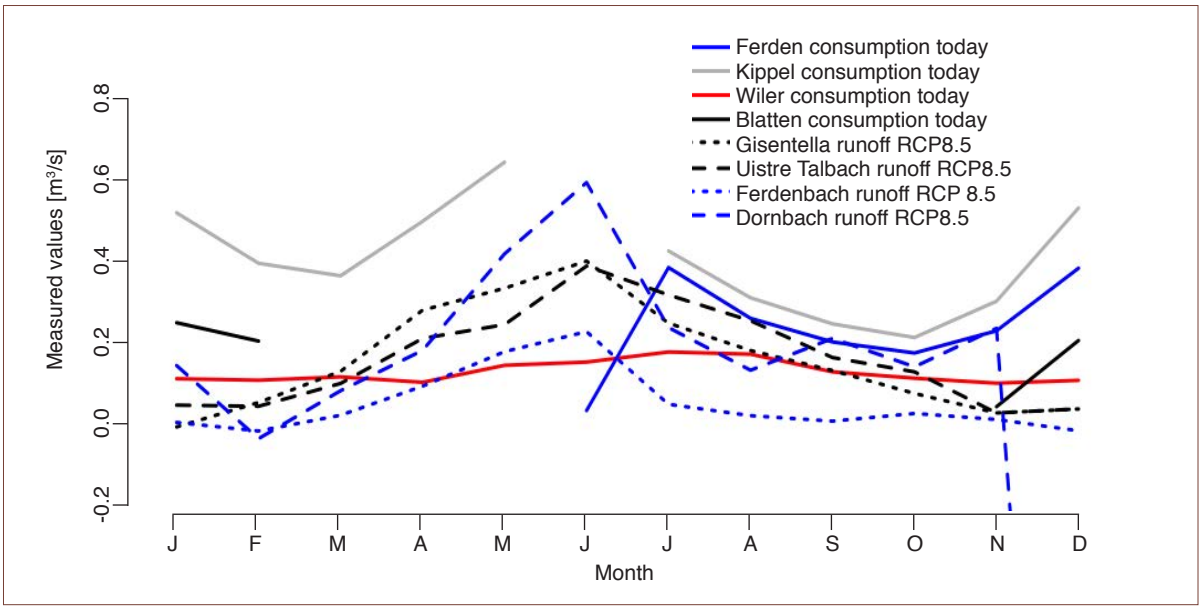

FIG. 38: Correlation between the water consumption of today and the modelled RCP8.5 scenarios for specific tributary torrents. Ferden uses springs in the area of Ferdenbach and Dornbach, while Uistre Talbach drains beneath the spring Chaltr Brunn of Blatten. Gisentella acts also as indicator for the future runoff signal in the area of Blatten. For Kippel and Wiler, no data regarding tributary torrents was available. A future water scarcity can be interpreted. (Source: municipalities & own data)

The decrease in summer can affect the valley in a severe way. The loss of up to -50 % of the average runoff (-80 % in summer) for Lonza in BLA illustrates the significant changes based on glacier loss (FIG. 34). Uistre Talbach as indicator for the source Chaltr Brunn in Blatten reveals a runoff loss of up to -84 % in August, which impacts the local population and tourists (FIG. 37). Based on a daily consumption of 1‘900 litre per person (see chapter 2.5) and a population of 350 people, Blatten has a daily usage of 665 m^3. Today this volume is transported by Uistre Talbach within five minutes (July) and will increase for the RCP8.5 calculations up to 35 minutes.

In FIG. 38 the consumption of the municipalities is correlated with the modelled runoff volumes of spring-similar tributary torrents at the end of the 21st century (RCP8.5). Uistre Talbach and Gisentella act as indicator for the spring Chaltr Brunn of Blatten, while Ferdenbach and Dornbach reveal informations about the springs used in Ferden. Even if the data base is not sufficient and the models reveal high uncertainties, critical phases during winter can be recognised. Also in the summer months an approximation of the graphs can be seen. CH2018 (2018: 10) states: *«The long-term trend will be associated with high variability, and heavy rainfall will continue to occur on an irregular basis. The intensity of peak events will increase much more strongly than mean precipitation and may increase even in seasons with decreasing mean precipitation.»* Based on this, the valley will be confronted with longer dry periods and heavier rainfall events which lead to strong runoff variabilities and a possible drop below the minimum runoff volume needed. The shown monthly averaged values in FIG. 38 can not illustrate short-time fluctuations and therefore, a water scarcity can not be pictured for the future specifically - but it also can not be ruled out. Here, the critical point of «peak water» would give a good indication about the relative processes and could help to classify future measures.

4 SEDIMENTS

4.1 Study area

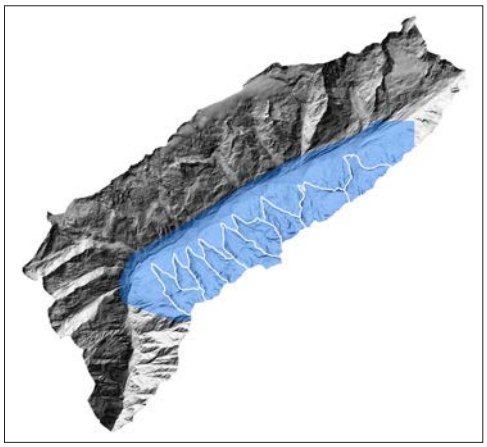

FIG. 39: Overview about the study area for the sediment analyses (blue shaded). The white outlines illustrate the specific catchments. (Source: SWISSTOPO, 2018a)

The study area (FIG. 39) is located on the north face of the Bietschhorn ridge and covers around a third of the valley area (48 km^2). It focuses on the catchments of Gitzi-, Bätzla-, Wiler-, Tänner-, Näst-, Birch-, Stamp-, Loibin- and Beichbach. Due to the orientation of the valley and the steep slopes, the area is shadowed a long time of the year.

In the study area 3.11 km^2 are glaciated, 1.71 km^2 are covered by trees and 2.43 km^2 by grass and bushes. The biggest percentage is characterized by bedrock (7.44 km^2) and debris cover (5.63 km^2). The south side is strongly affected by mass movements like avalanches and debris flows. Especially massive debris flows, sometimes in correlation with floods, represent a huge problem. The municipality of Blatten invested already over 3 million Swiss francs into prevention measures in their district.

4.1.1 Catchment description

Gitzibach

The most south-eastern catchment of the north faced Bietschhorn flank, is the one of the small river Gitzibach. The catchment has its apex at 1‘430 m a.s.l. and reaches up to Chastlerhorn and Hogleifa (highest point at 3‘278 m a.s.l.). The area is «L» shaped and can be sectioned into two parts: The lower part is defined by the straight line from the Apex via Gitziwanne up to the top of Discheltschuggen at 2‘340 m a.s.l. (FIG. 40). It is confined on the left side by the Gattunmandli and on the right side by the Bätzlerigg. From there on the catchment turns eastward and a wide goblet opens. It is limited by the Opental on the east following up the ridge until the point 2‘799 m a.s.l. and then turning south again to north eastern ridge of Hogleifa. On the western side, the north-western ridge of Hogleifa limits the catchment of Gitzibach. In total it covers an area of 2.17 km² whereof 0.7 km² are vegetated (trees, bushes and grass) and 1.46 km² are dominated by bedrock or debris. Ice is only in small amounts at G1 present (0.01 km²) (FIG. 41).

GEOPLAN AG (2007) registered in the year 2000 a flooding event and estimated the maximal transportable solid capability of a debris flow to 4‘000-5‘000 m³ (EHQ).

Bätzlabach

The catchment of Bätzla is the smallest on the northernly Bietschhorn flank (1.05 km²) and also the one with the smallest elevation difference between apex (1‘500 m a.s.l) and the the highest point (2‘684 m a.s.l.). The catchment includes the south-westerly located trough called Bätzlerfridhof at 2‘247 m a.s.l. (FIG. 40). The area is covered by 0.27 km² trees, 0.41 km² bushes and grass, 0.11 km² bedrock and 0.26 km² debris and is limited above 2‘200 m a.s.l. by the westerly Bätzlerrig and the Uistre Wilerrigg on the eastern side. There is no ice present (FIG. 41).

GEOPLAN AG (2007) registered no events and estimated the maximal transportable solid capability of a debris flow to 4‘800-7‘600 m³ (EHQ).

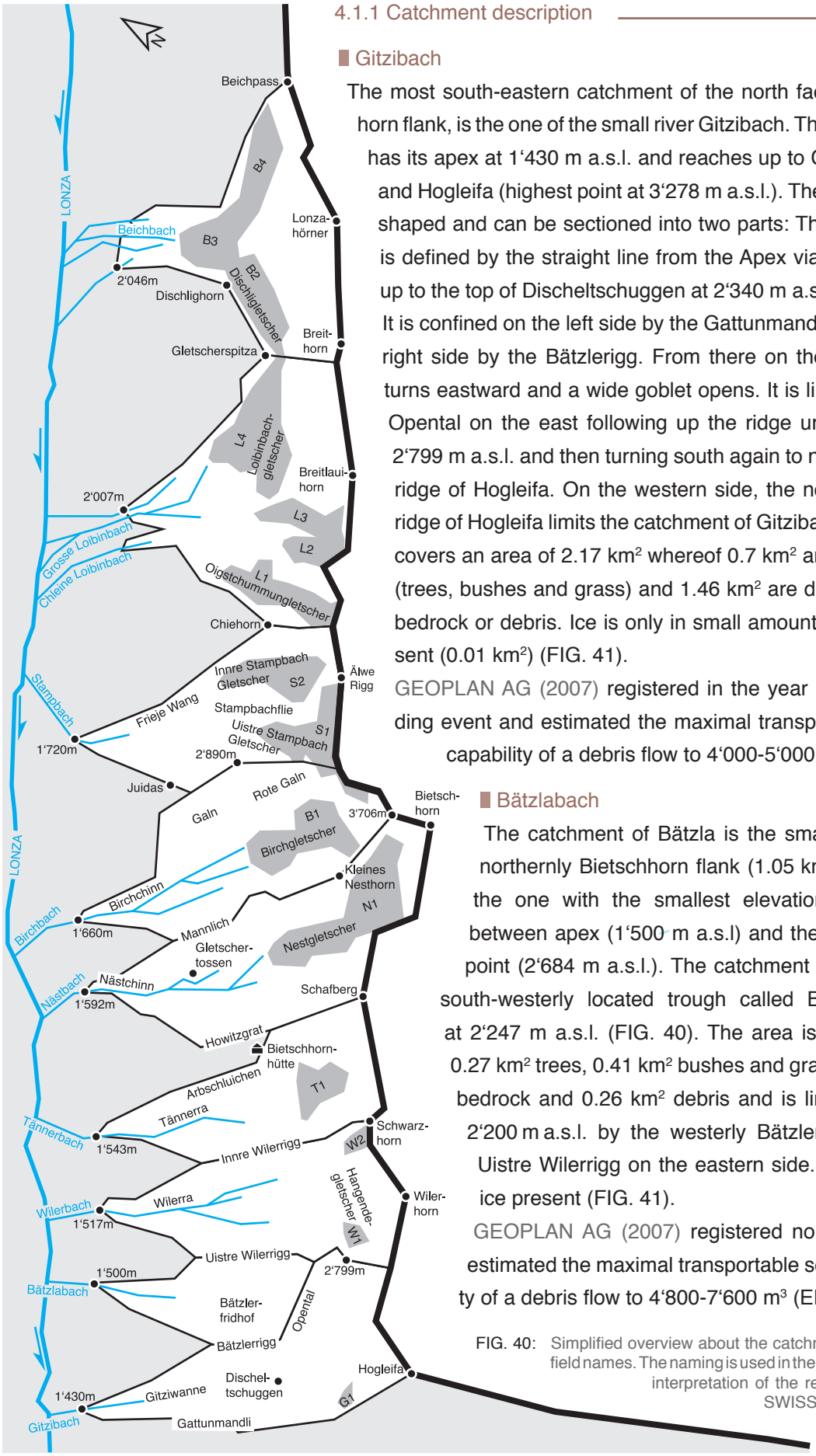

FIG. 40: Simplified overview about the catchments and their field names. The naming is used in the description and interpretation of the results. (Source: SWISSTOPO, 2018a)

Wilerbach

The Wilerbach is fed by a nearly symmetrical catchment. It is limited by the Wilerhorn (3‘307 m a.s.l.) in the south east, by the Uistre Wilerrigg (west) and the Innre Wilerrigg (east) and ends with the apex at 1‘517 m a.s.l. (FIG. 40). Between the apex and 2‘100 m a.s.l. the river flows through a narrow gorge (Wilerra) which opens up at 1‘900 m a.s.l. The whole catchment is 2.19 km^2 big and is mainly covered by bedrock (0.82 km^2) and includes the small Hangende Gletscher and an ice field on the north side of Schwarzhorn (in total 0.08 km^2) (FIG. 41).
GEOPLAN AG (2007) registered between 2003 and 2007 three debris flow events and estimated the maximal transportable solid capability of a debris flow to 13‘000-15‘000 m^3 (EHQ).

Tännerbach

From 1‘543 m a.s.l. the catchment reaches up to the Bietschhorn ridge, defined by Schafberg (3‘240 m a.s.l.) and Schwarzhorn (3‘114 m a.s.l.). On 2‘700 m a.s.l. remnants of a former glacier are located (T1) which draines between the Innre Wilerrig (left) and the Arbschluichen (right) through the narrow gorge of Tännerra into the the valley floor (FIG. 40). The catchment covers nearly 2 km^2, whereof 0.57 km^2 are vegetated (trees, bushes and grass), 0.69 km^2 are debris covered and 0.06 km^2 are ice, 0.67 km^2 are massive bedrock (FIG. 41).
GEOPLAN AG (2007) registered between 1950 and 2007 seven events (floods and debris flows) and estimated the maximal transportable solid capability of a debris flow to 90‘000-100‘000 m^3 (EHQ).

Nästbach

The 2.76km^2 large catchment of Nästbach begins in the south east at 3‘901 m a.s.l. near the Bietschhorn summit and steeply descends between Schafberg (3‘240 m a.s.l.) and Kleines Nesthorn (3‘336 m a.s.l.) in north westerly direction and turns more northward at around 2‘900 m a.s.l. The contained Nestgletscher (N1) reaches from 3‘500 m a.s.l. nearly 1‘000 m down and draines between Howitzgrat (west) and Mannlich (east) through the Nästchinn gorge and apex (1‘592 m a.s.l.) into Lonza (FIG. 40). With 2‘309 m difference in altitude, it is the catchment with the largest drop between the highest point and the apex. It includes 0.23 km^2 trees, 0.34 km^2 bushes and grass, 0.97 km^2 rock face, 0.68 km^2 debris cover and 0.54 km^2 ice (whereof 0.14 km^2 are covered) (FIG. 41).

Birchbach

The catchment of Birchbach ends at 1‘660 m a.s.l. at the apex near Blatten. Beside the Nästbach catchment, also the Birchbach catchment origins from the Bietschhorn at an altitude of 3‘706 m a.s.l. and includes the 0.38 km^2 large Birchgletscher (B1). It is located between Rote Galn (right) and Kleines Nesthorn (left). The glacier drains between Galn (east) and Mannlich (west) via Birchchinn into Lonza (FIG. 40). Beside the glacier, the catchment area is covered by trees (0.19 km^2), bushes and grass (0.31 km^2), bedrock (0.82 km^2) and debris (0.78 km^2) (FIG. 41).
GEOPLAN AG (2007) registered two debris flow events (1989 and 2007), followed by a third in 2013. The maximal transportable solid capability (EHQ) of a debris flow is estimated to 80‘000 m^3.

Stampbach

The Stampbach catchment (2.07 km^2) is dominated by the Innre (S2) and Uistre (S1) Stampbach glaciers which are separated by the Stampbachflie. On the highest point of the catchment, Älwa Rigg (3‘381 m a.s.l.) marks the south-eastern catchment border (FIG. 40). The glaciers cover nearly a fourth of the whole area (FIG. 41), while the main cover is based on debris (0.69 km^2) and bedrock (0.73 km^2). Below Frieje Wang, only small patches of trees can be found (0.1 km^2) until the lowest point is reached

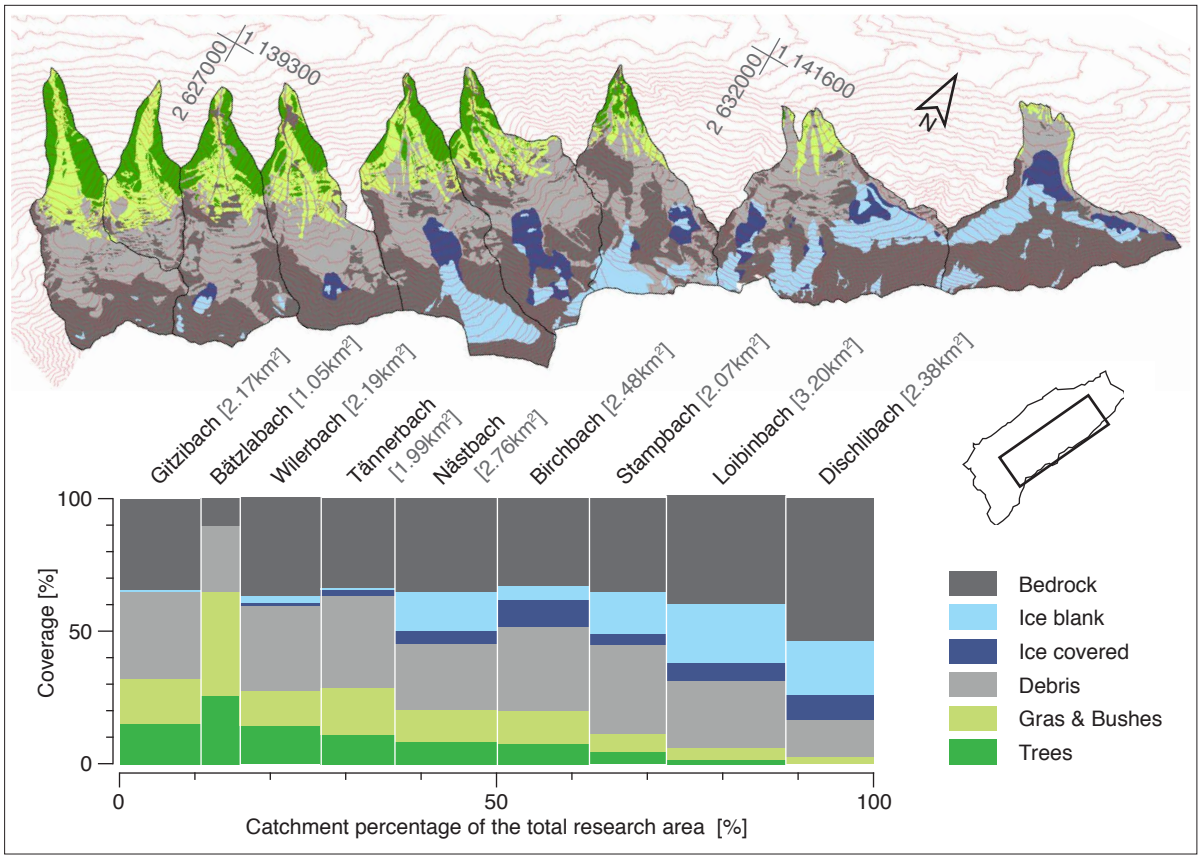

FIG. 41: Overview about the coverage of the analysed catchments. The mapping is based on the orthophoto of 2014 (Source: SWISSTOPO, 2018a) while the ice covered areas are defined in accordance to field work during July and September 2018. Due to rounding of the coverages, the different catchments do not always reveal a total coverage of exactly 100%. (Source: own illustration)

at 1‘720 m a.s.l. Stampbach is the catchment with the highest activity of debris flows. GEOPLAN AG (2007) registered eleven debris flow events between 1978 and 2007, followed by seven cascading events between the 7th of July and the 10th of August 2015. GEOPLAN AG (ibid.) estimated the maximal transportable solid capability of a debris flow to 90‘000 m³ (EHQ).

Loibinbach

The big (Grosse) and small (Chleine) Loibinbach are fed by the largest catchments of the investigated area (3.2 km²) and include the highest amount of glaciated area (0.93 km²). The triangular catchment is located on the north face of the Breitlauihorn (3‘655 m a.s.l.) which reveals the Oigstchummungletscher (L1), Loibinbachgletscher (L4) and two other ice fields (L2 and L3). They are situated between the Chiehorn (left) and the Gletscherspitza (east), both on a similar altitude of around 3‘060 m a.s.l. (FIG. 40). The broad catchment narrows until 2‘200 m a.s.l. where it is separated into an eastern and western apex, which represent the outflows of the two rivers. Because no distinct apex could be estimated, it is defined on an altitude of 2‘007 m a.s.l. The Chleine Loibinbach also includes a block glacier with a tongue altitude at 2‘050 m a.s.l. Due to the fact that the vegetated area is nearly inexistent (0.2 km²), the main area is dominated by the north face of Breitlauihorn with 1.3 km² of pure rock face (FIG. 41). GEOPLAN AG (2007) registered for the Grosse Loibinbach one debris flow event in 1944 and for Chleine Loibinbach three events (1944, 1993 and 2000), whereas the catchments are not always clearly differentiable. They estimated the maximal transportable solid capability of a debris flow for the whole Loibinbach catchment to 45‘000-50‘000 m³ (EHQ).

Beichbach

The Beichbach catchment is the most eastern one of the investigated area and covers 2.38 km^2. It reveals the form of a reversed «T» (FIG. 40) which is limited by the ridge from the Breithorn (3‘785 m a.s.l.) to the Beichpass (3‘128 m a.s.l.) and steeply descends into the glaciated areas of the western Dischligletscher (B2), the eastern glacier area B4 and the glacier tongue B3 (in total 0.7 km^2). At the altitude of Dischlighorn, the catchment turns into a northerly direction with an apex at 2‘046 m a.s.l.
The catchment is sparsely vegetated (0.07 km^2) and reveals large amounts of bedrock (1.28 km^2) and debris coverage (0.33 km^2) (see FIG. 41).

4.2 Data and methods

To evaluate possible surface processes and displacements on the southern valley side, the difference between two DEMs was calculated. The so-called «DEM-differencing» is variously used, especially in volume change assessments regarding surface shifts in geomorphology, hydrology or glaciology (e.g. ADAMS et al., 2016; BÜHLER et al., 2016; FISCHER et al., 2014).
The applied process is illustrated in FIG. 42 and shows the used DEMs. DEM18 originates from 2018 and is retrieved out of this thesis. After an introduction into the process of «Structure from Motion», the different steps of the applied methodology are explained.

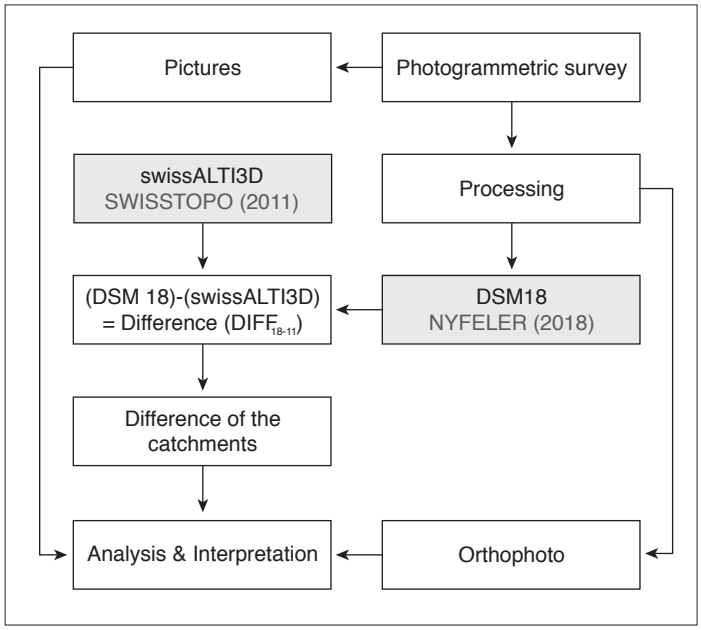

FIG. 42: Process for DEM-differencing. (Source: own diagram)

4.2.1 Structure from Motion (SfM) photogrammetry

In alpine regions the data acquisition of surface data is challenging. Steep slopes and lacking satellite coverage hinder precise measurements by GPS. Other terrestrial methods like laser-scanning are very expensive and impractical due to their equipment masses. WESTOBY et al. (2012: 301) states: *«Airborne surveys, including LiDAR and photography are also of restricted use due to the high three-dimensionality of mountainous landscapes, which results in significant line of sight losses and image foreshortening. Moreover, deploying survey platforms, including helicopters and smaller scale UAVs at altitude is highly dependent on favourable weather conditions and may often be hampered by high wind speed and cloud cover.»* To avoid high risks, photogrammetry is a reliable method based on stereo-pairs. During the recording process, data of position, time and orientation are collected for each picture to be able to locate it in the three dimensional space afterwards. Out of the given picture references and geolocated Ground Control Points (GCP), which are marked in the photographs, the

terrain model can be calculated. With efficient computer programs and higher processing power, the Structure from Motion (SfM) photogrammetry was developed. It was originally educed to create a three dimensional model out of random pictures showing one object or scene from different point of views (BROWN & LOWE, 2005) and it *«(...) differs fundamently from the conventional photogrammetry, in that the geometry of the scene, camera positions and orientation is solved automatically without the need to specify a priori, a network of targets which have known 3-D positions.»* (WESTOBY et al. 2012: 301). This leads to a much faster, efficient and cost-efficient workflow. Multiple views of the investigated object or area are captured with a camera system from different positions. The used software establishes a *«(...) spatial relationship between the original image locations in an arbitary 3-D coordinate system.»* (MICHELETTI et al., 2015: 2). Based on that, the retrieved three-dimensional locations form a sparse point cloud which operates as fundament for a further more detailed calculation (dense cloud) and ends in the generation of the digital elevation model (DEM). If needed geotagged ground control points (GCPs) can be implemented, to georeference the system even during the process. Because the GCPs also acts as reference for the calculations, their precision is important. Cameras use nowadays internal GPS receivers, to add the location of capture as metadata onto the picture, which also can improve the accuracy of the retrieved DEM.
It is distinguished between the digital elevation model (DEM) which represents the surface without vegetation or buildings (digitally subtracted) and the digital surface model (DSM) which represents the total surface including the structure of objects (e.g. trees, buildings, constructions).

4.2.2 swissALTI3D

The foundation for the research is the swissALTI3D DEM from 2011 which is provided by SWISSTOPO (2018a) and regularly updated.
The DEM in the area of the Lötschental is retrieved out of laser scans (below 2‘000m a.s.l.) and of aerial images (above 2‘000m a.s.l.) with a photogrammetric processing (SWISSTOPO, 2018b). A bad coverage and also the interpolation between the two systems lead to a rough surface with lower resolution in between (FIG. 43). The swissALTI3D has a spatial resolution of 2 m and an uncertainty in elevation of around 0.5 m (SWISSTOPO, 2012). Based on the regular update of the DEM (every 6 years), the DEM of the Lötschental will be refreshed in the next years.

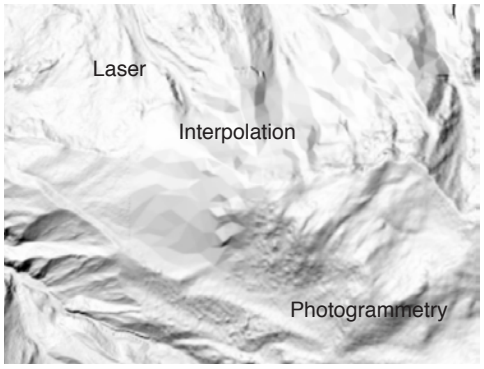

FIG. 43: Low spatial resolution due to lack of coverage or faulty interpolation between the measurement systems. (Source: SWISSTOPO, 2018b)

4.2.3 DSM18

To compare the swissALTI3D with the actual situation, a current DEM / DSM has to be retrieved. Based on the photogrammetry, a DSM is achieved with the following methodology:

Aerial system

To retrieve pictures of the study area in a meaningful time, a fast and reliable system is needed. First, the nearly fully automatic SenseFly eBee Drone developed by senseFly (a former startup of the École Polytechnique Fédéral de Lausanne EPFL) was planned to be in service. But the temporally restricted availability and the limited range of the system, based on battery endurance, led to the decision to look

for alternatives. Finally the decision was made to use a helicopter, since it is fulfilling all requirements regarding efficiency, height and range for the photogrammetric purpose.
The used helicopter is a Robinson R66 (FIG. 44) from the operator Mountainflyers 80 Ltd., located in Bern-Belp. It is a light single-engine turbine helicopter with five seats which is cost-efficient and fast. The photographer sits in the rear and takes pictures out of the left and right hand side.

FIG. 44: The Robinson R66 on the Petersgrat above the Lötschental in early March 2019. (Source: Thomas Graf)

Camera

To get useful results a good ground sampling (GSD) distance is required. The GSD describes *«(...) the distance between two consecutive pixel centres measured on the ground. The bigger the value of the image GSD, the lower the spatial resolution of the image and the less visible details. The GSD is related to the flight height: the higher the altitude of the flight, the bigger the GSD value.»* (PIX4D, 2018c). The camera used is a Canon EOS 5D Mark III in combination with a Canon EF 50 mm lens. The pictures are triggered manually in different angles to get a good coverage of the whole surface. Based on the formula by LISEIN et al. (2013: 4)

$$GSD = \frac{Pixel\ size\ [\mu m] \bullet Flight\ Altitude\ [m]}{Focal\ Length\ [mm]} \qquad (7)$$

and the «GSD calculator tool» developed by Pix4D (PIX4D, 2018a) the following settings led to a theoretically calculated GSD of 9.85 cm:

- Sensor width of the camera: 25.6 mm
- Focal length of the camera: 50 mm
- Assumed flight heigth: 1‘000 m above ground
- Image size (width x height): 5‘200 pixels x 2‘800 pixels
- Calculated GSD: 9.85 cm/pixel
- Calculated image footprint size on the ground (width x height): 512 m x 276 m

Even if it is possible to tag the images with GPS coordinates, the georeferencing of the photographs is not applied. Due to the mountainous and steep area, the GPS signals are probably affected by deflection and would return wrong data. Unfortunately no information about the accuracy of the integrated Canon GPS receiver could be found. But the paper of KÜNG et al. (2012), which appeared in the same year as the 5D Mark III camera, refers to a GPS signal accuracy of 5-10 m of a specialized mapping

drone. Even though the systems are not related, it can be assumed that the latest developments led to a higher precision of the signal. Nevertheless, the accuracy of normal GPS antennas is assumably in the area of meters and therefore not useful to photogrammetric purposes with an aimed resolution of centimetres. Due to the fact that the author is flying the helicopter, a photographer is on board to collect the pictures.

Software

To create the 3D digital elevation model, the Pix4D modelling software is used. Pix4D is a Swiss spin-off of the EPFL which develops specialized software tools for photogrammetric purposes. Based on the existing licenses at the University of Zurich, Pix4D was used for data processing. The EGM96 Geoid acted as reference with the CH1903+/LV95 applied.

DSM generation

Pix4D calculates the DSM in the following steps (see FIG. 45):

1. Key points (specific features on several images) are identified and matched to other pictures. Out of the two dimensional key points, the 3D tie points on the surface model are calculated. In the same step, the camera parameters (for example focal length and orientation) and location of the model are retrieved based on available georeferences. Because no integrated georeferences are used, the model has to be georeferenced on manually inserted ground control points (GCPs). It is possible to measure the GCPs with a differential GPS in the field, to label them on the ground and to search and link them afterwards on the picture. Because the area is large and measuring only a small number of GCPs would have been very time consuming, the GCPs are red out of the respective map provided by SWISSTOPO (2018a).

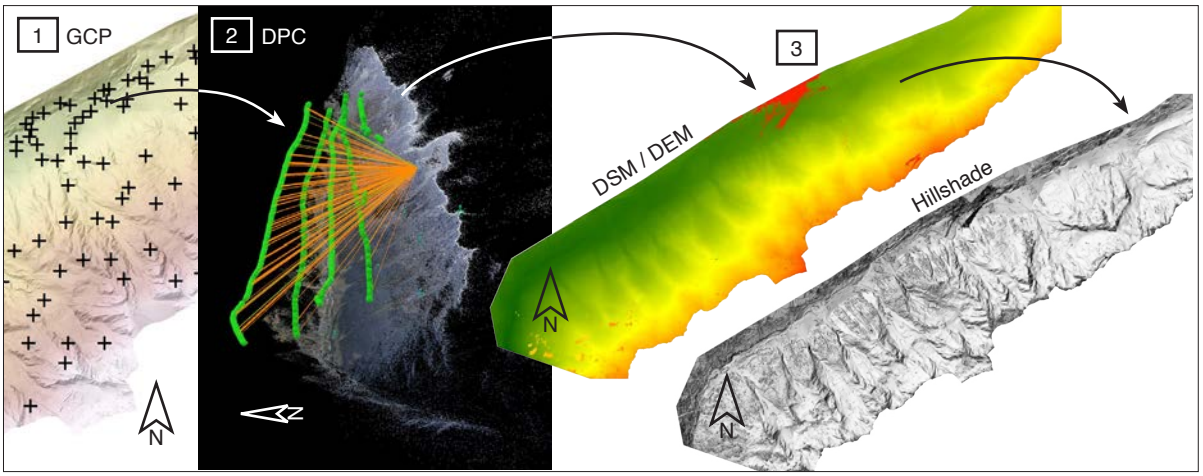

FIG. 45: Pix4D processing steps. Step 2 (middle left) shows the DPC which is based on correlated pixels. Illustrated in orange are the traces of one exemplary pixel to every picture which includes it. Step 3 (middle right) shows the transformed DEM based on the DPC, with the final hillshade (right). (Source: own illustration)

2. Additional and automatic retrieved tie points (TPs) are created, which lead in total to the densified point cloud (DPC) and illustrates every correlated pixel. Based on this high resolution DPC, a 3D texture mesh (3TM) is calculated. It represents a surface reconstruction based on triangles between pixels.

3. Out of the 3TM, the digital surface and elevation model (DSM/ DEM) is calculated. While the 3TM is built on triangles, the DEM is based on a 2D area with a z-axis attribute (elevation) for each pixel.

Out of the DEM a hillshade and the orthorectified orthomosaic (including the pictures) are compiled. Independently of the GSD, the DSM18 resolution has to be downgraded to 2 m/pixel to be correlatable to swissALTI3D.

DSM validation

A surface can be classified into changing (e.g. plants and glaciers) and non-changing (e.g. rocks and walls) surface areas. Therefore stable terrain reveals no difference if the same area is measured with a difference in time and acts as verification of the reliability of the photogrammetric output. If the calculation shows a surface change, there are two possibilities:

1. The calculation is faulty (shift of big and not specific areas) - or
2. The area retrieved a real change in elevation (shift of clearly defined areas)

The first case implies a recalculation until the stable parts match. The second case leads to further analysis and interpretation of the change.

The DSM18 validation is based on large and small scale error identification. The large scale error of DSM18 is based on a possible shift in X-,Y- and Z-axis regarding the reference swissALTI3D. NUTH & KÄÄB (2011) developed a method based on *«(...) the similarity of elevation differences with hillshade of the terrain (...), a function that is based upon terrain slope and aspect.»* (NUTH & KÄÄB, 2011: 275) which is applied. Because a shift of the whole DEM is affecting the terrain homogeneously, the procedure is executed on assumably stable surfaces without the influence of additional geomorphologic processes. The method calculates the horizontal and vertical difference between the reference and the model (FIG. 46). The result will be applied to co-registrate DSM18 onto swissALTI3D. The small scale error is more difficult to detect. The program can misinterpret structures or pixels, what can lead to wrong surface reconstructions. It has therefore to be distinguished between real surface changes and miscalculations. To exclude inexistent surface over- or underestimations between DSM18 and swissALTI3D, pictures of the photogrammetric flight, aerial images of the ETH image archive (E-PICS, 2018) and all data available of SWISSTOPO (2018a) including orthophotos, will be considered.

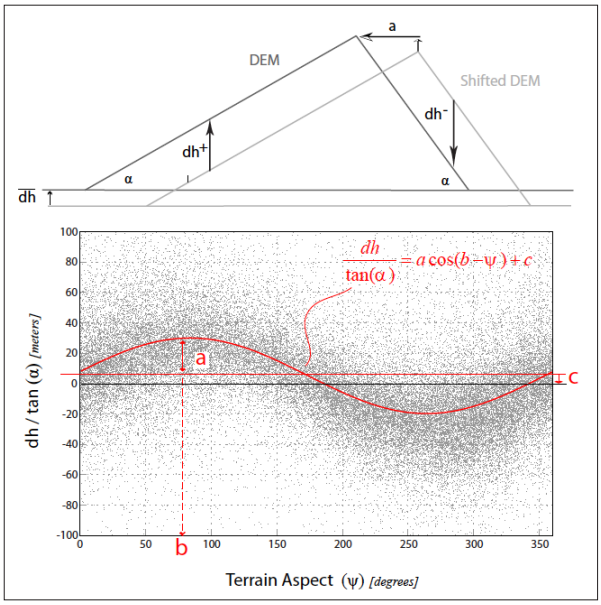

FIG. 46: Illustrated procedure of co-registration by NUTH&KÄÄB (2011).

4.2.4 DEM-differencing

After both DEM/DSMs are calculated, the differencing is achieved with the geoinformation system software ArcGis and the respective tools (e.g. «Raster Calculator»).

4.2.5 Interpretation

The surface changes are based on the following assumed and existing phenomenons:

- Deepening or development of debris flow channels
- Rock face decay or rock fall
- Ice melt
- Moving soil or rock/ debris package

The interpretation is conducted with the consultation of existing researches, projects and analyses from GEOPLAN AG (all reports), pictures of the photogrammetric flight, aerial images of the ETH image archive (E-PICS, 2018) and all data available of SWISSTOPO (2018a). Further on the mapped glaciated areas of the Swiss Glacier Inventory Project SGI2010 (FISCHER et al., 2014) are compared to the own mapping (based on the glacier extent 2011). The surface change will show subsurface ice melt and will therefore qualify the precision of the mapping. The given data fundament is also supported by fieldwork results during the summer 2018. The aim is to have a perception of the actual situation and ongoing processes. The catchments of Beich-, Loibin-, Birch- and Nestbach are visited.

4.3 DSM18

4.3.1 Survey

On the 21st of September 2018 the photogrammetric survey was executed (FIG. 47).
After different appointment changes due to bad weather and in consideration of possible upcoming snow events, the flight was conducted even if the weather was inconsistent and the forecast indicated precipitation in the late afternoon.
The sky was covered with thin clouds which led to a hazy light without shadows on the surface. That condition supported the photographer due to small changes in light conditions and therefore an uncomplicated camera operation.
On the date of the flight, the hunting season was on and several clarifications with the local preserver had to be made in advance. After informing of local authorities and the permission from the preserver, the helicopter flew from Bern to the Balmhornhut, a hut of the Swiss Alpine Club (SAC) above the Gasterntal in the Bernese Oberland. There all the equipment and the machine was finally prepared and the photographer was equipped with a harness. To get good visibility and free movement for the

FIG. 47: The helicopter is ready for take-off (left). The hazy light conditions during the flight (right). (Source: Elias Kaiser)

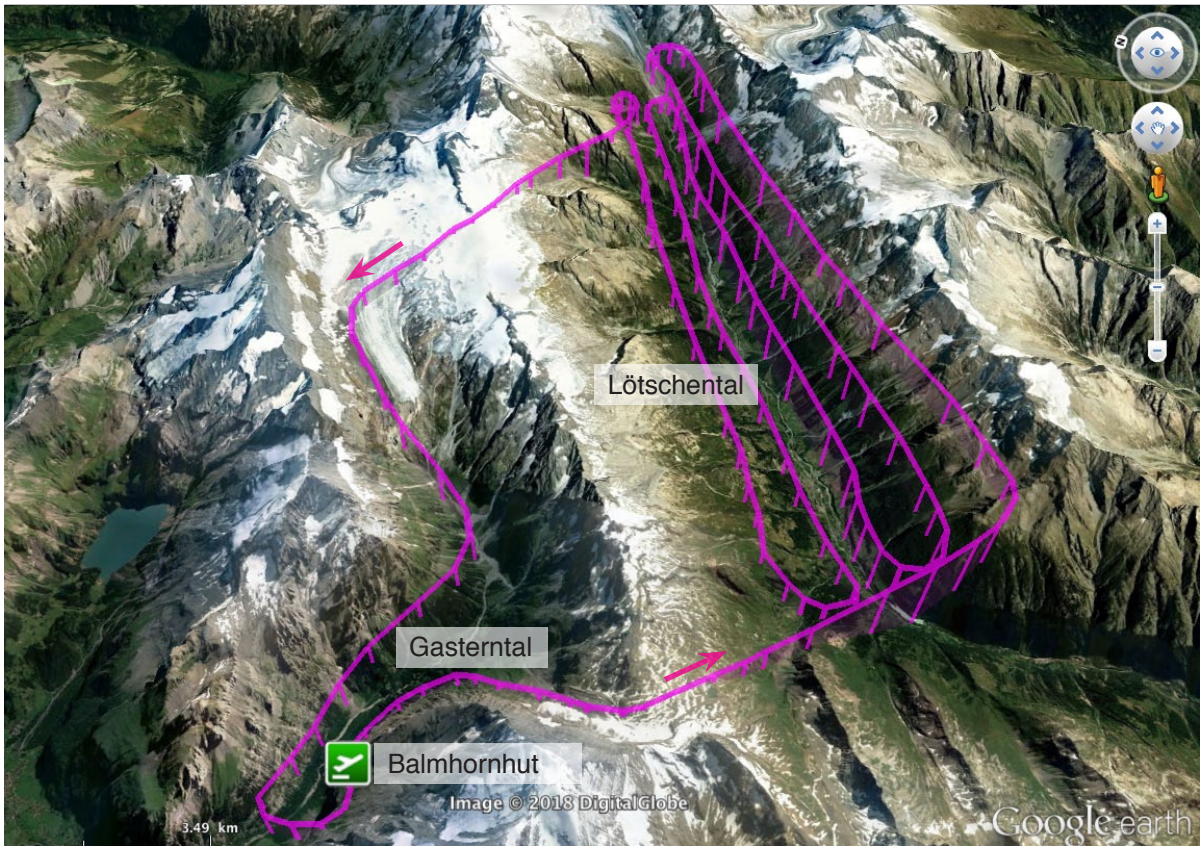

FIG. 48: Shown is the flight route for the photogrammetric survey on the 21st of September 2018. The Balmhornhut of the Swiss Alpine Club (SAC) served as stopover to prepare the helicopter for the mission. (Source: GoogleEarth)

photographer, the doors in the rear were removed. Afterwards the helicopter headed via Lötschenpass into the valley and passed four times along the northern flank of the Bietschhorn. The photographer had to switch places during the turns to catch pictures out of the left and right hand side of the helicopter. The flightpath was performed in adaption to the slope of the mountain ridge (at 3‘000, 2‘500 and 2‘000 m a.s.l.) with a vertical distance of approximately 800 m. This height enabled a compromise between minimal helicopter noise in consideration of the hunters in the terrain and enough GSD resolution. An additional overview was captured from the opposite valley side at a height of 2‘000 m a.s.l. to cover possible missed areas (FIG. 48).
During the 30 minute flight from and to the Balmhornhut a total of 4036 pictures with a total size of 20,28 GB (5 MB each), was generated.

4.3.2 Pix4D results

The program was able to calculate an average GSD of 26.36 cm but due to following correlation to the swissALTI3D, the GSD was downsized to 2 m. The quality check of the DEM calculation which was automatically released by Pix4D after the processing, revealed the following information:

- Out of the given images a median of 24‘164 keypoints per image was set (10‘000 are requested) which reveals a good coverage.
- From the 4‘038 taken photos (total coverage was 99.4 km^2) 3‘571 were used and calibrated (88 %).
- 3.36% relative difference between initial and optimized internal camera parameters was calculated. *«An initial camera model should be within 5 % of the optimized value to ensure a fast and*

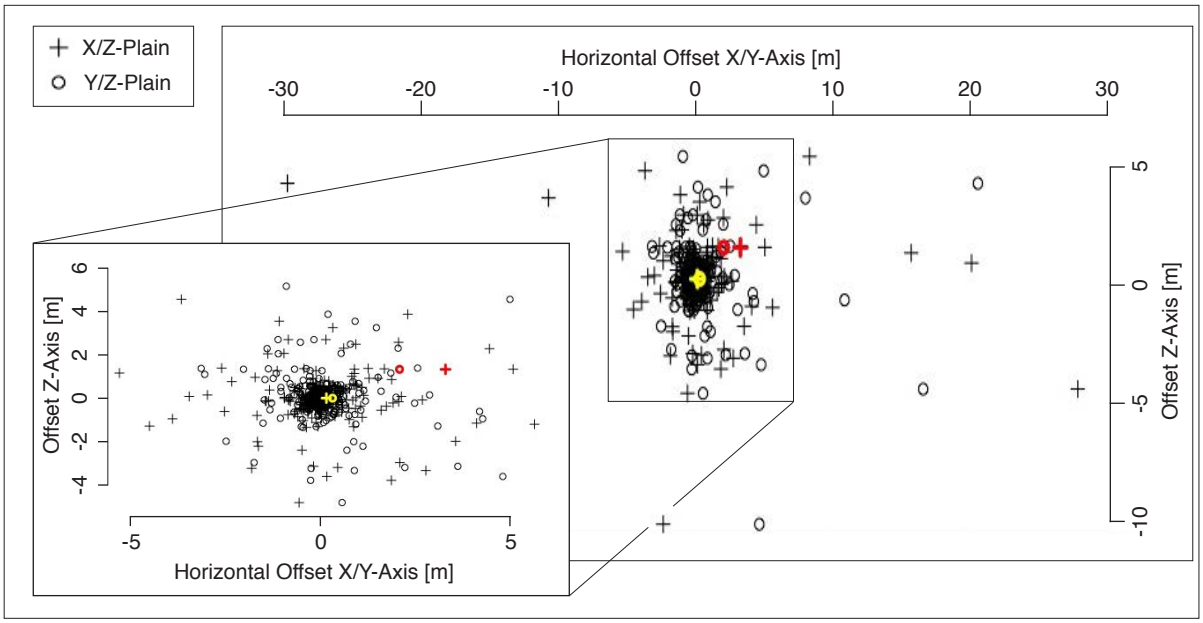

FIG. 49: Correlation between the GCP offset in the different axes. The mean (yellow) and the RMSE (red) are marked. (Source: own graph)

robust optimization.» (PIX4D, 2018d).

- A median of 12‘121.5 matches per calibrated image was calculated.
- 261 GCPs were inserted and a root mean square error (RMSE) of 2.238 m was calculated (FIG. 49). X-axis: 2.09 m, Y-axis: 3.30 m and Z-axis: 1.35 m.

4.3.3 Pix4D discussion

Dataset

As it can be seen in figure 5 of the Pix4D report (APP-A2), the excluded images are located in the south-western part of the valley, represented by the beginning of the flight, while the overlap revealed no problems. This is assumably based on the image quality: in the beginning of the flight, the camera was first set to a too short time of exposure and therefore a lot of images were too dark. On top of that, the images were blurred due to an increased exposure time (FIG. 50). This problem is well known and SIEBERTH et al. (2015) analysed the problem and revealed, that blurred images influence the processing steps significantly. The presented filter technique was too complex to apply it on over four 4‘000 images. Based on that, the program could not define enough clear TPs on some pictures. Nevertheless, since several shots of the same area in different angles and distances were made, the resulting overlap and grade of detail was sufficient for the program to calculate a DEM. The problem of dark and blurred pictures existed as well for other parts of the flight, but only the south western area was affected by the automatic exclusion of pictures by the software. It is unclear why.

Georeferencing

In a first step a series of 18 Ground Control Points was inserted and the result was compared to the swissALTI3D. The difference calculations showed a «wobbling» torsion of the model. The light red areas in the south western and north eastern part and also the uplift around Blatten revealed problems with the georeferencing (FIG. 51). Pix4D itself proposes that *«a minimum number of 5 GCPs is recommended. 5 to 10 GCPs are usually enough, even for large projects. More GCPs do not contribute sig-*

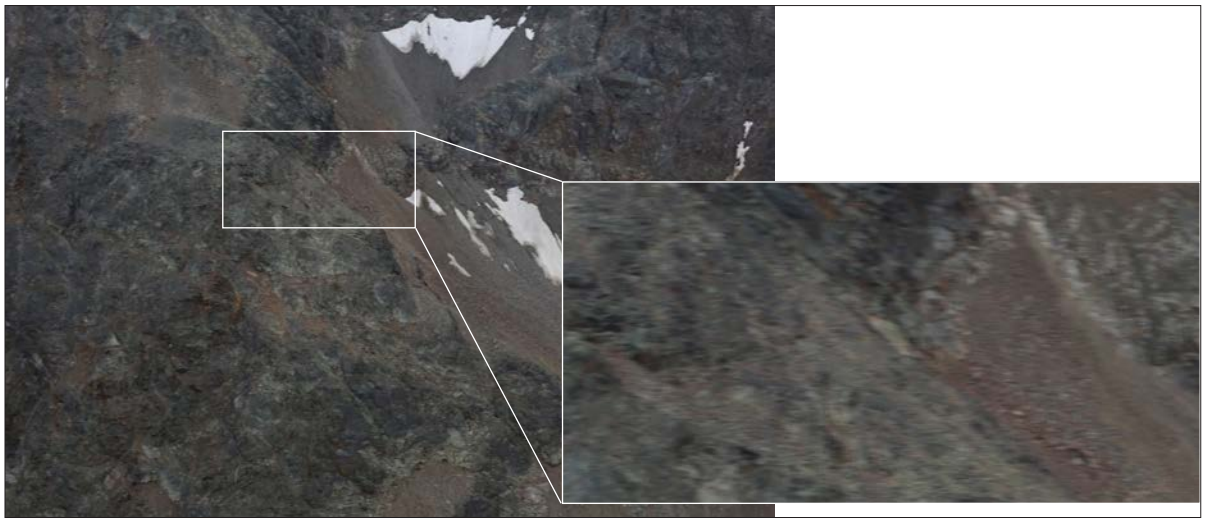

FIG. 50: The analysis of a blurred image. Comparison between the original picture (left) and the magnification of a section with blurring (right). Although other pictures revealed the same problem, only the south-western part of the DEM lost information. (Source: own photography)

nificantly to increasing the accuracy.» But based on the complex topography *«(...) more GCPs will, indeed, lead to better (more accurate) reconstruction.»* (PIX4D, 2018e) and therefore more GCPs were inserted. After marking 243 GCPs more, the model was bent into shape and the bulking effect disappeared (FIG. 51). The GCPs were homogeneously distributed over the whole area on assumably solid ground and on distinct positions like road markings, surface patches, rocks, cracks (in walls), trails and buildings (coordinates under APP-C5). The number of points developed randomly and is based on the identification of GCP locations and their usability. Therefore narrow gorges are more marked than regions with vegetation (see FIG. 52).

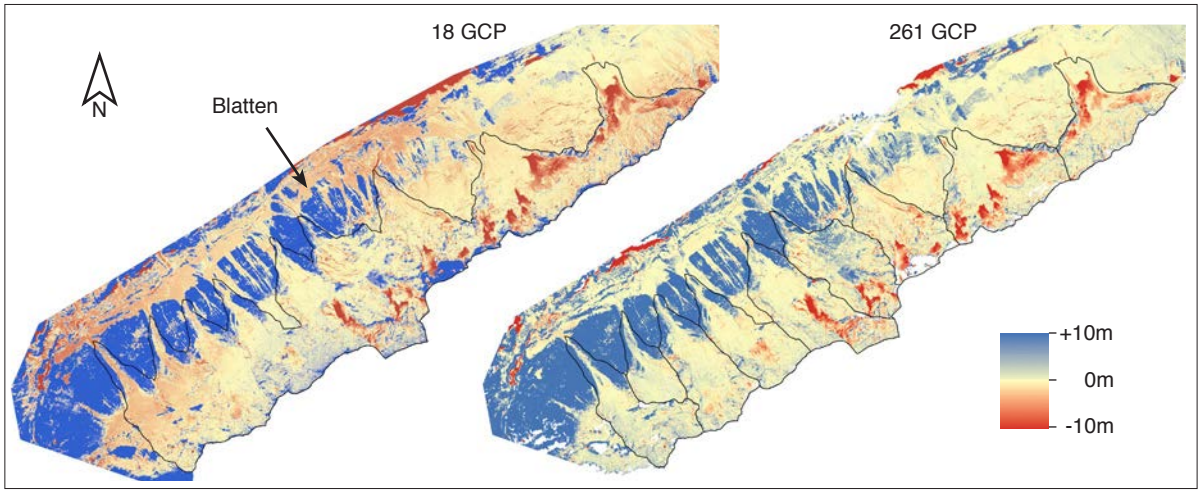

FIG. 51: The correlation between the number of GCPs and possible torsion effects. Left: Wobbling DSM18, the colourization is not homogeneously distributed and represents large areas of wrong shape (compared to the swissALTI3D). Right: After the implementation of 261 GCPs, the wobbling effect disappeared. (Source: own illustration)

Out of the 261 GCPs a mean RMS error of 2.24 m was retrieved and indicates therefore only DEM differences with a change of several meters. For a correctly reconstructed project the RMS should be around 1-2 GSD horizontally and 1-3 GSD vertically (PIX4D, 2018d), which was not accomplished

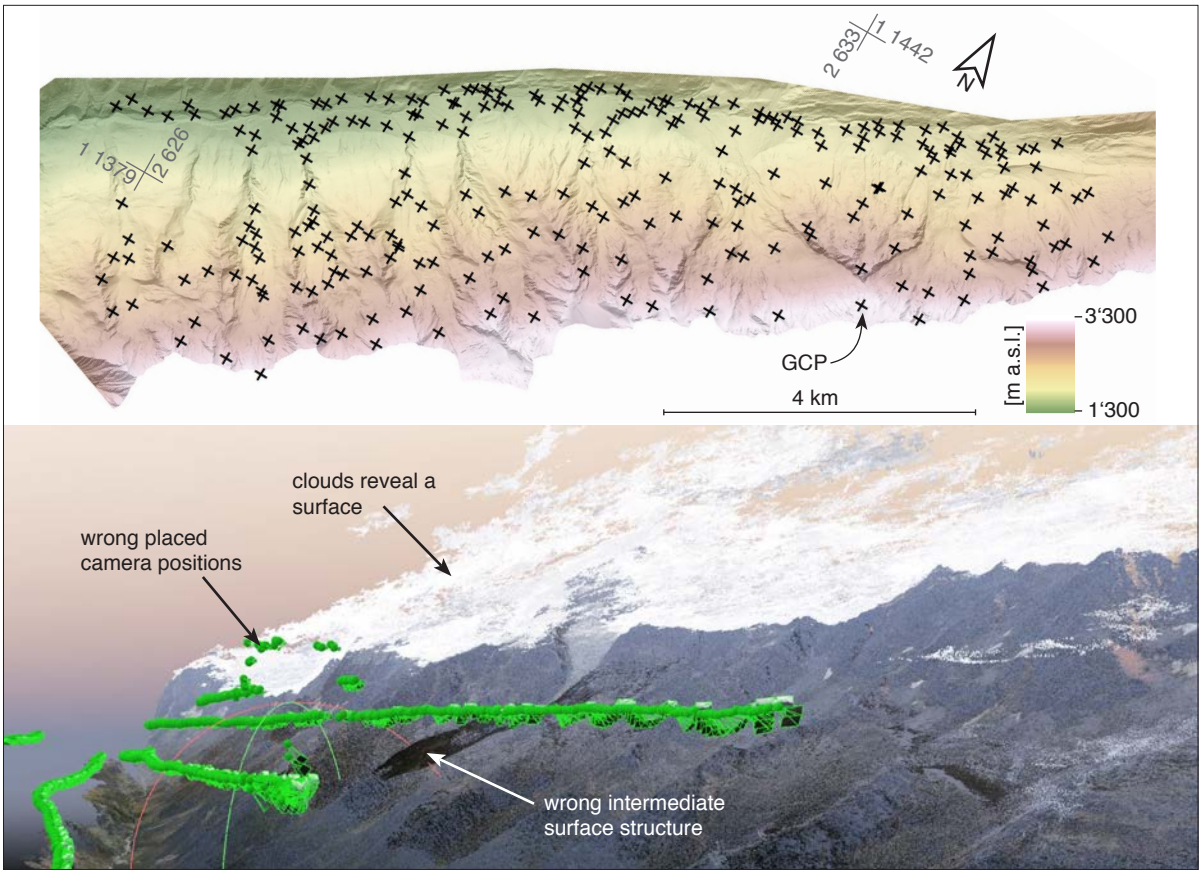

FIG. 52: The applied 261 GCPs are located on assumably stable terrain (top). Point Cloud visualisation of Pix4D. The surface is based on single correlated pixels (TPs) which is a precalculation of retrieving a DEM. The problem is based on the interpretation of clouds as existing layer. Interesting fact: the Bietschhorn vanishes behind the clouds. Green represented are the positions where images were taken (bottom). (Source: own illustrations)

by the retrieved values. Pix4D proposes severe issues with the dataset or an error when marking or defining the GCPs. Pix4D writes further on *«[...] Sharp edges, trees, reflective surfaces and certain type of roads and rooftops may be locally less accurate.»* (PIX4D, 2018d). It is an open discussion, if more GCPs really equal a higher precision of the result or not. GINDRAUX et al. (2017) assessed the relation between GCPs and the accuracy on three Swiss glaciers in mountainous terrain. They could show, *«(...) that the DSM accuracy increases with increasing the number of GCPs until a certain GCP density is reached (...)»* (ibid: 8) which corresponds to the result of ROCK et al. (2011) and TONKIN & MIDGLEY (2016). Based on the applied 261 GCPs, 12.8 GCP/km^2 are calculated, which is above the proposed 7 GCP/km^2 by GINDRAUX et al. (2017:8). GINDRAUX et al. (2017) and also CHUDLEY et al. (2018) applied SfM on flat glacier tongues but not on steep and canyoned mountainous slopes. It can be assumed, that in winding surfaces a lot more GCPs are needed and a GCP/km^2 resolution well above seven has to be aimed for.

The GCPs were manually red out and inserted as GCPs into the software. It can be stated, that this procedure was not sufficient. It can not be excluded, that during the readout or by inserting the 3‘500 digits typing errors occurred. Especially in steep terrain a small shift in the marking can lead to huge offsets in the calibration afterwards. The picture tagging itself was sometimes challenging due to different angles of the photography. Another factor arised by the software itself. The automatic generated TPs were sometimes faulty linked. Pixels were matched between pictures which were not at the same position, but assumably located in similar areas.

Based on the fact that the pictures revealed problems with blurring, the GCPs reveal a high uncertainty and the program had some troubles with the correlation of different TPs itself. The reason for this huge error is multilayered and can not be located in one specific wrong data process. The main problems which led to the offset have to be located in:

- Inaccurate GCP precision
- Blurred photos
- Difficult topography

In conclusion it can be summarized: the bigger and more winded the study area is, the smaller the single photogrammetric patch should be selected. The connection and dependency on pixels over large distances seem to have a negative effect on the result, especially in rough terrain.

Orthophoto

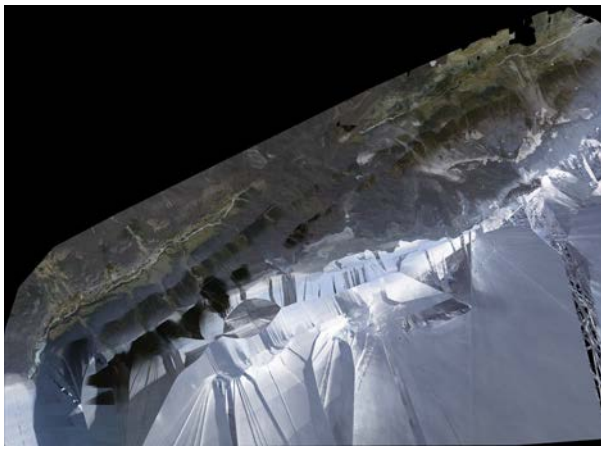

FIG. 53: The calculated orthophoto is not usable due to interfering background noise of the cloudy sky. (Source: own illustration)

The calculated orthophoto (FIG. 53) revealed problems with interfering background noise and it can be used as indicator for problems in the calculation process. Like WIEDEMANN & BECKMANN (2016) write in their paper abstract *«It is no problem to produce good orthophotos in small areas, whereas production of good and homogeneous orthophotos in large areas remains a challenge.»*

Due to the faulty point cloud generation, the orthophoto is composited based on a wrong initial position. Unfortunately, the product was not useful for this thesis and was replaced by the comparison between the taken photographies and older orthophotos (SWISSTOPO, 2018a).

4.3.4 DSM18 discussion

The calculations of Pix4D already revealed issues with uncertainties in the different axis (FIG. 49) and therefore NUTH & KÄÄB (2011) was applied to examine a possible shift. The areas shown in FIG. 54 were used as reference for the calculations (first run: red, second run: green).

In the first calculation the retrieved DSM18 shift was 0.0m for ΔX, 2.9 m for ΔY and -1.1 m for ΔZ. The contrary values were used to set the DSM18 onto the right position, but the result showed a more negative correlation than without the application (see FIG. 54). Due to the surprising result, the method was applied a second time (FIG. 54/55, green areas). The second run revealed no shift for ΔX and ΔY, but a minor offset of -0.1 m for ΔZ, which is in no correlation to the first calculation. If the colour grade resolution of $DIFF_{18\text{-}11}$ is artificially increased by lowering the upper and lower colour scheme boundary (before: +/-10 m, afterwards: +/-5 m), it reveals that the wobbling effect of the DSM18 could not be erased completely and every catchment is influenced differently (FIG. 55). While the catchment of Bätzlabach shows large elevation increases (assumably overestimations, A), the Stampbach catchment illustrates the contrary (B) and the Loibinbach catchment is consistent with swissALTI3D (C). On steep walls with increasing altitude a surface gain can be seen (overestimation, D). Based on

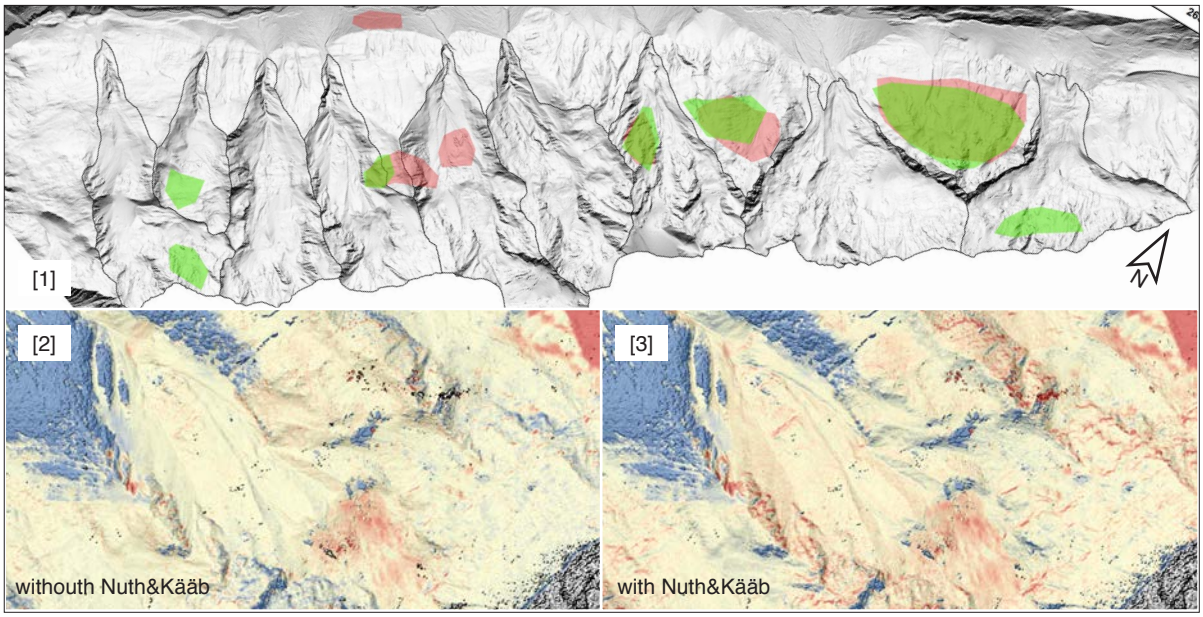

FIG. 54: Illustration about the applied co-registation. In [1], the assumed stable areas which acted as reference for the co-registration are shown (red and green), while the images on the bottom show the DEM difference between DSM18 and DEM11 on the first run without [2] and with [3] the application of NUTH & KÄÄB (2011). It is visible that [3] reveals a bigger shift than [2]. (Source: own illustrations)

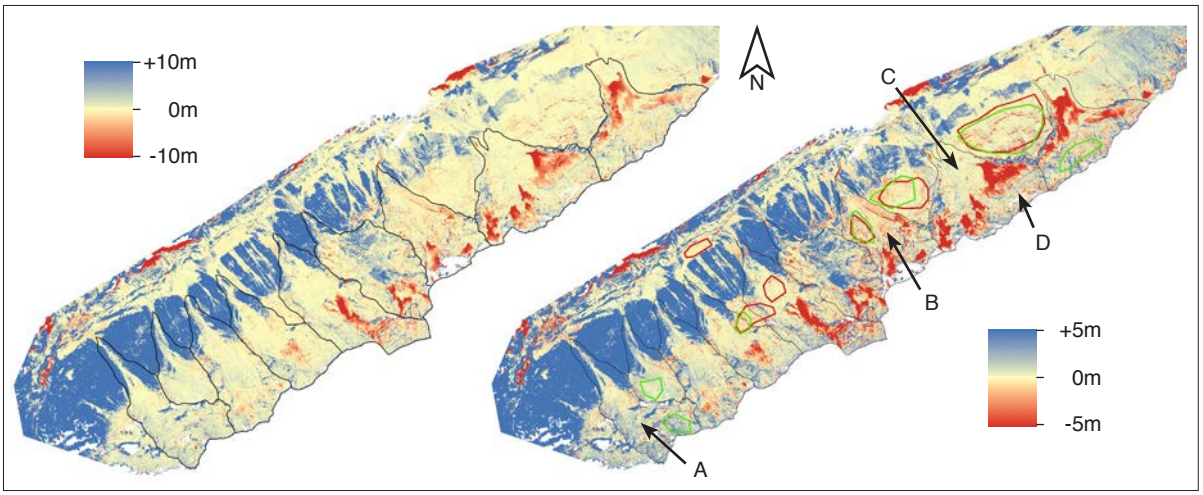

FIG. 55: DSM18 with the different colour grades -10/+10 m (left) and -5/+5 m (right). On the right graph the stable terrains for the co-registration are also shown. The catchments reveal specific surface imbalances. A: overestimation of the whole catchment, B: underestimation of the whole catchment, C: consistent catchment, D: rockwall inconsitency. (Source: own illustrations)

the inhomogeneity, NUTH & KÄÄB (2011) was performed on only one catchment (Bätzlabach) to see if the method is able to retrieve any shift for the specific area. The result showed a shift of $\Delta X = 0.7$ m, $\Delta Y = 0.9$ m and $\Delta Z = -0.3$ m. After application the result did still not show a satisfying correlation. The final conclusion was that the contrary information, which are generated due to the bulking and torsion effects, lead to an equalization of the shifts. Therefore DSM18 is internally so much distorted that an application of NUTH & KÄÄB (2011) was not useful.

Beside the distortion of the DSM18, the calculated surface topography revealed some further issues which led to wrong indications:

Lack of coverage («C»)

Because the topography of the north face is very rough, the parallel flight axis prevented a more

detailed coverage of all areas. As shown in the SfM theory (see chapter 4.2.1), an object has to be fully covered in all three dimensions to get a reliable volume assessment. Sections behind ridges, on plateaus above or directly on the flight altitude, or areas with deep chutes in nearly level angles to the flight path were therefore shadowed and insufficiently covered. The result were missing TPs which led to over- and underestimations of the surface elevation. A detailed analysis why the indicated volume change is based on a coverage problem and not on real surface changes is not given for each case. The exclusion of such areas is based on the following explanations:

- No difference in pictures between 2011 and 2018 and therefore no surface change.
- A negative balance would involve a positive balance below or would indicate a path where the material was transported to (and vice versa).
- Trough or gully behind a ridge without indications of material loss.

The exclusion of those areas includes the inability to investigate processes in these sections. In the following catchment descriptions, the corresponding areas are marked with a «C».

Noise («N»)

Noise is based on the misinterpretation of TPs and GCPs with a surface elevation generation at places where it does not exist. But why is Pix4D generating an inexistent surface? SfM works on single objects, where the background can be erased and the object is liberated of the environment. Due to this the camera angle during the photogrammetric survey was not defined to be downwarded and pictures in direction to the sky included the hazy cloudy sky. But the colour of the sky reveals a similar colour like the glaciers and the ice (FIG. 47). Based on the upwards oriented pictures and the existent clouds, the program calculated an inexistent mid-layer surface which was connected to the actually retrieved surface (FIG. 52). This «cloud surface» is also wrong in altitude and cuts off the Bietschhorn. The cloud layer and other misinterpretations of the Point Cloud led to noise in the DEM which is marked with a «N» in the following descriptions.
Values over +40 m and -70 m elevation difference between DSM18 and swissALTI3D are assumed as calculation errors and are zeroed. Smaller margins would interfere the correct reconstruction of height differences in steep areas, exemplarily represented on the Nestgletscher.

Vegetation («V»)

While the swissALTI3D reveals a topography with subtracted vegetation and buildings, DSM18 represents the actual surface without exclusion of obstacles. Therefore buildings and especially vegetation (trees and bushes) are indicated with a positive surface difference corresponding to swissALTI3D. Below 2‘200 m a.s.l. the forested areas are nearly continuous and additional areas at higher altitudes are sparsely vegetated. Based on shadowing effects, single trees at high altitudes can lead to a wrong surface generation and bias the calculations. The affected areas are located by virtue of aerial images. In the following catchment descriptions, the corresponding areas are marked with a «V».

4.4 Catchments

4.4.1 Results & interpretations

For simplicity the interpretation of each catchment follows directly after the result description. A sum-

marized discussion for all catchments can be found at the end of the chapter. The whole calculation process of the DSM was repeated five times and the best result gets discussed.
The quoted numbers in the descriptions (e.g. [3]) are also marked in the respective figures and should help to orientate.

Gitzibach catchment (FIG. 56)

[1] The elevation changes on the eastern side of Discheltschuggen at around 2‘300 m a.s.l. are accompanied by calculation errors. The patchy negative structure lost around -3 m in surface elevation (APP-B1 [A]). Based on the aerial images, the present scree field did not change noticeable since 2011. But the negative indication can be interpreted as result of ongoing rockfall processes which are changing the surface continuously.

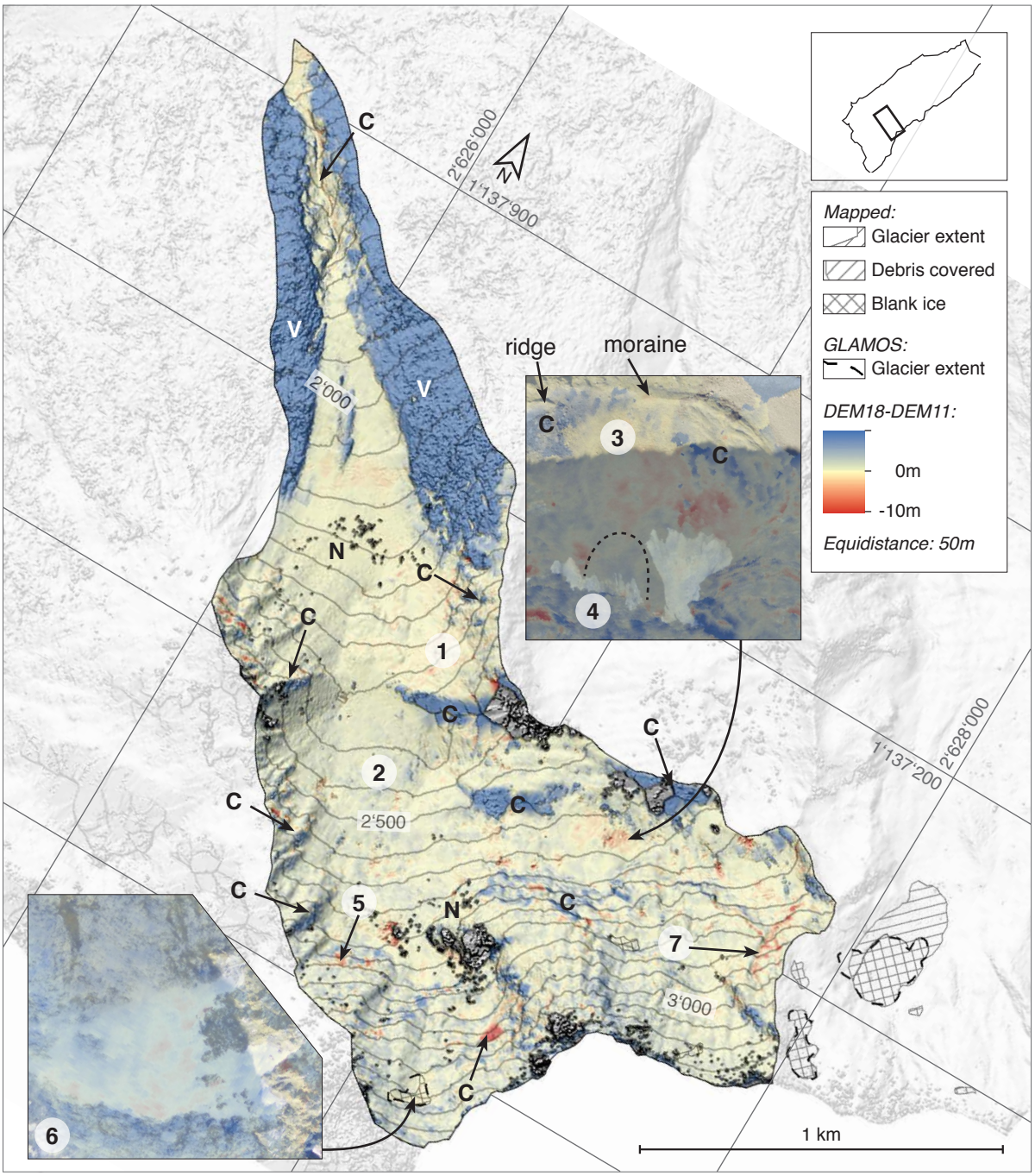

FIG. 56: The Gitzibach catchment. (Source: own illustration)

[2] Above Discheltschuggen the scree area reveals a positive surface balance. The elevation increase is calculated to be around +1 m and it is interpreted as accumulation zone of ongoing rockfall processes above.

[3] The small area east of the Opental reveals a negative surface balance of around -2 m since 2011. It is northerly surrounded by different areas with calculation errors. Based on the flight angle and the aerial images, the marked ridge and moraine shadowed lower areas which resulted in a miscalculation of obstacle near hidden deepenings. The reddish area received enough photogrammetric coverage and describes a negative elevation change. Because no erosional processes can be recognised, the surface lowering is assumably based on melting dead ice. If there is still ice present can not be distinguished.

[4] Directly beneath [3] below the rocky slope, a surface increase of around +2 m can be seen. A closer look on the aerial images reveal a fresh rockfall event (see APP-B2).

[5] Small areas of high negative indication (up to -8 m) are located at [5]. Because calculation errors are assumed around the respective area, it is unclear if the elevation change is correct or misleading. The consultation of the photos (APP-B1 [B]) showed some indications of existing erosional processes.

[6] The ice field on 3‘200 m a.s.l. shows a negative surface balance of around -1.5 m.

[7] The surface lowering of up to -10 m is located in steep rocky terrain. The photographies only show insufficient details and no fresh rock detachment could be recognised. If it is a calculation error or an ongoing erosional process can not be stated.

Bätzlabach catchment (FIG. 57)

[1] On the east side of the catchment patches of a surface lowering are visible (-2 m). The area is vegetated with bushes and calculation errors are possible. The photographs reveal small debris flow channels (APP-B3), which are also visible on older orthophotos. Based on the negative indication it can be assumed that the channels are still active. An extension or development of new channels is not visible.

[2] The trough of Bätzlerfridhof reveals no changes. The surrounding scree fields are not vegetated and seem to be active, even some parts are greener than others. While the calculations show no elevation differences between 2011 and 2018, the photos show a red rock face decay zone directly above the Bätzlerfridhof. The consultation of older orthophotos showed, that the phenomenon and process is not fresh but probably still ongoing. It is assumed, that the Bätzlerfridhof is a glacial overdeepening («Cirque«), eroded by strong glacial forces of a former steep glacier hanging and flowing on the southern lying rock faces (ZEPP, 2014).

Wilerbach catchment (FIG. 58)

[1] A sharp transition between light blue and light yellow areas can be seen. But the surface and the orthophoto do not show any explanation for a possible topography transformation. The reason can be found in the reference swissALTI3D.An issue of interpolation between LiDAR and photogrammetry reveals wrong $DIFF_{18\text{-}11}$ results (see chapter 4.2.2).

[2] Here a small negative surface elevation balance of -3 m is measured. It is directly below a rock face at 2‘800 m a.s.l. Based on pictures of the survey, a snow field is present. Old topographic maps (SWISSTOPO, 2018a) show a former glacier between Hangende Gletscher (former Wilergletscher) and the glacier on the north face of Schwarzhorn. The negative balance is therefore attributable to ice melt, representing the remnants of the glacier. Beside the small patch, no surface

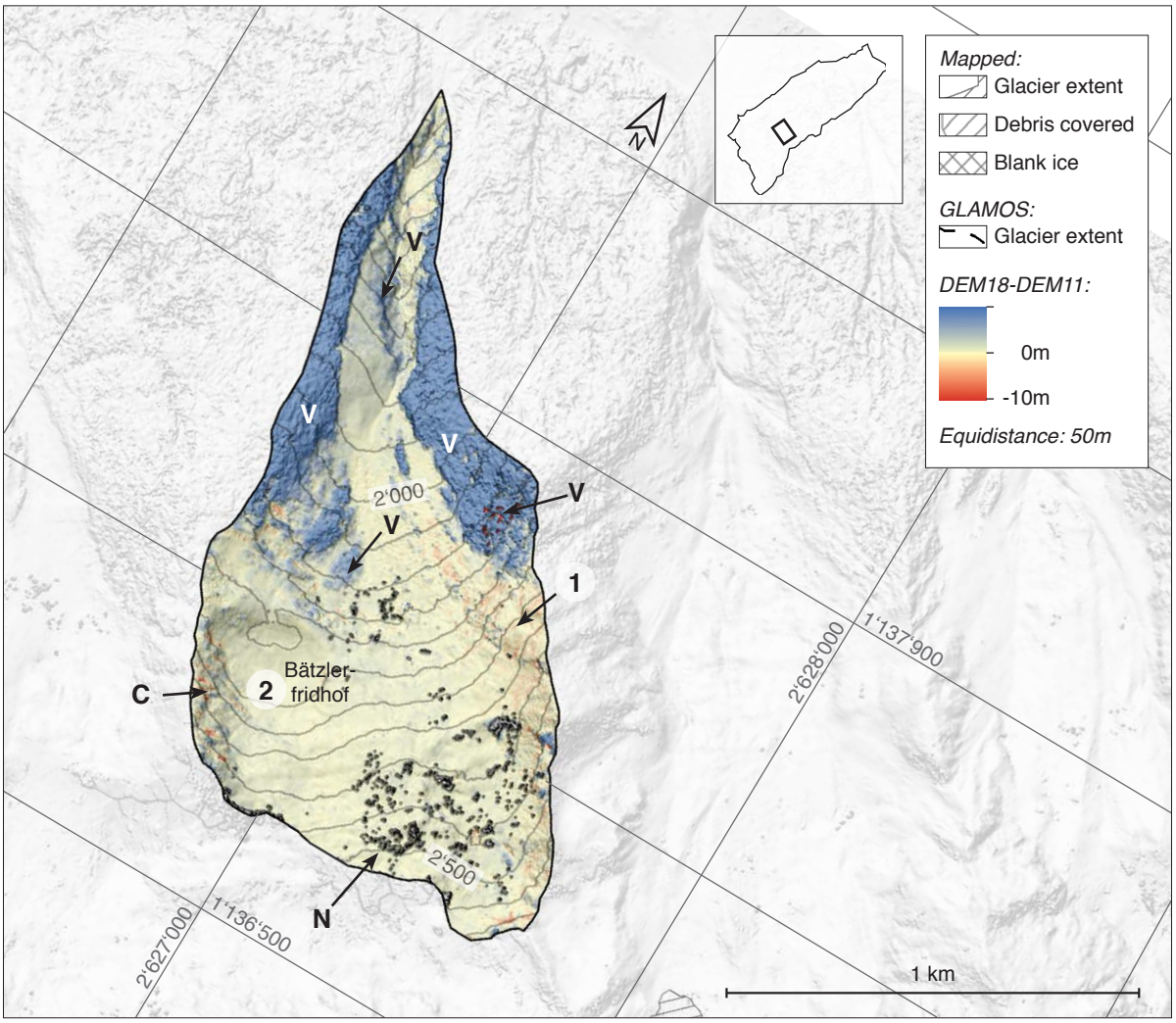

FIG. 57: The Bätzlabach catchment. (Source: own illustration)

lowering is observed and therefore no dead ice assumed (APP-B4 [C/D]).

[3] Even if a glaciated area is mapped, no surface changes are retrieved. Because the ice is on high altitude (around 3'150 m a.s.l), steep sloped and north faced, it can be assumed that the ice is not affected by warm temperatures as much as the Hangende Gletscher. Nevertheless, a zero or small positive indication would be unlikely and therefore a measurement error is assumed. It is assumed that the measurement was insufficient to cover any changes.

[4] The glacier on the north side of Schwarzhorn shows a surface lowering of around -6m based on melting processes. The area of negative balance is smaller than the mapped outlines. The photo (APP-B4 [A]) shows a massive debris coverage of roughly the half of the glacier surface.

[5] The Hangende Gletscher was mapped nearly the half of the extension which was mapped for this thesis. The $DIFF_{18\text{-}11}$ reveals an even bigger extent. While the bare and visible ice reveals a strong negative balance (-5 m), areas down at 2'650 m a.s.l. indicate also surface lowering. It can be assumed, that the glacier extension under the debris was around twice as big from 2011-2018 compared to the visual bare ice. APP-B4 [C] shows possible crevasses which implies the interpretation, that the (debris covered) glacier extent is much bigger than expected. The negative surface balance reaches 2'600 m a.s.l., lower than the small indicated ridge (APP-B4 [D]). If there is still ice present can not be said. It is possible that during the time between swissALTI3D and DSM18

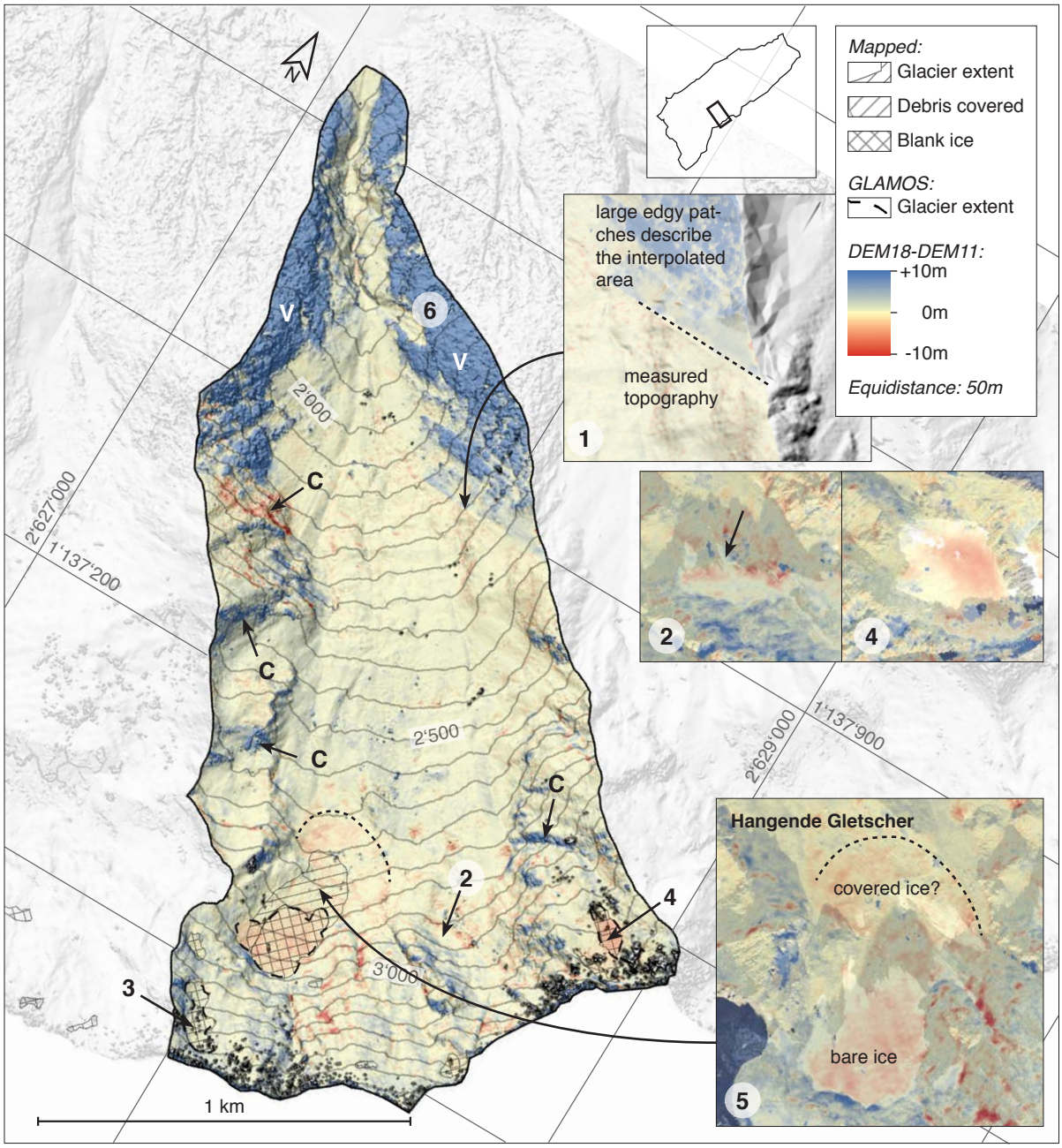

FIG. 58: The Wilerbach catchment. The dashed line indicates the assumed covered ice front. (Source: own illustration)

the ice melt out.

[6] The area around [6] seems to be stable without any surface changes. The picture (APP-B4 [B]) shows channels, but young vegetation and stable trees on top of the tear-off edge reveal no unexpected and recent movements.

Tännerbach catchment (FIG. 59)

[1] No. 1 indicates an area of negative balance. The slope is steep and erosion processes could have carried off material. While the orthophoto of 2014 (SWISSTOPO, 2018a) shows a grassed area, the flight revealed strong erosion with lacking vegetation (APP-B5 [A]). Even though the area is steep and difficult to access correctly for the software, the calculated loss of height is assumably correct (up to -2 m).

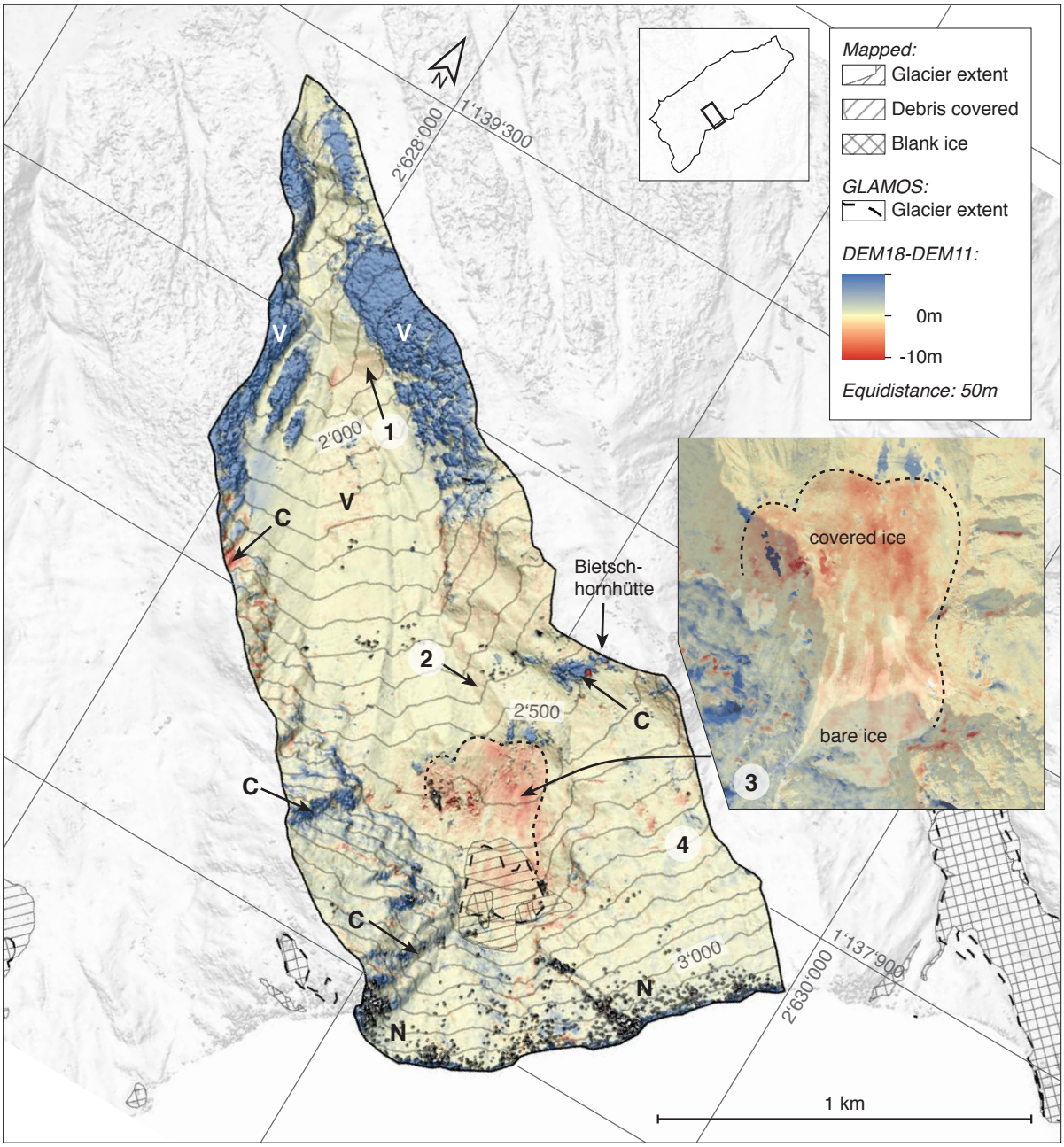

FIG. 59: The Tännerbach catchment. The indication shows the assumed subsurface ice extent. (Source: own illustration)

[2] The balance reveals a negative offset of around -1.5 m. The deep chute of the moraine bastion is affected by erosional processes, nevertheless the marked rock (APP-B5 [C/D) is already visible on aerial images from 1997 and therefore the channel seems to be stable. It is not clear if a surface lowering of -1.5 m occurred or if it is based on miscalculations.

[3] The biggest impact on the surface change has the area [3]. The red foot shaped area with an indicated surface lowering of up to -8 m extends 280 m further down than the mapped glacier extend. The borders are more or less sharp and end around 2‘520 m a.s.l. at the moraine bastion. It is not known and only vaguely assessable how much sediment the bastion includes. Because of the long existence, it can be assumed that the moraine is stabilized by bedrock structures. This interpretation is supported by the fact, that the Tännerbach flowing through the channel of the bastion did not deepen for years (SWISSTOPO, 2018a). It is also not clear if below the plateau on 2‘550 m a.s.l. an

overdeepening of the bedrock is located and how deep it is. It is interpreted, that under the debris cover of the plateau, ice is or was present. It is probable that the visible glacier ice is connected to the covered ice masses. Nevertheless the negative total indication (blank ice: -2.5 m) reveals the melting processes. Therefore the glaciated area is nearly 300 % as big as assumed (APP-B5 [C]).

[4] The north western slope of Schafberg indicates a surface lowering of around -4 m on a scree field. It is not clear if the surface really lowered or if it is a calculation error. It is assumed, that underneath debris covered dead ice is or was present. Also the consultation of older maps revealed no further informations.

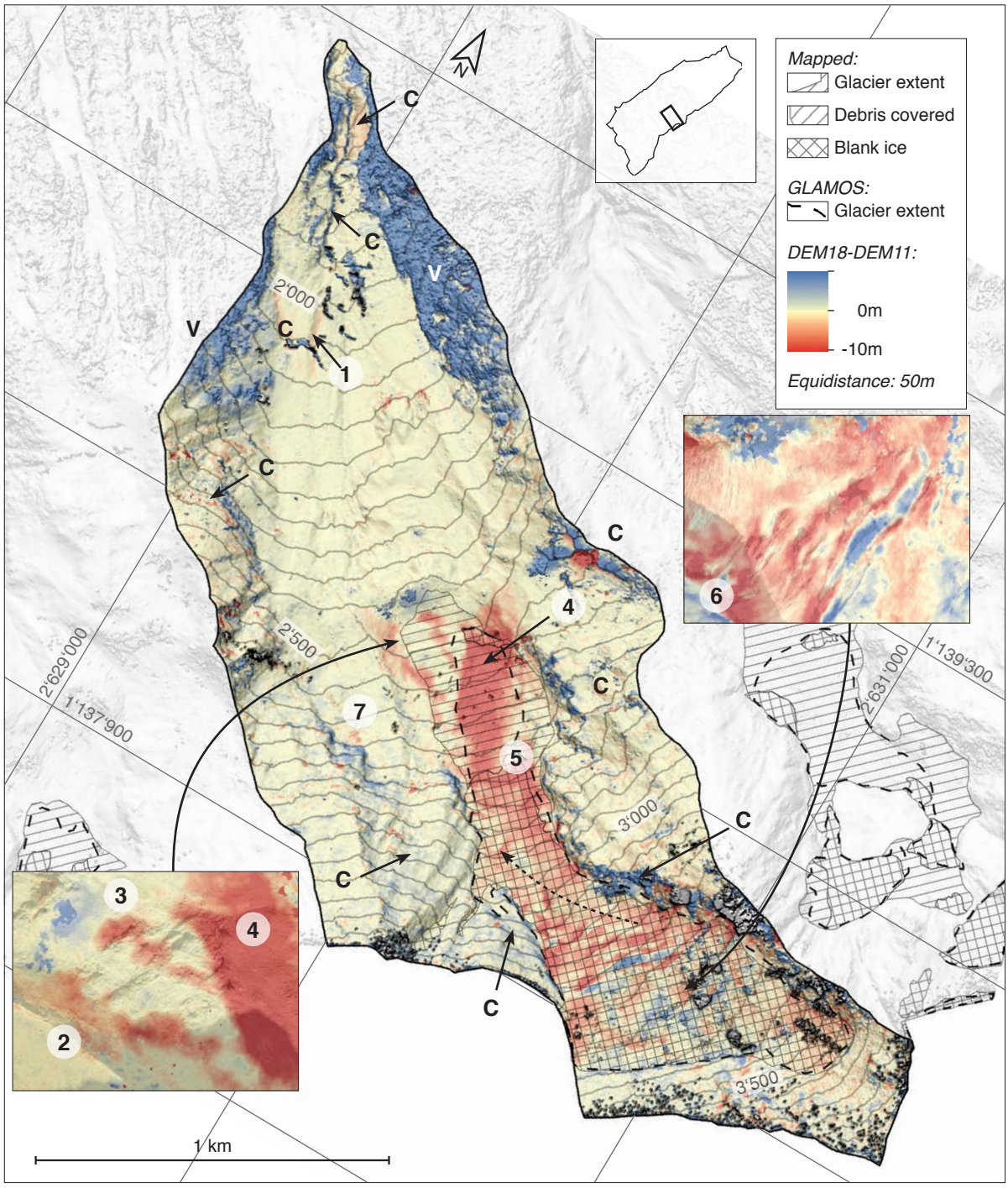

FIG. 60: The Nästbach catchment. (Source: own illustration)

Nästbach catchment (FIG. 60)

[1] The thin line indicates a surface lowering of around -2.5 m. The aerial images show an active gully and therefore the negative balance is reasonable (APP-B6 [A]).

[2] In this area a negative balance of around -5 m is calculated. Based on the fieldwork, the lateral moraine of Nestgletscher is ice cored (APP-B6 [B]) and the surface lowering is assumed to be based on ice melt.

[3] It shows single dots of negative balance up to -10 m (at 2‘500 m a.s.l.). The glacier tongue of 2011 was around the same altitude as the lowest negative indications. Therefore the negative patches illustrate former ice residuals which were located between the stepped bedrock ground. They disappeared until today. On the same spot but in altitude a couple of meters lower, a positive balance is measured (+5 m). During the fieldwork the area showed a flat debris covered surface. It is assumed, that a former small surface deepening of the bedrock was filled up with sediments which is represented by today‘s plain (APP-B6 [C]).

[4] On the same altitude as [3] and a couple of meters eastwards, a surface lowering of -20 m is calculated which is based on ice decay. While 2011 ice was present, today bedrock is on the surface. This negative balance can followed up to 2‘650 m a.s.l.

[5] At 2‘700 m a.s.l the slope increases and the glacier begins to crack. Here the negative balance decreases to around -10 m. The icefall up to 3‘200 m a.s.l. reveals indications about the flow behaviour. The middle of the ice stream lost less ice than the surrounding (marked on FIG. 68 with a dashed arrow) which illustrates the main flow direction of the ice. It is assumed, that the eastern part of the glacier tongue (directly by the labelling) will disappear first.

[6] Based on the icefall and crevasse movement, the difference between the DEMs should reveal a regular positive and negative pattern. While the upper section above 3‘200 m a.s.l shows a similar characteristic, the icefall itself only reveals a negative total balance. Therefore the glacier lost homogeneously around -10 m of ice over the whole area.

[7] On the eastern side of the Nestgletscher, a surface gain is calculated (+2.5 m). The pictures show the lobe of a rock glacier (APP-B6 [C]). But the DEM difference does not show any large scale movement of the whole tongue. It is therefore not clear, if the rock glacier is still active or not. BAFU indicates a probability for extensive permafrost existence (SWISSTOPO, 2018a).

Birchbach catchment (FIG. 61)

[1] Near the apex, the channel of Birchbach reveals a negative balance of around -7m. Between the two DEMs, three huge events with debris flows occurred (GEOGPLAN AG, 2010 & 2014). Hence, the deepening of the river bed is plausible (APP-B7 [A]).

[2] The calculated deepening of -8 m is relatively high, especially because the river flows directly on bedrock and therefore erosive processes are lower. It is estimated, that erosional processes occurred but with less erosion. The gorge is very narrow and a lacking photogrammetric coverage is assumed to be the origin of the miscalculation.

[3] The eastern channel of Birchbach has a negative surface balance of -3 m, which can be explained with the same events as [1] and [2]. It has to be noted, that the conduit is not vegetated and therefore active (APP-B7 [B]).

[4] Like for [3], the western channel lowered around -4 m but is, in contrary to the eastern channel, vegetated with bushes and grass. This describes a former phase of activity in the western channel which decreased again between 2011 and 2018.

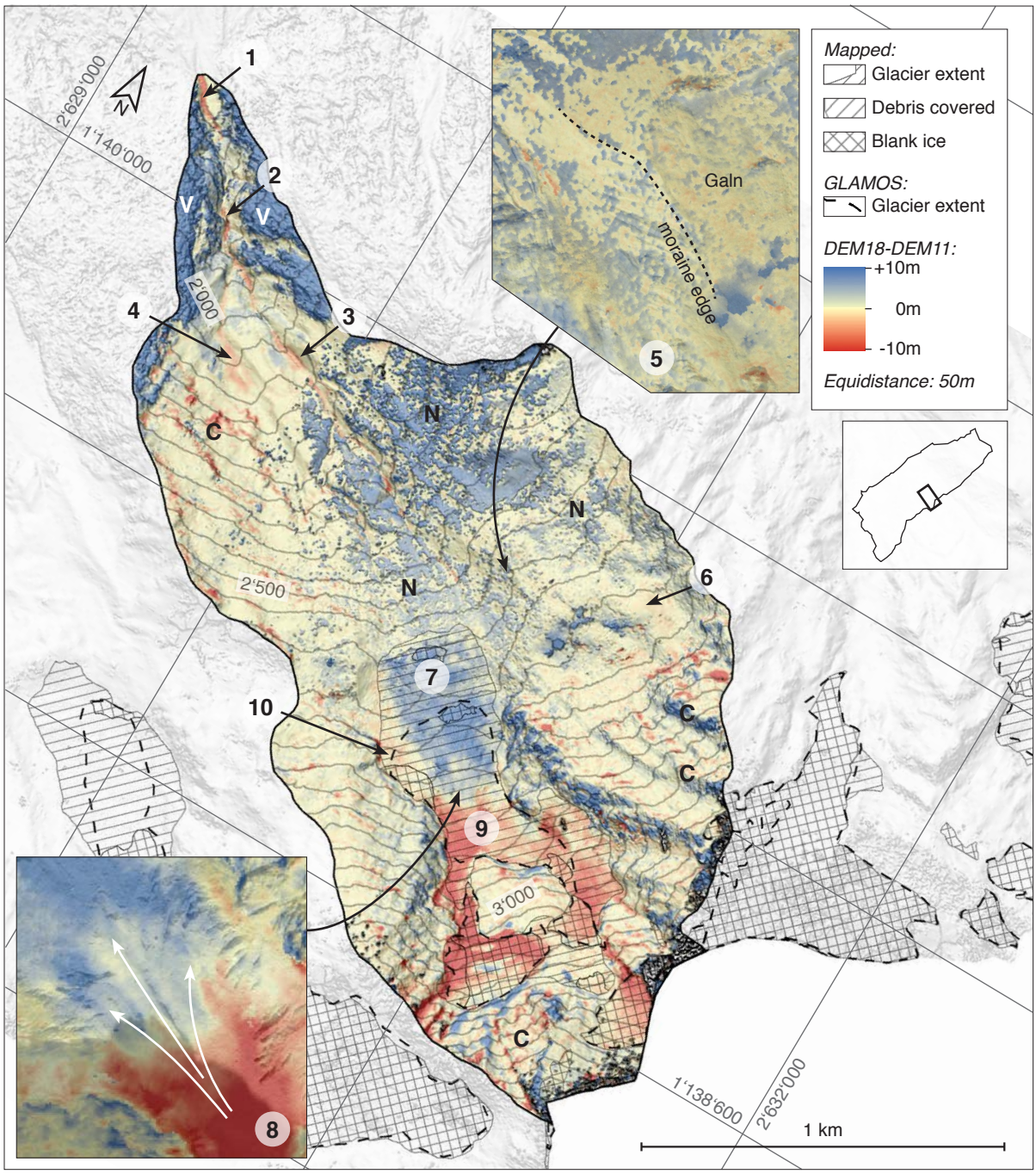

FIG. 61: The Birchbach catchment. (Source: own illustration)

[5] This area is disturbed by a huge amount of noise. The noise can lead to wrong indications, between the faulty values patches of small surface changes are visible. Hidden by the noise is also the big lateral moraine «Galn» on the east side of the glacier at around 2'600 m a.s.l. Hence no statement about detailed changes can be made. The consultation of aerial images and postcards showed, that the mass did not change significantly (APP-B7 [C/D]). The explanation for this long-time stability is assumably similar as for the moraine bastion of Tännerbach. Galn reveals some outcrops of bedrock on every side, even on the steep slopes in direction to the glacier. It is assumed, that the whole sedimentary body is supported by two different rock ridges (marked in APP-B7 [C]). These prevent an increasing erosional process while the lateral flanks are limited in angle and

the whole system is kept in place. Internal stability is also interpreted by permafrost. BAFU indicates a probability for extensive permafrost occurrence (SWISSTOPO, 2018a). This is supported by periglacial forms (APP-B7 [E]) which indicate the (former) existence of permafrost. It is not known, if permafrost is still present or not.

[6] A surface lowering of around -1.5 m is indicated. Based on the pictures, a periglacial form with different lobes can be seen. If a miscalculation or a real surface movement is present, can not be stated.

[7] At 2‘600 m a.s.l. begins the blue area with a positive surface balance of around +10 m. It is the debris covered glacier tongue of Birchgletscher, which is relatively stable since the 90ies. The glacier extent was underestimated by SGI (FISCHER et al., 2014) and smaller mapped than it actually was. The increase of surface elevation is surprising. As APP-B8 [A/B] shows the glacier front steepened from 2011 until 2017, which corresponds to an increasing amount of ice. The lateral glacier limits are extended. Because no positive mass-balance took place during the period (GLAMOS, 2018), the accumulation can only be explained with a higher flow velocity. STOCKER-WALDHUBER et al. (2018) could show, that alpine glaciers react very quickly to changes of forcing (e.g. the temperature). It is assumed, that the very warm year of 2015 could have triggered a rapid increase in ice flow velocity. Like an elastic band, the ice fall stretched and thinned while more ice was accumulated on the relatively flat area of the glacier tongue. Leading to a steeper and bulked ice front which reveals the characteristically cracked frontal zone (APP-B7 [F]). Going up the glacier tongue, the ice mass increase reaches a value of up to +13 m (at 2‘700 m a.s.l.).

[8] At 2‘750 m a.s.l. the balance changes from a surface increase to a decrease within short distance (equilibrium zone). The balance structure reveals the internal flow paths and shows, how the ice is squeezed through the narrow flanks.

[9] Above the equilibrium zone, the surface lowered around -12 m while the glacier splits into two arms. The western arm reveals an ice thinning of up to -60 m. This is possible due to the vertical measurement of the steep north face DEMs. The real thickness loss will be smaller. In 2011 the upper part of the western Birchgletscher was still connected with the glacier tongue. Today it is separated. Birchgletscher is only fed by the eastern arm, which reveals a loss of around -10 m since 2011.

[10] Aside of the bulking glacier tongue, the lateral scree indicates a surface lowering of around -2 m. Based on the calculated differences it is assumed that covered ice melted, while the glacier tongue in the middle pushed in. Therefore, the lateral small ice occurrences are melting uninterrupted.

Stampbach catchment (FIG. 62)

[1] The apex of the Stampbach catchment reveals a lowering of the surface of around -8 m. This is based on the construction of the different protection measures including a deflecting dam and the excavation of a new riverbed into northerly direction. The elevation can be therefore verified and can be assumed to be correct (APP-B9 [A]).

[2] On 2‘000 m a.s.l., the surface changes abruptly from stable terrain to a negative balance indication of around -5 m. The area is located within a debris flow channel and the sharp transition is based on the border between bedrock and sedimentary accumulations. Even though the channel seems to be sparsely vegetated in the lower section, the upper part looks more recent. The orthophoto showed, that until 2017 the channel was relatively small. The aerial images of 2018 reveal now a different picture. The channel is wide, debris covered but still ends abruptly at 2‘000 m a.s.l. (APP-

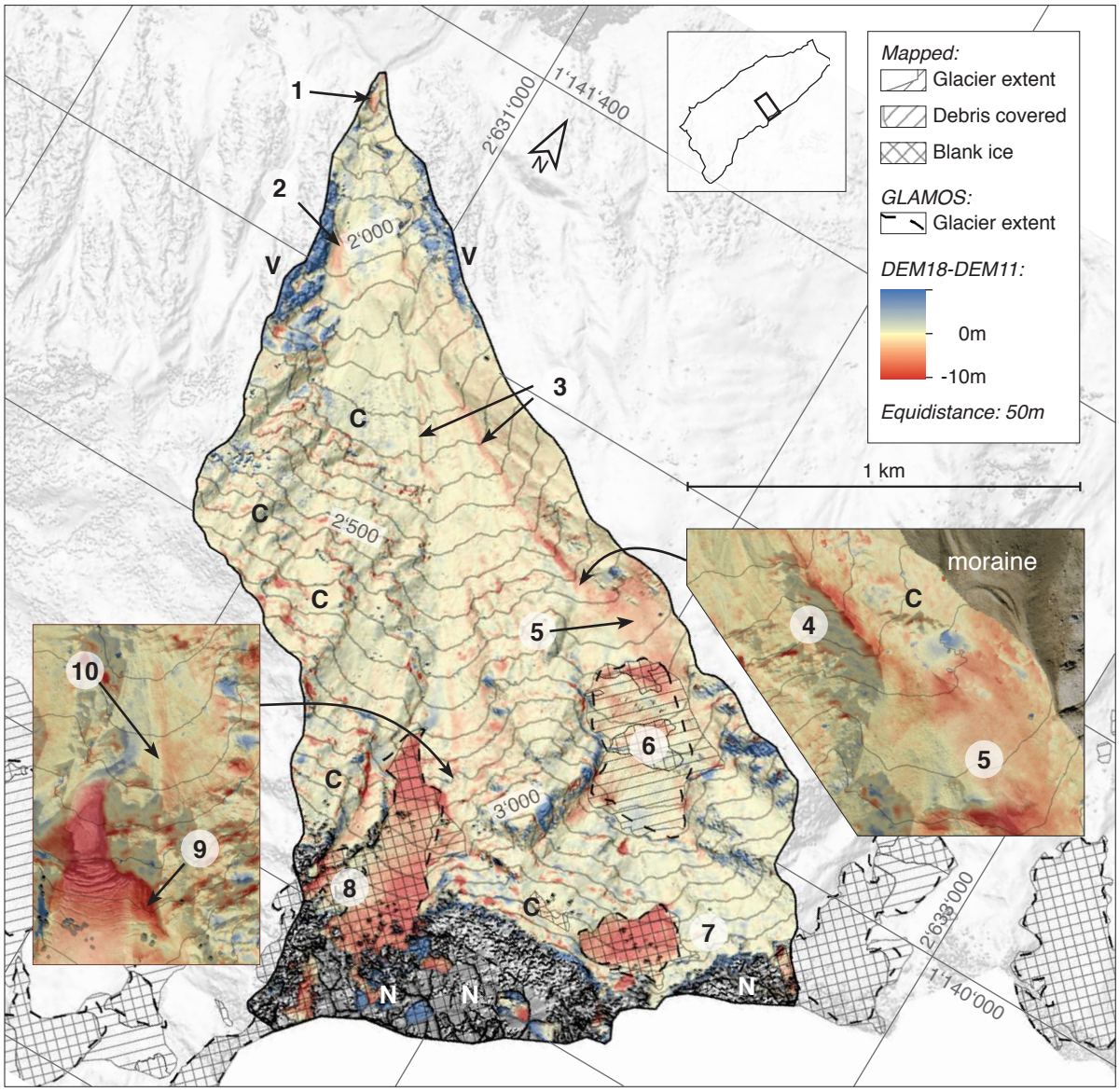

FIG. 62: The Stampbach catchment. (Source: own illustration)

B9 [B]). It seems that the channel became active during the last years.

[3] Both channels reveal a lowering of around -12 m, while the deepening of the Innre Stampbach Gletscher is more explicit.

[4] Around 2'500 m a.s.l. the channel is -22 m deeper than 2011. The orthophoto between 2011 and 2017 reveal the reason: the erosion «climbed» upwards and reached the moraine at 2'600 m a.s.l. (APP-B10 [A/B]).

[5] The reddish area revealed a surface lowering of around -1 to -2 m. Because the glacier tongue of Innre Stampbachgletscher is not debris covered and can be visually seen, the affected area has to include dead ice. The ice melt results in a lowering of the surface and the transportation of sediments in direction of the funnel. Based on the orthophotos (APP-B9 [D/E]) the calculated volume loss is verified. The illustrated paths in APP-B10 [C] show how the material is assumably transported. The area also reveals a small area which reveals little surface increase. Similar to Birchbach, one part is decreasing and directly beneath, the ice is accumulating. Why is unclear and would need to be investigated. Further on, the frontal / lateral moraine of [5] is not shown in FIG. 62, but

it does not reveal any changes of the surface. Similar to the moraine bastion of Tännerbach, an underlying bedrock step is assumed which stabilises the moraine.

[6] The Innre Stampbachgletscher itself reveals negative surface indications (at 2‘700 m a.s.l. up to -9 m), but the loss is not very big. Some parts at 2‘900 m a.s.l. show a positive result (+3 m).

[7] In contrary to [6], the ice field north of Alwä Rigg indicates a high negative balance (-21 m).The calculation result is supported by the consultation of pictures from 2009 (APP-B10 [F/G]). It is estimated, that around three-quarters of the ice mass already disappeared. The loss can be used as explanation why Innre Stampbachgletscher was relatively stable: the ice decay of the hanging glacier felt onto the underlying glacier, which was regularly fed by the ice masses. This process will now stop very fast and also Innre Stampbachgletscher will begin to melt quickly.

[8] The Uistre Stampbachgletscher reveals an extensive surface lowering of -8m over the whole glacier with an increased negative balance at [9] (-25 m), while the glacier extension did not change significantly between 2011 and 2018 (APP-B10 [F/G]).

[10] The area below the Uistre Stampbachgletscher indicates a small surface lowering of around -4 m. Based on aerial images of GEOPLAN AG (2015), underneath the debris cover dead ice is present, which induced a debris flow event in 2015. Therefore the negative balance is correct and illustrates large scale subsurface ice existence.

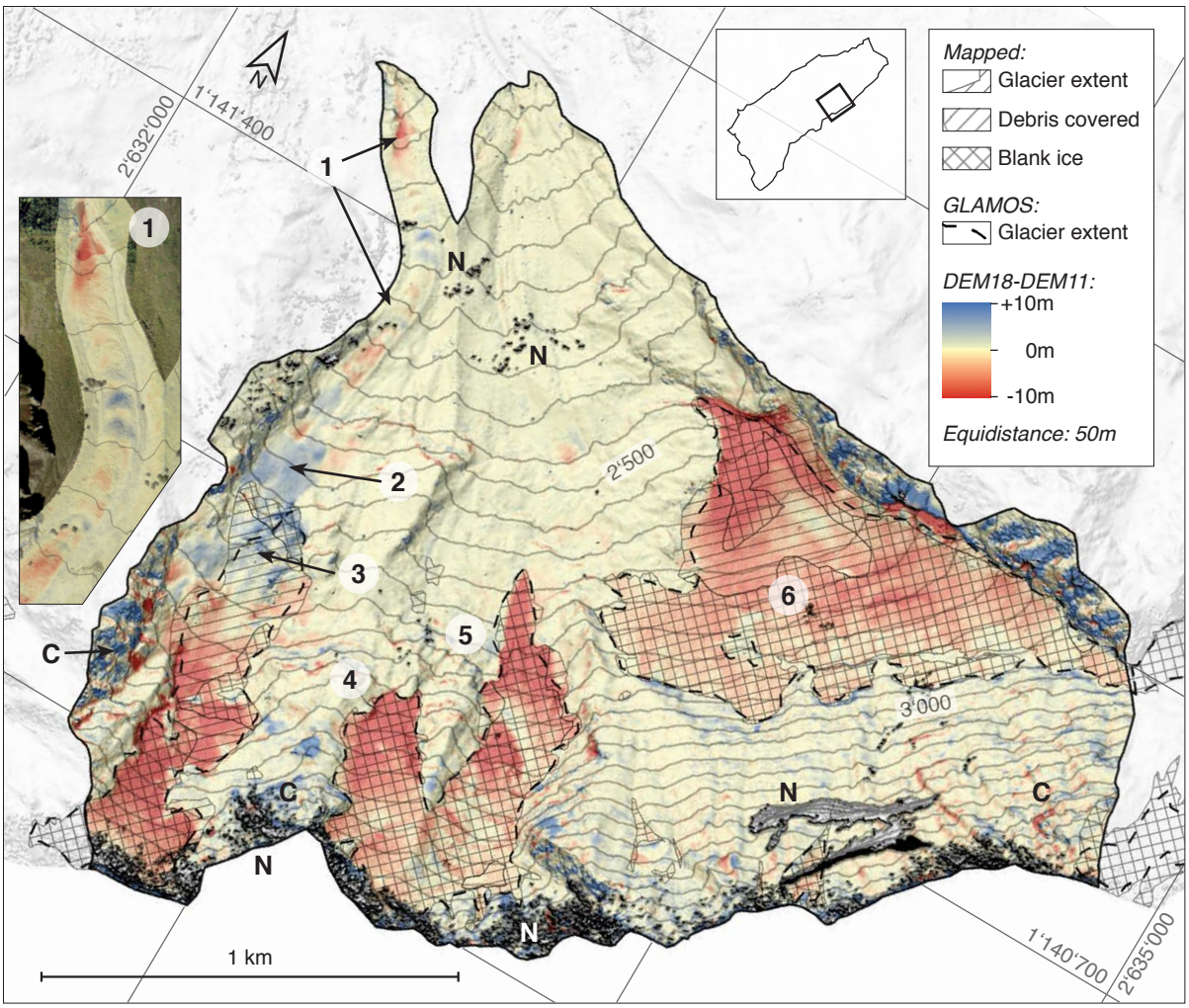

FIG. 63: The Loibinbach catchment. (Source: own illustration)

Loibinbach catchment (FIG. 63)

[1] The western catchment tongue with the Chleine Loibinbach reveals a surface lowering of around -7 m at 2‘050 m a.s.l., followed by alternating positive and negative balances (around +8 m to -2 m) in direction to south-east. The ogive similar form is characteristic for alternating processes which left behind a regular form. Based on the orthophotos and pictures of the measurement, the phenomenon resembles a rock glacier. But none of the considered map shows the assumed process. The research on past postcards and aerial images revealed the fact, that during the 80ies a glacier advancement occurred where the Oigstchummunglacier pushed forward (APP-B11). When in time this process started and for how long the pushing movement took place is not retraceable. It is assumed, that the main glacier ice disappared fast and left over the debris. This assumption is based on the fact, that the rock glacier did not lost volume since 2011 but rather a shift of the ogives and debris on the surface can be seen. As FIG. 64 shows, the rock glacier is still moving but it is not clear, why the structure reveals bulking and lowering areas.

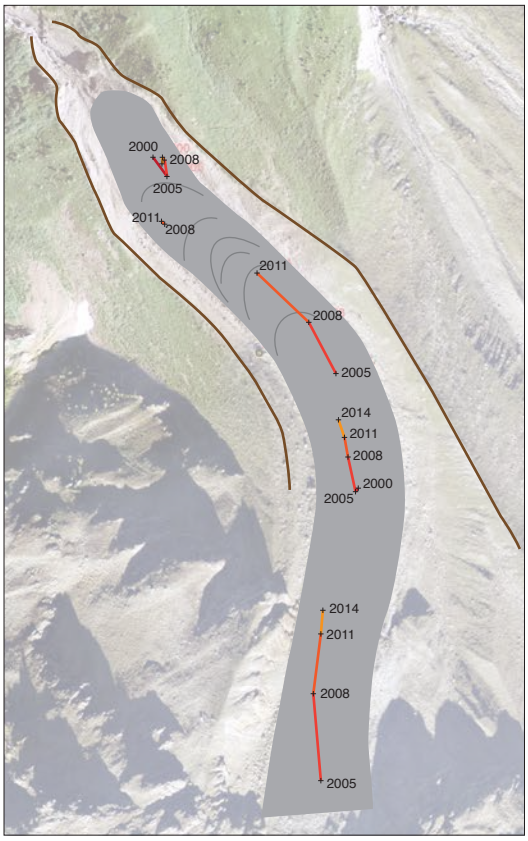

FIG. 64: The relative movement of the Oigstchummun rock glacier, based on visually tracked boulders on the surface. (Source: own illustration)

[2] Between 2‘400 m and 2‘750 m a.s.l. in the western channel, the balance reveals mainly positive values (up to +7 m). While the bedrock topography seems to be stable and the elevation increase is large, it can be assumed that under the partly debris covered surface ice is accumulated. Otherwise the increase of around +6 m can not be explained. It is assumed that the ice fall at 2‘650 m a.s.l. supplies the underlying dead ice with ice fragments, which are directly merged with accumulated debris from the surrounding areas. The resulting medley is the basis for a developing rock glacier which flows out of the source area below 2‘500 m a.s.l. (APP-B12 [A]).

[3] The glacier tongue of Oigstchummunglacier reveals a surface increase of up to +9 m. Like for the Birchbachgletscher, the positive balance with a surface increase of several meters can be assumably explained with faster flowing ice masses, correlated with less ice accumulation above the ELA. Oigstchummunglacier reveals a balance equilibrium between 2011 and 2018 at 2‘750 m which is followed by surface lowering up to -16 m at 3‘000 m a.s.l. On top at 3‘300 m a.s.l. the ice surface lowered around -6 m (APP-B12 [B]).

[4] Until 3‘150 m a.s.l. the glacier tongue reveals a surface lowering of up to -25 m. Above, the loss is around several meters. It is assumed, that due to the steep terrain, the glacier flows faster and loses much quicker volume. At 3‘130 m a.s.l. the glacier loss is nearly zeroed due to the inflow of ice masses from above, combined with a slower flow rate. It can be assumed, that underneath the glacier a bedrock step will appear (APP-B12 [C]).

[5] Similar to [4], above 3‘100 m a.s.l. the surface lowering is small (several metres) while below at

3‘000 m a.s.l. a first ice fall reveals losses around -25 m. At 2‘900 m a.s.l. again a platform indicates small increased surface elevation (+3 m) which is based on slower flow velocities and the ice input from above. Below 2‘850 m a.s.l. the glacier ends up into a steep ice fall with losses up to -20 m (APP-B12 [C]).

[6] The Loibinbachgletscher decays more and more into smaller patches. While the surface lowering at 2‘900 m is only a few meters (around -5 m), the glacier tongue retreated significantly and therefore represents the highest value of -36 m (APP-B13).

Beichbach catchment (FIG. 65)

[1] Up to 2‘100 m a.s.l. the catchment reveals two small areas with little indicated volume loss. The western area shows an elevation difference around -1 m up to -2 m in correlation to the swissALTI3D. The area is debris covered and beside some small trees sparsely vegetated. It is assumed, that erosional or settlement processes of the debris led to the negative balance. But it can not be verified (APP-B14 [C]).

[2] More east and in the centre of the catchment tongue, the marked area indicates a surface lowering of around -2 m in the riverbed of Beichbach. Based on possible erosional processes, it is assumed that the calculations are correct and the river either transported more debris away or incised into the underlying bedrock (APP-B14 [A]). Due to the geomorphological setting of the cone, the former is assumed.

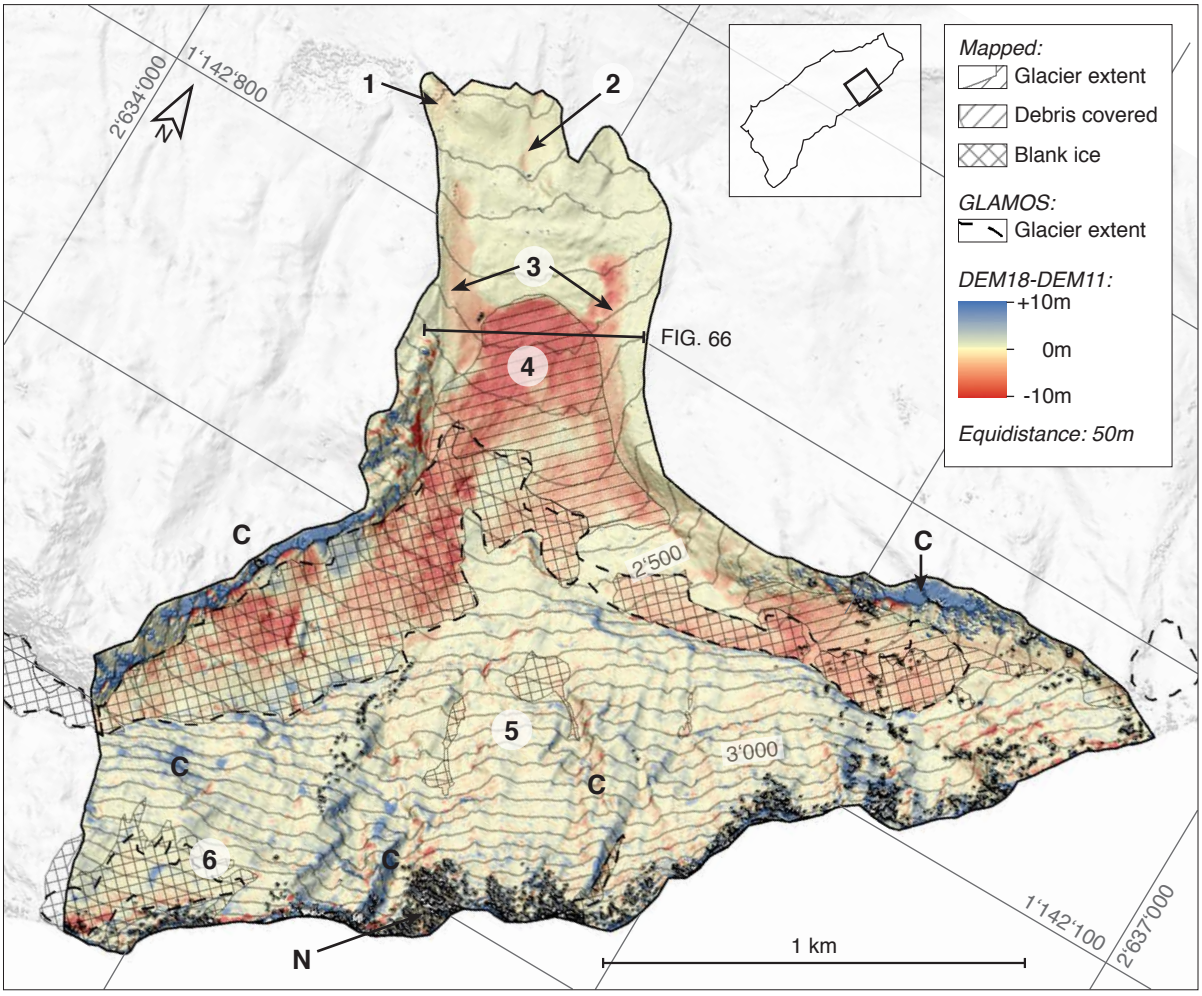

FIG. 65: The Beichbach catchment. (Source: own illustration)

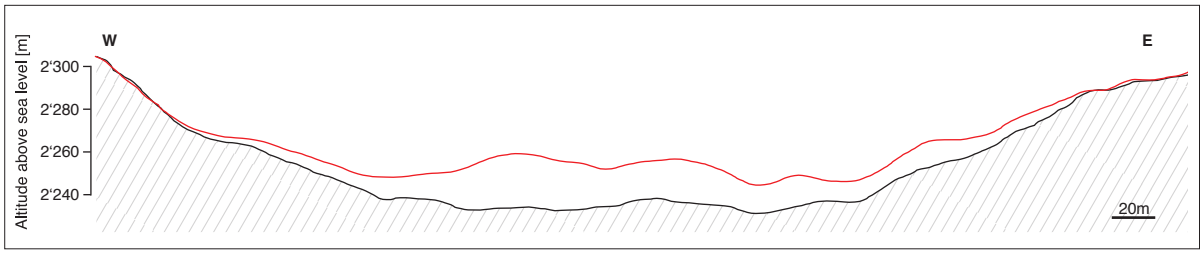

FIG. 66: Cross section of Dischligletscher at 2‘250 m a.s.l. (marked in FIG.65). (Source: own illustration)

[3] The flat intermediate area between the two red shaded patches is stable and shows no differences, while the red patches east and west of it indicate large surface lowering. While the western part reveals up to -3 m surface differences, the eastern one has a -12 m lower surface than 2011. Based on orthophotos, the western surface change is located on a lateral moraine which was probably ice cored. Field observations could not reveal any indications for ice. But because erosional deposits can neither be seen underneath on pictures nor on the difference calculations, an ice cored moraine is assumed, which lost volume through melting processes and hence the surface lowered. The eastern patch however is based on a relatively flat area which is also debris covered on the surface. The connection to the mapped glacier indicates covered ice remnants which melt out. This assumption is supported by old orthophotos and pictures (APP-B14 [B/D]).

[4] The tongue of Dischligletscher is shaped by a surface lowering of up to -26 m (FIG. 66). The glacier tongue retreated only 50 m since 2011 (ABB-P14 [D/E]). It is assumed, that higher flow velocities led to a stable glacier front. The glacier tongue lost volume especially in the lower 100 m, while the central area above 2‘300 m reveals a less negative balance (around -2 m). Both upper glacier arms lost around -5 to -10 m in ice and can not support the glacier tongue in the lower parts anymore. The separation of the eastern glacier already cut the ice input, while the western arm will separate in the next years.

[5] The granitic north face of the Lonzahörner reveals no change and can be assumed to be stable.

[6] The ice field on the steep north face of Breithorn reveals only little change. But also here a loss of ice on the upper parts can be seen (-3 m), while the lower part volume accumulated (+1 m).

4.4.2 Discussion & outlook

The results mainly show differences of the glaciers and their surrounding, while the large parts of the catchments are assumably stable. No hidden slides or other surprising processes could be found. But, the catchments reveal different predominant processes. While Gitzi-, Bätzla- und Wilerbach show only small changes based on rock fall events or fluvial erosion, the catchments east of Tännerbach are severely dominated by the retreating glaciers. Therefore the preconditions for debris flow events are different. GEOPLAN AG (2007) assessed the debris flow susceptibility of each channel with the already named

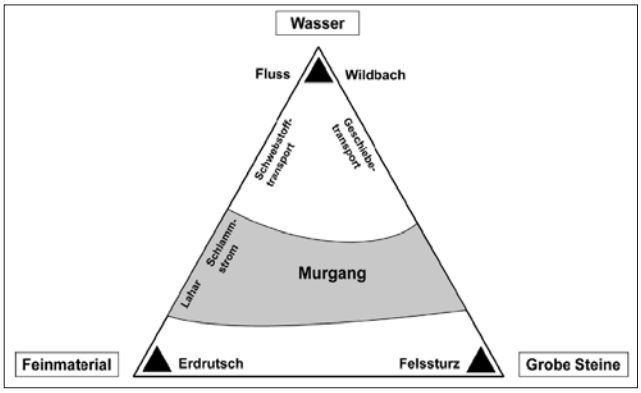

FIG. 67: Main composition of a debris flow, based on a three-phase-diagram. (Source: RICKENMANN, 2014)

results in chapter 4.1.1. But based on the calculations of the photogrammetric survey, the different parameters should be discussed after the debris flow definition by RICKENMANN (2014: 48): *«Ein Murgang ist ein in der Regel schnellfliessendes Gemisch von Lockermaterial und unterschiedlichen Anteilen von Wasser. Murgänge weisen an der Front eine hohe Feststoffkonzentration auf und zeichnen sich durch ein schubartiges Fliessverhalten aus, das sich deutlich vom Reinwasser-Abfluss unterscheidet.»* (see FIG. 67). While the water availability will be discussed in chapter 5., here the focus is based on debris availability and the water independent preconditions. Following the DEM-differencing, three main sediment reservoirs can be found:

1. At the huge depositions of Galn and the moraine bastions of Tännerbach and Stampbach («Massifs»).
2. On the glacier tongues and / or directly in front of them («Coverage»).
3. Widespread above the treeline («Scatter»).

After the description from where the debris is mainly originating, the three reservoir types are discussed.

Debris formation

The erosive effectiveness of glaciers is mainly based on basal process, influenced by ice and water pressure and the flow velocity (BOULTON, 1979). HERMAN et al. (2015) showed that the bedrock strength reveals also a huge impact. Neglecting the influence of topography and flow velocity, a weak material is faster eroded than a strong one. The glaciers in the Lötschental mainly develop in altitudes of existing granite (around 3‘100 m a.s.l.) and flow steeply into the underlying gneisses. During the fieldwork water leaked from small cracks in massive gneissic bedrock (2‘400 m a.s.l.) and indicated the susceptibility of the material (FIG. 68). Beside the assumption that gneisses and their sub-categories are physically weaker than granite and are therefore easier erodible by glacier activity, water availability in fissures can lead to a physical destruction of the rock, based on temperature cycles and is well known as frost weathering in alpine regions (ZEPP, 2014). The dark colour of the biotite-gneisses reveal high temperature differences between day and night and can shed due to high internal temperature gradients, even if no water or ice is present. Based on practical experiences, the surface temperature of such dark rocks can exceed the limit to be touched by hand. GRUNER (2008) could show, that warm temperatures lead to a closure of cracks due to the extension of the material. The highest rate of rock destruction can be located in spring, when the fissures are open, melt water is available and big temperature differences are present. The upcoming increasing temperatures could therefore lower the process of bedrock fragmentation. It is questionable if a decrease will be observed due to the fact, that on the steep north faces still huge temperature variabilities can be assumed.

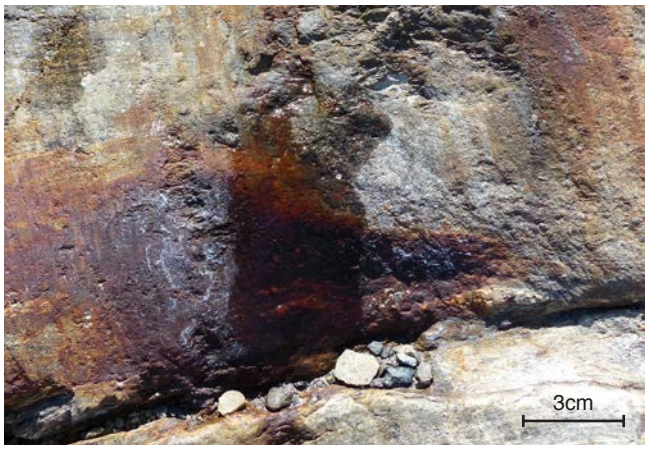

FIG. 68: Water discharge out of a gneiss on basal bedrock in the Nästbach catchment. (Source: own photography)

While during the 80ies the glacier glossed in the sunlight (SWISSTOPO, 2018a), today they are covered with several meters of debris. Even the glaciers on the north face are less exposed to solar radi-

ation, the ice masses are below the modelled mean ELA. The temperature correlated ablation process (e.g. HOCK, 2003) leads to an ongoing ice melt which should result in glacier retreat. But the debris covered glaciers do not retreat significantly and are nearly stable. As it can be seen on the retrieved DEM-differencing maps, the increased melt sets in over the whole glacier surface and not only on the glacier tongue. PRATAP et al. (2014) could show, that even small debris coverage of ice can lead to a reduced ablation rate. The accompanied insulation effect also minimises the ablation dependency on altitude. Based on the reduced ablation rate with the assumably higher flow velocity of some glaciers, it can be stated, that the debris coverage decelerated the ice melt. Beside other glaciological factors, the glacier tongues of Nest-, Birch-, Oigstchummun- and Dischligletscher assumably would have been already vanished without the debris cover.

While the catchments of Gitzi-, Bätzla-, Wiler- and Tännerbach are relatively calm regarding debris flow activity, Nest-, Birch- and Stampbach reveal high recurring flow rates, followed by several events of Loibin- and Beichbach (GEOPLAN AG, all reports).

Massifs

Obvious sediment reservoirs are located on the topographic steps in the Tänner-, Birch- and Stampbach catchment. These steps hinder the huge sedimentary deposits (Galn, moraine bastion of Tännerbach and Stampbach) to be moved or eroded. The slopes of the debris reservoirs reveal a slope of around 33° (FIG. 69), which is comparable to the measurements and modellings of the debris slopes of CURRY et al. (2009) at Feegletscher. The critical angle depends on the composition of the sediment (internal friction) and leads to mobilisation of material if the angle is exceeded. This explains why the huge sedimentary deposits are stable for years not only in size, but also in detailed surface characteristics: based on the conducted photogrammetric survey and after the consultation of orthophotos between 1980 and 2018 (SWISSTOPO, 2018a), neither a structure of the moraine bastions nor of Galn showed any changes. It is questionable which role permafrost comprises. Following the official map of BAFU (SWISSTOPO, 2018a), permafrost is probably existent in the respective areas. However the steep south westerly oriented face of Galn is stable since decades, in place and in appearance, the gullies did not develop further on. If permafrost would have been present, the uppermost layers would have been continuously eroded due to ongoing thawing. Like DAMM & FELDERER (2013) on page 146 state: *«(...) the lowering of permafrost table may increase the susceptibility of slopes for instabili-*

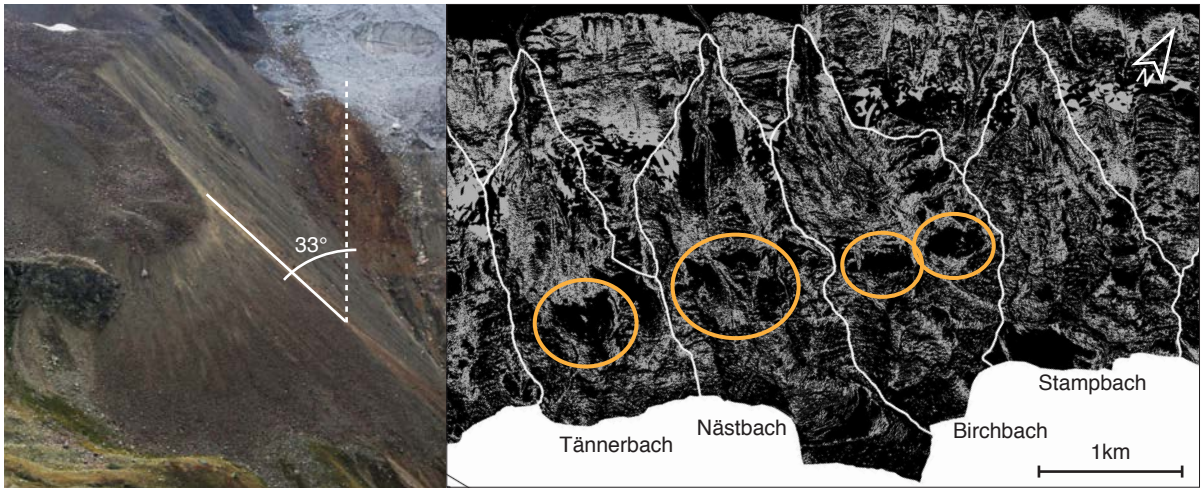

FIG. 69: Left: Slope angle of Galn (left). In the background, Birchgletscher is visible. Right: A map with indicated slope angles between 33°-40° (grey). The topographic steps are marked with orange circles. (Source: own photography & SWISSTOPO, 2018a)

ties and consequently the initiation of debris flows. In this case, the thickening of the active layer can increase sediment availability in potential debris flow initiation zones and may also reduce the shear strength of debris.» It is therefore not fully clear, if the big sedimentary reservoirs are supported by internal permafrost or not. Another factor can be presumed in the composition of the respective bodies: a possible majority of coarse grained sediments and boulders could result in an unhindered runoff of fluvial inputs. Even if the sediments are stabilised by possible permafrost underneath, no water can be dammed and therefore no material can be triggered as debris flows.

The stability of the accumulations implicates the question about their age. The Dufourmap of the little ice age extent (SWISSTOPO, 2018a) illustrates a maximal glacier extent just to the discussed forms and not further. Based on the glacial history of the valley (chapter 2.3) it is estimated that the sediment bodies are several thousand years old. In summary the huge debris accumulations represent an impressive appearance, but they did not build the foundation for debris flow activity in the past years.

Even if the former history did not show any changes, the situation can drastically change when the slopes get undercut by erosion of the fundament. While some parts of the massive accumulations are based on solid rock, the slopes often end on quaternary and sometimes vaguely vegetated surface coverage. If these underlying sediments are mobilised, the on top lying package will be transported too. Galn shows indications of such processes (marked in APP-B7 [C]), but also these scars are stable since decades.

Coverage

Based on the retrieved data the correlation between debris flows and glaciers can be defined by the position of the glacier tongue. All catchments reveal a stepped topography whereas the glacier tongues are lying on a trough edge between 2‘200-2‘600 m a.s.l. There they stayed for several decades more or less stable and revealed a conveyor belt similar sedimentary transport.

In the Birchbach catchment sediments accumulate on pure bedrock below exactly this topographic step at 2‘500 m a.s.l. (FIG. 70). This reservoir was identified by GEOPLAN AG (2010) as source for a

FIG. 70: The Birchgletscher transport mechanism. It transports mainly granite from the Bietschhorn, while the lateral flanks are characterized by weathered (reddish) biotite-gneisses. Illustrated are the different processes which leads to susceptible debris accumulations. (Source: own photography)

major debris flow event of Birchbach in 2009 which was triggered by an intensive rainfall. That shows exemplarily, that beside the availability of debris and water, also the underground and permeability of the material plays an important role. The bedrock prevented the water from percolation into the underground. The delayed runoff led to an oversaturation of the sediments which triggered immediately a mass movement. Similar events happened in 2013, when debris was mobilised on the ice front of Birchgletscher (GEOPLAN, 2014) and also in 2015, when in the Stampbach catchment debris flows sheared off from dead ice (GEOPLAN AG, 2015 & illustrated in FIG. 62 as [10]).
The described ice accumulation at the Birchbach glacier tongue (indicated as surface uplift in FIG. 61) was accompanied by a steepening of the ice front at the same location where the topography steepens. Such processes facilitate the accumulation of debris on areas below. Stampbach reveals a similar case: the Innre Stampbachgletscher accumulates debris in the former glacier basin which is eroded through the narrow gorge, seen in APP-B10 [C]. The gorge and the channel are limited by bedrock, the debris comes directly out of the glacier basin. The Uistre Stampbachgletscher accumulates the debris on the dead ice field directly aside of the active glacier tongue.

Scatter

The large debris coverage above the treeline is a common appearance in the alps and is mainly originating from rock decay. But for the analysed catchments, not only the widespread obvious debris cover ,but also the fine grained sedimentary deposits in the near surrounding (sole, embankment) of channels have to be considered. It is possible that debris deposits within a rock face or on a random slope are mobilised, but moreover it is probable, that a debris flow grows in size due to lateral erosion processes into these accumulations or by lateral input from smaller catchments.
Signs of these processes can be observed in the area and reveal a scared surface, especially in the vegetated zones. Based on the slope angles and the catchment preconditions, every catchment on the south side is endangered by debris flow activity like GEOPLAN AG (2007 & 2013) stated in their several reports.

Triggering

Finally the sediment availability has to be discussed by the size of the debris flow. Debris flows are defined by the water capability of a river and its debris carriage (RICKENMANN, 2014). Floods with lower intensity (30-year event HQ_{30}) transport less material than larger events (HQ_{300}) due to their water content. GEOPLAN (2007 & 2013) calculated these volumes with the respective methods (TAB. 10).

TAB. 10: Calculated debris volumes for flood events (GEOPLAN, 2007 & 2013). For Gitzi-, Nest- and Beichbach no data was available. Some rivers are not debris flow endangered for HQ_{30} events.

[m^3]	Gitzi-bach	Bätzla-bach	Wiler-bach	Tänner-bach	Nest-bach	Birch-bach	Stamp-bach	Loibin-bach	Beich-bach
HQ_{30}			11‘000			25‘000	30‘000		
HQ_{100}		7‘000	18‘000	45‘000		40‘000	45‘000	15‘000	
HQ_{300}		9‘300	24‘000			50‘000	60‘000		
EHQ		60‘000	15‘0000	90‘000		80‘000	90‘000	35‘000	

Because HQ_{30} events are based on relatively small volumes, nearly every catchment of the Lötschental reveals the possibility of limited debris flow activity. But larger events do not only need more severe triggering factors but also more available debris. Therefore the location of the trigger event is important.

Small amounts in steep slopes can result in a debris flow, while huge amounts in flat areas reveal no danger. The observed debris flows normally followed the already existing riverbed (GEOPLAN AG, different reports) and are therefore crucial for the build-up of a mass movement. While Nestbach and Birchbach are similar catchments, Birchbach had several debris flow events in the past years while Nestbach had no activities. The difference can be found in the position of the glacier tongue in correspondence with the glacial outflow and the position of the channels. The glacier tongue of Nestbach retreated more and is located above the topographic bedrock nose at 2'450 m a.s.l. The glacial torrent flows directly from glacier tongue over the nose down the slope. While the glacier reveals a slope of around 24° in the area of the tongue, below the ice and on top of the bedrock shoulder the slope flattens to 1° for 130 m in distance and increases again up to 31° below the step. Following RICKENMANN (2014) debris flows can be stopped if the slope angle decreases below 18° due to increased friction and the loss of water content. Thus this topographic step blocks the whole width of the valley for around 430 m and prevents material of the glacier to be mobilised and stops a beginning mass movement.

Birchbach also reveals such a step, but it does not traverse the whole trough valley and stops directly east of the glacier tongue. A 130 m wide gully is built out between the glacier and Galn (FIG. 71). It is exactly the place, where in 2013 the debris flow was initiated (GEOPLAN AG, 2014). The retrieved calculations of the DEM-differencing revealed, that this part included dead ice and assumably still does.

FIG. 71: Photography of a debris flow evnt on th 29th of July 2013 in the Birchbach catchment. It is exactly on the same spot, where the topographic step decreases and ice is still present.
(Modified after GEOPLAN AG, 2014)

For both catchments can be stated, that not only the debris accumulation is crucial, but also the underground which decides about the triggering or not. Therefore it does not surprise that GEOPLAN AG (2015) stated, that three of seven Stambach debris flow events of 2015 were not triggered by rain, but rather on high glacier melt rates which resulted in slipping debris patches. Based on those events further questions about possible decollement horizons arise, especially regarding the presence of possible permafrost. Therefore the perspective of sediment availability changes. It is out of scope of this thesis to analyse how permafrost can influence debris flow events. The relation between permafrost degradation in a non-creeping slope area and the possible initiation or increase of debris flow activity is intensively discussed (DAMM & FELDERER, 2013).

Based on the reports from GEOPLAN AG and the performed calculations of the DEMs, the debris availability can be stated as following: The «Massifs» are calculated and are rated as stable, while the debris around the glaciated areas revealed the main source for debris availability due to their unstable underground and easy triggerability («Coverage»). Neither «Scatter» nor the topography reveal any large changes or hidden slides.

Future

To have a glimpse into the future researches about past processes can be helpful. During different conversations local people told about the increasing activities of the debris flow channels and natural

hazards in total. But PEDOTH et al. (2014) made researches in Tyrol and showed, that local inhabitants who were affected by one or more events are variously influenced and can therefore divert in perception from the real situation. So could STOFFEL et al. (2008) show, that the debris flow activity of the Ritigraben, southerly of the Lötschental, was relatively stable for the last 300 years. Based on data of GEOPLAN AG (2008), they stated that for Stampbach the amount of transported volumes increased between the periods of 1989-2007 (averaged 7‘700 m^3/year) and 2000-2007 (averaged 15‘000 m^3/year) but no declaration about the recurrency was made.
It is assumed that the debris flow recurrency rate stayed the same, while the volumes increased, based on more available debris. How the sediment availability will change in the future is difficult to predict. The glaciers will be gone and the glacial erosion will be zeroed. The future availability depends on the coverage and the location with the corresponding topography. It can be separated into two timespans which are derived from the glacial coverage:

1. In a first phase until the glaciers completely have disappeared, the periglacial sediment transport will assumably increase. This is mainly based on unconsolidated surface structures and higher melt rates of the glaciers (DELANEY et al., 2018). The main issue for the Lötschental are the sediment deposits around the critical glacier tongues (Nest-, Birch- Stampbach) where widespread accumulations on bedrock are easily erodible. Steep glacier tongues like Birchgletscher reveal in the near future the problem of acute ice fall and high amounts of meltwater which could trigger a debris flow during warm and sunny periods. The effects of permafrost thawing are assumed to be initially minor due to a delayed signal (STAUB, 2015) and to increase instability processes only in a slow way, especially on steep north faces (HAEBERLI & HOHMANN, 2008).
2. In a second phase it can be speculated, that based on GRUNER (2008) the frost weathering processes will be shifted to higher altitudes and that lower areas will reveal more vegetation. This can result in a lower rate of erosion due to relatively strong bedrock (granite) and to more consolidated surface structures. On one hand, HAEBERLI & HOHMANN (2008) describe higher erosional rates due to more destabilized surfaces. But on the other hand, RAYMOND-PRALONG et al. (2015) reveal a scenario, where the reduced average runoff and it‘s peak will limit sediment transport, because the time when the critical threshold is exceeded will decrease. STOFFEL et al. (2013) concludes, that the rate of debris flow events assumably will stay constant, while the debris flow magnitude will increase. In the Lötschental the decreased permafrost tables can also destabilise old structures like Galn what could increase the rate of erosion and therefore the sediment availability.

Even though the glacier retreat after Egesen stadial led to an increased erosion rate, a reactivation of manifold debris flow activities has not to be assumed. Permafrost is decreasing and northerly exposed flanks will be destabilized. It can be assumed, that the changing processes are compensating each other and will result in a similar sediment availability than today - preconditioned the «Massifs» are stable.

5 DISCUSSION

5.1 Research questions

To discuss the remains of the glacier melt, the research questions (framed) about water and sediment availability, will be answered in the following sections.

Water availability

1. What are the different contributors to the runoff of the Lonza river and how can they be quantified? How do glaciers influence the runoff?
2. How does the runoff change in future?
3. Is there a possibility of a developing water scarcity in the valley?

1. The developed and applied water model could show how the different contributors of rain, snow melt, ice melt and evapotranspiration influence the runoff of the main river Lonza. The quantification of the parameters is based on the measurements of MeteoSwiss (temperature and precipitation) and BAFU (runoff Lonza) in Blatten. It revealed two different areas of in Lötschental: the catchment of BLA is mainly influenced by glacial melt (51 %) and is responsible for 71 % of the measured runoff in FER (FIG. 27 / 29). Therefore a strong dependency of ice melt is recognised. Also the tributary torrents show the same behaviour and the main differences between the torrents can be defined in the amount of glacial coverage.
2. Based on the CH2018 (2018) scenarios, the temperatures increase and the precipitation pat-

terns change. Due to the temperature dependency of the glaciers, the main consequence can be perceived in the glaciated catchments. The modelled glacier disappearance until the end of the century results in a runoff collapse of around -25 % for RCP2.6, -43 % for RCP4.5 and -48 % for RCP8.5 for the catchment BLA, while the percentages for FER are around 2-3 % smaller. The tributary torrents show a similar picture based on their main catchment reference (BLA or FER). Ferdenbach which is mainly influenced by snow melt and rain reveals a modelled runoff decrease of -38 % (RCP8.5) while the strongly glaciated Uistre Talbach loses around -75 % for the same scenario (see FIG. 37 / page 51).

3. The water scarcity was assessed through the correlation between the known water consumption and the modelled tributary torrents, which are presumed to represent the runoff pattern of the used water springs. Even if the water consumption is with 948 litre per day and person very high today, the springs provide enough water for the municipalities. The future modelled projections show a significant decrease of the torrent runoff volumes, nevertheless a water scarcity could not clearly be modelled (FIG. 38). It has to be taken into account, that the revealed data is based on a monthly resolution and therefore any short-term scarcities can not be pictured. But even if no water shortcomings can be recognised here, it is assumed that the water situation in the valley will be influenced by strong fluctuations without any damping processes regarding the runoff behaviour.

Sediment availability

4. Where are the main sedimentary reservoirs? And how did they form?
5. How could they be triggered as mass flows and why?
6. Is an effect of decreasing permafrost visible or assumable?

4. The main sedimentary reservoirs were assessed with the DEM-differencing of two elevation models of 2011 and 2018. It was recognised, that the main reservoirs can be separated into the three group «Massifs», «Coverage» and «Scatter». The «Massifs» describe old sedimentary accumulations, originating from former ice ages several thousand years ago. The «Coverage» can be found on strongly debris covered ice such as glacier tongues or dead ice bodies. This phenomenon is acute and is based on retreating ice masses which are unable to transport sedimentary deposits. The third reservoir named «Scatter» describes the widespread debris cover above the treeline, which results out of little ongoing erosive processes in the alpine area.
5. The study has shown, that the «Massifs» and the «Scatter» can be estimated to be stable in location, while the «Coverage» implies the highest risk of being triggered as debris flow. The sediment accumulation on ice reveals a lower triggering threshold due to a prevented water infiltration. A possible water input is forced to drain above the ice surface, destabilizing the on top lying sediments. Depending on where the ice body is located, sliding sediments can result in a debris flow if the topographic (steep terrain) and material (composition) preconditions are given (seen at Birchbach). These preconditions can change and the debris flow activity of a channel can vary significantly. The triggering of a debris flow is based on a fluvial input which can be based on rain or melt water. Several events of Stampbach have shown, that high amounts of melt water led to debris flow events during days without any precipitation.
6. If decreasing permafrost is important for the investigated sedimentary reservoirs can not be stated conclusive. There was no detailed permafrost analysis conducted. But the stable «Massifs»

reveal a phenomenon which should have or should be influenced by a permafrost table. Due to the fact, that no changes can be recognised, it is questionable how and when permafrost was (or is) influencing the sediment availability in the valley. Beside other indications, the developed rock glacier in the Dischlibach catchment indicates ongoing periglacial processes.

5.2 Outlook

To assess and discuss the results of the glacier retreat, the risk of the processes has to be taken into account. Risk is defined as a function of the parameters «hazard», «exposure» and «vulnerability» which are specified as following (IPCC, 2012 & CH2018, 2018: 106):

- «Hazard»: *«(...) weather events such as storms, floods, droughts, or heat waves both in terms of the probability of occurrence as well as the physical intensity.»*
- «Exposure»: *«(...) geographical distribution of people, livelihoods, and assets or infrastructure - generally speaking, of all items potentially exposed to hazards including ecosystems in their services.»*
- «Vulnerability»: *«(...) describes how specific exposure will be affected by a specific hazard; that is, it relates the intensity of a given hazard to its impact, such as wind damage to buildings as a function of wind speed or the effect of a flood on a local community and the livelihoods of its residents.»*

The factors of «exposure» and «vulnerability» will change only in small ranges due to a given infrastructure and an existing knowledge about possible dangerous alpine processes. The factor which will be significantly affected by climate change is «hazard».
The glacier retreat leads to an increased risk due to hazards such as debris flows, droughts and floods. STOFFEL et al., (2008: 232) writes: *«However, even if the frequency of summer events decreases (...), the magnitude and related impacts of future summer debris flows could be greater than currently (...) because warmer temperatures and higher precipitation intensities could result in greater runoff, an increase in the transport capacity of surges leading to a greater erosive potential of debris flows.»* Even though there will be no glaciers which can transport sediments to possible easily triggerable locations in future, the volume and energy of single debris flow events could increase due to a higher fluvial input based on heavy precipitation events (CH2018, 2018). In the same way, the recurrency rate of events could decrease due to a higher triggering threshold for single events.
This phenomenon can already be presumed in the existing records of debris flow events of Birch- and Stampbach and in data of the catchment dam sediment inputs at Ferden (FIG. 72).
After peak water, the missing precipitation during the summer months can not be balanced by ice melt which results in the widely discussed projections of chapter three. In combination with the debris flow occurrences, an estimated hazard overlay is presumed.
Especially during dry periods, heavy rainfall events could trigger debris flows while the low water of Lonza reveals an immediate and unhindered fluvial runoff. Beside the loss of usable water, the heavy input can result in severe floods. Like for the sedimentary flux, the possible decrease in recurrency combined with an increase in intensity can already be interpreted in the statistics of floods of Lonza at Blatten (BAFU, 2019a). Possible cascading effects like in 2011 (GEOPLAN AG, 2012; RÖSSLER et al.

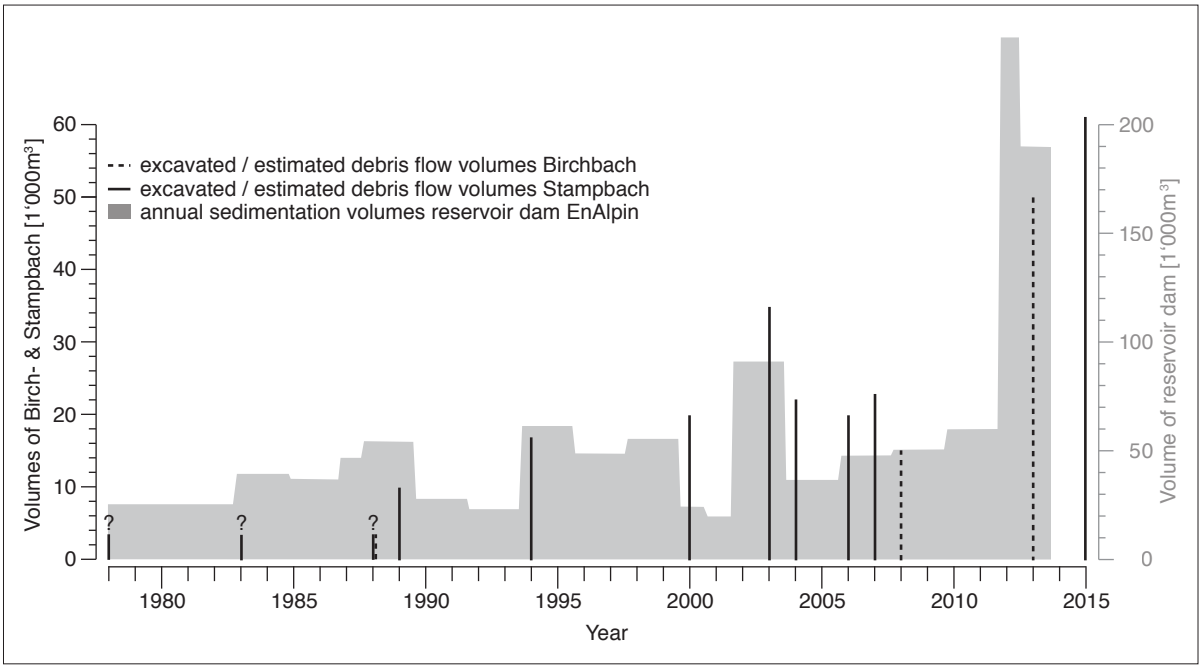

FIG. 72: An overview about the sedimentary fluxes. Correlation between the sedimentary input at the Stampbach catch basin (Blatten), estimates of debris flows of Birchbach and the accumulations in the reservoir dam at Ferden. The excavation of the dam is not executed regularly (always in August). The peak 2015 is based on 7 different events within 34 days. (Source: GEOPLAN AG 2008 / 2010 / 2014 / 2015; ENALPIN AG (2018); BÖCKLI & RICKENMANN, 2015)

2013) could therefore increase in consequences. Regarding such effects STOFFEL & CORONA (2018: 459) write: «*In many mountain areas across the world, increasing air temperature has resulted in a reduced frequency of snowfall, as well as an increasing proportion of rain. These trends are projected to continue, with more rain-on snow events very likely to lead to changes in snow avalanche activity and character, as well as winter landsliding. The projected changes to mountain environments, combined with socio-economic, cultural and political developments, will probably produce conditions and mass wasting without historical precedent. With the exposure of people and assets in high mountain regions to such natural hazards expected to increase in the future, the lessons learned from the extreme month of January 2018 can help authorities beyond the European Alps plan for the emerging risks.*» The ice melt also increases the susceptibility of the Lötschental. Based on the loss of the major summer water input (glacier melt), the valley reveals a higher dependency on water input by precipitation, which will be influenced by stronger short-time fluctuations (CH2018, 2018). Possible future water collection measures, which could dampen high runoff fluctuations or water scarcity phenomenons, could be located in trough valleys or could be built onto natural overdeepenings of Lang- and Anengletscher (HAEBERLI et al., 2016) which will appear in the next decades. Such measures would be highly endangered by mass flow events. Impacts could destroy the constructions or could trigger a flood wave which threatens the local population (HAEBERLI et al., 2013). The increased susceptibility of the system affects the valley in various perspectives and should be assessed carefully.

Based on the increasing factor «hazard», the risk increases too. Until then, the sediment and water availability was controlled by glacial processes which will change in the near future. The ice melt leads to a higher water runoff without damping, while the unconsolidated sedimentary remnants are affected by heavy precipitation events. Two effects which are directly depending on the retreating ice masses and which increase the risk for the local population.

6 CONCLUSION

This study has assessed the water and sediment availability in the Lötschental. For the main river Lonza a model has been developed which included the factors of rain, snow melt, ice melt and evapotranspiration. It has shown, that the Lonza catchment can be separated into two areas which represent a glaciated and a non-glaciated runoff pattern. The upper glaciated area, measured in Blatten by BAFU (BLA), reveals a modelled ice melt runoff contribution of 51 % and is responsible for a mean water input into the lower catchment, measured in Ferden by EnAlpin AG (FER), of 71 % in total (FIG. 29). This implies a strong dependency on the glaciers which is also illustrated in the model results of future runoff conditions under the RCP8.5 scenario (FIG. 33/34), where a decrease in total runoff of -46 % is calculated for FER (BLA: -49 %). The highest variabilities are retrieved during the summer months, where -87 % of the runoff is lost (FER, August), while the winter months increase around factor four in the modelled runoff (FER, January). The tributary torrents, which are assumed to reflect the input pattern of the municipality water springs, are modelled based on the results of the catchments of Ferden (FER) and Blatten (BLA) and describe the patterns of Lonza. Especially the strong glaciated catchments (Gisentella, Innre & Uistre Talbach) will decrease in runoff (FIG. 37). Uistre Talbach as indicator for the source Chaltr Brunn will assumably lose -84 % of the runoff volume in August, if the RCP8.5 sets in. Even if the averaged water consumption is very high in the valley (TAB. 01), the Lötschental is not directly affected by water scarcity problems today. The melting glaciers contribute with an increased water input to the system. When the glaciers are gone, the valley will be more depending on precipitation inputs. Because the precipitation variability will increase also (CH2018, 2018), the applied model with a monthly resolution can not describe short-time water scarcities based on increasing appearances of droughts and heavy precipitation events. The correlation of today‘s water consumption

with the RCP8.5 model results, reveals a first glimpse how it could look like (FIG. 38).
Here, detailed information about the springs are crucial. Today, the springs are used without having any knowledge about their origin and composition which leads to a huge uncertainty regarding future projections. To be able to describe the future water availability in a detailed way, more specific information about the springs are needed. The automatic surveillance system is a first step into more data gathering and helps to understand how rain, snow melt and ice melt are influencing the springs. Possible delays and dependencies can impact the springs in a distinct way. To be more confident about the future developments, a specific water source analysis should be approached soon. Otherwise the future changes in water availability will be unclear and the community may be endangered by possible water scarcity situations, especially if dry periods are accumulative.
Beside the origins of the springs, also the water consumption itself reveals a huge issue. The water usage is around a factor eight higher than Swiss average (chapter 2.5). It is assumed, that the former constant water availability could reveal a wrong perception of the upcoming challenges. To prevent water scarcity scenarios in a first place, the consumption should be lowered. A high water consumption reveals a lower threshold of being endangered by a water shortage. But even if the water consumption can be reduced, high runoff variabilities imply the need of water collection basins to bridge dry periods. Where and how such basins could be built needs to be assessed.

The sediment availability was assessed with DEM differencing based on data of 2011 and 2018. The main sedimentary reservoirs can be found in massive accumulations, supported by underlying and integrated bedrock structures («Massifs») and are located in specific areas around or on the glacier tongues («Coverage»), or are found widespread above the treeline without a specific location («Scatter»). While the «Scatter» mainly originates from rock decay, the «Massifs» were presumably built during former ice ages and are several thousand years old (chapter 2.3). The «Coverage» is a phenomenon of the actual glacier retreat and describes an acute process. The most active debris flow channels are fed by glacier tongues which transport high amounts of sediments to easy triggerable locations (e.g. on top of topographical steps). The ice builds a good decollement horizon which mobilises debris faster than other underground and high meltwater runoff volumes can trigger debris flows without any precipitation inputs. The «Massifs» reveal a possible sediment reservoir for debris flows, if their structure is undercut by ongoing surface erosion and / or possible permafrost is decreasing which destabilises the internal setup. This thesis was not able to discuss the topic of permafrost deeper. In the future, permafrost should be investigated especially regarding the «Massifs». A beginning collapse of the sediment bodies reflects a huge danger for the local population in the valley. However, during this study, no changes of the «Massifs» could be measured.

The future of the Lötschental can be separated into two timespans:

1. The first phase describes the situation until the total runoff of Lonza stops to increase. The steep and still coherent glaciers on the south side of Lonza will increase their flow velocities due to higher temperatures. The ice will aggregate in the lower parts, contributing more debris to triggerable areas. Afterwards the glacier tongues will be separated (or are already divided) into a lower dead ice glacier tongue and a steep ice fall, hanging on the north face of the Bietschhorn ridge. The dead ice bodies lead to a delayed runoff signal, because ice melt is reduced. The ice falls will rapidly decay which could release suddenly water quantities due to the liberated impact energy of the collapsing ice. It is presumed, that the southern glaciers will vanish rapidly once the glacier tongues are se-

parated from the firn (already visible at Stampbach). In this timespan, the water availability will be characterized by an increased runoff volume due to enhanced ice melt input which also leads to a higher sediment availability.

This phase will inevitably take place, but it depends on the applied RCP scenario when it takes place. Based on CH2018 (2018) it is modelled, that for RCP2.6 the glacier retreat will stop at an ice extension of around 20 % of today until the end of the 21st century (APP-C1). If RCP8.5 arises, this situation is expected to set in after the first half of century has passed (due to delay). But in contrary to RCP2.6, the retreat of RCP8.5 will not stop and will continue with the second phase.

2. In the second phase, the glaciers vanish completely and the valley significantly changes in appearance. The runoff will assumably increase slowly or will stay constant after the ELA has reached an altitude above 3‘200 m a.s.l. At this altitude the ice cap of Petersgrat and the Anengletscher will be fully affected by ablation processes and could equalize the missing ice of the south side (FIG. 36, points A and C). Once the remaining ice masses have reached a specific volume, the runoff will decrease rapidly (peak water). It is estimated that peak water is reached around the middle of the century. The unconsolidated debris, sometimes still aggregated on dead ice bodies, is easily triggerable by heavy rainfall events and could lead to severe debris flows. After the glaciers have vanished and the risk of «Coverage» will be decreased, the remaining sedimentary bodies («Massifs» and «Scatter») are mainly influenced by precipitation patterns. While the mean water input will decrease, the sediment availability is depending on the permafrost table retreat and the rate of solidification and vegetation coverage. It is possible, that missing glaciers and less precipitation in summer lead to a reduced debris flow activity, while the size and impact of events will increase due to stronger rain fall events and the high amount of triggerable sedimentary freight. If the RCP8.5 scenario will arise, it is assumed, that the valley will be ice free until the end of the century.

Even if the year of 2018 was dry and the mean air temperature was higher than average (FIG. 02), the valley was not affected by water scarcity. As widely discussed, the glaciers presumably dampen the missing precipitation input. Based on the increased factor of «hazard», the glacier retreat increases the risk in the Lötschental in general. Measures which can deal with droughts, heavy rainfall events and debris flow activities are needed to withstand the upcoming climatic challenges. It will be important, to develop adaption measures and management processes which comprise several aims in one.

The present change in glacier existence reveals a system transformation which was formerly unknown. Glaciers dominated our alps for hundred of years and after their vanishing, the basic processes in the alps will be different. Today the Lötschental already indicates effects in debris flow system changes, while the water system seems to be constant. With the ongoing climate change, the consequences will increase in severity. The separation point between the different temperature curves based on the RCP scenarios 2.6, 4.5 and 8.5, is estimated to be around 2030 (CH2018, 2018). Then it will be clearer how the future of the glaciers, including the water and sediment availability, in the Lötschental will look like at the latest.

BIBLIOGRAPHY

ADAMS, M. S., FROMM, R., & LECHNER, V. (2016). High-resolution debris flow volume mapping with unmanned aerial systems (UAS) and photogrammetric techniques. International Archives of the Photogrammetry, Remote Sensing and Spatial Information Sciences - ISPRS Archives, 2016-January(July), 749–755. http://doi.org/10.5194/isprsarchives-XLI-B1-749-2016

ALLEN, M.R., O.P. DUBE, W. SOLECKI, F. ARAGÓN-DURAND, W. CRAMER, S. HUMPHREYS, M. KAINUMA, J. KALA, N. MAHOWALD, Y. MULUGETTA, R. PEREZ, M. WAIRIU, AND K. ZICKFELD (2018). Framing and Context. In: Global Warming of 1.5°C. An IPCC Special Report on the impacts of global warming of 1.5°C above pre-industrial levels and related global greenhouse gas emission pathways, in the context of strengthening the global response to the threat of climate change, sustainable development, and efforts to eradicate poverty [Masson-Delmotte, V., P. Zhai, H.-O. Pörtner, D. Roberts, J. Skea, P.R. Shukla, A. Pirani, W. Moufouma-Okia, C. Péan, R. Pidcock, S. Connors, J.B.R. Matthews, Y. Chen, X. Zhou, M.I. Gomis, E. Lonnoy, T. Maycock, M. Tignor, and T. Waterfield (eds.)]. In Press.

AUBERT, D. (1980). Les stades de retrait des glaciers du haut-valais, 97, 101–169. Unknown.

BAFU (2018). Sommer 2018: Trockenheit in der Schweiz. https://www.bafu.admin.ch/bafu/de/home/themen/wasser/dossiers/trockenheit-in-der-schweiz-juli-2018.html (request: 06.08.18)

BAFU (2019a). Hochwasserwahrscheinlichkeiten (Jahreshochwasser), Lonza - Blatten (EDV: 2269). https://www.hydrodaten.admin.ch/de/2269.html (request: 07.01.2019)

BAFU (2019b). Abflussdatenpaket der Messstation 2269; Lonza. Zur Verfügung gestellt durch das Bundesamt für Umwelt (BAFU) in diversen Mails. https://www.bafu.admin.ch/bafu/de/home/themen/wasser/zustand/daten/messwerte-zum-thema-wasser-beziehen.html (request: 22.04.2019)

BARRY, R.G., CHORLEY, R.J. (1987). Atmosphere, weather and climate, 5th edition, Routledge: London.

BAVAY, M., GRÜNEWALD, T., & LEHNING, M. (2013). Response of snow cover and runoff to climate change in high Alpine catchments of Eastern Switzerland. Advances in Water Resources, 55, 4–16. http://doi.org/10.1016/j.advwatres.2012.12.009

BELLWALD, B. (2009). Gletscherveränderungen und deren Auswirkungen am Beispiel des Lötschentales. Bachelorarbeit, ETH Zürich.

BELLWALD, W. (2009). Historisches Lexikon der Schweiz, Lötschental. http://www.hls-dhs-dss.ch/textes/d/D12907.php (request: 10.04.2019)

BINI, A., BUONCRISTIANI, J.F., COUTERRAND, S., ELLWANGER, D., FELBER, M., FLORINETH, D., GRAF, H.R., KELLER, O., KELLY, M., SCHLÜCHTER, C., SCHÖNEICH, P. (2009). Die Schweiz während des letzteiszeitlichen Maximums (LGM), Karte 1:500 000. Federal Office of Topography swisstopo, Wabern, Switzerland.

BÖCKLI, M., & RICKENMANN, D. (2015). Lonza: Geschiebetransportsimulationen mit sedFlow.

BÖRST, U.-J. (2006). Nachhaltige Entwicklung im Hochgebirge. Eine Systemanalyse von Mensch-Umwelt-Szenarien im Lötschental (Zentral-Alpen). These, 1–214.

BOULTON, G.S. (1979). Processes of glacier erosion on different substrata. Journal of Glaciology, 23(89), 1-24.

BROWN, M., & LOWE, D.G. (2005). Unsupervised 3D object recognition and reconstruction in unordered datasets, 5th Int. Conf. 3-D Digital Imag. Modeling. 56-63.

BÜHLER, Y., ADAMS, M. S., BOSCH, R., & STOFFEL, A. (2016). Mapping snow depth in alpine terrain with unmanned aerial systems (UASs): Potential and limitations. Cryosphere, 10(3), 1075–1088. http://doi.org/10.5194/tc-10-1075-2016

BURGA, C. A, PERRET, R., & ZOLLER, H. (2001). Swiss localities of early recognized Holocene climate oscillations. Vierteljahresschrift der naturforschenden Gesellschaft in Zürich, 146(2–3), 65–74.

BURGA, C. A. (1988). Swiss vegetation history during the last 18'000 years. New Phytologist, 110(1988), 581–602. http://doi.

org/10.1111/j.1469-8137.1988.tb00298.x

CH2018 (2018). CH2018 – Climate Scenarios for Switzerland, Technical Report, National Centre for Climate, Services, Zurich, 271 pp., ISBN: 978-3-9525031-4-0

CHUDLEY, T. R., DOYLE, S. H., SNOOKE, N., ABELLAN, A., & CHRISTOFFERSEN, P. (2018). High accuracy UAV photogrammetry of ice sheet dynamics with no ground control. The Cryosphere Discussions, (December), 1–22. http://doi.org/10.5194/tc-2018-256

CHY, Swiss Hydrological Commission (2009). Snow, ice and water in the Alpine Region: The system is undergoing radical change. Conference: Snow, Ice and Water in the Alpine Region - more topical than ever.

CLARK, P.U., DYKE, A.S., SHAKUN, J.D., CARLSON, A.E., CLARK, J., WOHLFARTH, B., MITROVICA, J.X., HOSTTLER, S.W., MCCABE, A.M. (2009). The Last Glacial Maximum. Science, 325(5941), 710–714. http://doi.org/10.1126/science.1172873

COSTA. A., MOLNAR, P., STUTENBECKER, L., BAKKER, M., SILVA, T.A., SCHLUNEGGER, F., LANE, S.N., LOIZEAU, J.-J., GIRARDCLOS, S. (2018). Temprature signal in suspended sediment export from an Alpine catchment. Hydrology and Earth System Sciences, 22, 509-528. https://doi.org/10.5194/hess-22-509-2018.

CURRY, A. M., SANDS, T. B., & PORTER, P. R. (2009). Geotechnical controls on a steep lateral moraine undergoing paraglacial slope adjustment. Geological Society, London, Special Publications, 320(1), 181–197. http://doi.org/10.1144/sp320.12

DAMM, B., & FELDERER, A. (2013). Impact of atmospheric warming on permafrost degradation and debris flow initiation - a case study from the eastern European Alps. E&G Quarternary Science Journal, 62(2), 136–149. http://doi.org/10.3285/eg.62.2.05

DEBRET, M., CHAPRON, E., DESMET, M., ROLLAND-REVEL, M., MAGAND, O., TRENTESAUX, A., BOUT-ROUMAZEILLE, V., NOMADE, J., ARNAUD, F. (2010). North western Alps Holocene paleohydrology recorded by flooding activity in Lake Le Bourget, France. Quaternary Science Reviews, 29(17-18), 2185–2200. http://doi.org/10.1016/j.quascirev.2010.05.016

DELANEY, I., BAUDER, A., HUSS, M., & WEIDMANN, Y. (2018). Proglacial erosion rates and processes in a glacierized catchment in the Swiss Alps. Earth Surface Processes and Landforms, 43(4), 765–778. http://doi.org/10.1002/esp.4239

DER BUND (2011). Unwetter kostet Lötschental 20 Millionen Franken. https://www.derbund.ch/panorama/vermischtes/unwetter-kostet-loetschental-20-millionen-franken-/story/30207694 (request: 13.01.19)

DEWALLE, D.R., RANGO, A. (2008). Principles of Snow Hydrology. Cambridge University Press, Cambridge.

DIXON, J. L., VON BLANCKENBURG, F., STÜWE, K., & CHRISTL, M. (2016). Glaciation's topographic control on Holocene erosion at the eastern edge of the Alps. Earth Surface Dynamics, 4(4), 895–909. http://doi.org/10.5194/esurf-4-895-2016

E-PICS (2018). Bildarchiv Online, ETH Zürich. https://www.e-pics.ethz.ch/de/home/ (request: 18.12.2018)

E-PICS (2019a). Bildarchiv Online, ETH Zürich. http://ba.e-pics.ethz.ch, picture code: LBS_R1-970953 (request: 12.02.2019)

E-PICS (2019b). Bildarchiv Online, ETH Zürich. http://ba.e-pics.ethz.ch, picture code: Fel_090723-RE (request: 12.02.2019)

EKK, Cryospheric Commission (2017). Glaciological Report (Glacier) No. 135/136 The Swiss Glaciers 2013/14 and 2014/15. (eds.) Andreas Bauder. Publication of the Cryospheric Commission of the Swiss Academy of Sciences, (135). http://doi.org/ http://doi.org/10.18752/glrep 135-136

ELLENBERG, H., LEUSCHNER, C., (2010). Vegetation Mitteleuropas mit den Alpen in ökologischer, dynamischer und historischer Sicht. Ulmer, Stuttgart.

ENALPIN AG (2018). Datenpaket der Lonza-Zuflüsse in den Stausee Ferden. Mail von Michel Salzgeber, 06.11.2018.

FAO, Food and Agriculture Organization of the United Nations (2018a). ETo Calculator. http://www.fao.org/land-water/databases-and-software/eto-calculator/en/ (request: 07.09.18)

FAO, Food and Agriculture Organization of the United Nations (2018b). Chapter 6 - ETc - Single crop coefficient (Kc). http://www.fao.org/docrep/X0490E/x0490e0b.htm#crop%20coefficients (request: 12.11.18)

FARINOTTI, D., USSELMANN, S., HUSS, M., BAUDER, A., FUNK, M. (2011). Runoff evolution in the Swiss Alps: projections for selected high-alpine catchments based on ensembles scenarios. Hydrological Processes, 26(13), 1909–1924. http://doi.org/10.1002/hyp.8276

FISCHER, M., HUSS, M., BARBOUX, C., & HOELZLE, M. (2014). The New Swiss Glacier Inventory SGI2010: Relevance of Using High-Resolution Source Data in Areas Dominated by Very Small Glaciers. Arctic, Antarctic, and Alpine Research, 46(4), 933–945. http://doi.org/10.1657/1938-4246-46.4.933

FOSTER, G., & RAHMSTORF, S. (2011). Global temperature evolution 1979–2010. Environmental Research Letters, 6(4), 044022. http://doi.org/10.1088/1748-9326/6/4/044022

GEOPLAN AG (2007). Schutzkonzept und Hochwassergefahrenkarten Gemeinden Ferden, Kippel, Wiler und Blatten. HWSK Lötschental. Bericht Nr. VS 1923, September 2007.

GEOPLAN AG (2008). Ereignisbericht Murgänge Stampbach Blatten im August/September 2008, revidiert. Bericht Nr. VS 1994. Oktober 2008.

GEOPLAN AG (2010). Beurteilung der Murganggefahr im Birchbach nach dem Ereignis vom 09.08.2009. Bericht Nr. VS 2021. Juni 2010.

GEOPLAN AG (2012). Hochwasserereignis vom 10.11.2011 im Lötschental, Ereignisanalyse. Bericht Nr. 2077, März 2012.

GEOPLAN AG (2013). Aktualisierung Gefahrenkarte Hochwasser, Gemeinde Ferden, Kippel, Wiler, Blatten. Bericht Nr. VS 3048 / 3049 / 3051, Oktober 2013.

GEOPLAN AG (2014). Ereignisanalyse Murgang Birchbach vom 29.07.2013. Bericht Nr. VS 3087. Februar 2014.

GEOPLAN AG & PRONAT UMWELTINGENIEURE AG (2015). Murgänge Stampbach Juli / August 2015. Ereignisanalyse Sofortmassnahmen Umweltbaubegleitung. Bericht Nr. VS 3210. November 2015.

GEORGOPOULOU, E., HARZHAUSER, M., NEUBAUER, T., MANDIC, O. & KROH, A. (2015). An outline of the European Quaternary localities with freshwater gastropods: Data on geography and updated stratigraphy. Palaeontologia Electronica, 2017(October), 10–13. http://doi.org/10.26879/527

GIGUET-COVEX, C., ARNAUD, F., POULENARD, J., DISNAR, J. R., DELHON, C., FRANCUS, P., DAVID, F., ENTR, D., REY,P.-J., DELANNOY, J. J. (2011). Changes in erosion patterns during the holocene in a currently treeless subalpine catchment inferred from lake sediment geochemistry (lake anterne, 2063 m a.s.l., NW french alps): The role of climate and human activities. Holocene, 21(4), 651–665. http://doi.org/10.1177/0959683610391320

GINDRAUX, S., BOESCH, R., & FARINOTTI, D. (2017). Accuracy assessment of digital surface models from Unmanned Aerial Vehicles' imagery on glaciers. Remote Sensing, 9(2), 1–15. http://doi.org/10.3390/rs9020186

GLAMOS (2018). Swiss Glacier Length Change. Glacier Monitoring Switzerland. Release 2018. doi:10.18750/lengthchange.2018.r2018.

GLETSCHERVERGLEICHE (2019). Interaktive Vorher-Nachher Bildvergleiche verschiedener Alpengletscher. http://gletschervergleiche.ch (request: 16.03.2019)

GLORI, Glaciers-to-rivers sediment transfer in alpine basins (2018). https:/glori.projects.unibz.it (request: 22.03.19)

GROSJEAN, M., SUTER, P.J., TRACHSEL, M., WANNER, H. (2007). Ice-borne prehistoric finds in the Swiss Alps reflect Holocene glacier fluctuations. Quaternary Science, 22(3), 203-207. DOI: 10.1002/jqs.1111

GRUNER, U. (2008). Climatic and Meteorological Influences on Rockfall and Rockslides. Interpraevent, 147–158.

HADES, Hydrologischer Atlas der Schweiz (2018). Daten- und Analyseplattform. https://www.hydromaps.ch (request: 16.11.18).

HAEBERLI, W., BÜTLER, M., HUGGEL, C., MÜLLER, H., SCHLEISS, A. (2013). Neue Seen als Folge des Gletscherschwundes im Hochgebirge - Chancen und Risiken. Forschungsbericht des Nationalen Forschungsprogramms. Schleiss, A. (Hrsg.). http://doi.org/10.3218/3534-6

HAEBERLI, W., & HOHMANN, R. (2008). Climate, Glaciers and Permafrost in the Swiss Alps 2050: scenarios, consequences and recommendations. Proceedings Ninth International Conference on Permafrost, 1(July), 607–612.

HAEBERLI, W., & PENZ, U. (1985). An attempt to reconstruct glaciological and climatological characteristics of 18 ka BP Ice Age glaciers in and around the Swiss Alps. Zeitschrift Gletscherk. Glazialgeol., 21 (January 1985), 351–361.

HAEBERLI, W., FRAUENFELDER, R., HOELZLE, M., & MAISCH, M. (1999). On rates and acceleration trends of global glacier mass changes. Physical Geography, 81(4), 585–591. http://doi.org/10.1111/j.0435-3676.1999.00086.x

HAEBERLI, W., LINSBAUER, A., COCHACHIN, A., SALAZAR, C., & FISCHER, U. H. (2016). On the morphological characteristics of overdeepenings in high-mountain glacier beds. Earth Surface Processes and Landforms, 41(13), 1980–1990. http://doi.org/10.1002/esp.3966

HAEBERLI, W., SCHAUB, Y., & HUGGEL, C. (2017). Increasing risks related to landslides from degrading permafrost into new lakes in de-glaciating mountain ranges. Geomorphology, 293, 405–417. http://doi.org/10.1016/j.geomorph.2016.02.009

HÄFELIN, J. (1955). Die Gliederung der Schweiz in Wetterprognosenbezirke. Geographica Helvetica, 10(1), 12–15. http://doi.org/10.5194/gh-10-12-1955

HAFNER, A., (2015). Schnidejoch und Lötschenpass, Archäologische Forschung in den Berner Alpen. Band 1, Volume 1. Archäologischer Dienst des Kantons Bern, Bern. ISBN: 978-3-907663-35-6.

HEIRI, O., KOINIG, K. A., SPÖTL, C., BARRETT, S., BRAUER, A., DRESCHER-SCHNEIDER, R., GAAR, D., IVY-OCHS, S., KERSCHNER, H., LUETSCHER, M., MORAN, A., NICOLUSSI, K., PREUSSER, F., SCHMIDT, R., SCHOENEICH, P., SCHWÖRER, C., SPRAFKE, T., TERHOST, B., TINNER, W. (2014). Palaeoclimate records 60-8 ka in the Austrian and Swiss Alps and their forelands. Quaternary Science Reviews, 106, 186–205. http://doi.org/10.1016/j.quascirev.2014.05.021

HERMAN, F., BEYSSAC, O., BRUGHELLI, M., LANE, S.N., LEPRICE, S., ADATTE, T., LIN, J.Y.Y., AVOUAC, J.-P., COX, S.C. (2015). Erosion by an Alpine glacier. Science, 350(6257), 193–195. http://doi.org/10.1126/science.aab2386

HERRNEGGER, M., NACHTNEBEL, H.-P., & HAIDEN, T. (2012). Evapotranspiration in high alpine catchments – an important part of the water balance. Hydrology Research, 43(4), 460–475. http://doi.org/10.2166/nh.2012.132

HOCK, R. (2003). Temperature index melt modelling in mountain areas. Journal of Hydrology, 282(1-4), 104–115. http://doi.org/10.1016/S0022-1694(03)00257-9

HOCK, R., (1999). A distributed temperature-index ice- and snowmelt model including potential direct solar radiation. Journal of Glaciology, 45(149), 101-111.

HUGGEL, C., HAEBERLI, W., KÄÄB, A., BIERI, D., & RICHARDSON, S. (2005). An assessment procedure for glacial hazards in the Swiss Alps. Canadian Geotechnical Journal, 41(6), 1068–1083. http://doi.org/10.1139/t04-053

HÜGI, TH., LEDERMANN, H., SCHLÄPPI, E. (1988). Geologischer Atlas der Schweiz, Lötschental. Schweizerische Geologische Kommission

HUSS, M., & HOCK, R. (2018). Global-scale hydrological response to future glacier mass loss. Nature Climate Change, 8(2), 135–140. http://doi.org/10.1038/s41558-017-0049-x

HUSS, M., JOUVET, G., FARINOTTI, D., & BAUDER, A. (2010). Future high-mountain hydrology: A new parameterization of glacier retreat. Hydrology and Earth System Sciences, 14(5), 815–829. http://doi.org/10.5194/hess-14-815-2010

IPCC (2012). Field, C. B., Barrros, V., Stocker, T. F., Qin, D., Dokken, D., Ebi, K. L., Mastrandrea, M. D., March, K. J., Plattner, G. K., Allen, S. K., Tignor, M. & Midgley, P. M. (eds.). Managing the Risks of Extreme Events and Disasters to Advance Climate Change Adaptation. Cambridge, UK, and New York, NY, USA: Cambridge Univeristy Press.

IPCC (2013). Stocker, T.F., D. Qin, G.-K. Plattner, M. Tignor, S.K. Allen, J. Boschung, A. Nauels, Y. Xia, V. Bex and P.M. Midgley (eds.). Climate Change 2013: The Physical Science Basis. Contribution of Working Group I to the Fifth Assessment Report of the Intergovern- mental Panel on Climate Change. Cambridge University Press, Cambridge, United Kingdom and New York, NY, USA, 1535 pp.

IVY-OCHS, S. (2015). Glacier variations in the European Alps at the end of the last glaciation. Cuadernos de Investigación Geográfica, 41(2), 295. http://doi.org/10.18172/cig.2750

IVY-OCHS, S., KERSCHNER, H., KUBIK, P. W., & SCHLÜCHTER, C. (2006). Glacier response in the European Alps to Heinrich Event 1 cooling: The Gschnitz stadial. Journal of Quaternary Science, 21(2), 115–130. http://doi.org/10.1002/jqs.955

IVY-OCHS, S., KERSCHNER, H., MAISCH, M., CHRISTL, M., KUBIK, P. W., & SCHLÜCHTER, C. (2009). Latest Pleistocene and Holocene glacier variations in the European Alps. Quaternary Science Reviews, 28(21-22), 2137–2149. http://doi.org/10.1016/j.quascirev.2009.03.009

IVY-OCHS, S., KERSCHNER, H., REUTHER, A., PREUSSER, F., HEINE, K., MAISCH, M., KUBIK, P.W., SCHLÜCHTER, C. (2008). Chronology of the last glacial cycle in the European Alps. Quarternary Science, 23(6-7), 559-573. DOI: 10.1002/jqs.1202

IVY-OCHS, S., SCHÄFER, J., KUBIK, P. W., SYNAL, H. A., & SCHLÜCHTER, C. (2004). Timing of deglaciation on the northern Alpine foreland (Switzerland). Eclogae Geologicae Helvetiae, 97(1), 47–55. http://doi.org/10.1007/s00015-004-1110-0

JENNINGS, K. S., WINCHELL, T. S., LIVNEH, B., & MOLOTCH, N. P. (2018). Spatial variation of the rain-snow temperature threshold across the Northern Hemisphere. Nature Communications, 9(1), 1–9. http://doi.org/10.1038/s41467-018-03629-7

JOERIN, U. E., NICOLUSSI, K., FISCHER, A., STOCKER, T. F., & SCHLÜCHTER, C. (2008). Holocene optimum events inferred from subglacial sediments at Tschierva Glacier, Eastern Swiss Alps. Quaternary Science Reviews, 27(3-4), 337–350. http://doi.org/10.1016/j.quascirev.2007.10.016

JOERIN, U. E., STOCKER, T. F., & SCHLÜCHTER, C. (2006). Multicentury glacier fluctuations in the Swiss Alps during the

Holocene. Holocene, 16(5), 697–704. http://doi.org/10.1191/0959683606hl964rp

JOHANNESSON, M., RAYMOND, C., & WADDINGTON, E., (1989). Time-Scale for adjustment of glaciers to changes in mass balance. Journal of Glaciology, 35(121).

JONAS, T., MARTY, C., & MAGNUSSON, J. (2009). Estimating the snow water equivalent from snow depth measurements in the Swiss Alps. Journal of Hydrology, 378(1-2), 161–167. http://doi.org/10.1016/j.jhydrol.2009.09.021

JORDA, M., & ROSIQUE, T. (1994). Le Tardiglaciaire des Alpes françaises du Sud : Rythme et modalités des changements bio-morphoclimatiques. Quaternary, 5(3), 141-149.

JOSS, J., SCHÄDLER, B., GALLI, G., CAVALLI, R., BOSCACCI, M., HELD, E., DELLA BRUNA, G., KAPPENBERGER, G., NESPOR, V., SPIESS, R., (1997). Operational Use of Radar for Precipitation Measurements in Switzerland. 1-13.

JOUVET, G., SEGUINOT, J., IVY-OCHS, S., & FUNK, M. (2017). Modelling the diversion of erratic boulders by the Valais Glacier during the last glacial maximum. Journal of Glaciology, 63(239), 487–498. http://doi.org/10.1017/jog.2017.7

JUTEBRING STERTE, E., JOHANSSON, E., SJÖBERG, Y., HUSEBY KARLSEN, R., & LAUDON, H. (2018). Groundwater-surface water interactions across scales in a boreal landscape investigated using a numerical modelling approach. Journal of Hydrology, 560, 184–201. http://doi.org/10.1016/j.jhydrol.2018.03.011

KANTON WALLIS (2016). Tourismuspolitik des Kanton Wallis. Kanton Wallis, 1-40.

KANTON WALLIS (2018). Hitzewellenplan für den Kanton. Department für Gesundheit, Soziales und Kultur, Dienststelle für Gesundheitswesen, 1-11.

KERSCHNER, H. (2009). Gletscher und Klima im Alpinen Spätglazial und frühen Holozän. Alpine Space - Man & Environment, 6(January), 1–26. Retrieved from http://www.uibk.ac.at/alpinerraum/publications/vol6/kerschner.pdf

KRAUSE, P., BOYLE, D. P., & BÄSE, F. (2005). Comparison of different efficiency criteria for hydrological model assessment. Advances in Geosciences, 5, 89–97. http://doi.org/10.5194/adgeo-5-89-2005

KUHN, M. (1980). Climate and glaciers, IAHS 131, 3-20.

KÜNG, O., FUA, P., BEYELER, A., FLOREANO, D., GERVAIX, F., ZUFFEREY, J.-C., & STRECHA, C. (2012). the Accuracy of Automatic Photogrammetric Techniques on Ultra-Light Uav Imagery. ISPRS - International Archives of the Photogrammetry, Remote Sensing and Spatial Information Sciences, XXXVIII-1/, 125–130. http://doi.org/10.5194/isprsarchives-xxxviii-1-c22-125-2011

LINSBAUER, A., PAUL, F., & HAEBERLI, W. (2012). Modeling glacier thickness distribution and bed topography over entire mountain ranges with glabtop: Application of a fast and robust approach. Journal of Geophysical Research: Earth Surface, 117(3). http://doi.org/10.1029/2011JF002313

LINSBAUER, A., PAUL, F., MACHGUTH, H., & HAEBERLI, W. (2013). Comparing three different methods to model scenarios of future glacier change in the Swiss Alps. Annals of Glaciology, 54(63), 241–253. http://doi.org/10.3189/2013aog63a400

LISEIN, J., LINCHANT, J., LEJEUNE, P., BOUCHÉ, P., & VERMEULEN, C. (2013). Aerial surveys using an unmanned aerial system (UAS): Comparison of different methods for estimating the surface area of sampling strips. Tropical Conservation Science, 6(4), 506–520. http://doi.org/10.1177/194008291300600405

LÖTSCHENTAL MARKETING AG (2019). Website of the Lötschental, https://www.loetschental.ch/ (request: 04.01.19)

MAISCH, M. (1987). Zur Gletschergeschichte des alpinen Spätglazials. Analyse und Interpretation von Schneegrenzdaten. Geographie Helvetica 42, 63-71.

MARCOTT, S. A., SHAKUN, J. D., CLARK, P. U., & MIX, A. C. (2013). A reconstruction of regional and global temperature for the past 11,300 years. Science, 339(6124), 1198–1201. http://doi.org/10.1126/science.1228026

MEEHL, G. A., ARBLASTER, J. M., & TEBALDI, C. (2005). Understanding future patterns of increased precipitation intensity in climate model simulations. Geophysical Research Letters, 32(18), 1–4. http://doi.org/10.1029/2005GL023680

METEOSWISS (2016). Niederschlag. https://www.meteoschweiz.admin.ch/home/wetter/wetterbegriffe/niederschlag.html (request: 29.11.2018)

METEOSWISS (2017). Schneegrenze / Schneefallgrenze. https://www.meteoschweiz.admin.ch/home/wetter/wetterbegriffe/schneegrenze-schneefallgrenze.html (request: 15.01.2019).

METEOSWISS (2019a). Klimabulletin Jahr 2018. Zürich.

METEOSWISS (2019b). IDAweb, Datenportal für Lehre und Forschung. https://gate.meteoswiss.ch/idaweb/login.do (request:

15.04.2019)

MICHELETTI, N., CHANDLER, J.H., LANE, S.N. (2015). Structure from Motion (SfM) Photogrammetry. Geomorphological Techniqus, Chap. 2, Sec. 2.2. British Society for Geomorphology. 1-12.

MORIASI, D. N., ARNOLD, J. G., LIEW, M. W. VAN, BINGNER, R. L., HARMEL, R. D., & VEITH, T. L. (2007). Model evaluation guidelines for systematic quantification of accuracy in watershed simulations. 50(3), 885–900.

NASH, J. E., & SUTCLIFFE, J. V. (1970). River flow forecasting through conceptual models, Part I. A discussion of principles. Journal of Hydrology, 10, 282–290. http://doi.org/10.1016/0022-1694(70)90255-6

NICOLUSSI, K., KAUFMANN, M., PATZELT, G., VAN DER PLICHT, J., THURNER, A., (2005). Holocene tree-line variability in the Kauner Valley, Central Eastern Alps, indicated by dendrochronological analysis of living trees and subfossil logs. Vegetation History History and Archaeobotany 14, 221–234.

NUSSBAUMER, S. U., BREITENMOSER, P., HOLZHAUSER, H., GROSJEAN, M., TRACHSEL, M., HAFNER, A., HOLZHAUSER, H., WANNER, H., ZUMBÜHL, H. J. (2011). Alpine climate during the Holocene: a comparison between records of glaciers, lake sediments and solar activity. Journal of Quaternary Science, 26(7), 703–713. http://doi.org/10.1002/jqs.1495

NUTH, C., & KÄÄB. (2011). Co-registration and bias corrections of satellite elevation data sets for quantifying glacier thickness change. Cryosphere, 5(1), 271–290. http://doi.org/10.5194/tc-5-271-2011

OTTO, J.-C., SCHROTT, L., JABOYEDOFF, M., DIKAU, R. (2009). Quantifying sdiment storage in a high alpine valley (Turtmanntal, Switzerland). Earth Surface Processs and Landforms 34, Issue 13. 1726-1742. https://doi.org/10.1002/esp.1856.

PAUL, F., MAISCH, M., ROTHENBÜHLER, C., HOELZLE, M., & HAEBERLI, W. (2007). Calculation and visualisation of future glacier extent in the Swiss Alps by means of hypsographic modelling. Global and Planetary Change, 55(4), 343–357. http://doi.org/10.1016/j.gloplacha.2006.08.003

PEDOTH, L., MITTERHOFER, P., & SCHNEIDERBAUER, S. (2014). Understanding risk perception and risk attitude of an Alpine community to improve risk management procedures. Proceedings of the 5th International Disaster and Risk Conference: Integrative Risk Management - The Role of Science, Technology and Practice, IDRC Davos 2014, (December 2018), 556–559.

PFAUNDLER, M. & ZAPPA, M. (2002). Die mittleren Abflüsse über die ganze Schweiz, ein optimierter Datensatz im 500x500m Raster. Fachzeitschrift «Wasser Energie Luft».1-15.

PIX4D (2018a). Pix4D Support, GSD calculator. https://support.pix4d.com/hc/en-us/articles/202560249-TOOLS-GSD-calculator (request: 22.09.18)

PIX4D (2018b). Pix4D Support, Accuracy of Pix4D outputs. https://support.pix4d.com/hc/en-us/articles/202558889 (request: 12.02.19)

PIX4D (2018c). Pix4D Support, Ground sampling distance (GSD). https://support.pix4d.com/hc/en-us/articles/202559809-Ground-sampling-distance-GSD- (request: 12.04.19)

PIX4D (2018d). Pix4D Support, Quality Report Help. https://support.pix4d.com/hc/en-us/articles/202558689-Quality-Report-Help (request: 12.04.19)

PIX4D (2018e). Pix4D Support, Step 1. Before Starting a project. https://support.pix4d.com/hc/en-us/articles/202557489-Step-1-Before-Starting-a-Project-4-Getting-GCPs-on-the-field-or-through-other-sources-optional-but-recommended- (request: 12.04.19)

PRATAP, B., DOBHAL, D. P., MEHTA, M., & BHAMBRI, R. (2015). Influence of debris cover and altitude on glacier surface melting: A case study on Dokriani Glacier, central Himalaya, India. Annals of Glaciology, 56(70), 9–16. http://doi.org/10.3189/2015AoG70A971

RABATEL, A., LETRÉGUILLY, A., DEDIEU, J. P., & ECKERT, N. (2013). Changes in glacier equilibrium-line altitude in the western Alps from 1984 to 2010: Evaluation by remote sensing and modeling of the morpho-topographic and climate controls. Cryosphere, 7(5), 1455–1471. http://doi.org/10.5194/tc-7-1455-2013

RASMUSSEN, S.0., BIGLER, M., BLOCKLEY, S.P., BLUNIER, T., BUCHARDT, S.L., CLAUSEN, H.B., CVIJANOVIC, I., DAHL-JENSEN, D., JOHNSEN, S.J., FISCHER, H., GKINIS, V., GUILLEVIC,M., HOEK, W.Z., LOWE, J.J., PEDRO, J.B., POPP,T., SEIERSTAD, I.K., STEFFENSEN, J.P., SVENSSON, A.M., VALLELONGA, P., VINTHER, B.M., WALKER, M.J.C., WHEATLEY, J.J., WINSTRUP, M. (2014). A stratigraphic framework for abrupt climatic changes during the Last Glacial period based on three synchronized Greenland ice-core records: refining and extending the INTIMATE event stratigraphy. Quaternary Science Reviews, 106, 14–28. http://doi.org/10.1016/j.quascirev.2014.09.007

RAYMOND-PRALONG, M., TUROWSKI, J., RICKENMANN, D., ZAPPA, M. (2015). Climate change impacts on bedload transport in alpine drainage basins with dydropower exploitation. Earth Surface Processes and Landfroms 40: 1587-1599.

REITNER, J. M., IVY-OCHS, S., DRESCHER-SCHNEIDER, R., HAJDAS, I., & LINNER, M. (2016). Reconsidering the current stratigraphy of the Alpine Lateglacial: Implications of the sedimentary and morphological record of the Lienz area (Tyrol/ Austria). E & G Quaternary Science Journal, 65(2), 113-144.

REMOTEPIXEL (2018). Plattform for Remote Images. https://viewer.remotepixel.ca/#3/40/-70.5 (request: 14.11.2018)

RICKENMANN, D. (2014). Methoden zur quantitativen Beurteilung von Gerinneprozessen in Wildbächen. WSL Berichte, Heft 9. 1-105. www.wsl.ch/publikationen/pdf/13549.pdf.

ROCK, G., RIES, J. B., & UDELHOVEN, T. (2011). Sensitivity Analysis of Uav-Photogrammetry for Creating Digital Elevation Models (Dem). ISPRS - International Archives of the Photogrammetry, Remote Sensing and Spatial Information Sciences, XXXVIII-1/C22(September), 69–73. http://doi.org/10.5194/isprsarchives-xxxviii-1-c22-69-2011

RÖSSLER, O., DIEKKRÜGER, B., & LÖFFLER, J. (2012). Potential drought stress in a Swiss mountain catchment. Ensemble forecasting of high mountain soil moisture reveals a drastic decrease, despite major uncertainties. Water Resources Research, 48(4), 1–19. http://doi.org/10.1029/2011WR011188

RÖSSLER, O., FROIDEVAUX, P., BÖRST, U., RICKLI, R., MARTIUS, O., & WEINGARTNER, R. (2013). Ereignisanalyse Extremhochwasser Lötschental, Wallis, 10. Oktober 2011. 21.

RUTISHAUSER, A., MAURER, H., & BAUDER, A. (2016). Helicopter-borne ground-penetrating radar investigations on temperate alpine glaciers: A comparison of different systems and their abilities for bedrock mapping. Geophysics, 81(1), WA119–WA129. http://doi.org/10.1190/geo2015-0144.1

SCAPOZZA, C. (2016). Evidence of paraglacial and paraperiglacial crisis in Alpine sediment transfer since the last glaciation (Ticino, Switzerland), Quaternary [online], Vol. 27(2). http://journals.openedition.org/quaternaire/7805 (request: 13.04.2019),

SCHADEGG, J. (2019), Dendrogeomorphologische Untersuchung einer Rutschung oberhalb von Ferden, VS. Masterarbeit.

SCHÄDLER, B. & WEINGARTNER, R. (2002): Komponenten des natürlichen Wasserhaushaltes 1961-1990. In: BWG: Hydrologischer Atlas der Schweiz (Tafel 6.3), Bern.

SCHAEFLI, B., HINGRAY, B., NIGGLI, M., & MUSY, A. (2005). A conceptual glacio-hydrological model for high mountainous catchments. Hydrology and Earth System Sciences Discussions, 2(1), 73–117. http://doi.org/10.5194/hessd-2-73-2005

SCHÜRCH, M., KOZEL, R., BIAGGI, D., & WEINGARTNER, R. (2010). Typisierung von Grundwasserregimenin der Schweiz. GWA. Gas, Wasser, Abwasser, 11, 955–965.

SCNAT, Swiss Academy of Sciences (2018). Ein Jahr der Extreme für Schweizer Gletscher, Medienmitteilung EKK SCNAT. https://naturwissenschaften.ch/service/news/106404-ein-jahr-der-extreme-fuer-schweizer-gletscher (reuqest: 20.10.18)

SECKLER, D., BARKER, R., & AMARASINGHE, U. (1999). Water scarcity in the twenty-first century. International Journal of Water Resources Development, 15(1-2), 29–42. http://doi.org/10.1080/07900629948916

SEIBERT, J., JENICEK, M., HUSS, M., & EWEN, T. (2014). Snow and Ice in the Hydrosphere. Snow and Ice-Related Hazards, Risks, and Disasters. http://doi.org/10.1016/B978-0-12-394849-6.00004-4

SEIERSTAD, I. K., JOHNSEN, S. J., VINTHER, B. M., & OLSEN, J. (2005). The duration of the Bølling-Allerød period (Greenland Interstadial 1) in the GRIP ice core. Annals of Glaciology, 42(3), 337–344. http://doi.org/10.3189/172756405781812556

SIEBERTH, T., WACKROW, R., & CHANDLER, J. H. (2015). UAV image blur-its influence and ways to correct it. International Archives of the Photogrammetry, Remote Sensing and Spatial Information Sciences - ISPRS Archives, 40(1W4), 33–39. http://doi.org/10.5194/isprsarchives-XL-1-W4-33-2015

SPREAFICO, M., & WEINGARTNER, R. (2005). Hydrologie der Schweiz. Rapports de l'OFEG, Série Eaux, (7), 1–138.

SRP AG (2008). Technischer Bericht und Kostenschätzung. Wasserkraftwerk Fafleralp, Blatten. 1-30. SRP / 3240-03-020-CD. doc

STAUB, B. (2015). The evolution of mountain permafrost in the context of climate change : towards a comprehensive analysis of permafrost monitoring data from the Swiss Alps, 207. Retrieved from https://www.swissbib.ch/Record/374561141/ Description#tabnav

STECK, A. (1983). Geologie Der Aletschregion (Vs). Bulletin de La Murithienne, 101, 135–154.

STOCKER-WALDHUBER, M., FISCHER, A., HELFRICHT, K., & KUHN, M. (2018). Ice flow velocity as a sensitive indicator of glacier state. The Cryosphere Discussions, (March), 1–18. http://doi.org/10.5194/tc-2018-37

STOFFEL, M., & CORONA, C. (2018). Future winters glimpsed in the Alps. Nature Geoscience, 11(7), 458–460. http://doi.org/10.1038/s41561-018-0177-6

STOFFEL, M., BOLLSCHWEILER, M., HASSLER, G.-M. (2006). Differentiating past events on a cone influenced by debris-flow and snow avalanche activity - a dendrogeomorphological approach. Earth Surface Processes and Landforms 31, 1424-1437. DOI: 10.1002/sp.1363

STOFFEL, M., CONUS, D., GRICHTING, M. A., LIÈVRE, I., & MAÎTRE, G. (2008). Unraveling the patterns of late Holocene debris-flow activity on a cone in the Swiss Alps: Chronology, environment and implications for the future. Global and Planetary Change, 60(3-4), 222–234. http://doi.org/10.1016/j.gloplacha.2007.03.001

STOFFEL, M., MENDLIK, T., SCHNEUWLY-BOLLSCHWEILER, M., & GOBIET, A. (2013). Possible impacts of climate change on debris-flow activity in the Swiss Alps. Climatic Change, 122(1-2), 141–155. http://doi.org/10.1007/s10584-013-0993-z

STRASSER, U., BERNHARDT, M., WEBER, M., LISTON, G. E., MAUSER, W. (2008). Is snow sublimation important in the alpine water balance. The Cryosphere, 2, 53-66.

SWISSTOPO, Federal Office of Topography (2012). swissALTI3D Ausgabebericht 2012, 1-5.

SWISSTOPO, Federal Office of Topography (2018a). Webbrowser with different layers. https://map.geo.admin.ch/ (request: 15.12.2018)

SWISSTOPO, Federal Office of Topography (2018b). swissALTI3D Ausgabebericht 2018, 1-7.

TINNER, W., & THEURILLAT, J.-P. (2003). Uppermost Limit, Extent, and Fluctuations of the Timberline and Treeline Ecocline in the Swiss Central Alps during the Past 11,500 Years. Arctic, Antarctic, and Alpine Research, 35(2), 158–169. http://doi.org/10.1657/1523-0430(2003)035[0158:uleafo]2.0.co;2

TONKIN, T. N., & MIDGLEY, N. G. (2016). Ground-control networks for image based surface reconstruction: An investigation of optimum survey designs using UAV derived imagery and structure-from-motion photogrammetry. Remote Sensing, 8(9), 16–19. http://doi.org/10.3390/rs8090786

UCPH, Centre for Ice and Climate (2018). Climate during Holocene. http://www.iceandclimate.nbi.ku.dk/research/climatechange/glacial_interglacial/climate_holocene/ (reguest: 30.12.18)

UN WATER (2019). Water Scarcity. http://www.unwater.org/water-facts/scarcity/ (request: 12.02.19)

VAN HUSEN, D. (1997). Institut für Geologie der Technischen Universität, Karlsplatz 13, A-1040 Wien, Austria. Quaternary International, 38/39(96), 109–118. http://doi.org/10.1016/S1040-6182(96)00017-1

VS (2018). Aussergewöhnliche Trockenheit im Wallis hält an - Anpassung der Gefahrenkarte für das französischsprachige Wallis. https://www.vs.ch (request: 27.09.18).

VSGIS (2019). Geographic Information System of Canton Valais. https://www.vsgis.ch/ (request: 13.03.2019)

WEHREN, B., WEINGARTNER, R., SCHÄDLER, B., & VIVRIOLI, D. (2010). Alpine Waters. Handbook of Environmental Chemistry (Vol. 6). http://doi.org/10.1007/978-3-540-88275-6

WELPMANN, M. (2003). Bodentemperaturmessungen und -simulationen im Lötschental (Schweizer Alpen).

WESTOBY, M. J., BRASINGTON, J., GLASSER, N. F., HAMBREY, M. J., & REYNOLDS, J. M. (2012). “Structure-from-Motion” photogrammetry: A low-cost, effective tool for geoscience applications. Geomorphology, 179, 300–314. http://doi.org/10.1016/j.geomorph.2012.08.021

WIEDEMANN, A., & BECKMANN, S. (2016). Quality aspects of aerial digital orthophotos, the producers point of view. International Archives of the Photogrammetry, Remote Sensing and Spatial Information Sciences - ISPRS Archives, 41(July), 449–453. http://doi.org/10.5194/isprsarchives-XLI-B2-449-2016

WITTMANN, H., VON BLANCKENBURG, F., KRUESMANN, T., NORTON, K. P., & KUBIK, P. W. (2007). Relation between rock uplift and denudation from cosmogenic nuclides in river sediment in the Central Alps of Switzerland. Journal of Geophysical Research: Earth Surface, 112(4), 1–20. http://doi.org/10.1029/2006JF000729

WULF, H., BOOKHAGEN, B., & SCHERLER, D. (2016). Differentiating between rain, snow, and glacier contributions to river discharge in the western Himalaya using remote-sensing data and distributed hydrological modeling. Advances in Water Resources, 88, 152–169. http://doi.org/10.1016/j.advwatres.2015.12.004

WWF (2012). The Swiss Water Footprint Report, a global picture of Swiss water dependence. 1-36.

YUWEI, W., JIANQIAO, H., ZHONGMING, G., & ANAN, C. (2014). Limitations in identifying the equilibrium-line altitude from the optical remote-sensing derived snowline in the Tien Shan, China. Journal of Glaciology, 60(224), 1093–1100. http://doi.

org/10.3189/2014jog13j221

ZEMP, M. (2006). Glaciers and Climate Change Spatio-temporal Analysis of Glacier Fluctuations in the European Alps after 1850.2006, University of Zurich, Faculty of Science. https://doi.org/10.5167/uzh-34258.

ZEPP, H. (2004): Geomorphologie. Eine Einführung. Paderborn, Deutschland: Verlag Ferdinand Schöningh GmbH. ISBN: 978-3-82524030-1.

APPENDIX

APP-A / GRAPHS

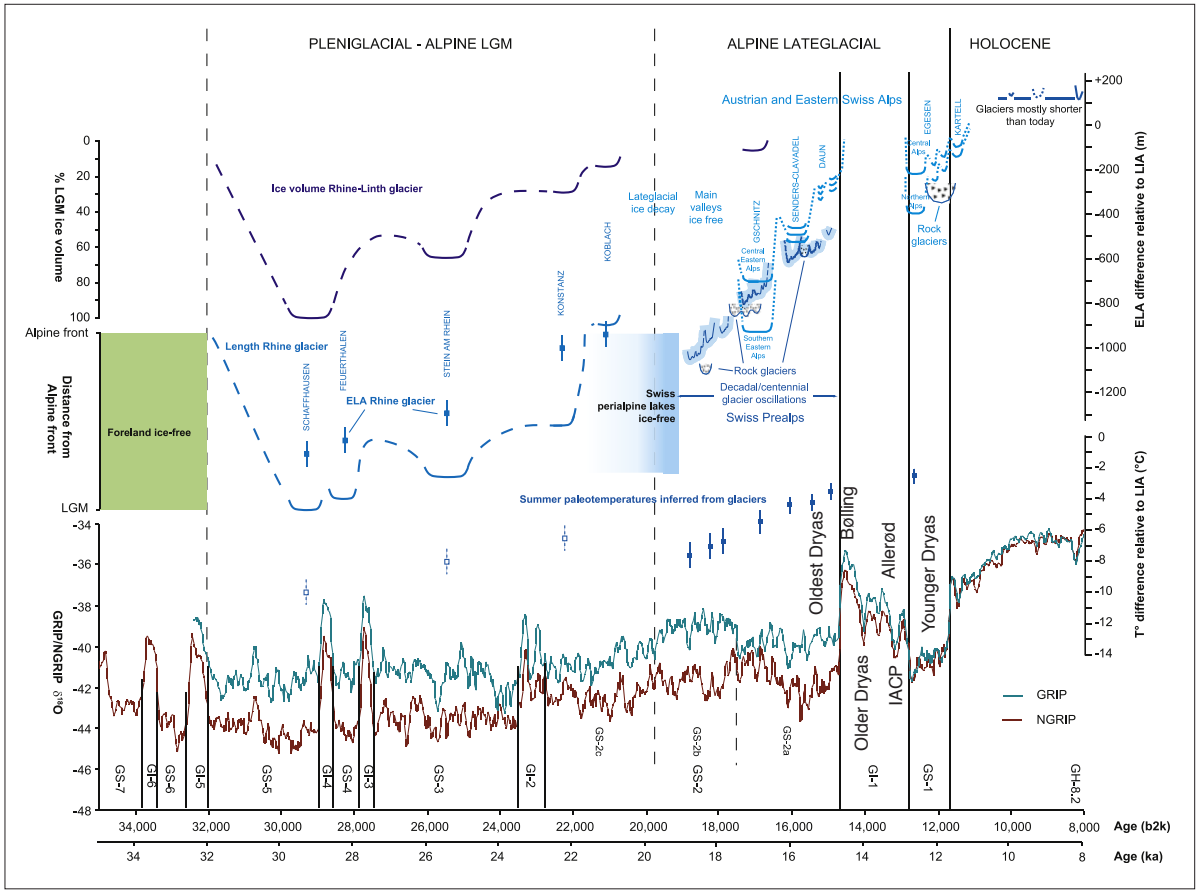

APP-A1: Modified overview about the last 34‘000 years. The given Rhine glacier extent can be used as indication for an alpine signal. Nevertheless, the LGM of the discussed Rhone glacier is assumed to be later, around 19-20 ka BP. See chapter 2.3 for further informations. (Source: HEIRI et al., 2014)

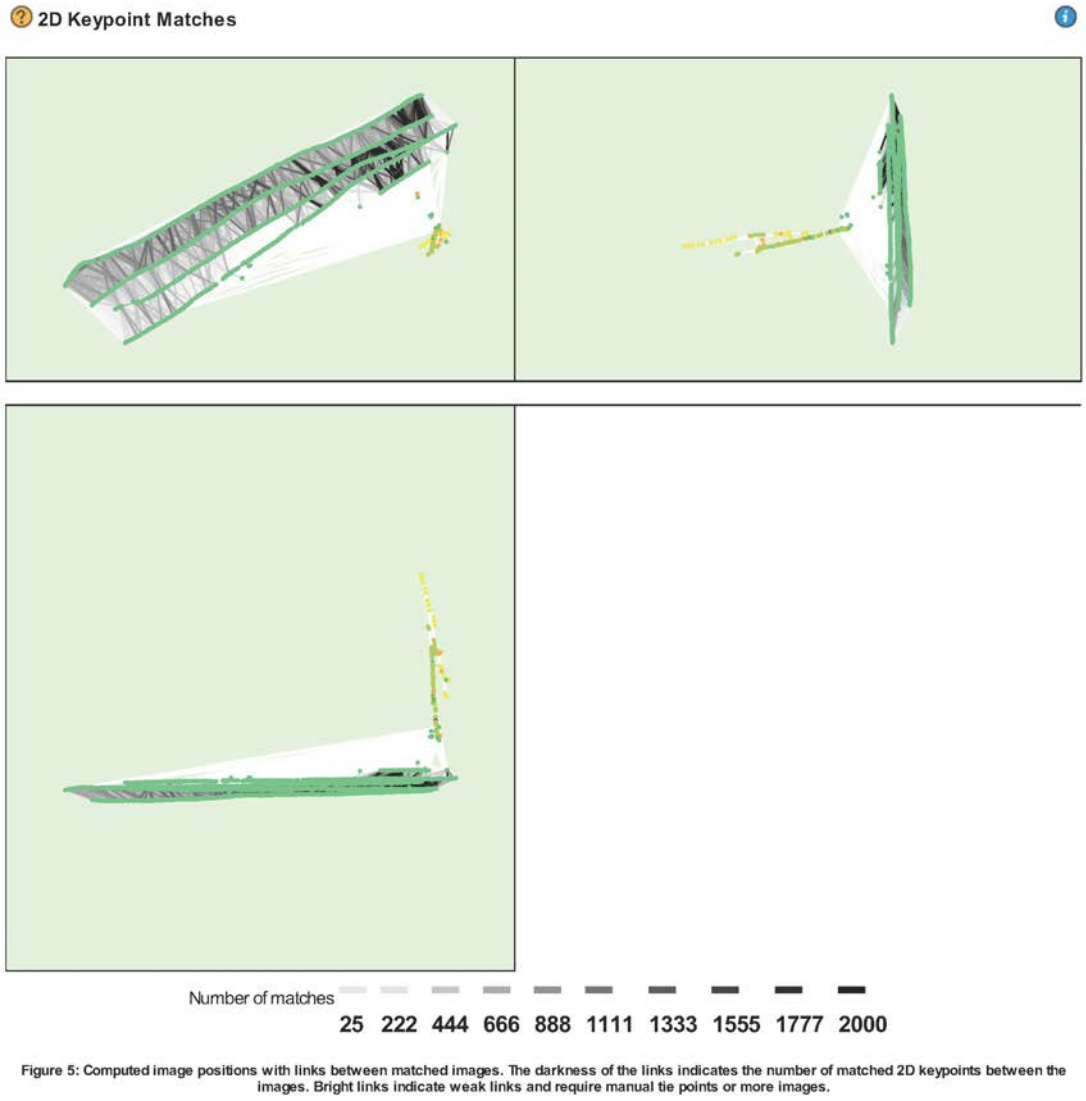

APP-A2: Extract of the quality report of Pix4D. (Source: own illustration)

APP-B / PHOTODOCUMENTATION

The numbers and descriptions correspond to chapter 4.4.4 catchment results & interpretations.

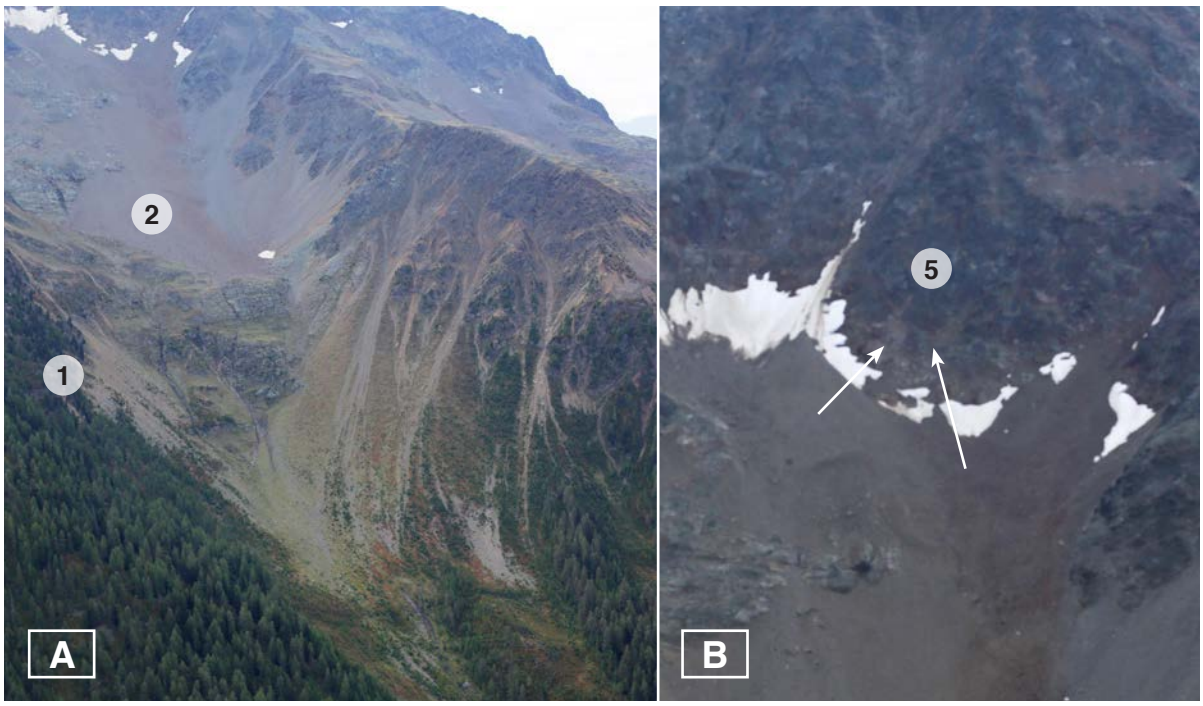

APP-B1: The lower part of Gitzibach with assumably stable terrain (left), while the upper part reveals some doubtful rock-faces (right). (Source: own photographies)

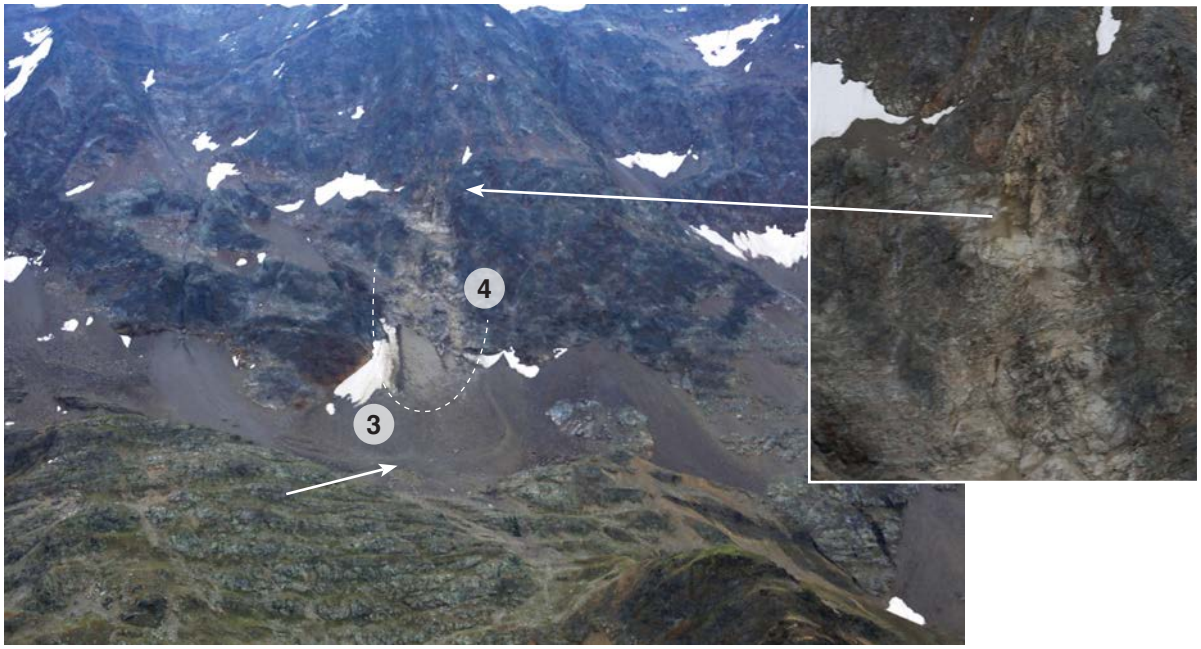

APP-B2: The upper part of the Gitzibach catchment. The fresh rockfall event is obvious. (Source: own photographies)

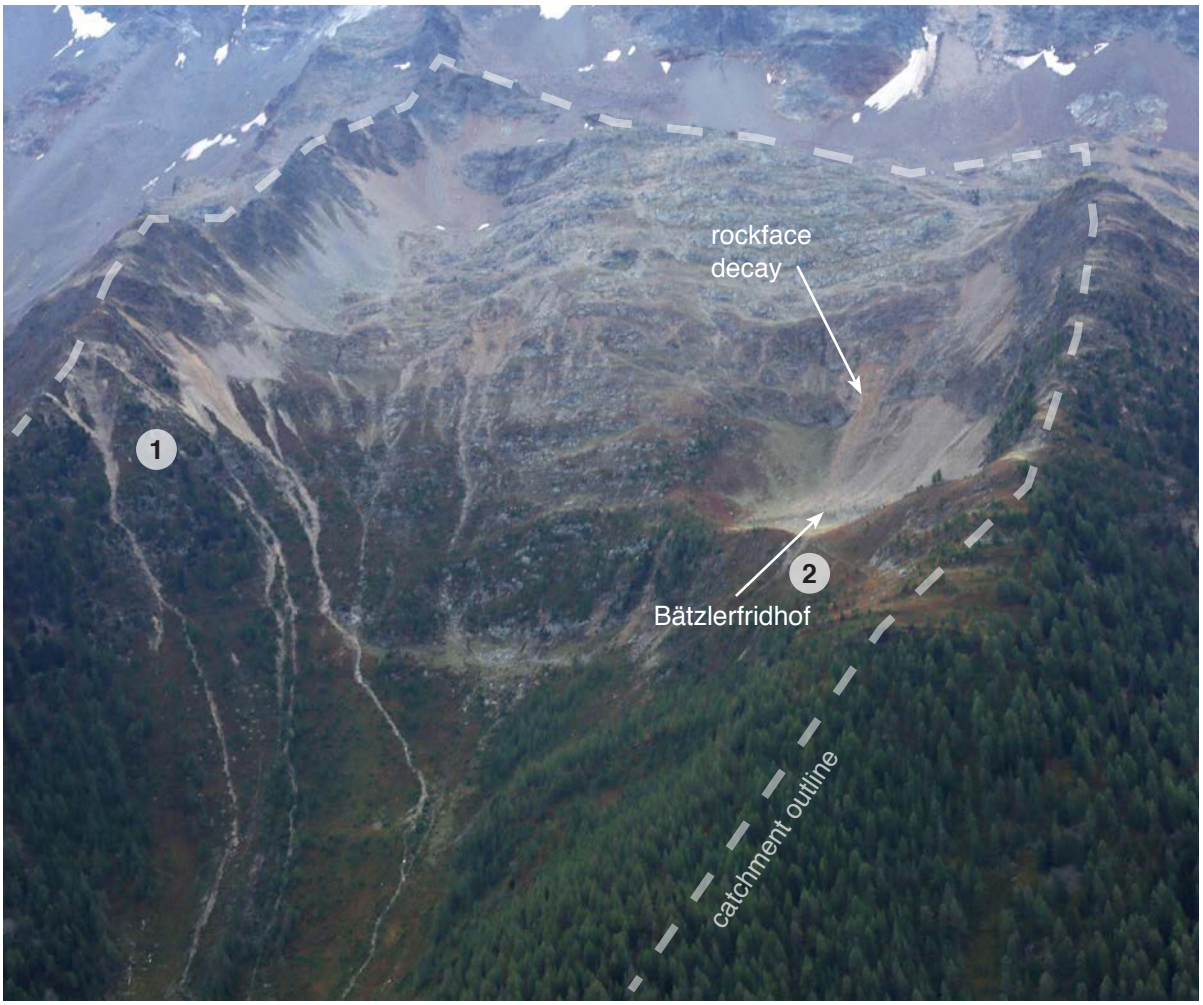

APP-B3: The catchment of Bätzlabach is strongly vegetated and reveals only small amounts of visible surface processes. (Source: own photographies)

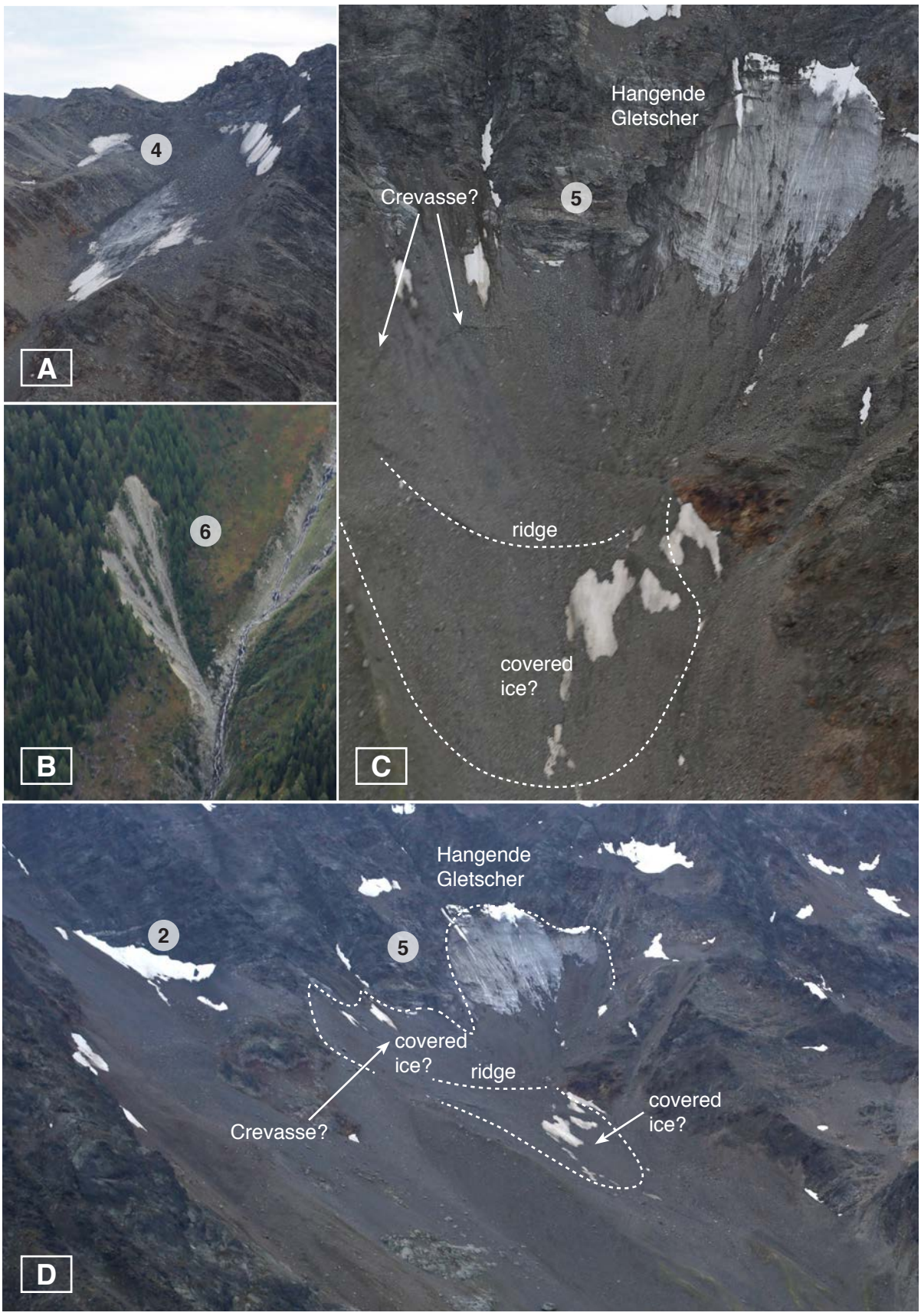

APP-B4: Hangende Gletscher in detail. A larger extent is assumed. (Source: own photographies)

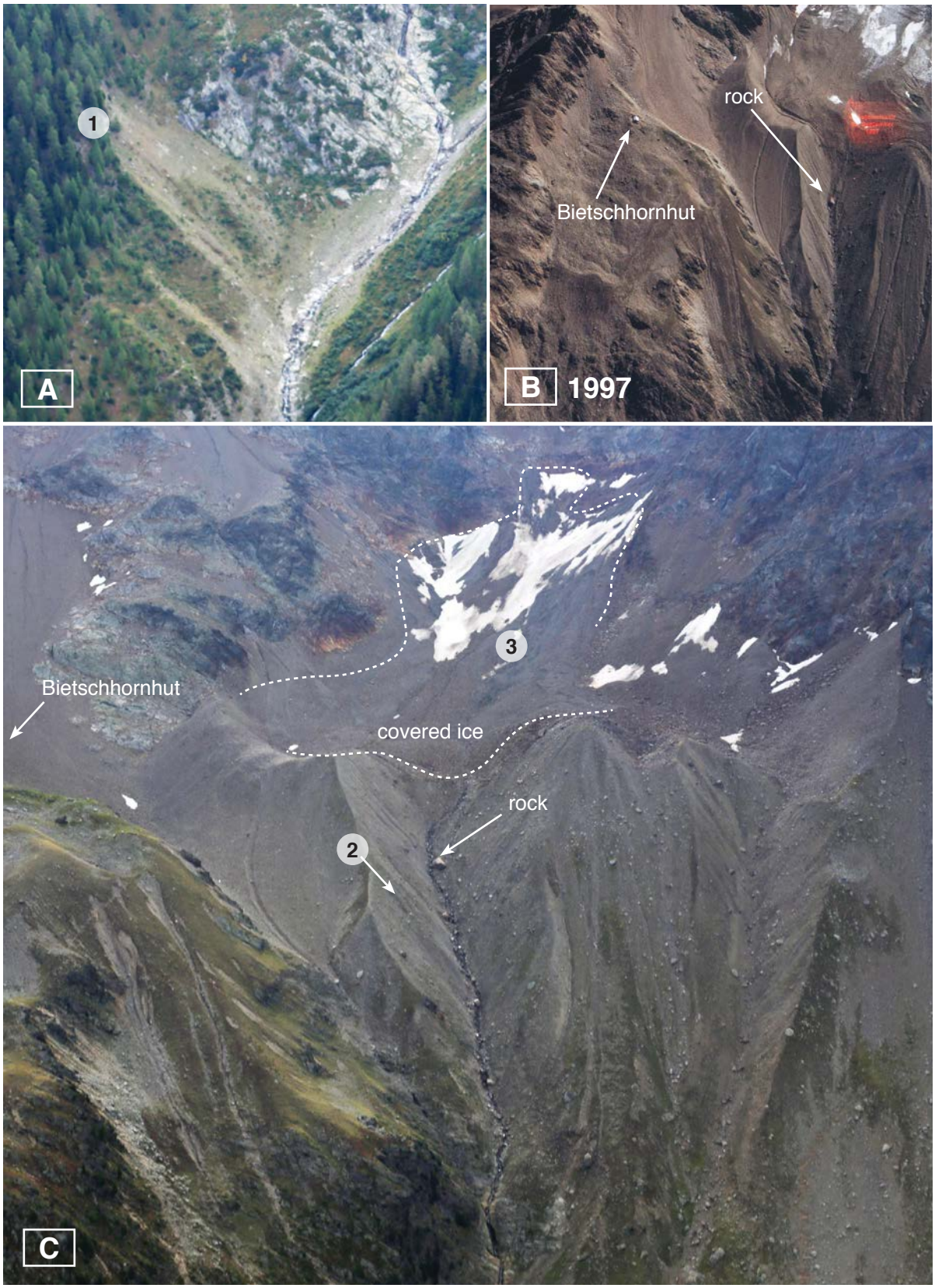

APP-B5: The catchment of Tännerbach in detail. Picture B shows an aerial image of 1997, including the huge rock within the bastion channel. (Source: own photographies; E-PICS, 2019a [B])

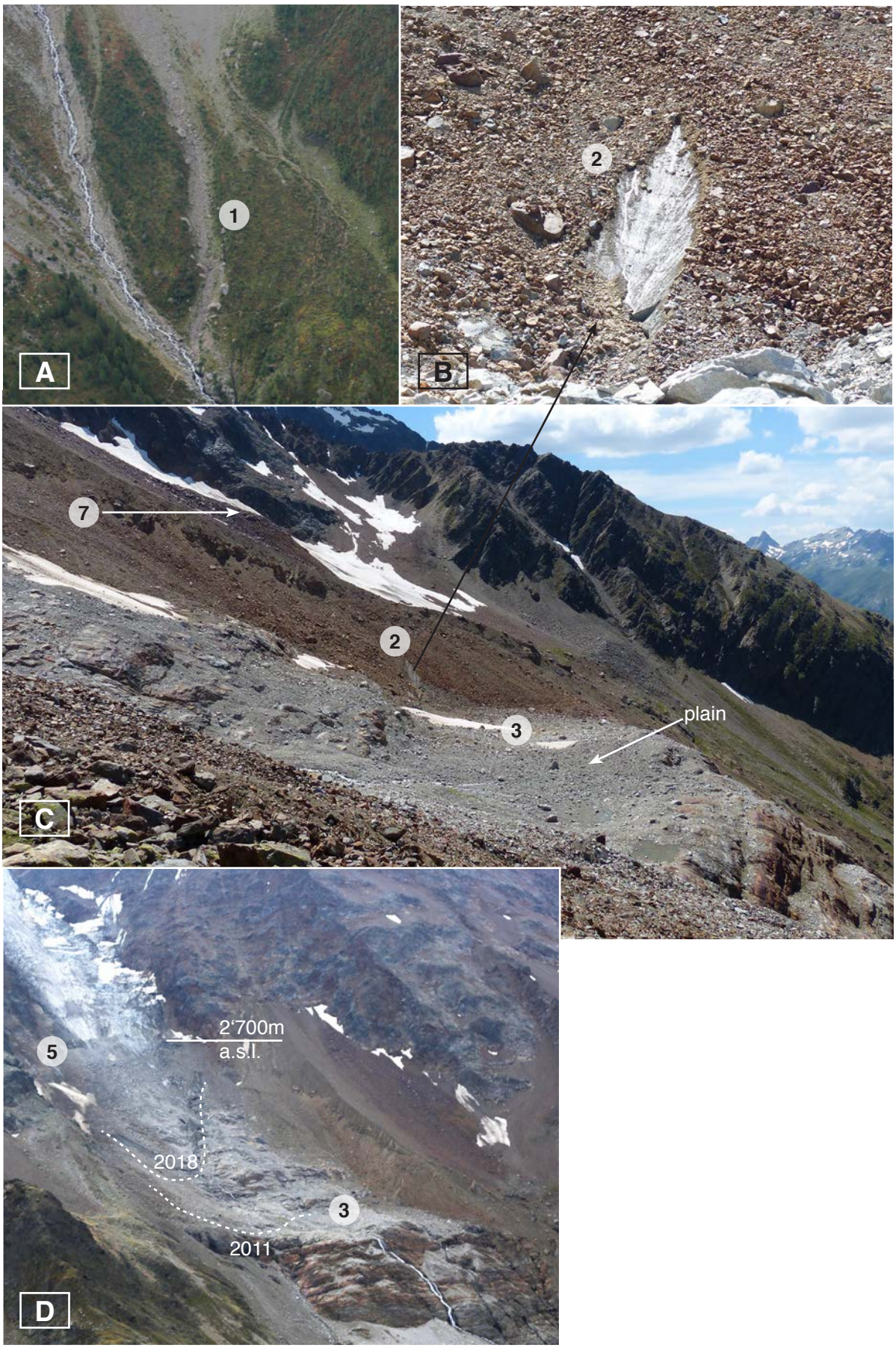

APP-B6: The catchment of Nästbach in detail. (Source: own photographies)

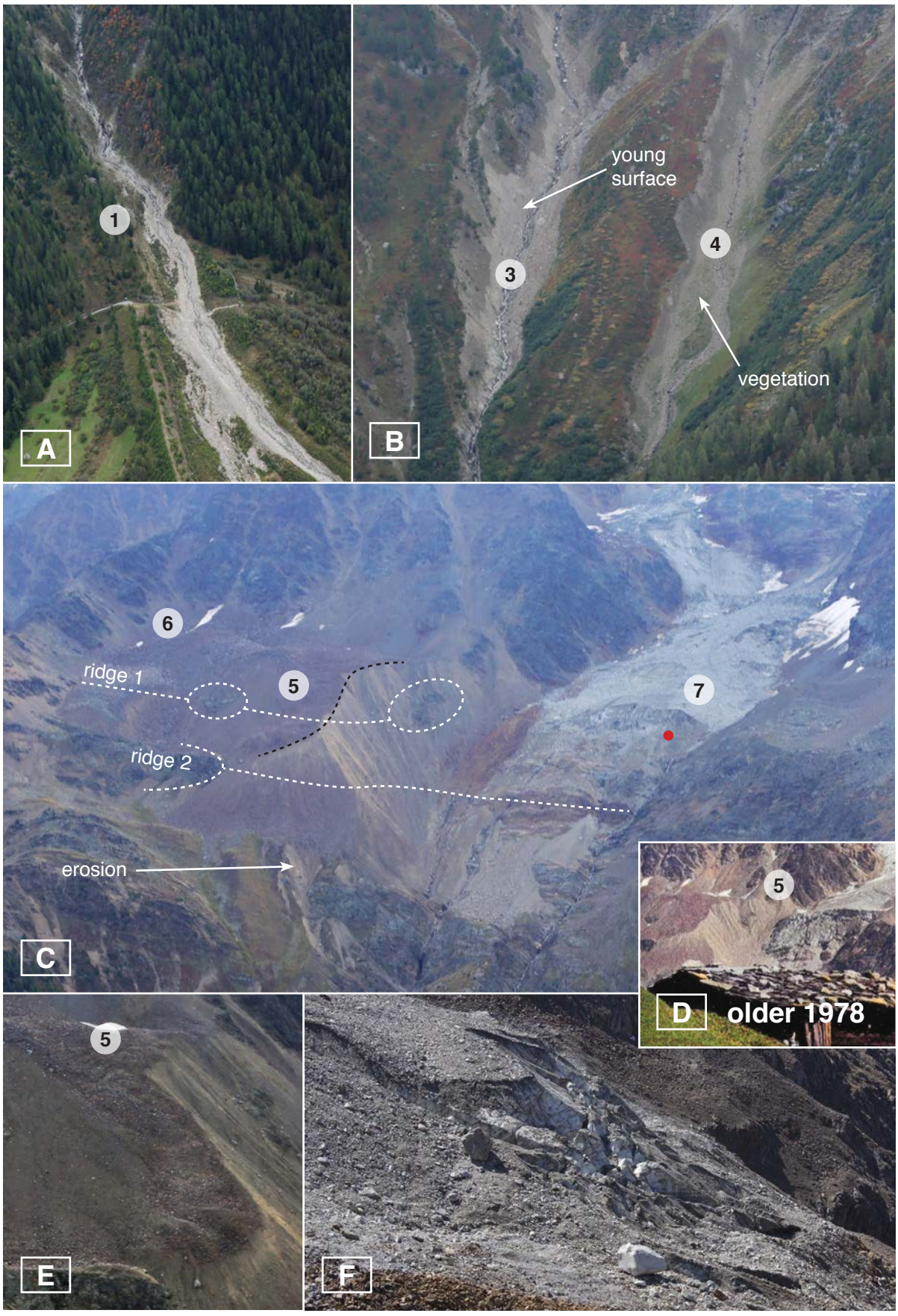

APP-B7: The catchment of Birchbach in detail. In [D] a segment of a postcard is illustrated which is older than 1978. (Source: own photographies; private collection of Werner Bellwald [D])

APP-B8: The glacier advancement between 2011 and 2017 shows different aspects. The black arrows indicate a lateral extension gain and the red circle shows the movement of a boulder. The red dot acts as reference. (Source: SWISSTOPO, 2018a)

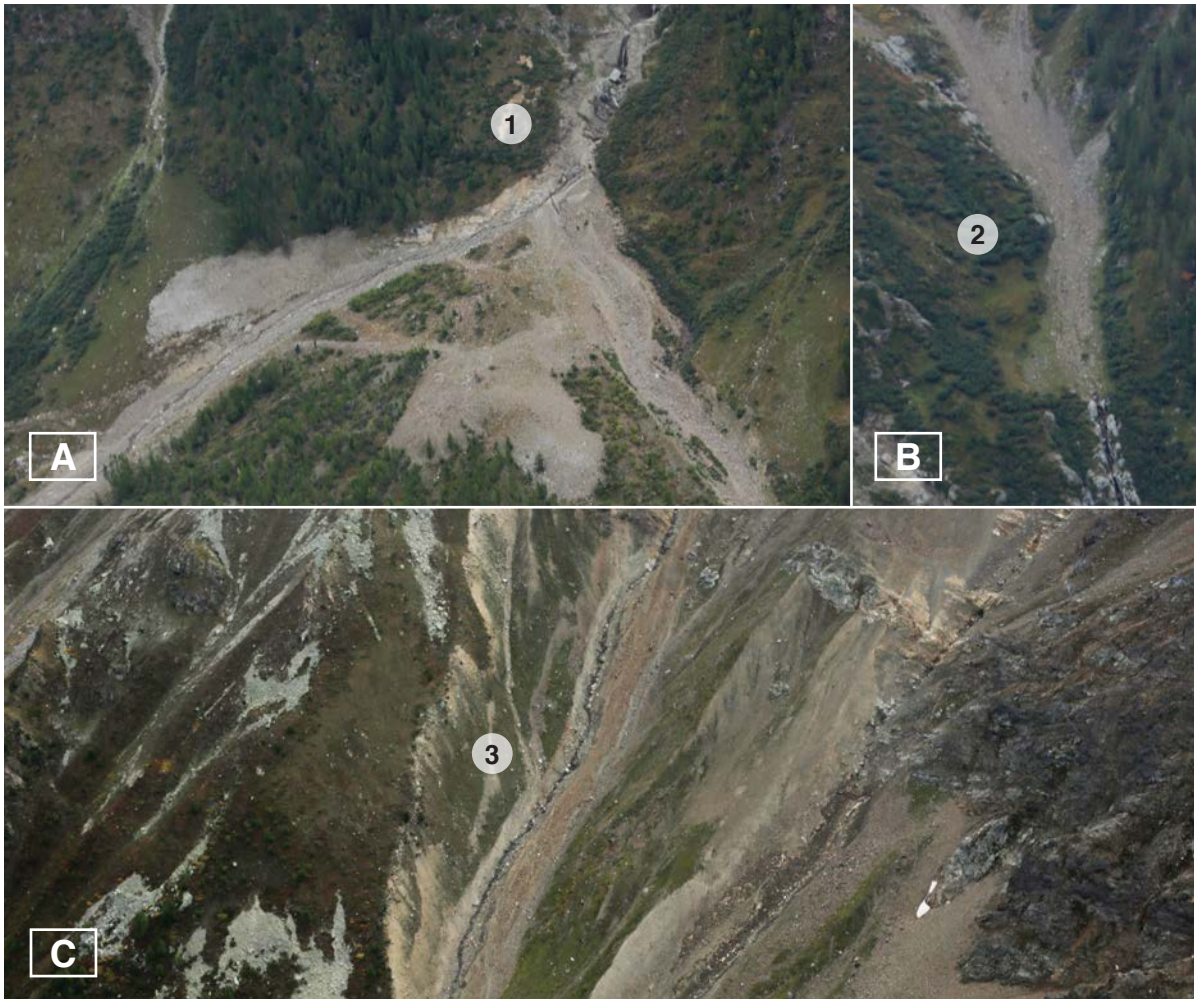

APP-B9: The lower parts of the Stampbach catchment. (Source: own photographies)

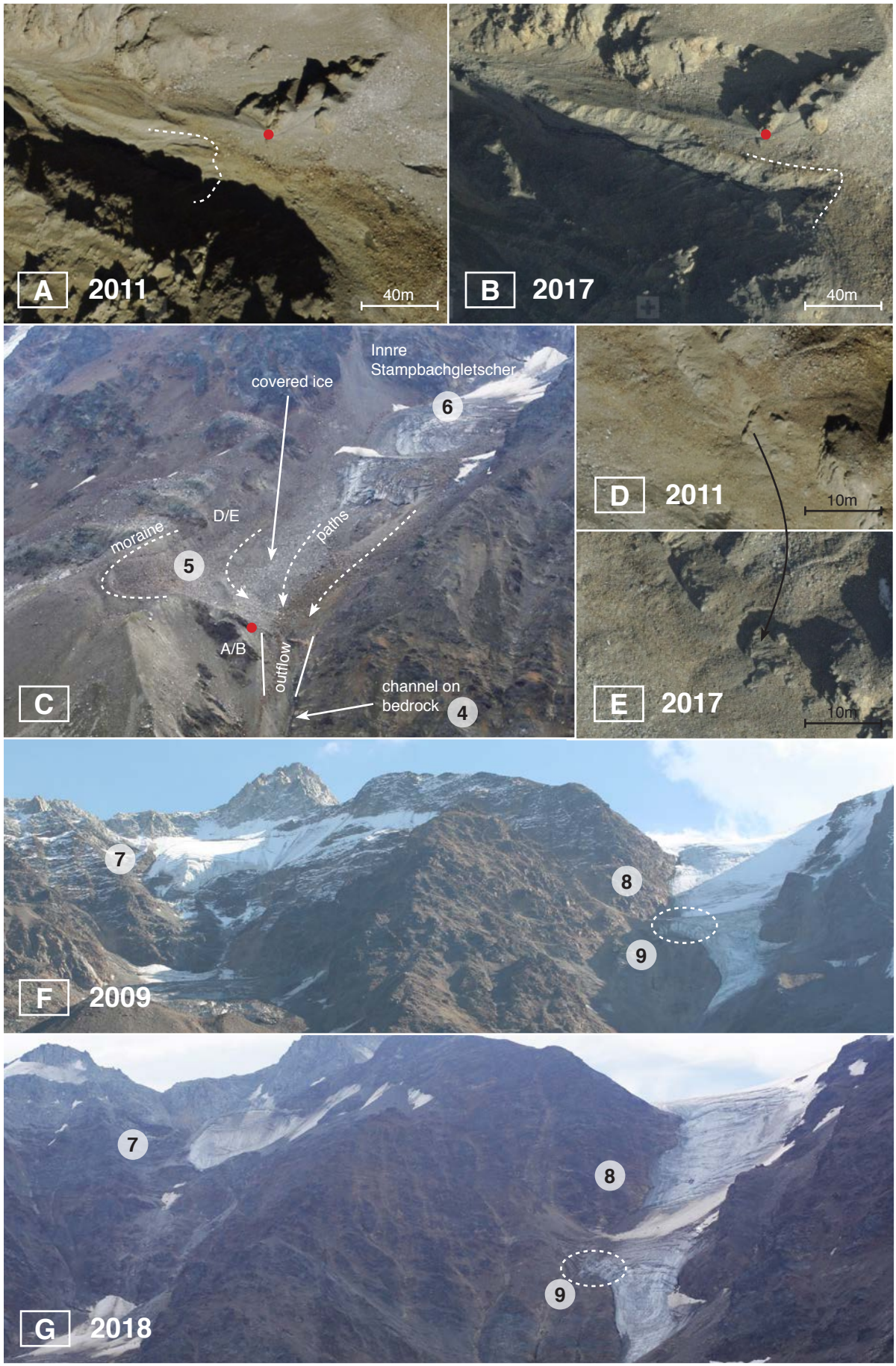

APP-B10: Detailed overview about the Stampbach catchment. (Source: own photographies; SWISSTOPO, 2018a [A, B, D, E])

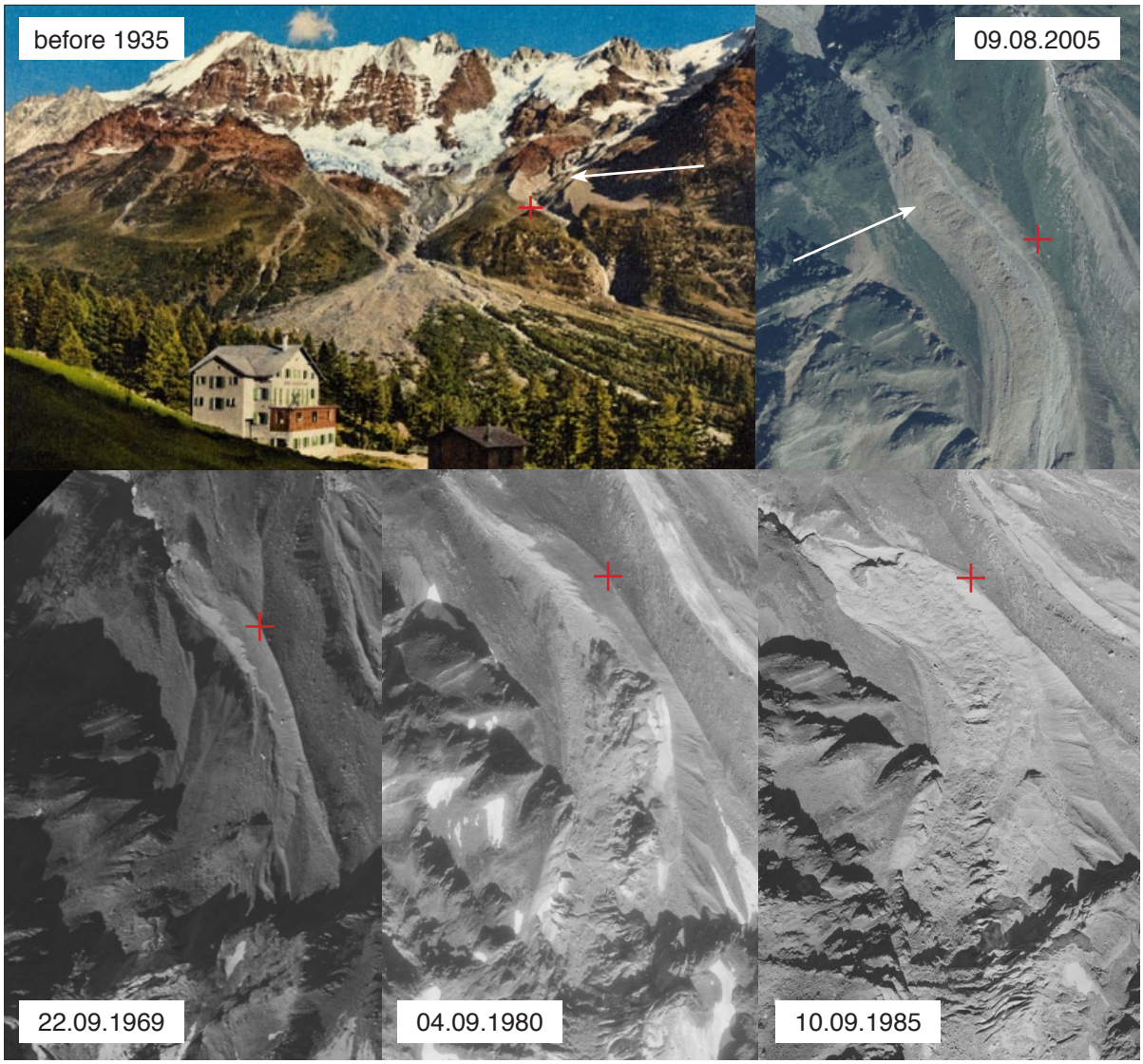

APP-B11: On the top left a postcard before the 19th July of 1935 shows the hotel Fafleralp with the Breitlauihorn in the background. The deep channel on the right side (marked) is the remnant of the Oigstchummungletscher. On the top right the aerial picture of 2005 shows the same channel but filled with an assumed block glacier. The red cross serves as relative orientation based on a sharp edge of the middle moraine. Below a time sequence between 1969 and 1985 shows the glacial advancement during the 80ies (Source: SWISSTOPO 2018a; E-PICS, 2019b)

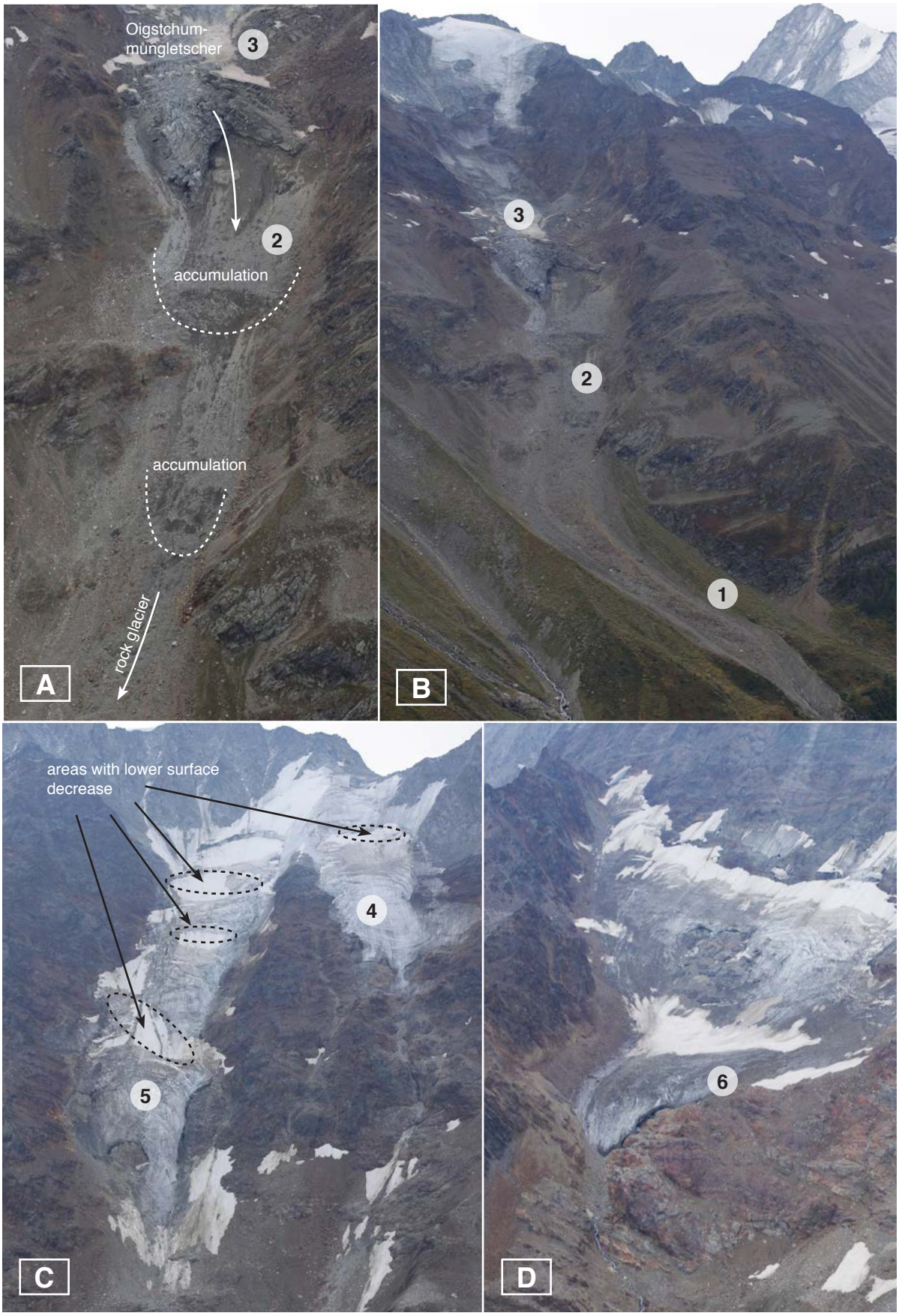

APP-B12: Detailed overview about the Loibinbach catchment. (Source: own photographies)

APP-B13: The retreat of the Loibinbachgletscher within 11 years. (Source: own photographies)

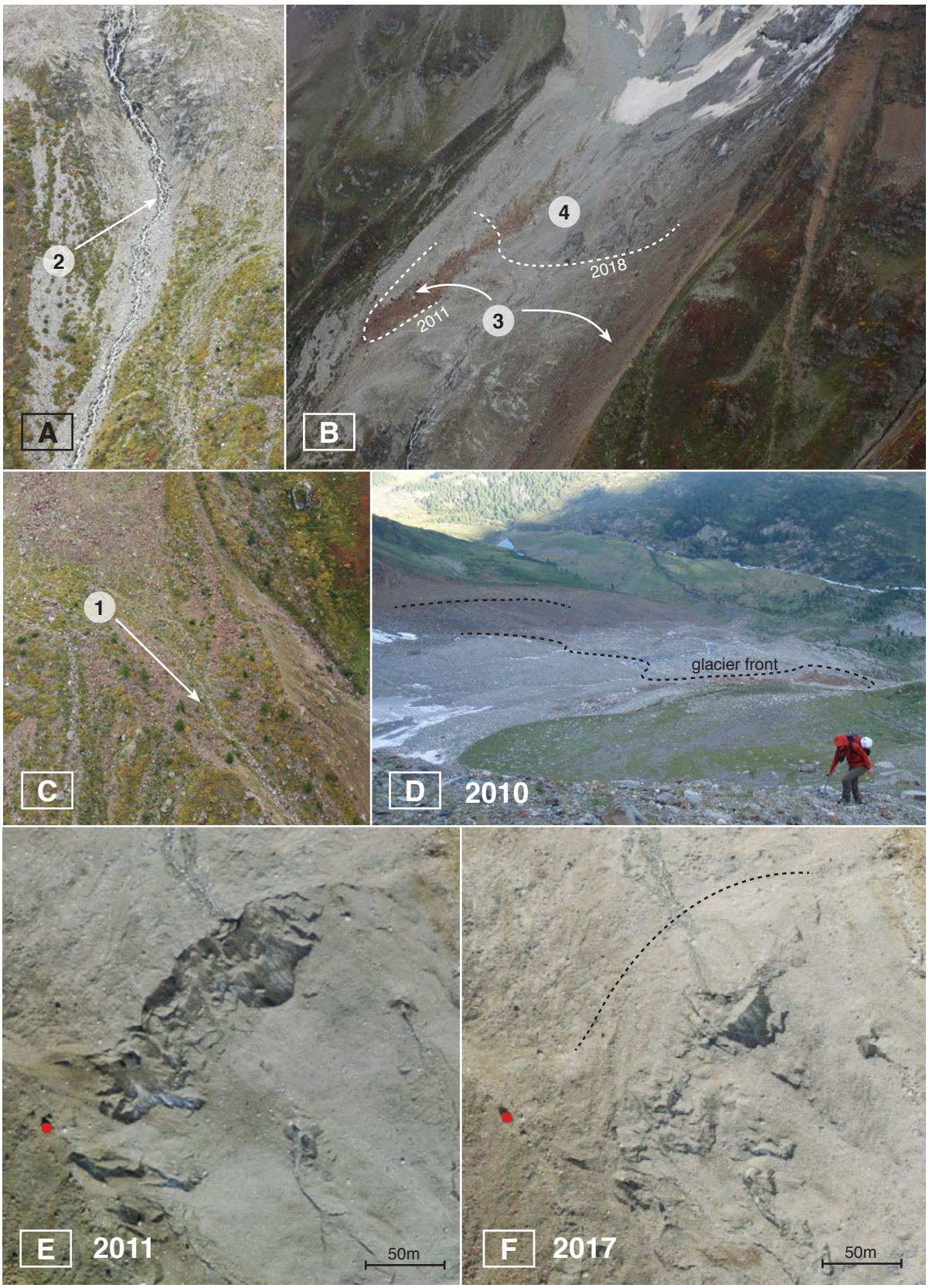

APP-B14: A detailed overview on the Beichbach catchment. (Source: own photographies; SWISSTOPO, 2018a [E, F])

APP-C / TABLES

APP-C1: Modelled glaciated area depending on temperature increase from today (2018).

$T_{increase}$	[+°C]	0	0.5	1	1.5	2	2.5	3	3.5	4	4.5	5
ELA_{calc}	[m a.s.l.]	3000	3085	3170	3255	3340	3425	3510	3595	3680	3765	3850
ELA_{round}	[m a.s.l.]	3000	3100	3200	3300	3300	3400	3500	3600	3700	3800	3900
BLA												
$Area_{Acc.}$	[km^2]	11.34	6.13	2.87	1.78	1.78	1.07	0.76	0.51	0.28	0.07	0
$Area_{Abl.}$	[km^2]	7.56	4.09	1.91	1.19	1.19	0.71	0.51	0.34	0.19	0.05	0
Sum	[km^2]	18.9	10.21	4.79	2.96	2.96	1.78	1.27	0.85	0.47	0.12	0
	[%]	100	54.0	25.3	15.7	15.7	9.4	6.7	4.5	2.5	0.6	0
FER												
$Area_{Acc.}$	[km^2]	12.14	6.49	3.12	1.87	1.87	1.1	0.77	0.51	0.28	0.07	0
$Area_{Abl.}$	[km^2]	8.1	4.33	2.08	1.25	1.25	0.73	0.52	0.34	0.19	0.05	0
Sum	[km^2]	20.24	10.82	5.19	3.12	3.12	1.84	1.29	0.86	0.47	0.12	0
	[%]	100	53.5	25.6	15.4	15.4	9.1	6.4	4.2	2.3	0.6	0

APP-C2: Comparison between modelled and measured values for the catchment FER.

	Jan	Feb	Mar	Apr	Mar	Jun	Jul	Aug	Sep	Oct	Nov	Dec
Measured [m^3/s]	1.15	1.22	1.38	3.40	9.30	17.67	16.38	13.31	7.95	4.43	2.47	1.41
Modeled [m^3/s]	0.64	0.39	1.62	4.50	10.13	14.83	15.02	10.84	5.49	2.73	0.65	0.34
Offset [%]	-44.5	-67.8	17.3	32.3	9.0	-16.1	-8.3	-18.6	-30.9	-38.4	-73.5	-76.2

APP-C3: Comparison between modelled and measured values for the catchment BLA.

	Jan	Feb	Mar	Apr	Mar	Jun	Jul	Aug	Sep	Oct	Nov	Dec
Measured [m^3/s]	0.60	0.52	0.65	1.81	5.67	11.33	12.42	10.42	5.62	2.65	0.07	0.72
Modeled [m^3/s]	0.22	0.14	0.74	2.33	8.20	12.99	13.88	9.84	5.86	2.18	0.70	0.14
Offset [%]	-63.6	-72.2	12.7	29.0	44.7	14.7	11.8	-5.6	4.2	-17.5	-39.1	-81.1

APP-C4: Applied factors for the RCP calculations of the tributary torrents

	P_{Rain}			*Sm* BLA			*Sm* FER			*Gm* BLA			*Gm* FER			*ETc* BLA			*ETc* FER		
RCP	2.6	4.5	8.5	2.6	4.5	8.5	2.6	4.5	8.5	2.6	4.5	8.5	2.6	4.5	8.5	2.6	4.5	8.5	2.6	4.5	8.5
1	1.08	1.07	1.12	1.26	2.16	5.02	1.23	1.99	4.07	1.00	1.00	1.00	1.00	1.00	1.00	1.47	2.74	29.23	10.72	10.72	10.72
2	1.08	1.07	1.12	1.19	1.82	3.62	1.19	1.73	3.15	1.00	1.00	1.00	1.00	1.00	1.00	1.44	2.91	8.82	1.36	2.41	44.68
3	1.00	0.99	1.00	1.02	1.31	2.12	1.02	1.27	1.86	1.00	1.00	1.00	1.00	1.00	1.00	1.06	1.82	4.58	1.04	1.62	27.44
4	1.00	0.99	1.00	1.02	1.19	1.48	1.01	1.13	1.30	1.00	1.00	1.00	1.00	1.00	1.00	1.03	1.34	2.15	1.02	1.29	15.37
5	1.00	0.99	1.00	1.01	1.05	1.02	1.00	1.01	0.92	0.41	0.10	0.02	0.41	0.10	0.02	1.02	1.18	15.40	1.00	1.00	1.00
6	0.96	0.91	0.79	1.04	1.00	0.74	1.04	0.96	0.66	0.52	0.15	0.04	0.51	0.15	0.04	0.98	0.94	0.82	1.00	1.00	0.09
7	0.96	0.91	0.79	1.01	0.79	0.36	1.01	0.75	0.30	0.52	0.15	0.04	0.52	0.15	0.04	0.97	0.93	0.81	1.00	1.00	1.00
8	0.96	0.91	0.79	0.93	0.46	0.05	0.93	0.42	0.04	0.52	0.15	0.04	0.51	0.15	0.04	1.00	1.00	0.09	1.00	1.00	1.00
9	0.96	0.96	0.94	0.82	0.37	0.07	0.81	0.37	0.07	0.49	0.13	0.03	0.48	0.13	0.03	0.98	1.00	1.01	1.00	1.00	1.00
10	0.96	0.96	0.94	0.94	0.81	0.52	0.92	0.78	0.49	0.32	0.03	0.00	0.32	0.03	0.00	1.00	1.00	1.00	1.00	1.00	1.00
11	0.96	0.96	0.94	1.10	1.33	1.66	1.08	1.26	1.47	1.00	1.00	1.00	1.00	1.00	1.00	1.18	1.74	19.40	1.00	1.00	1.00
12	1.08	1.07	1.12	1.19	1.70	2.49	1.14	1.52	2.04	1.00	1.00	1.00	1.00	1.00	1.00	1.40	2.58	6.38	1.34	2.17	38.25

APP-C5: Used ground control points (GCPs). The numbering is not continuous.

GCP	Easting	Northing	Altitude	GCP	Easting	Northing	Altitude	GCP	Easting	Northing	Altitude
1	626241.7	136419.4	2522.0	84	629788.2	141301.3	1551.1	139	635504.1	143920.2	1993.1
10	628124.3	137300.9	2498.9	85	629868.8	141267.8	1554.4	140	635627.3	144004.3	2005.7
12	628617.8	136428.5	3304.7	86	630122.8	141432.6	1586.6	141	635847.8	144210.9	2040.1
15	629097.5	138250.8	2566.9	87	630120.4	141316.9	1591.9	143	636510.2	143870.5	2350.6
17	627088.4	139355.2	1403.4	88	630242.1	141660.5	1614.0	144	636424.4	143739.1	2372.8
19	629041.0	139368.7	1954.7	89	630286.5	141498.1	1603.6	145	636123.5	143717.8	2230.6
23	629250.2	140992.6	1525.3	90	630327.6	141740.3	1604.4	146	635770.6	143808.6	2120.3
25	630742.9	138606.2	3116.5	91	630309.9	141585.6	1595.6	147	635930.8	143411.6	2263.2
30	630642.8	141189.5	1717.6	92	630468.5	141794.6	1605.4	148	635652.2	143425.2	2158.9
31	631341.5	140407.5	2351.5	94	630678.4	141921.8	1640.9	149	635422.2	143593.2	2059.2
37	632725.0	141469.0	2221.6	95	630803.0	141898.5	1607.8	150	635611.4	143315.3	2193.2
39	632848.4	142735.7	1779.7	96	630862.5	141669.1	1615.1	151	635329.3	143090.9	2226.9
40	633919.7	140482.2	3296.2	97	631068.8	141821.4	1619.7	152	635055.4	143262.0	2047.8
42	634101.6	142267.7	2363.6	98	631117.3	141984.4	1625.7	153	634730.2	143401.4	1959.0
45	635854.4	141874.7	3082.0	99	631270.3	141956.9	1643.2	154	634884.3	142868.4	2169.8
47	635252.5	143792.2	1977.2	100	631234.2	142086.2	1636.3	155	634882.4	143167.1	2065.8
50	629130.1	138817.9	2207.8	101	631297.5	142102.6	1640.3	156	634504.7	143287.5	1943.1
51	625256.8	138416.9	1378.3	102	631526.7	141975.4	1679.4	157	634529.8	143007.6	2030.2
52	625385.6	138596.3	1380.3	103	631481.2	141880.2	1676.6	158	634585.1	143233.4	1976.4
53	626173.9	138842.1	1357.8	104	631540.0	142217.8	1666.1	159	637021.8	143521.8	2695.8
54	626779.3	139320.1	1419.7	105	631686.2	142244.9	1687.6	160	637020.9	143151.4	2881.4
55	627010.1	139493.1	1397.5	106	631783.9	142175.6	1704.8	161	636600.0	143162.3	2665.7
56	627063.7	139505.9	1398.0	107	631794.4	142396.6	1726.1	162	636500.5	143060.4	2724.2
57	626587.6	139170.1	1406.4	108	632028.5	142511.9	1755.5	163	636232.8	143219.8	2507.7
58	627441.6	139767.9	1428.6	109	632223.3	142226.8	1799.8	164	636325.4	142735.9	2843.2
59	627553.2	139823.0	1435.4	110	632378.1	142591.7	1767.5	165	636634.0	142540.2	3099.5
60	625640.6	138573.3	1365.6	111	632402.8	142500.9	1765.4	166	636406.6	142646.4	2867.5
61	625893.6	138645.4	1348.1	112	632487.4	142584.9	1764.4	167	635851.3	142580.3	2652.2
62	626042.8	138909.9	1394.8	113	632574.4	142617.9	1766.1	168	635812.9	142781.9	2519.4
63	626506.9	139060.6	1400.1	114	632645.6	142567.0	1771.5	169	635377.3	142705.1	2358.2
64	628092.3	139870.1	1447.9	115	632705.7	142720.1	1769.9	170	635630.2	142397.9	2507.2
65	627687.4	139982.4	1442.3	116	632904.8	142626.3	1770.6	171	635741.5	142199.2	2716.5
66	627994.5	140193.1	1459.2	117	633147.6	142751.8	1822.2	172	635411.5	141723.9	2953.0
67	627744.5	139673.8	1429.1	119	633437.0	142967.4	1840.8	173	635490.7	141367.1	3346.3
68	628211.3	140288.2	1481.9	120	633614.6	143112.6	1846.1	174	635081.8	141619.7	2904.9
69	628363.9	139983.4	1486.7	121	633680.7	142992.1	1847.2	175	634757.2	141986.7	2665.0
70	627949.1	139808.4	1440.2	122	633814.8	143162.1	1854.6	176	634189.1	142554.1	2172.7
71	628462.1	140439.6	1494.0	123	633751.7	143240.1	1850.0	177	634662.9	142448.3	2358.1
72	628572.6	140281.1	1499.6	124	633990.7	143358.6	1868.1	178	634518.4	141540.4	2989.7
73	628755.4	140757.1	1514.3	125	634032.1	143228.1	1870.3	179	634762.7	141138.9	3418.1
74	628967.0	140687.4	1547.1	129	634312.9	143488.9	1881.9	180	634090.2	142057.3	2490.3
75	628600.9	140488.3	1490.6	130	634374.3	143320.6	1914.5	181	633744.2	141577.1	2646.2
76	629007.5	140916.8	1525.5	131	634482.4	143639.6	1902.4	182	633692.8	142864.8	1899.0
77	629090.2	140974.9	1526.8	132	634710.6	143624.3	1930.9	183	634164.8	142536.3	2183.0
78	629217.6	141059.7	1535.4	133	634782.8	143562.8	1942.5	184	633564.0	142247.4	2184.0
79	629174.4	140604.9	1580.2	134	634702.8	143455.6	1943.1	185	632930.8	142008.8	2075.5
80	629306.8	140836.7	1537.3	135	635025.4	143697.8	1969.1	186	633265.6	142630.1	1887.9
81	629420.8	140972.9	1532.0	136	635130.1	143628.4	1972.7	187	633656.2	141647.5	2590.9
82	629395.7	141105.1	1530.1	137	635098.2	143864.8	1970.6	188	633142.1	140898.4	2567.0
83	629557.6	141000.3	1538.7	138	635310.5	143713.9	1986.8	189	633428.1	141192.1	2554.6

190	632830.6	141584.9	2162.2	242	629798.3	138073.5	2871.1	281	627715.5	137785.3	2117.3
191	632875.7	141198.9	2361.6	243	629625.8	138692.3	2430.6	282	627833.4	137691.8	2219.7
192	632985.8	140856.1	2613.0	244	629270.3	138563.0	2404.4	283	627682.4	137344.0	2435.3
193	632895.5	140412.4	2804.7	245	629290.3	138723.6	2287.2	284	627897.8	137404.3	2403.0
194	633134.1	140071.6	3295.4	246	629815.0	138399.6	2601.4	285	628433.0	137618.2	2582.2
195	632583.8	141062.6	2423.3	247	628889.6	138667.9	2414.8	286	628074.2	137354.9	2460.6
196	632398.9	141541.3	2098.4	248	628708.1	138691.1	2295.6	287	628776.9	137205.6	2948.8
197	632613.3	141591.1	2125.1	249	628695.8	138542.6	2333.7	288	628477.8	136850.1	2865.1
198	632212.8	141912.8	1847.5	250	628748.4	138040.1	2411.1	289	628128.7	136373.0	3109.3
199	632136.3	140894.9	2431.1	251	628602.6	138199.6	2275.2	290	627356.0	137215.0	2415.6
200	630967.2	141748.6	1619.2	252	628439.0	138372.2	2163.5	291	626742.9	137223.9	2243.1
201	630810.8	141538.2	1638.9	253	628403.0	138199.8	2236.3	292	627153.1	136959.9	2443.8
202	630809.2	141350.1	1704.9	254	628187.8	138449.0	1991.8	293	627545.8	136563.4	2750.3
203	630978.6	141174.8	1848.4	255	628114.7	138575.9	1928.1	294	627518.2	136259.1	2963.7
204	631545.8	140845.1	2345.6	256	628162.7	138373.6	2029.7	295	626577.0	136137.7	2569.6
205	631226.2	141153.2	2037.6	257	627899.5	138831.7	1737.0	296	626744.6	136345.7	2482.4
206	631894.4	140640.6	2541.7	258	627695.3	139099.4	1571.5	297	625963.3	137389.1	1931.7
207	631764.4	141252.8	2160.0	259	627541.0	139271.0	1502.7	298	626275.0	137038.6	2100.7
208	631464.2	140708.7	2388.9	260	627694.2	139556.6	1434.4	299	626230.2	136738.4	2250.7
209	632143.8	139655.9	3108.6	261	627638.2	139370.8	1472.4	300	626407.1	136823.8	2204.4
210	632469.4	139750.9	3147.3	262	627520.0	139460.6	1453.5				
211	631486.5	139680.3	2901.3	263	627511.1	139204.9	1507.5				
212	631323.0	139929.8	2695.4	264	627338.2	139336.3	1442.5				
213	631152.4	140453.3	2268.6	265	628053.8	138217.8	2112.4				
214	630778.6	140873.6	1960.1	266	628225.1	138023.9	2265.0				
215	630386.2	141394.9	1637.9	267	628630.6	137671.1	2580.1				
216	630446.2	141201.1	1686.3	268	628759.6	137860.3	2510.0				
217	630751.2	140404.9	2314.0	269	629232.9	137406.6	2821.1				
218	630968.7	139921.1	2704.5	270	629039.7	137211.4	3059.3				
219	630408.4	140167.6	2399.7	271	629479.6	137769.1	2835.4				
220	630673.8	139783.3	2532.4	272	629683.7	137515.4	3089.2				
221	630476.5	139407.6	2494.6	273	628865.2	138060.6	2483.0				
222	630776.5	138860.3	2851.0	274	626979.6	139015.6	1440.3				
236	629533.2	139198.7	2214.6	275	626776.4	138968.4	1415.1				
237	629276.4	138763.9	2261.2	276	627038.9	138827.9	1498.7				
238	629768.8	138789.2	2447.9	277	627458.0	138204.4	1871.3				
239	630274.7	138861.1	2687.3	278	627514.8	137985.7	1969.5				
240	630299.6	138058.2	2961.6	279	627643.3	137932.9	2016.9				
241	631821.3	140057.7	2793.3	280	627530.4	137774.7	2080.9				

Personal Declaration

I hereby declare that the submitted thesis is the result of my own, independent work.
All external sources are explicitly acknowledged in the thesis.

Matthias Nyfeler
Greifensee, 28th of April 2019